NANOTEC
a member of NSTDA

NATIONAL E-SCIENCE
INFRASTRUCTURE CONSORTIUM

DEPARTMENT OF COMPUTER SCIENCE
FACULTY OF SCIENCE, KASETSART UNIVERSITY

COMPUTATIONAL SCIENCE & BIG DATA FOR SUSTAINABLE AND INNOVATIVE FUTURE

August 2-5, 2017

Thailand Science Park, Pathum Thani, Thailand

ANSCSE 21

The 21^{st} International Annual Symposium on Computational Science and Engineering

01100100011
01100100011
0111010011
0001
01100100011
00100011
01100100011
0101
1010
1011101001
01100100011
1110100010010
110011010

Program & Abstract

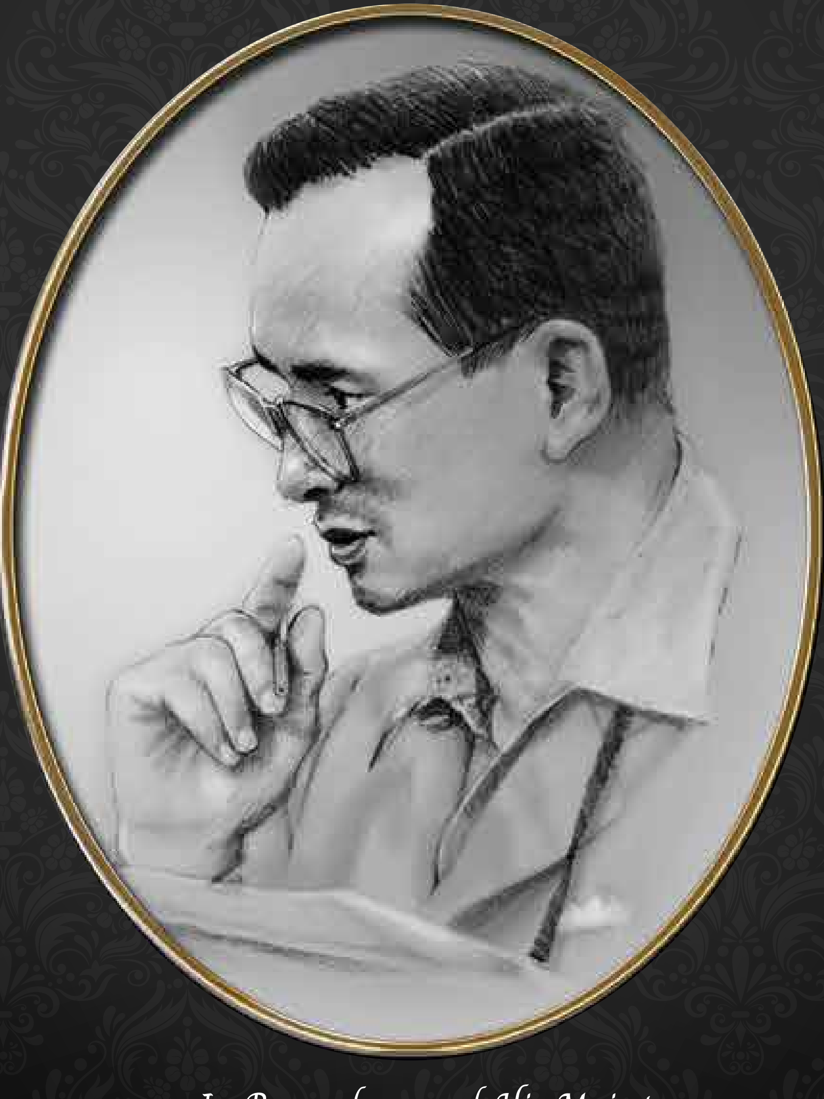

In Remembrance of His Majesty

King Bhumibol Adulyadej

1927–2016

เทิด ธ พระพ่อหลวง
เสด็จสรวง ล่วงลาแล้ว
น้อมส่ง องค์พ่อแก้ว
สถิตแล้ว สุราลัย
เสียงโศก ดั่งโลกสิ้น
พระภูมินทร์ ธ ดวงใจ
เสด็จสู่ สวรรคาลัย
ราษฎร์ร่ำไห้ ไปทั่วแดน

ประพันธ์โดย ธนภัทร ศรีโมรา

* * *

ด้วยเกล้าด้วยกระหม่อม ขอเดชะ
ข้าพระพุทธเจ้า คณะผู้จัดงานประชุมวิชาการ
ANSCSE21

WELCOME MESSAGE

Dr. Wannee Chinsirikul

Executive Director,
National Nanotechnology Center (NANOTEC),
National Science and Technology
Development Agency (NSTDA), Thailand

Welcome to Thailand!

It is my great pleasure to welcome you to the 21st International Annual Symposium on Computational Science and Engineering (ANSCSE21). ANSCSE serves as an annual international forum for computational scientists and engineers and is one of the largest gathering of Thai computational research community.

In late 2016, the Thai government promoted “Thailand 4.0” as the new economic model aimed at pulling Thailand out of the middle-income trap, and push the country in the high-income range. The model focuses on creating a Value-based Economy supported by three elements: High Income Nation, Inclusive Society, and Sustainable growth and development. Science, technology, and innovation will play a key role in driving the success of this model.

As you are aware, digital innovation is one of the fastest growing technology and business in this decade and one which has considerable impact on the world economy. For this reason, it is without a doubt that ANSCSE21 theme of “Computational Science and Big Data for Sustainable and Innovative Future” ties well with the emerging digital era and direction of Thailand 4.0 model. In so doing, this symposium will provide opportunities for researchers and scholars from private sectors, academia, and research institutes in the field of computational science and engineering to exchange technical information, stimulate ideas and foster collaboration for driving sustainable innovation and economy.

Again, Welcome and best wishes for a successful ANSCSE21, and thank you for your participation.

Dr. Wannee Chinsirikul

Executive Director of National Nanotechnology Center (NANOTEC)
National Science and Technology Development Agency (NSTDA), Thailand

WELCOME MESSAGE

Asst. Prof. Dr. Putchong Uthayopas

Acting President of Computational Science and Engineering Association (CSEA), Thailand

Dear Friends and Colleagues,

It is a great pleasure and an honor to extend to you a warm invitation to attend the ANSCSE21, the 21st International Annual Symposium on Computational Science and Engineering, to be held August 2-5, 2017. This year the symposium is organized by Nanoscale Simulation Laboratory of the National Nanotechnology Center (NANOTEC), Computational Science and Engineering Association (CSEA) and National e-Science Infrastructure Consortium. ANSCSE21 has always been one of the greatest gatherings of computational scientists, computer science, and engineering researchers. After 21 years, we have seen many signs of progress and so many interesting researches being conducted in this area. In this digital age, rapid progress has been driven by artificial intelligence, big data, and much higher computing power enabled by new technology such as GPU, FPGA. Thus, the vital role that computational science plays in human social development becomes clearer and clearer every day.

One of the great spirits of ANSCSE is the live discussion among fellow international researchers. After a few days of intense discussion on our works, the organizer kindly arranges an excursion to the ancient city of Ayutthaya, the UNESCO world heritage site. I am certain that everyone will enjoy the talk along with the rich history and the beauty of Ayutthaya.

Finally, I look forward to meeting all of you. Thank you for sharing your thoughts and ideas in ANSCSE21.

Best Wishes,

Asst.Prof.Dr. Putchong Uthayopas
Kasetsart University
Acting President of Computational Science and Engineering Association (Thailand)

WELCOME MESSAGE

Dr. Supawadee Namuangruk

Head of Nanoscale Simulation Laboratory,
National Nanotechnology Center (NANOTEC),
National Science and Technology Develop
Agency (NSTDA), Thailand

Dear Colleagues,

On behalf of the organizing committee, I am honored and delighted to welcome you to the 21st International Annual Symposium on Computational Science and Engineering (ANSCSE21). It is a great honor for NANOTEC to be the host of ANSCSE21. Our co-hosts are Computer Science and Engineering Association, National e-Science Infrastructure Consortium and Department of Computer Science, Kasetsart University

Over twenty years, ANSCSE has a long history of gathering researchers who are in the field of computational science and engineering to cross-fertilize ideas and to strengthen both local and international networks. The theme of this year is "Computational Science and Big Data for Sustainable and Innovative Future". Under this theme, ANSCSE21 covers various disciplines of computational science and engineering including fields of Biology, Chemistry, Physics, Fluid Dynamics, Solid Mechanics, High Performance Computing, Cloud Computing, and Computer Science and Engineering.

There are 5 plenary talks, 38 invited talks and about 84 oral and poster presentations. This year, the scientific programs are accompanied with the Big Data Analytics workshop. This conference aims to provide an exciting venue for scientists to present and exchange ideas, as well as to renew existing collaborations and developing new ones. ANSCSE21 also offers the great opportunity for academics and industrial people to meet and exchange ideas and information.

As a conference chair of ANSCSE21, I would like to express my appreciation to the steering committee, the honorary chairs, the international advisory board, the scientific committee chair, the program chairs, the scientific committee, the reviewers, our sponsors and the organizing team. Last but not the least; recognition should also go to the local organizing committee members who have worked extremely hard in planning and organizing the technical programs and supporting social arrangements.

Finally, ANSCSE21 truly serves the venue for networking and knowledge sharing as a consequence of the comprehensive presentations as well as high-level plenary and panel sessions. We hope you will take the utmost advantage of this event to explore new innovation.

Sincerely yours,

Dr. Supawadee Namuangruk
Conference Chair,
Nanoscale Simulation Laboratory
National Nanotechnology Center (NANOTEC)
National Science and Technology Development Agency (NSTDA), Thailand

PLENARY LECTURES

PL-1: Utilizing IBM Power Systems to Optimize Genomic Applications Compute

Denise Ruffner

Business Development Executive,
Worldwide Genomic Solutions,
IBM, USA

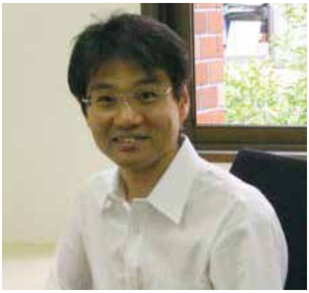

PL-2: Structure and Catalytic Activity of Nanocluster Catalysts

Prof. Dr. Masahiro Ehara

Institute for Molecular Science, Japan
SOKENDAI, the Graduate University for Advanced Studies, Japan
Element Strategy Initiative for Catalysts and Batteries, Kyoto University, Japan

PL-3: Extreme-scale Atomistic Simulations of Nanomaterials

Prof. Dr. Aiichiro Nakano

University of Southern California,
Los Angeles, CA, USA

PL-4: Chemistry and Our Common Future

Dr. Ito Chao

Institute of Chemistry, Academia Sinica,
Taipei, Taiwan

PL-5: Designing a Massive Coil to Shield JUNO from the Earth's Magnetic Field

Prof. Dr. Sukit Limpijumnong

Suranaree University of Technology,
Thailand

INVITED SPEAKERS

Computational Physics, Fluid Dynamics and Solid Mechanics

PFD-I-1	Arthit	Vongachariya	Siam Cement Chemicals	Thailand
PFD-I-2	Somboon	Otarawanna	MTEC, NSTDA	Thailand
PFD-I-3	Siegfried	Fritzsche	University of Leipzig	Germany
PFD-I-4	Sittipong	Komin	Ubon Ratchathani University	Thailand
PFD-I-5	Jessada	Chureemart	Mahasarakham University	Thailand
PFD-I-6	Phanwadee	Chureemart	Mahasarakham University	Thailand
PFD-I-7	Norraphat	Srimanobhas	Chulalongkorn University	Thailand
PFD-I-8	Teparksorn	Pengpan	Prince of Songkla University	Thailand
PFD-I-9	Komsilp	Kotmool	Mahidol Wittayanusorn School	Thailand
PFD-I-10	Piti	Ongmongkolkul	Mahidol University International College	Thailand

Computational Chemistry

CHE-I-1	Tetsuya	Taketsugu	Hokkaido University	Japan
CHE-I-2	Panida	Surawatanawong	Mahidol University	Thailand
CHE-I-3	Minh Tho	Nguyen	KU Leuven	Belgium
CHE-I-4	Jun-ya	Hasegawa	Hokkaido University	Japan
CHE-I-5	Kaito	Takahashi	Academia Sinica	Taiwan
CHE-I-6	Jyh-Chiang	Jiang	National Taiwan University of Science and Technology	Taiwan
CHE-I-7	Arkira	Nakayama	Hokkaido University	Japan
CHE-I-8	Chao-Ping	Hsu	Academia Sinica	Taiwan
CHE-I-9	Vinich	Promarak	Vidyasirimedhi Institute of Science and Technology	Thailand
CHE-I-10	Lam	Hunynh	Vietnam National University	Vietnam
CHE-I-11	Tim	Kowalczyk	Western Washington University	USA
CHE-I-12	Min	Gao	Hokkaido University	Japan
CHE-I-13	Manussada	Ratanasak	Hokkaido University	Japan

Computational Biology and Bioinformatics

BIO-I-1	Ras	Pandey	The University of Southern Mississippi	USA
BIO-I-2	Norio	Yoshida	Kyushu University	Japan
BIO-I-3	Hisashi	Okumura	Institute for Molecular Science	Japan
BIO-I-4	Kiattawee	Choowongkomon	Kasetsart University	Thailand
BIO-I-5	Jen-Shiang	Yu	National Chiao Tung University	Taiwan
BIO-I-6	Satoru	Itoh	Institute for Molecular Science	Japan
BIO-I-7	Shinji	Saito	Institute for Molecular Science	Japan
BIO-I-8	Vannajan	Lee	University of Malaya	Malaysia
BIO-I-9	Peter	Wolschann	University of Vienna	Austria
BIO-I-10	Varomyalin	Tipmanee	Prince of Songkla University	Thailand
BIO-I-11	Syed Sikander	Azam	Quaid-i-Azam University Islamabad	Pakistan
BIO-I-12	Sissades	Tongsima	BIOTEC, NSTDA	Thailand

High Performance Computing, Cloud Computing, Computer Science and Engineering

CSE-I-1	Zong-Yao	Chen	ACER	Taiwan
CSE-I-2	Ekasit	Kijsipongse	NECTEC, NSTDA	Thailand
CSE-I-3	Waranyu	Wongseree	King Mongkut University of Technology North Bangkok	Thailand
CSE-I-4	Chantana	Chantrapornchai	Kasetsart University	Thailand

COMMITTEE

Steering Committee Chair

Asst. Prof. Dr. Putchong Uthayopas
Kasetsart University and Acting President of Computational Science and Engineering Association (CSEA), Thailand

Assoc. Prof. Dr. Vudhichai Parasuk
Chulalongkorn University and President-elect of Computational Science and Engineering Association (CSEA), Thailand

Prof. Dr. Supa Hannongbua
Dean of Faculty of Science, Kasetsart University, Thailand

Honorary Chair

Dr. Wannee Chinsirikul
Executive Director, National Nanotechnology Center (NANOTEC), National Science and Technology Development Agency (NSTDA), Thailand

Dr. Uracha Ruktanonchai
Deputy Executive Director Research & Development, National Nanotechnology Center (NANOTEC), National Science and Technology Development Agency (NSTDA), Thailand

Dr. Kajornsak Faungnawakij
Director of Nanomaterials and Nanosystems Engineering Research Unit, National Nanotechnology Center (NANOTEC), National Science and Technology Development Agency (NSTDA), Thailand

Conference Organizers

National Nanotechnology Center (NANOTEC), National Science and Technology Development Agency (NSTDA), Thailand

Computational Science and Engineering Association (CSEA), Thailand

National E-Science Infrastructure Consortium, Thailand

Department of Computer Science, Faculty of Science, Kasetsart University, Thailand

Conference Organizing Committee Chair

Dr. Supawadee Namuangruk
Head of Nanoscale Simulation Laboratory, National Nanotechnology Center (NANOTEC), National Science and Technology Development Agency (NSTDA), Thailand

International Advisory Board

Prof. Dr. Peter Wolschann
University of Vienna, Austria

Prof. Dr. Siegfried Fritzsche
University of Leipzig, Germany

Prof. Dr. Masahiro Ehara
Institute for Molecular Science, Japan

Prof. Dr. Tetsuya Taketsugu
Hokkaido University, Japan

Dr. Ito Chao
Academia Sinica, Taiwan

Prof. Dr. Aiichiro Nakano
University of Southern California, USA

Scientific Committee Chair

Assoc. Prof. Dr. Siriporn Jungsuttiwong
Ubon Ratchathani University, Thailand

Technical Program Committee Chair

Computational Chemistry Chair:

Assoc. Prof. Dr. Pornpan Pungpo
Ubon Ratchathani University, Thailand

Computational Physics Chair:

Assoc. Prof. Dr. Anucha Yangthaisong
Ubon Ratchathani University, Thailand

Asst. Prof. Dr. Worasak Sukkabot
Ubon Ratchathani University, Thailand

Computational Biology and Bioinformatics Chair:

Asst. Prof. Dr. Thanyada Rungrotmongkol
Chulalongkorn University, Thailand

Computational Fluid Dynamics and Solid Mechanics Chair:

Assoc. Prof. Dr. Vejapong Juttijudata
Kasetsart University, Thailand

High Performance Computing and Cloud Computing Chair:

Asst. Prof. Dr. Putchong Uthayopas
Kasetsart University, Thailand

Computer Science and Engineering Chair:

Assoc. Prof. Dr. Vara Varavithya
King Mongkut's University of Technology North Bangkok, Thailand

Dr. Supakit Prueksaaroon
Thammasat University, Thailand

International Scientific committee

Prof. Dr. Shinji Saito
Institute for Molecular Science, Japan

Assoc. Prof. Dr. Hisashi Okumura
Institute for Molecular Science, Japan

Asst. Prof. Dr. Satoru Itoh
Institute for Molecular Science, Japan

Prof. Dr. Jun-ya Hasegawa
Hokkaido University, Japan

Assoc. Prof. Dr. Akira Nakayama
Hokkaido University, Japan

Asst. Prof. Dr. Min Gao
Hokkaido University, Japan

Dr. Manussada Ratanasak
Hokkaido University, Japan

Assoc. Prof. Dr. Norio Yoshida
Kyushu University, Japan

Assoc. Prof. Dr. Vannajan Sanghiran Lee
University of Malaya, Malaysia

Prof. Dr. Jen-Shiang K. Yu
National Chiao Tung University, Taiwan

Dr. Cherri Chao-Ping Hsu
Academia Sinica, Taiwan

Dr. Kaito Takahashi
Academia Sinica, Taiwan

Prof. Dr. Jyh-Chiang Jiang
National Taiwan University of Science and Technology, Taiwan

Prof. Dr. Lam K. Huynh
Vietnam National University, Vietnam

Prof. Dr. Ras B. Pandey
The University of Southern Mississippi, USA

Scientific committee

Prof. Dr. Supa Hannongbua
Kasetsart University, Thailand

Dr. Chalee Vorakulpipat
National Electronics and Computer Technology Center (NECTEC), NSTDA, Thailand

Asst. Prof. Dr. Duangkamol Tantanak
King Mongkut's Institute of Technology Ladkrabang, Thailand

Asst. Prof. Dr. Nawee Kungwan
Chiang Mai University, Thailand

Asst. Prof. Dr. Bundet Boekfa
Kasetsart University, Thailand

Asst. Prof. Dr. Jakkapan Sirijaraensre
Kasetsart University, Thailand

Asst. Prof. Dr. Patchreenart Saparpakorn
Kasetsart University, Thailand

Asst. Prof. Dr. Songwut Suramitr
Kasetsart University, Thailand

Asst. Prof. Dr. Chan Inntam
Ubon Ratchathani University, Thailand

Dr. Piti Treesukul
Kasetsart University, Thailand

Asst. Prof. Dr. Supaporn Dokmaisrijan
Walailak University, Thailand

Dr. Pornthip Boonsri
Srinakharinwirot University, Thailand

Dr. Potjaman Poolmee
Kasetsart University Kamphaengsaen Campus, Thailand

Dr. Malinee Promkatkaew
Kasetsart University Si Racha Campus, Thailand

Assoc. Prof. Dr. Duangkamol Gleeson
King Mongkut's Institute of technology Ladkrabang, Thailand

Assoc. Prof. Dr. PhonThep Somphonphisut
Chulalongkorn University, Thailand

Asst. Prof. Dr. Panida Kongsawadworakul
Mahidol University, Thailand

Asst. Prof. Dr. Khatcharin Siriwong
Khon Kaen University, Thailand

Asst. Prof. Dr. Somsak Pianwanit
Chulalongkorn University, Thailand

Asst. Prof. Dr. Nadtanet Nunthaboot
Mahasarakham University, Thailand

Dr. Varomyalin Tipmanee
Prince of Songkla University, Thailand

Assoc. Prof. Dr. Udomsilp Pinsook
Chulalongkorn University, Thailand

Dr.Sittipong Komin
Ubon Ratchathani University, Thailand

Asst. Prof. Dr. Kanchana Savalertporn
Ubon Ratchathani University, Thailand

Assoc. Prof. Dr. Teparksorn Pengpan
Prince of Songkla University, Thailand

Dr. Pruet Kalasuwan
Prince of Songkla University, Thailand

Dr. Jessada Chureemart
Mahasarakham University, Thailand

Dr. Sujin Suwanna
Mahidol University, Thailand

Organizing committee

Dr. Supawadee Namuangruk
National Nanotechnology Center (NANOTEC), NSTDA, Thailand

Dr. Chalee Vorakulpipat
National Electronics and Computer Technology Center (NECTEC), NSTDA, Thailand

Asst. Prof. Nawee Kungwan
Chiang Mai University, Thailand

Asst. Prof. Phornphimon Maitarad
Shanghai University, China

Tortrakul Poolsopha
National Nanotechnology Center (NANOTEC), NSTDA, Thailand

Sasinee Watcharaput
National Nanotechnology Center (NANOTEC), NSTDA, Thailand

Benyapa Suwan
National Nanotechnology Center (NANOTEC), NSTDA, Thailand

Wipaporn Ekamornthanakul
National Nanotechnology Center (NANOTEC), NSTDA, Thailand

Channarong Prommakan
National Nanotechnology Center (NANOTEC), NSTDA, Thailand

Sukunya Phramkhao
National Nanotechnology Center (NANOTEC), NSTDA, Thailand

Chayuda Karaphol
National Nanotechnology Center (NANOTEC), NSTDA, Thailand

Yaninee Khantapat
National Nanotechnology Center (NANOTEC), NSTDA, Thailand

Pongsit Rattanakonvit
National Nanotechnology Center (NANOTEC), NSTDA, Thailand

Jariyamas Amornprapaipis
National Nanotechnology Center (NANOTEC), NSTDA, Thailand

Amornpan Koysungnoen
National Nanotechnology Center (NANOTEC), NSTDA, Thailand

Pannee Santiveeraphan
National Nanotechnology Center (NANOTEC), NSTDA, Thailand

Worawut Khoonkrong
National Nanotechnology Center (NANOTEC), NSTDA, Thailand

Dr. Chompoonut Rungnim
National Nanotechnology Center (NANOTEC), NSTDA, Thailand

Dr. Pussana Hirunsit
National Nanotechnology Center (NANOTEC), NSTDA, Thailand

Dr. Manaschai Kunaseth
National Nanotechnology Center (NANOTEC), NSTDA, Thailand

Dr. Monrudee Liangruksa
National Nanotechnology Center (NANOTEC), NSTDA, Thailand

Dr. Anchalee Junkaew
National Nanotechnology Center (NANOTEC), NSTDA, Thailand

Jittima Meeprasert
National Nanotechnology Center (NANOTEC), NSTDA, Thailand

Chirawat Chitpakdee
National Nanotechnology Center (NANOTEC), NSTDA, Thailand

GENERAL INFORMATION

Registration Desk

Registration desk is located on the 3rd floor in front of the auditorium of the convention center

Registration Hours

Thursday, August 3rd	8.00 AM – 5.00 PM
Friday, August 4th	8.00 AM – 12.00 PM

Exhibition

The Exhibition booths are located on the 3rd floor in front of the auditorium of the convention center. The hours are from 8.00 AM – 5.00 PM.

Poster Stand Location

The poster stands are located inside the Grand Hall on the 1st floor of the convention center

Conference rooms

The conference rooms are the auditorium and room cc305, cc306, cc307 and cc308 which are located on the 3rd floor of the convention center

Internet access

Two internet access codes (1 day per code) are inserted in a participant badge.

Lunch

Lunch will be served at the Event Square located on the 2nd floor in front of the Science Café.

Lost and Found

The lost and found counter is located at the registration desk on the 3rd floor of the convention center

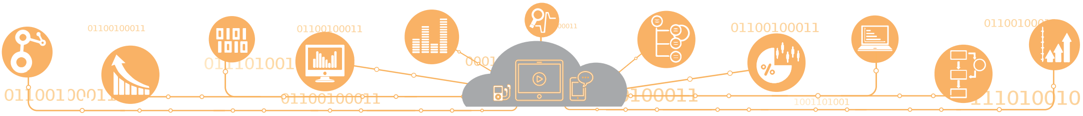

AUDITORIUM, GRAND HALL, AND CONFERENCE ROOM FLOOR PLAN

First Floor

Poster stand and Welcome Dinner Party at Grand Hall

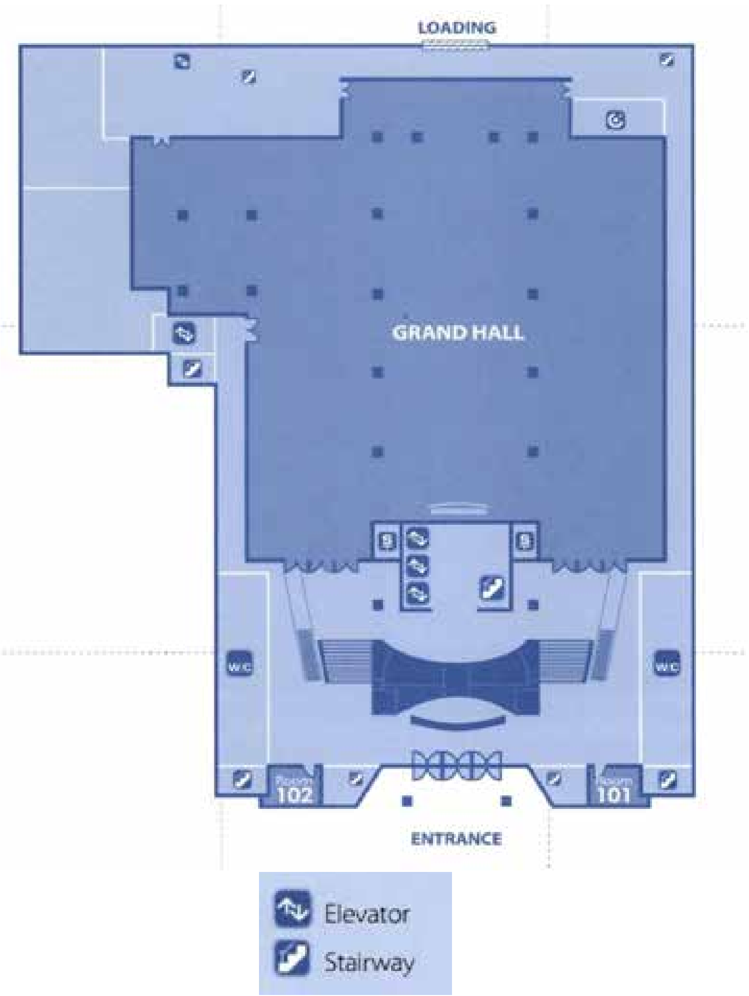
LOADING
GRAND HALL
WC
WC
Room 102
Room 101
ENTRANCE
Elevator
Stairway

Second Floor

Lunch at Event Square

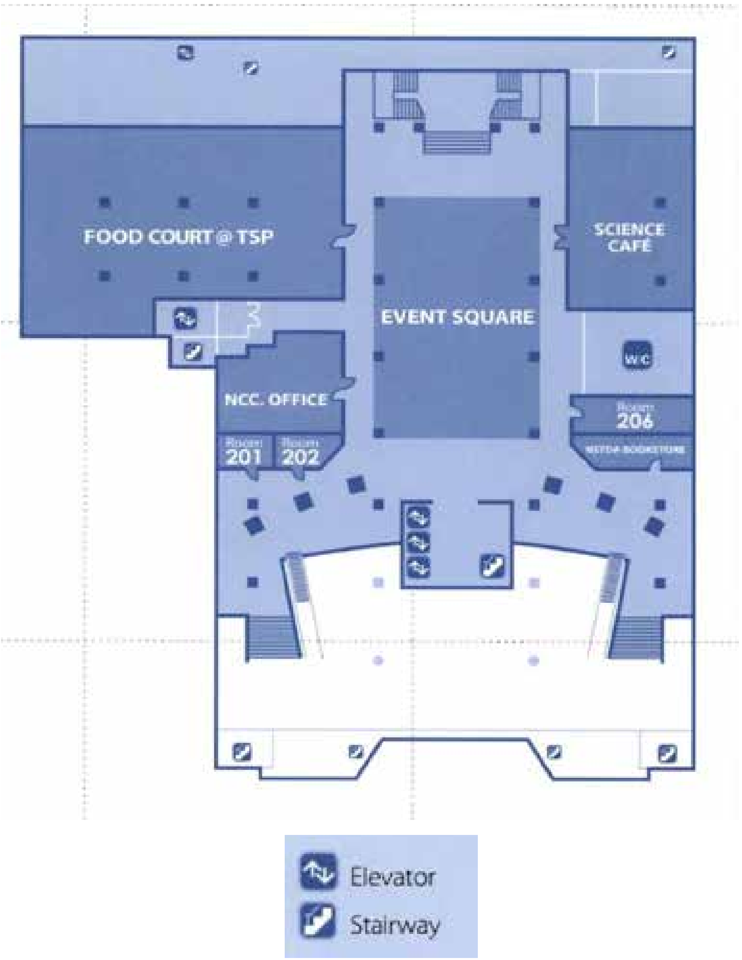
FOOD COURT @ TSP
SCIENCE CAFÉ
EVENT SQUARE
W C
NCC. OFFICE
Room 206
Room 201
Room 202
Elevator
Stairway

Third Floor

Auditorium and Conference rooms (Room 305, 306, 307 and 308)

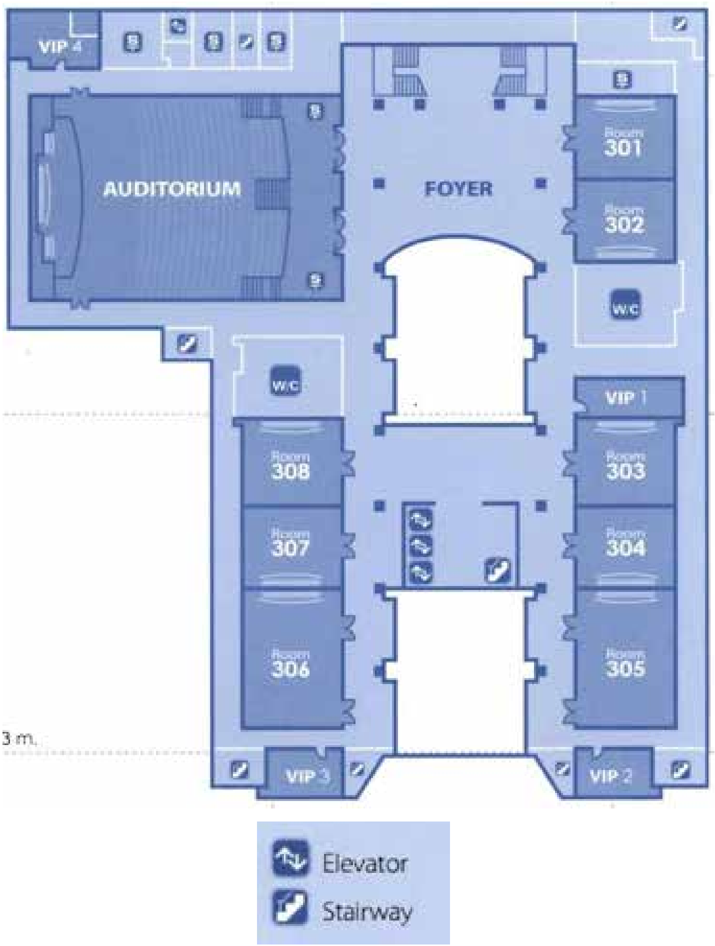
VIP 4
AUDITORIUM
FOYER
Room 301
Room 302
W.C
W.C
VIP 1
Room 308
Room 303
Room 307
Room 304
Room 306
Room 305
3 m.
VIP 3
VIP 2
Elevator
Stairway

INFORMATION FOR PRESENTERS & AUTHORS

Session Codes

PL	Plenary Lecture
PFD	Computational Physics, Fluid Dynamics and Solid Mechanics
CHE	Computational Chemistry
BIO	Computational Biology and Bioinformatics
CSE	High Performance Computing, Cloud Computing, Computer Science and Engineering

Presentation Codes

Presentation codes are assigned for each presentation in form of

PL-00	for **Plenary** lectures
AAA-**I**-00	for **Invited** speakers
AAA-**O**-00	for **Oral** presentation
AAA-**P**-00	for **Poster** presentation

AAA is the session codes shown above.

00 is identification number for each presented title.

Oral Presentation

Oral presentation room will be equipped with the following items:

- A computer equipped with Microsoft Office
- A LCD Projector

Presenters can upload their presentation file to the computer in the **room 301** located on the 3rd floor of the convention center from 8.00 am onwards.

The time slot for i**nvited speaker** is **25 minutes** including discussion.

The time slot for **oral presentation** is **20 minutes** including discussion (17 minutes for presentation and 3 minutes for discussion).

Poster Presentation

The poster session is on Thursday August 3rd, 2017 at t**he Grand Hall located on 1st** floor of the convention center.

Your poster code can be seen in this abstract book and is put on the poster board in the Grand Hall.

Mounting materials will be provided in the poster session area.

The presenters are kindly requested to mount up the poster on Thursday August 3rd during 8.00 AM – 4.45 PM. and remove by 7.00 PM.

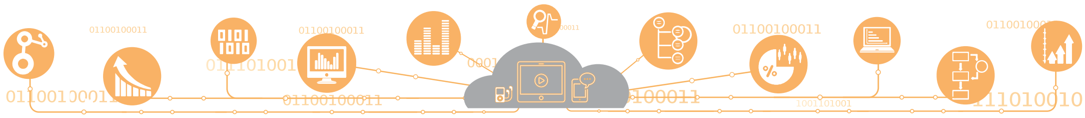

PROGRAM

OVERALL PROGRAM
Thursday, 3 August 2017

Time				Location
08.00 - 09.00	Registration			3rd Floor
09.00 - 09.35	Opening Ceremony			Auditorium on the 3rd Floor
09.35 - 09.50	Group Photo			
09.50 - 10.35	**Plenary Lecture (I) Denise Ruffner**			
	Title: Utilizing IBM Power Systems to Optimize Genomic Applications Compute			
10.35 - 10.50	Coffee Break			3rd Floor
10.50 - 12.00	Oral Presentation (4 parallel sessions)			
	Room: CC307	Room: CC305	Room: CC306	Room: CC308
	Computational Physics, Fluid Dynamics and Solid Mechanics	Computational Chemistry	Computational Biology and Bioinformatics	High Performance Computing, Cloud Computing, Computer Science and Engineering
	Session: PFD1	**Session: CHE1**	**Session: BIO1**	**Session: CSE1**
	PFD-I-1 10.50-11.15	CHE-I-1 10.50-11.15	BIO-I-1 10.50-11.15	CSE-I-1 10.50-11.15
	PFD-I-2 11.15-11.40	CHE-I-2 11.15-11.40	BIO-I-2 11.15-11.40	CSE-O-1 11.15-11.35
	PFD-O-1 11.40-12.00	CHE-I-3 11.40-12.05	BIO-O-1 11.40-12.00	CSE-O-2 11.35-11.55
12.00 - 13.00	Lunch			2nd Floor
13.00 - 13.45	**Plenary Lecture (II) Prof. Dr. Masahiro Ehara**			Auditorium
	Title: Structure and Catalytic Activity of Nanocluster Catalysts			
13.45 - 15.00	Oral Presentation (4 parallel sessions)			
	Room: CC307	Room: CC305	Room: CC306	Room: CC308
	Session: PFD2	**Session: CHE2**	**Session: BIO2**	**Session: CSE2**
	PFD-I-3 13.45-14.10	CHE-I-4 13.45-14.10	BIO-I-3 13.45-14.10	CSE-I-2 13.45-14.10
	PFD-I-4 14.10-14.35	CHE-I-5 14.10-14.35	BIO-I-4 14.10-14.35	CSE-O-3 14.10 -14.30
	PFD-O-2 14.35-14.55	CHE-O-1 14.35-14.55	BIO-O-2 14.35-14.55	CSE-O-4 14.30 -14.50
15.00 - 15.15	Coffee Break			3rd Floor
15.15 - 16.45	Room: CC307	Room: CC305	Room: CC306	Room: CC308
	Session: PFD3	**Session: CHE3**	**Session: BIO3**	**Session: CSE3**
	PFD-I-5 15.15 -15.40	CHE-I-6 15.15 -15.40	BIO-I-5 15.15 -15.40	CSE-I-3 15.15 -15.40
	PFD-I-6 15.40-16.05	CHE-I-7 15.40-16.05	BIO-I-6 15.40-16.05	CSE-O-5 15.40 -16.00
	PFD-O-3 16.05 -16.25	CHE-O-2 16.05 -16.25	BIO-O-3 16.05 -16.25	CSE-O-6 16.00 -16.20
	PFD-O-4 16.25 -16.45	CHE-O-3 16.25 -16.45	BIO-O-4 16.25 -16.45	CSE-O-7 16.20 -16.40
17.00-18.30	Poster Session			Grand Hall
18.30-19.30	Welcome Party			Grand Hall

Friday, 4 August 2017

Time				**Location**
08.00 - 09.00	Registration			3rd floor
09.00 - 09.45	**Plenary Lecture (III) Prof. Dr. Aiichiro Nakano**			Auditorium on the 3rd Floor
	Title: Extreme-Scale Atomistic Simulations of Nanomaterials			
09.45 - 10.30	**Plenary Lecture (IV) Dr. Ito Chao**			
	Title: Chemistry and Our Common Future			
10.30 - 10.45	Coffee Break			3rd Floor
10.45 - 12.00	Oral Presentation (4 parallel sessions**)**			
	Room: CC307	Room: CC305	Room: CC306	Room: CC308
	Computational Physics, Fluid Dynamics and Solid Mechanics	Computational Chemistry	Computational Biology and Bioinformatics	High Performance Computing, Cloud Computing, Computer Science and Engineering
	Session: PFD4	**Session: CHE4**	**Session: BIO4**	**Session: CSE4**
	PFD-I-7 10.45-11.10	CHE-I-8 10.45-11.10	BIO-I-7 10.45-11.10	CSE-I-4 10.45-11.10
	PFD-I-8 11.10-11.35	CHE-I-9 11.10-11.35	BIO-I-8 11.10-11.35	CSE-O-8 11.10 -11.30
	PFD-O-5 11.35-11.55	CHE-O-4 11.35-11.55	BIO-O-5 11.35-11.55	CSE-O-9 11..30 -11.50
12.00 - 13.00	Lunch			2nd Floor
13.00 - 13.45	**Plenary Lecture (V) Prof. Dr. Sukit Limpijumnong**			Auditorium
	Title: Designing a Massive Coil to Shield JUNO from the Earth's Magnetic Field			
13.50 - 15.00	Oral Presentation (4 parallel sessions)			
	Room: CC307	Room: CC305	Room: CC306	Room: CC308
	Session: PFD5	**Session: CHE5**	**Session: BIO5**	
	PFD-I-9 13.50-14.15	CHE-I-10 13.50-14.15	BIO-I-9 13.50-14.15	Special session
	PFD-O-6 14.15-14.35	CHE-I-11 14.15-14.40	BIO-I-10 14.15-14.40	
	PFD-O-7 14.35-14.55	CHE-O-5 14.40-15.00	BIO-O-6 14.40-15.00	
14.55 - 15.15	Coffee Break			3rd Floor
15.15 - 16.45	Room: CC307	Room: CC305	Room: CC306	
	Session: PFD6	**Session: CHE6**	**Session: BIO6**	
	PFD-I-10 15.15-15.40	CHE-I-12 15.15-15.40	BIO-I-11 15.15-15.40	
	PFD-O-8 15.40-16.00	CHE-I-13 15.40-16.05	BIO-I-12 15.40-16.05	
	PFD-O-9 16.00-16.20	CHE-O-6 16.05 -16.25	BIO-O-7 16.05 -16.25	
	PFD-O-10 16.20-16.40	CHE-O-7 16.25 -16.45		

Plenary Lecture

Date Aug 3, 2017 **Room# Auditorium 3rd floor**

Chair: Asst. Prof. Putchong Uthayopas

Time	Code	Presenter	Title
09:50-10:35	PL-1	*Denise Ruffner* IBM, USA	Utilizing IBM Power Systems to Optimize Genomic Applications Compute

Chair: Assoc. Prof. Siriporn Jungsuttiwong

Time	Code	Presenter	Title
13:00-13:45	PL-2	*Prof. Dr. Masahiro Ehara* Institute for Molecular Science, Japan	Structure and Catalytic Activity of Nanocluster Catalysts

Plenary Lecture

Date Aug 4, 2017 **Room# Auditorium 3rd floor**

Chair: Dr. Manaschai Kunaseth

Time	Code	Presenter	Title
09:00-09:45	PL-3	*Prof. Dr. Aiichiro Nakano* University of Southern California, USA	Extreme-scale Atomistic Simulations of Nanomaterials
09:45-10:30	PL-4	*Dr. Ito Chao* Academia Sinica, Taiwan	Chemistry and Our Common Future

Chair: Dr. Anchalee Junkaew

Time	Code	Presenter	Title
13:00-13:45	PL-5	*Prof. Dr. Sukit Limpijumnong* Suranaree University of Technology, Thailand	Designing a Massive Coil to Shield JUNO from the Earth's Magnetic Field

Aug 3, 2017
Computational Physics, Fluid Dynamics and Solid Mechanics

Session PFD1 **Time 10:50-12:00** **Room# cc307**

Chair: Asst. Prof. Warasak Sukkabot

Time	Code	Presenter	Title
10:50-11:15	PFD-I-1	*Arthit Vongachariya* Siam Cement Chemicals, Thailand	Advanced Process Modelling: A Key to Accelerate Development of Petrochemical Products
11:15-11:40	PFD-I-2	*Somboon Otarawanna* MTEC, NSTDA, Thailand	Finite Element Analysis for Fatigue Life Prediction of Alloy Wheels under Radial Loading
11:40-12:00	PFD-O-1	*Krittidej Chanthawara* Ubon Ratchathani Rajabhat University, Thailand	A Variable Multiquadric Shape Parameter in the Dual Reciprocity Boundary Element Method for Convection-Diffusion Problems

Session PFD2 **Time 13:45-15:00** **Room# cc307**

Chair: Assoc. Prof. Anucha Yangthaisong

Time	Code	Presenter	Title
13:45-14:10	PFD-I-3	*Siegfried Fritzsche* University of Leipzig, Germany	The Role of Lattice Flexibility of ZIF - Materials Used for Gas Separation
14:10-14:35	PFD -I-4	*Sittipong Komin* Ubon Ratchathani University, Thailand	Variational Optimization of Capping Atom Potentials for QM/MM Method
14:35-14:55	PFD-O-2	*Churtpong Choodet* Khon Kaen University, Thailand	Insight into the Interaction of 8-oxo-dG and DNA Aptamer by Molecular Dynamics Simulation for the Application in Biosonsor

Session PFD3 **Time 15:15-16:45** **Room# cc307**

Chair: Assoc. Prof. Teparksorn Pengpan

Time	Code	Presenter	Title
15:15-15:40	PFD-I-5	*Jessada Chureemart* Mahasarakham University, Thailand	Hybrid Design for Advanced Magnetic Recording Media: Combining Exchange Coupled Composite Media with Coupled Granular Continuous Media
15:40-16:05	PFD-I-6	*Phanwadee Chureemart* Mahasarakham University, Thailand	Spin Transport in Read Elements via Spin Accumulation Model
16:05-16:25	PFD-O-3	*Noppamas Yolai* Khon Kaen University, Thailand	Effect of Size, Shape and Surface Charge on Cellular Uptake of Gold Nanoparticles
16:25-16:45	PFD-O-4	*Rutchapon Hunkao* Mahidol University, Thailand	Empirical Tight-Binding Calculation of Electronic Structure of Mn-Doped ZnS Nanocrystals

Aug 3, 2017
Computational Chemistry

Session CHE1 **Time 10:50-12:00** **Room# cc305**

Chair: Assoc. Prof. Akira Nakayama

Time	Code	Presenter	Title
10:50-11:15	CHE-I-1	*Tetsuya Taketsugu* Hokkaido University, Japan	Computational Approach to Design of Non-Platinum Catalyst for Oxygen Reduction Reaction: Boron Nitride with Gold
11:15-11:40	CHE-I-2	*Panida Surawatanawong* Mahidol University, Thailand	Mechanisms of C-O Bond Activation and Oxygen Activation: Density Functional Study
11:40-12:05	CHE-I-3	*Minh Tho Nguyen* KU Leuven, Belgium	Recent Advances in the Determination of Structure and Bonding of Elemental Clusters

Session CHE2 **Time 13:45-15:00** **Room# cc305**

Chair: Prof. Lam K. Huynh

Time	Code	Presenter	Title
13:45-14:10	CHE-I-4	*Jun-ya Hasegawa* Hokkaido University, Japan	Theoretical Study of Frustrated Lewis Pair for Activation of Stable Chemical Bonds
14:10-14:35	CHE-I-5	*Kaito Takahashi* Academia Sinica, Taiwan	Substitution Effect in the Reaction Rate of Criegee Intermediates with Water Vapor
14:35-14:55	CHE-O-1	*Suwit Suthirakun* Suranaree University of Technology, Thailand	First-Principles Study of Sn-Doped V_2O_5 as Cathode Material of Li-ion Batteries

Session CHE3 **Time 15:15-16:45** **Room# cc305**

Chair: Asst. Prof. Tim Kowalczyk

Time	Code	Presenter	Title
15:15-15:40	CHE-I-6	*Jyh-Chiang Jiang* National Taiwan University of Science and Technology, Taiwan	Theoretical Approaches for Improving Overall Performances of Dye-Sensitized Solar Cells
15:40-16:05	CHE-I-7	*Arkira Nakayama* Hokkaido University, Japan	Catalytic Reactions at the Liquid/Metal-Oxide Interface: Role of the Acid-Base Sites
16:05-16:25	CHE-O-2	*Yuwanda Injongkol* Kasetsart University, Thailand	Nitrous Oxide Decomposition over Cu-BTC Metal-Organic Frameworks: A DFT Study
16:25-16:45	CHE-O-3	*Panchanit Piyakeeratikul* Vidyasirimedhi Institute of Science and Technology, Thailand	Influence of Metal Species in Porphyrin-Base Metal-Organic Frameworks on Carbon Dioxide Capture

Aug 3, 2017
Computational Biology and Bioinformatics

Session BIO1 **Time 10:50-12:00** **Room# cc306**

Chair: Asst. Prof. Thanyada Rungrotmongkol

Time	Code	Presenter	Title
10:50-11:15	BIO-I-1	*Ras Pandey* The University of Southern Mississippi, USA	Self-Organizing Structures of Proteins by a Coarse-Grained Model
11:15-11:40	BIO-I-2	*Norio Yoshida* Kyushu University, Japan	p*Ka* Prediction in Biological Systems Based on the Statistical Mechanics Theory of Liquids
11:40-12:00	BIO-O-1	*Sasiporn Rattanasupha* King Mongkut's University of Technology Thonburi, Thailand	Backward Bifurcation of SEIR Epidemic Model with Treatment Function

Session BIO2 **Time 13:45-15:00** **Room# cc306**

Chair: Prof. Jen-Shiang K. Yu

Time	Code	Presenter	Title
13:45-14:10	BIO-I-3	*Hisashi Okumura* Institute for Molecular Science, Japan	Simulational Studies of Aß Amyloid Fibrils by Equilibrium and Nonequilibrium Molecular Dynamics Method
14:10-14:35	BIO-I-4	*Kiattawee Choowongkomon* Kasetsart University, Thailand	Computer-aided Drug Discovery: From Small Compounds to Protein Inhibitors Against Tyrosine Kinase of EGFR
14:35-14:55	BIO-O-2	*Kanyani Sangpheak* Chulalongkorn University, Thailand	*In Vitro* and *In Silico* Studies of Chalcone as a New Anticancer Drug Candidate Against a Cancer Target Protein

Session BIO3 **Time 15:15-16:45** **Room# cc306**

Chair: Assoc. Prof. Vannajan Sanghiran Lee

Time	Code	Presenter	Title
15:15-15:40	BIO-I-5	*Jen-Shiang Yu* National Chiao Tung University, Taiwan	Enzyme Catalysis that Paves the Way for S-Sulfhydration *via* Sulfur Atom Transfer
15:40-16:05	BIO-I-6	*Satoru Itoh* Institute for Molecular Science, Japan	Oligomerization Pathway of Amyloid-Beta Fragments Studied by the Hamiltonian Replica-Permutation Method
16:05-16:25	BIO-O-3	*Suriyawut Kulatee* Thammasat University, Thailand	Enantioselectivity and Enzyme-Ligand Docking Studies of pfDHFR and Cycloguanil Compounds
16:25-16:45	BIO-O-4	*Kulpavee Jitapunkul* Thammasat University, Thailand	Molecular Modelling of 5-Lipoxygenase Enzyme with Antiasthmatic Substances from Plai

Aug 3, 2017

High Performance Computing, Cloud Computing, Computer Science and Engineering

Session CSE1 **Time 10:50-12:00** **Room# cc308**

Chair: Assoc. Prof. Vara Varavithya

Time	Code	Presenter	Title
10:50-11:15	CSE-I-1	*Zong-Yao Chen* ACER	AI in Practice: Application & Challenges
11:15-11:35	CSE-O-1	*Kunwithree Phramrung* King Mongkut's University of Technology Thonburi, Thailand	The Numerical Solution of Fractional Angiogenesis Problem by Meshless Local Petrov-Galerkin Method
11:35-11:55	CSE-O-2	*Naravadee Nualsaard* King Mongkut's University of Technology Thonburi, Thailand	The Meshless Local Petrov-Galerkin Method for Solving the New Black-Scholes-Schrodinger Model

Session CSE2 **Time 13:45-15:00** **Room# cc308**

Chair: Dr. Supakit Prueksaaroon

Time	Code	Presenter	Title
13:45-14:10	CSE-I-2	*Ekasit Kijsipongse* NECTEC, NSTDA, Thailand	Deep Learning on Hybrid GPU Cluster/Volunteer Computing
14:10-14:35	CSE-O-3	*Chanon Taupachit* Thammasat University, Thailand	Spinner: Failure Detection and Recovery Software in Software Define Network
14:35-14:55	CSE-O-4	*Soratouch Pornmaneerattanatri* Kasetsart University, Thailand	System Tuning for Energy Efficient Big Data Infrastructure

Session CSE3 **Time 15:15-16:45** **Room# cc308**

Chair: Dr. Chantana Chantrapornchai

Time	Code	Presenter	Title
15:15-15:40	CSE-I-3	*Waranyu Wongseree* King Mongkut University of Technology North Bangkok, Thailand	Climate Change Projections Using Statistical Downscaling
15:40-16:05	CSE-O-5	*Danupon Kumpanya* Rajamangala University of Technology Suvarnabhumi, Thailand	Application of Intensified Current Search to Design Optimal PIDD^2 Controller for BLDC Motor Speed Control with Back EMF Detection
16:05-16:25	CSE-O-6	*Peeranon Wattanapong* King Mongkut's University of Technology North Bangkok, Thailand	Express Lane Services on Software-Defined Networks
16:25-16:45	CSE-O-7	*Kanon Sujaree* Rajamangala University of technology Rattanakosin, Thailand	Blood Vehicle Routing Network Using Artificial Chemical Reaction Optimization Algorithm

Aug 4, 2017

Computational Physics, Fluid Dynamics and Solid Mechanics

Session PFD4 **Time 10:45-12:00** **Room# cc307**

Chair: Dr. Sittipong Komin

Time	Code	Presenter	Title
10:45-11:10	PFD-I-7	*Norraphat Srimanobhas* Chulalongkorn University, Thailand	CMS Software and Computing: From RAW Data to Physics Results
11:10-11:35	PFD-I-8	*Teparksorn Pengpan* Prince of Songkla University, Thailand	Bloch Spectral Functions of Palladium-Doped Iron Telluride from KKR-CPA Calculations
11:35-11:55	PFD-O-5	*Umaporn Nuntaplook* Mahidol University, Thailand	The Scattering of Electromagnetic Waves from the Two-Layer Sphere When Outer Layer Has Variable Refractive Index: Shape Resonance

Session PFD5 **Time 13:50-15:00** **Room# cc307**

Chair: Asst. Prof. Jessada Chureemart

Time	Code	Presenter	Title
13:50-14:15	PFD-I-9	*Komsilp Kotmool* Mahidol Wittayanusorn School, Thailand	Predicting the High-Pressure Phases of Materials Using Evolutionary Algorithm
14:15-14:35	PFD-O-6	*Pakawat Toomjeen* Khon Kaen University, Thailand	Designing DNA-Functionalized AuNP Dimer by Molecular Dynamics Simulation for the Application in Biosensor
14:35-14:55	PFD-O-7	*Nissaya Chuathong* King Mongkut's University of Technology North Bangkok (Rayong Campus), Thailand	A New Hybrid Radial Basis Function: The First Step towards Numerically Solving Nonlinear PDEs

Session PFD6 **Time 15:15-16:45** **Room# cc307**

Chair: Asst. Prof. Phanwadee Chureemart

Time	Code	Presenter	Title
15:15-15:40	PFD-I-10	*Piti Ongmongkolkul* Mahidol University International College, Thailand	Current Computational Technique in High Energy Physics
15:40-16:00	PFD-O-8	*Warittha Thongkham* King Mongkut's University of Technology Thonburi, Thailand	Electrical Conductivity of Flexible PEDOT Thermoelectric Foams
16:00-16:20	PFD-O-9	*Witthawat Phanchai* Khon Kaen University, Thailand	Designing Colorimetric Aptasensor Based on Disassembly of AuNP Dimers for Detection of Ochratoxin A
16:20-16:40	PFD-O-10	*Nuttapon Yodsin* Ubon Ratchathani University, Thailand	Effect of Platinum Decorated Carbon Nanocones on Hydrogen Storage Reactions: Theoretical Study

Aug 4, 2017
Computational Chemistry

Session CHE4 **Time 10:45-12:00** **Room# cc305**

Chair: Dr. Kaito Takahashi

Time	Code	Presenter	Title
10:45-11:10	CHE-I-8	*Chao-Ping Hsu* Academia Sinica, Taiwan	Electronic Coupling and Rates for Singlet Fission
11:10-11:35	CHE-I-9	*Vinich Promarak* Vidyasirimedhi Institute of Science and Technology, Thailand	Functional Organic Materials for Optoelectronic Devices
11:35-11:55	CHE-O-4	*Suwapich Pornsatitworakul* Kasetsart University, Thailand	The Preparation of 5,7-Dihydroxy-4-Methylcoumarin via the Pechmann Reaction

Session CHE5 **Time 13:50-15:00** **Room# cc305**

Chair: Asst. Prof. Nawee Kungwan

Time	Code	Presenter	Title
13:50-14:15	CHE-I-10	*Lam K. Hunynh* Vietnam National University, Vietnam	Multi-Scale Modeling and Simulation for Gas-Phase Chemistry and Materials Design: Computational Tools and Applications
14:15-14:35	CHE-I-11	*Tim Kowalczyk* Western Washington University, USA	The Role of the Chemical Environment in Simulations of Photoactive Organic Materials
14:35-14:55	CHE-O-5	*Preeyaporn Poldorn* Ubon Ratchathani University, Thailand	A DFT Study of Volatile Organic Compounds Adsorption on Transition Metals Doped Single Vacancy Graphene

Session CHE6 **Time 15:15-16:45** **Room# cc305**

Chair: Asst.Prof. Panida Surawatanawong

Time	Code	Presenter	Title
15:15-15:40	CHE-I-12	*Min Gao* Hokkaido University, Japan	Reactivity of Gold Clusters in the Regime of Structural Fluxionality
15:40-16:05	CHE-I-13	*Manussada Ratanasak* Hokkaido University, Japan	Theoretical Study on Enantioselective Hydrosilylation of Styrene Catalyzed by Palladium with Helical Poly(quinoxaline-2,3-diyl)s Chiral Phosphine Ligand
16:05-16:25	CHE-O-6	*Kunanon Chattrairat* King Mongkut's Institute of Technology Ladkrabang, Thailand	A Theoretical Study of Small Schiff Base Complexes with Heavy Metal
16:25-16:45	CHE-O-7	*Supawadee Sainimnuan* Kasetsart University, Thailand	Binding Mode Study of Genistein in Complex with Estrogen Receptor Beta by Computational Methods

Aug 4, 2017

Computational Biology and Bioinformatics

Session BIO4 **Time 10:45-12:00** **Room# cc306**

Chair: Assoc. Prof. Kiattawee Choowongkomon

Time	Code	Presenter	Title
10:45-11:10	BIO-I-7	*Shinji Saito* Institute for Molecular Science, Japan	Reaction Model for Circadian Rhythm of Kai System Considering Elementary Processes
11:10-11:35	BIO-I-8	*Vannajan Sanghiran Lee* University of Malaya, Malaysia	Computational Design of Protein Inhibitor for Dengue Envelope Protein
11:35-11:55	BIO-O-5	*Damrongrit Setsirichok* King Mongkut's University of Technology North Bangkok, Thailand	Effects of Incorporating Genetic Models into a Genetic Programming Tree Ensemble for Genetic Association Studies

Session BIO5 **Time 13:50-15:00** **Room# cc306**

Chair: Assoc. Prof. Norio Yoshida

Time	Code	Presenter	Title
13:50-14:15	BIO-I-9	*Peter Wolschann* University of Vienna, Austria	Databases in Chemistry and Biology
14:15-14:35	BIO-I-10	*Varomyalin Tipmanee* Prince of Songkla University, Thailand	Molecular Insight of Recombinant Interleukin-18 as a Model for Functional Protein Design
14:35-14:55	BIO-O-6	*Damrongrit Setsirichok* King Mongkut's University of Technology North Bangkok, Thailand	Incorporating a Genetic Model into a Logistic Regression Model Improves SNP Selection by Lasso for Genetic Association Studies

Session BIO6 **Time 15:15-16:45** **Room# cc306**

Chair: Dr. Varomyalin Tipmanee

Time	Code	Presenter	Title
15:15-15:40	BIO-I-11	*Syed Sikander Azam* Quaid-i-Azam University, Pakistan	The Vitality of Swivel Domain Motion in Performance of Enzyme I of Phosphotransferase System; A Comprehensive Molecular Dynamics Study
15:40-16:05	BIO-I-12	*Sissades Tongsima* BIOTEC, NSTDA, Thailand	Sequencing Data Deluge: Thailand Challenges in Big Data Analytics
16:05-16:25	BIO-O-7	*Charis Georgiou* University of Edinburgh, United Kingdom	Pushing the Limits of Detection of Weak Binding Using Fragment Based Drug Discovery: Identification of New Cyclophilin Binders

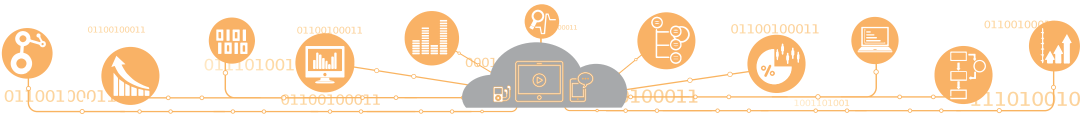

Aug 4, 2017

High Performance Computing, Cloud Computing, Computer Science and Engineering

Session CSE4 **Time 10:45-12:00** **Room# cc308**

Chair: Dr. Waranyu Wongseree

Time	Code	Presenter	Title
10:45-11:10	CSE-I-4	*Chantana Chantrapornchai* Kasetsart University, Thailand	On the Fine Tuning CNN with Pretained Networks
11:10-11:30	CSE-O-8	*Krailerk Manopattanagorn* Kasetsart University, Thailand	The Development of a VM Auto-Scaling Software for OpenStack Cloud
11:30-11:50	CSE-O-9	*Kanon Sujaree* Rajamangala University of Technology Rattanakosin, Thailand	Mobile Dental Unit Using Computer Simulation Theory

Time 13:50-15:00 **Room# cc308**

Chair: Assoc. Prof. Vannajan Sanghiran Lee

Time	Code	Presenter	Title
13:50-15:00			Special Session

Poster Session

Computational Physics, Fluid Dynamics and Solid Mechanics (PFD)

Code	Presenter	Title
PFD-P-1	Lanchakorn Kittiratanawasin	Finite Volume Scheme with Weighted Average Flux for Wet and Dry Shallow Water Simulations
PFD-P-2	Chewa Thassana	Image Processing for Astronomical Objects
PFD-P-3	Nuttapong La-Ongtup	Atomistic Simulation of Structural Evolution at Long Time Scales: Diffusion in the FCC NiAl System
PFD-P-4	Sorasit Buapong	The Effects of Stone-Wales Defect on Quantum Capacitance in Carbon Nanotube
PFD-P-5	Wiraporn Maithong	Stellar Spectrum Analysis from eShel Spectroscope

Poster Session

Computational Chemistry (CHE)

Code	Presenter	Title
CHE-P-1	Narissa Kanlayakan	Effects of Different Proton Donor and Acceptor Groups on Excited-State Intramolecular Proton Transfers of Amino-type and Hydroxy-type Hydrogen-Bonding Molecules: Theoretical Insights
CHE-P-2	Jack D'Amelio	Structural Screening of Photoactive Covalent Organic Frameworks
CHE-P-3	Chanatkran Prommin	Theoretical Studies of Excited State Proton Transfer of 2-Hydroxybenzaldehyde, 1-Hydroxy-2-naphthaldehyde, 1,8-Dihydroxy-2-naphthaldehyde, and Their Derivatives
CHE-P-4	Suparada Kimchompoo	Theoretical Study of Different Donor-and Acceptor-Type Effect in Push−Pull Porphyrin Dyes for Dye-Sensitized Solar Cells
CHE-P-5	Ruangchai Tarsang	Theoretical Study on Effect of Auxiliary Acceptor in Novel D-π-A-π-A Featured Sensitizers for Dye-Sensitized Solar Cells
CHE-P-6	Chattarika Sukpattanacharoen	Theoretical Study on Electronic and Optical Properties of Polythiophene, Polyfuran, Polypyrrole and Their Derivatives as Light-Emitting Materials
CHE-P-7	Malinee Promkatkaew	Theoretical Study on the Structural and Spectroscopic Properties of Cyanine Dyes as Fluorescent Dyes for DNA Detection
CHE-P-8	Rusrina Salaeh	Time-Dependent Density Functional Theory (TDDFT) Investigation on Electronic and Photophysical Properties of Derivatives of 3-Hydroxyflavone
CHE-P-9	Worawaran Thongnuam	Aldol Condensation of Benzaldehyde and Acetophenone on Zirconium Based Metal-Organic Framework: A DFT Study
CHE-P-10	Sarinya Hussadee	Carbon-Doped Boron Nitride Nanosheet: An Efficient Metal-Free Catalyst for Catalytic Oxidation of Carbon Monoxide

Code	Presenter	Title
CHE-P-11	Nattida Maeboonruan	Confinement Effect on the Adsorption of Glucose, Hydroxymethylfurfural and Levulinic Acid on H-Zeolites (H-ZSM5, H-MOR and H-BEA)
CHE-P-12	Rathawat Daengngern	Dynamics Simulations of ESIPT Reactions of 2,5-bis(2'-benzoxazolyl)hydroquinone
CHE-P-13	Yutthana Wongnongwa	Mechanistic Study of CO Oxidation by N_2O over Ag_7Au_6 Cluster Investigated by DFT Methods
CHE-P-14	Phornphimon Maitarad	Nitrous Oxide Decomposition with CO Reducing Agent over Oxotitanium Porphyrin: A Theoretical Study
CHE-P-15	Saowalak Phikulthai	The Catalytic Reaction of Ethanol to Ethylene : A DFT Study
CHE-P-16	Wasinee Panjan	The Conversion of Methane to Methanol over the [Cu-O-Cu]2+/ZSM-5 Zeolite : a Density Functional Theory Study
CHE-P-17	Chanchai Sattayanon	The Effect of Small Gas Detection on Metal-Embedded MoS_2: DFT Study
CHE-P-18	Chan Inntam	The Influence of Silver Cluster Size and Carbon Nanotubes on CO Adsorption: A DFT Study
CHE-P-19	Karan Bobuatong	Theoretical Mechanistic Investigation of Au_{20} and $Au_{16}Pd_4$ Catalyzed Aerobic Oxidation of Benzyl Alcohol to Benzaldehyde
CHE-P-20	Tanabat Mudchimo	Theoretical Study on Carbon-Doped Boron Nitride Nanosheet as a Metal-Free Catalyst for NO Reduction Reaction
CHE-P-21	Suppasith Assawabenjang	Theoretical Study on Olefin Polymerization Catalyst: Half-Titanocenes Containing Aryloxo Ligands
CHE-P-22	Thantip Roongcharoen	Warped Nanographene $C_{80}H_{30}$ as a Promising Catalyst for Nitric Oxide Decomposition
CHE-P-23	Warin Jetsadawisut	Coarse-Grained Molecular Dynamics Simulation of CorA Magnesium Channel in a Nanodisc
CHE-P-24	Paptawan Suwanhom	Computational Docking Study of 4-Oxo-N-(2-(Piperidin- 1-Yl)Ethyl)-4H-Chromene-2-Carboxamide as Acetylcholinesterase and Butyrylcholinesterase Inhibitors
CHE-P-25	Panisak Boonamnaj	Dimer Structure Stabilization of H_v1 C-terminal Domain by Salt Bridge Movements
CHE-P-26	Wiparat Hotarat	Enhanced Stability of Inclusion Complexes of Alpha-Mangostin with Hydrophilic Beta-Cyclodextrin; A Molecular Dynamics Simulation Study
CHE-P-27	Channarong Khrutto	MD Simulation of M2 Proton Channel in Different Phospholipid Bilayer Models
CHE-P-28	Pattama Wapeesittipan	Millisecond Protein Dynamics Does Not Control Catalysis in Cyclophilin A – Evidence from Molecular Dynamics Simulations
CHE-P-29	Theerayut Khempach	Molecular Calculations on Host-Guest Inclusion Complexes of Natural Insecticides: Squamocin and Nicotine
CHE-P-30	Nattaya Mekjirawat	Molecular Docking Investigation of WR99210 Analogues as Novel *M.tuberculosis* DHFR Inhibitors
CHE-P-31	Naruedon Phusi	Structure Based Drug Design of 4-Aminoquinilone Derivatives in DNA Gyrase B Subunit for Anti-Tuberculosis Agents Using Molecular Dynamic Simulations
CHE-P-32	Triet Le Huynh Minh	A Data Mining Approach to Determine the Hindered Internal Rotational Frequency for Chemical Species

Poster Session

Computational Biology and Bioinformatics (BIO)

Code	Presenter	Title
BIO-P-1	Wanwisa Panman	Amylose Wrapping on Single-wall Carbon Nanotube by Computational Study
BIO-P-2	Panupong Mahalapbutr	Computer-Based Drug Screening of Mansonone G Analogs Against Human DNA Topoisomerase II ATPase Domain
BIO-P-3	Phakawat Chusuth	Dynamics Behaviors of Active and Inactive EGFR TK Domains with Erlotinib Bound
BIO-P-4	Sirilak Kongkaew	How a T-Cell Antigen Receptor Recognizes Self-Peptide Leading Autoimmune
BIO-P-5	Nitchakan Darai	In Silico Screening of Chalcones Against Epstein-Barr Nuclear Antigen 1 Protein
BIO-P-6	Kamonpan Sanachai	In Silico Screening of Targeted Proteins for Developing Anticancer Agents
BIO-P-7	Napat Kongtaworn	MD Simulations of Three Designed TSX Structures with 50% Galactose-Removal in Explicit Water Solvent
BIO-P-8	Chonnikan Hanpaibool	Molecular Dynamics Study on MCR-1 In Mono-Zinc and Di-Zinc Forms
BIO-P-9	Peerapong Wongpituk	Structural Dynamics and Binding Free Energy of Neral Cyclodextrins Inclusion Complexes: Molecular Dynamics Simulation
BIO-P-10	Bodee Nutho	Susceptibility of Potent Inhibitors Against NS2B/NS3 Serine Protease of Zika Virus: A Molecular Dynamics Study
BIO-P-11	Nattawat Tantijaratchai	Virtual Screening for Tripeptide Inhibitors in Nnrti Binding Pocket of HIV-1 Reverse Transcriptase

Poster Session

High Performance Computing, Cloud Computing, Computer Science and Engineering (CSE)

Code	Presenter	Title
CSE-P-1	Pairat Tulyaprawat	A Numerical Model for Optimizing a Magnetic Regenerator
CSE-P-2	Prasarnphun Saisin	Automatic Control for Water Droplet on Metal Surface

PLENARY LECTURE
ABSTRACTS

PL-1 Utilizing IBM Power Systems to Optimize Genomic Applications Compute

Denise Ruffner
Business Development Executive at IBM,
Worldwide Genomic Solutions, IBM Systems Group

E-mail: *ruffner@us.ibm.com*

ABSTRACT

In this presentation, IBM will discuss optimizing compute by looking at application performance. IBM will show how the use of hybrid compute clusters allow faster results for key workloads. IBM will look at the key architecture for genomics, and discuss how this can impact performance. Finally, IBM will discuss research results on IBM Power8 where IBM show a great speedup for both compression/decompression as well as on GATK 3.5 performance.

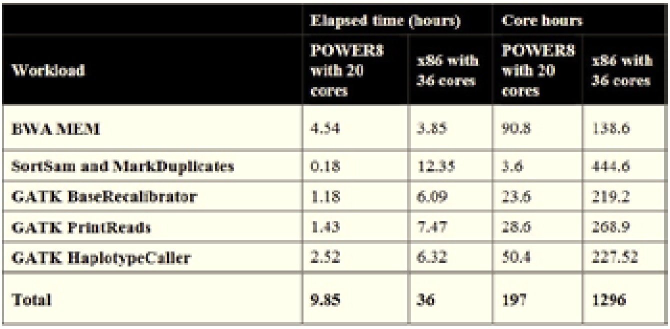

Workload	Elapsed time (hours)		Core hours	
	POWER8 with 20 cores	x86 with 36 cores	POWER8 with 20 cores	x86 with 36 cores
BWA MEM	4.54	3.85	90.8	138.6
SortSam and MarkDuplicates	0.18	12.35	3.6	444.6
GATK BaseRecalibrator	1.18	6.09	23.6	219.2
GATK PrintReads	1.43	7.47	28.6	268.9
GATK HaplotypeCaller	2.52	6.32	50.4	227.52
Total	**9.85**	**36**	**197**	**1296**

Figure 1: Comparative performance benchmark of GATK best practice pipeline on IBM Power server versus published data on an X86 platform (Intel Xeon process E5-2699 v3@2.3 GHz, 256 GB RAM

Keywords: Genomic, Utilizing IBM Power Systems

REFERENCES

Infrastructure for GATK Best Practices Pipeline Deployment:
https://www.intel.com/content/www/us/en/healthcare-it/solutions/documents

	Denise Ruffner is the business and strategy leader for genomics for IBM Power / Cognitive Systems. Her background is as a scientist in both molecular biology and neurobiology with 10 publications in journals such as Science and Journal of Neuroscience. She has worked for scientific instrument companies such as Beckman, DuPont and Transgenomic in Business Development and Marketing. She was recruited to join IBM in 2000 to do venture investing for their newly formed Life Science business unit.

PL-2

Structure and Catalytic Activity of Nanocluster Catalysts

Masahiro Ehara[1,2,3]
[1] *Institute for Molecular Science, Myodaiji, Okazaki 444-8585, Japan*
[2] *SOKENDAI, the Graduate University for Advanced Studies, Myodaiji, Okazaki 444-8585, Japan*
[3] *Element Strategy Initiative for Catalysts and Batteries, Kyoto University, Kyoto 615-8520, Japan*

***E-mail**: ehara@ims.ac.jp; **Fax**: +81 564 55 7025 **Tel.** +81 564 55 7461*

ABSTRACT

In the supported nanocluster (NC) catalysts, the structure and electronic states of NC are relevant for the catalytic activity. We have investigated these factors together with bond activation of Cu binary NCs using DFT calculations. We adopted the computational model of $Cu_{38-n}M_n$ (M=Ru, Rh, Pd, Ag, Os, Ir, Pt, and Au; n=1, 2, and 6). In the most stable structure of $Cu_{37}M_1$ (M=Ru, Ph, Os, Ir, Group 7 and 8), the M atom takes the core position, while in $Cu_{37}M_1$ (M=Pd, Ag, Pt, Au, Group 9 and 10), it takes the shell (center or corner) position. The segregation energy defined by the energy difference between the most stable $Cu_{37}M_1$ (core) and the next stable structure $Cu_{37}M_1$ (shell), was found to be proportional to d orbital population, suggesting that the M atom with unoccupied d orbitals tends to take the core position. Due to the alloy effect, the adsorption energy and bond activation to CO and NO are enhanced in binary NCs, for example, $Cu_{32}Ru_6$. We also studied the single atom catalyst, $M_1/\gamma\text{-}Al_2O_3$ (M=Pd, Fe, Co, Ni) for the low-temperature CO oxidation and found that the +II oxidation state of the M atom is crucial for its catalytic activity. We have theoretically proposed that $Ni_1/\gamma\text{-}Al_2O_3$ is an alternative efficient catalyst that has low energy barriers. In this talk, we overview our recent works.

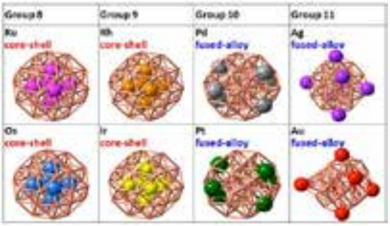

Figure 1. Structure of CuM (M=Ru, Rh, Pd, Ag, Os, Ir, Pt) NC

Keywords: Structure of Binary Nanocluster, Single-atom Catalyst

REFERENCES

1. N. Takagi, K. Ishimura, M. Matsui, R. Fukuda, M. Ehara, S. Sakaki, *submitted for publication.*
2. T. Yang, R. Fukuda, S. Hosokawa, T. Tanaka, S. Sakaki, M. Ehara, *ChemCatChem*, **9**, 1222-1229 (2017).

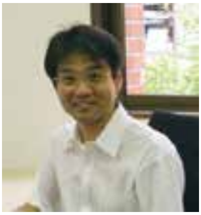	1993	Ph.D. at Kyoto University
	1993-1994	Postdoctral Fellow at Institute for Fundamental Chemistry
	1994-1995	Postdoctral Fellow at University of Heidelberg
	1995-2002	Assistant Professor at Kyoto University
	2002-2008	Associate Professor at Kyoto University
	2008-	Professor at Institute for Molecular Science
	2012-	Professor at ESICB, Kyoto University (concurrent position)

PL-3

Extreme-scale Atomistic Simulations of Nanomaterials

Aiichiro Nakano,[1,*] Rajiv K. Kalia,[1] Fuyuki Shimojo,[2] and Priya Vashishta[1]
[1] *Collaboratory for Advanced Computing and Simulations, Department of Computer Science, Department of Physics & Astronomy, Department of Chemical Engineering & Materials Science, and Department of Biological Sciences, University of Southern California, Los Angeles, CA 90089-0242, USA*
[2] *Department of Physics, Kumamoto University, Kumamoto 860-8555, Japan*

[*] ***E-mail**: anakano@usc.edu;* ***Fax**: +1 213 821 2664;* ***Tel.** +1 213 821 2657*

ABSTRACT

We have developed a divide-conquer-recombine algorithmic framework for large quantum molecular dynamics (QMD) and reactive molecular dynamics (RMD) simulations, which will continue to scale on future computing platforms, with minimal architectural assumptions. The framework has achieved over 98% of the perfect speedup on 786,432 IBM Blue Gene/Q processors for 40 trillion electronic degrees-of-freedom QMD in the framework of density functional theory and 68 billion-atom RMD. We will discuss several applications including (1) 16,616-atom QMD simulation of rapid hydrogen production from water using metallic alloy nanoparticles, (2) 6,400-atom nonadiabatic QMD simulation of exciton dynamics for efficient solar cells, and (3) 112 million-atom RMD simulation of metacarbon synthesis by high temperature oxidation of SiC nanoparticles. We will also discuss the merger of exaflop/s high performance computing and exabyte big data anaytics for the discovery of new materials at our MAterials Genome Innovation for Computational Software (MAGICS) center supported by the U.S. Department of Energy (DOE). MAGICS simulations under DOE INCITE and Aurora ESP projects on photoexcitation dynamics in transition metal dichalcogenide layers explain free-electron X-ray laser and ultrafast electron diffraction experiments at the SLAC National Accelerator Laboratory at exactly the same space and time scales.

Aiichiro Nakano is a Professor of Computer Science with joint appointments in Physics & Astronomy, Chemical Engineering & Materials Science, Biological Sciences, and the Collaboratory for Advanced Computing and Simulations at the University of Southern California (USC). He received a Ph.D. in physics from the University of Tokyo, Japan, in 1989. He has authored 350+ refereed articles in the areas of scalable scientific algorithms, high-end parallel computing, scientific visualization, and computational materials science.

PL-4 Chemistry and Our Common Future

Ito Chao
Institute of Chemistry, Academia Sinica, Taipei, Taiwan

***E-mail**: ichao@gate.sinica.edu.tw* ***Fax**: +886 2 27831237;* ***Tel.** +886 2 2789 8530*

ABSTRACT

Chemistry has been providing mankind the power to transform natural resources into things fulfilling its needs. Mother Nature also employs chemistry to keep the materials flow moving, fulfilling the needs of all species in the ecosystem by utilizing the consumption wastes of one species as resources of another species. Since industrial revolution, mankind has had a jumpstart period of harnessing chemical technologies for exploiting natural resources on an unprecedented scale. The consequences of massive exploitation are seriously disturbed ecosystem and an unsustainable future. In the 21st century, turning the post-consumption wastes into sustainable resources is a grand challenge and it bring tremendous opportunities. Importantly, green chemistry has to be adopted so that new technologies can become as innocuous as possible. In this talk, examples will be given to demonstrate the current status of natural resources, development of green chemistry, and game-changing collaborations among stakeholders.

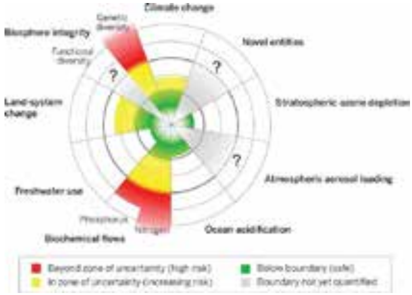

Figure 1. Current status of the control variables for seven of the planetary boundaries.[1]

Keywords: Sustainability, Green Chemistry, Collaboration.

REFERENCES

1. Steffen, W., et al., *Science*, 2015, **347** (6223), 1259855.
2. Matlin, S. A., Mehta, G., Hopf, H., Krief, A., *Nature Chemistry*, 2015, **7**, 941-943.
3. Whitesides, G. M., *Angew. Chem. Int. Ed.* 2015, **54**, 3196-3209.
4. Matlin, S. A., Mehta, G., Hopf, H., Krief, A., *Nature Chemistry*, 2016, **8**, 393-398.

	Research Fellow (2004-); Associate Research Fellow, (1998-2004); Assistant Research Fellow(1993-1998); Postdoctoral Scholar, University of California at Los Angeles, USA (1992-93); Ph.D., University of California at Los Angeles, USA (1992); B.S., National Taiwan University, Taiwan (1985) Secretary General, Chemical Society Located in Taipei (2015-) Deputy Director, Inst. of Chemistry, Academia Sinica(2009-2012)

PL-5 Designing a Massive Coil to Shield JUNO from the Earth's Magnetic Field

Sukit Limpijumnong[1,2], **Saroj Rujirawat**[1,2] **and Jiraroj T-Thienprasert**[2,3]

[1]*School of Physics, Suranaree University of Technology, Nakhon Ratchasima 30000, Thailand*
[2]*Thailand Center of Excellence in Physics, Commission on Higher Education, Bangkok 10400, Thailand*
[3]*Department of Physics, Faculty of Science, Kasetsart University, Bangkok 10900, Thailand*

E-mail: *sukit@sut.ac.th*

On behalf of the JUNO Collaboration

The Jiangmen Underground Neutrino Observatory (JUNO) is designed to detect antineutrinos from nuclear power plants to determine the neutrino mass hierarchy. JUNO's main component is the central detector (CD) - a 35-meter diameter acrylic glass sphere filled with 20 kton liquid scintillator surrounded by 43,000 photomultiplier tubes (PMT). The detector will be built in a 700 m deep underground laboratory. To successfully determine the neutrino mass hierarchy, JUNO must achieve an unprecedented energy resolution of 3% at 1 MeV, which requires the PMTs to have a high and homogeneous photon detection efficiency. To achieve this, the PMTs have to be shielded from the earth's magnetic field to 90% or better. Three institutions in Thailand (Suranaree University of Technology, Chulalongkorn University and National Astronomical Research Institute of Thailand) joined JUNO in 2016 with the task of collaborating in the design, testing and implementation of the magnetic field shielding system. Among several options to shield the magnetic field, building a set of massive electric coils to cover the entire CD emerges as the best option. There are several coil models with different advantages ranging from performance, cost, design, durability and most importantly easiness of installation. Each of the coil models requires the optimization of detailed electric current flow in each section to produce the best cancellation of the earth's magnetic field. Using a simple Biot–Savart law and a finite element method, we constructed a large non-square matrix for each coil model relating the set of electrical currents to the set of magnetic fields at target points. The best set of currents for each coil model can be obtained by using the least-squares method with constraints. The results and limitations of each coil model will be presented and discussed.

Sukit Limpijumnong received his Ph.D in physics from Case Western Reserve University, USA in 1999. For now, he is a professor of physics and director of Research Center in Computational and Theoretical Physics (ThEP) at Suranaree University of Technology, Thailand. His research interests cover: (1) Semiconductor alloys and structural phase transformation of nanoscale semiconductors under high pressure. (2) Characterization of hydrogen in materials. (3) Electronic properties of impurities and defects in III-V and II-VI semiconductors. (4) Structural identification of defects in semiconductors by various techniques such as IR spectroscopy, electron paramagnetic resonance, and photoluminescence. (5) Applications of x-ray absorption spectroscopy in material characterizations.

INVITED SPEAKER ABSTRACTS

PFD -I- 1	**Advanced Process Modelling:** **A Key to Accelerate Development** **of Petrochemical Products**

Arthit Vongachariya[1,C], **Choosak Kiwjaroen** [1], **Siricharn Jirapongphan**[1], **Nattawat Tiensai**[1] **and Khavinet Lourvanij** [1]

[1] *Process Innovation, Process Technology Center, SCG Chemicals co., LTD,*
271 Sukhumvit Rd., Map Ta Phut, Rayong, Thailand

[C] ***E-mail:*** *arthitvo@scg.co.th email;* ***Tel.*** *+66 8 9764 1682*

ABSTRACT

In modern petrochemical industry, development of process technology for producing high value-added products is crucial. Advanced process modelling (APM) is an important tool to minimize time, cost, and risks during the development process. This presentation demonstrates how SCG Chemicals apply the APM tool to various business/technical challenges. Deliverables from the APM technology is driven by multi-scale elements, including physical-property model, detailed kinetics model, and Computation Fluid Dynamics model (Figure 1). Integration of these elements makes the APM technology more effective to find solutions than conventional simulation.

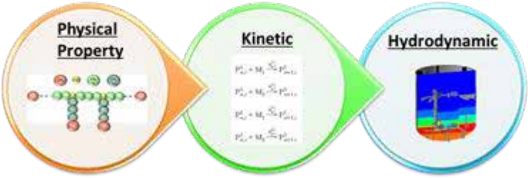

Figure 1. Integration of Multi-scale Elements in Advanced Process Modelling

Keywords: Advanced Process Modelling, Process Technology, Petrochemical Products

REFERENCES

1. Zheng H., Huang Z., Liao Z., Wang J., Yang Y., and Wang Y., *Ind. Eng. Chem. Res.*, 2014, **53** (38), 14865-14875.
2. Pladis P. and Kiparissides C., *J. Appl. Polym. Sci.*, 1999, **73** (12), 2327-2348.

	Arthit Vongachariya is a Lead Engineer that technically supports process and product development in petrochemical business by using Advanced Process Modelling (APM) technology at SCG Chemicals. His education background includes chemistry and physical chemistry from Chulalongkorn University and he had been trained on various simulation techniques in his career (6 years at UBE Group and 1 year at SCG Chemicals). His works have contributed to actual petrochemical plants, resulting in annual cost saving of several dozen million baht for the companies.

PFD
-I-
2

Finite Element Analysis for Fatigue Life Prediction of Alloy Wheels under Radial Loading

Wassamon Phusakulkajorn and Somboon Otarawanna[*]

Computer-Aided Engineering (CAE) Laboratory, Design and Engineering Research Unit,
National Metal and Materials Technology Center (MTEC),
National Science and Technology Development Agency (NSTDA),
114 Thailand Science Park, Pathum Thani, Thailand

[*]***E-mail***: *somboono@mtec.or.th;* ***Tel.*** *+66 2564 6500 ext. 4320*

ABSTRACT

The term 'alloy wheels' generally means wheels made from nonferrous alloys. Alloy wheels for passenger cars are typically made from an aluminium alloy by the low-pressure or gravity die casting process. Due to the processing technique, alloy wheels can be designed to have aesthetic appeal which often involves highly-complex shapes. The dynamic radial fatigue test is one of the mandatory mechanical tests for ensuring the structural integrity of alloy wheels produced. In the test, the wheel and tyre assembly is rolled on a rotating driven drum under radial fatigue loading (Figure 1) for a defined number of cycles, typically 5×10^5 to 1.1×10^6 cycles. This is to simulate the loading conditions when the wheel is attached with a moving vehicle under normal highway conditions.

Finite element analysis (FEA) plays an important role in designing alloy wheels to pass the mandatory mechanical tests including the dynamic radial fatigue test. Significant reduction in cost and time associated with the wheel design and testing processes can be obtained by the use of FEA. In addition, optimisation of the wheel design by using FEA can lead to superior product quality, such as stronger and/or lighter wheels [1].

Regarding the FEA of the wheel radial fatigue test, there are two modelling methods mainly reported in the literature. The first method is modelling the cyclic radial loading applied to the wheel by a number of static load cases [2]. The second is a more simplified model using only a single static load case with an empirical factor to estimate the equivalent cyclic stress [3]. In this work, the two modelling methods were evaluated in terms of solution accuracy, computational resources used and effort required in the fatigue evaluation procedure. For the comparison between prediction and real-test results, regions in the wheel where high stresses were predicted by FEA were compared with regions where cracking occurred in the wheel test.

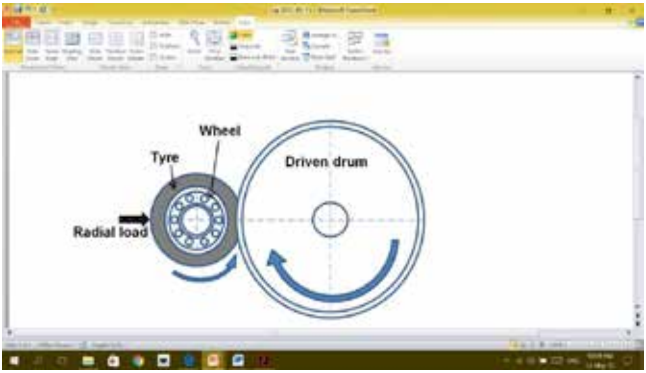

Figure 1. Schematic layout of the wheel radial fatigue test.

Keywords: dynamic radial fatigue test; alloy wheels; finite element; fatigue analysis; mean stress correction

REFERENCES

1. Hsu, Y. L. and Hsu, M. S., *Comput. Ind.*, 2001, **46**, 167-79.
2. Topaç, M. M., Ercan, S., and Kuralay, N. S., *Eng. Fail. Anal.*, 2012, **20**, 67-79.
3. Raju, P.R., Satyanarayana, B., Ramji, K., and Babu, K.S., *Eng. Fail. Anal.*, 2007, **14**, 791-800.

Somboon Otarawanna received his B. Eng. (Mechanical) and M. Eng. (Mechanical) from Chulalongkorn University (Thailand). He completed his Ph. D. (Materials Engineering) at the University of Queensland (Australia) in 2009. Since then, he has been active in the field of Computational Mechanics. Currently, S. Otarawanna is a Senior Researcher and Head of Computer-Aided Engineering Laboratory of MTEC, NSTDA.

PFD -I- 3

The Role of Lattice Flexibility of ZIF - Materials Used for Gas Separation

Siegfried Fritzsche[1]**, Tatiya Chokbunpiam**[2]
[1]*Institute of Theoretical Physics, Faculty of Physics and Geosciences, University of Leipzig, Postfach 100920, D- 04009 Leipzig, Germany*
[2]*Ramkhamhaeng University, Department of Chemistry, Faculty of Science, Bangkok 10240, Thailand*

***E-mail**: sfritzsc07@gmail.com;*

ABSTRACT

Zeolitic Imidazolate Frameworks (ZIF's) are new exciting materials which are a subgroup of Metal Organic Frameworks (MOF's). They consist of metal ions connected by organic linkers forming porous solids with permanent porosity. By exchange of the organic linkers they can be modified and thus be tailored for special purposes. While many MOF's are not stable over longer time, many ZIF's show an outstanding thermal and chemical stability. This makes them promising candidates for industrial use as adsorbents ore membranes for gas separation or gas storage purposes.

Because of the huge number of possible ZIF structures, some overview papers have been published in which Monte Carlo and Molecular Dynamics simulations investigate adsorption and diffusion of gases in ZIF's. In such papers usually rigid lattices have been used in order to save computational effort and thus to be able to scan many ZIF's in one paper. But, many ZIF's have very flexible lattices. This talk presents studies in which the importance of this flexibility has been investigated.

Examples:

In ref. [1] it has been shown that a previously published adsorption selectivity CH_4/H_2 obtained from simulation with rigid lattice was wrong by seven orders of magnitude. In ref. [1] good agreement with the experiment could be obtained from simulations with flexible lattice. The reason was breathing of the size of the windows connecting adjacent cavities that allowed CH_4 to pass the windows.

Besides the window breathing there is an effect called 'gate opening'. This means that the window size increases by a reversible rotation of the imidazolate linker without extension of the other parts of the lattice. Such effects have been published in refs. [2,3]. Figure 1 shows the gate opening in ZIF-8 caused by N_2 guest molecules[2].

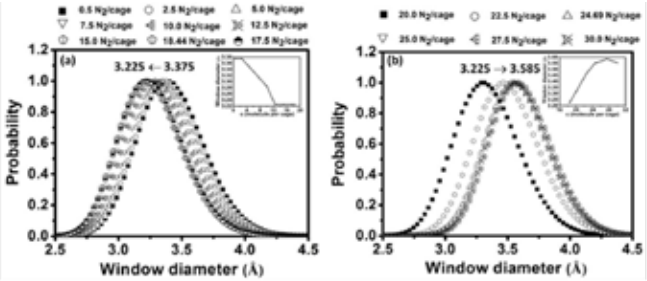

Figure 1. Distributions of ZIF-8 window diameters for different N_2 loadings at 300 K for parameter set A. (a) N_2 loading from 0.5 – 18.44 molecules/cage (b) N_2 loading from 20.0 – 30.0 molecules/cage.

Keywords: Molecular Dynamics computer simulations, Gibbs-Ensemble Monte Carlo simulations, Diffusion, Adsorption, Lattice Flexibility, Zeolitic Imidazolate Frameworks, Metal-Organic Frameworks.

REFERENCES

1. L. Hertäg, H. Bux, J. Caro, C. Chmelik, T. Remsungnen, M. Knauth, S. Fritzsche, *J. Membr. Sci.* **2011,** *377* (1–2), 36-41.
2. T. Chokbunpiam, R. Chanajaree, T. Remsungnen, O. Saengsawang, S. Fritzsche, C. Chmelik, J. Caro, W. Janke, S. Hannongbua, N2 in ZIF-8 *Micropor. and Mesopor. Mater.* **2014,** *187*, 1-6
3. T. Chokbunpiam, S. Fritzsche, C. Chmelik, J. Caro, W. Janke and S. Hannongbua, *Chem. Phys. Lett.* **2016,** *648*, 178-181

	1968-72 Study of physics in Halle (Germany). 1972 - 1991 Scientific coworker at the Central Institute for Isotope and Radiation Research of the German Academy of Sciences in Leipzig in the Group for Statistical and Chemical Physics. Since 1994 coworker at the Institute for Theoretical Physics at the University of Leipzig. 1972 Diploma in Physics, 1983 Ph.D., 1999 Habilitation (Dr. rer. nat. habil.), 2000 Private University Lecturer (Priv.-Doz. or PD) at the University of Leipzig, Germany

PFD
-I-
4

Variational Optimization of Capping Atom Potentials for QM/MM Method

Sittipong Komin[1] **and Sukit Limpijumnong**[2]
[1] Physics Department, Faculty of Science, Ubonratchathani University, Bangkok, Thailand
[2]School of Physics, Institute of Science, Suranaree University of Technology and Synchrotron Light Research Institute, Nakhon Ratchasima, Thailand

[C] ***E-mail***; *sittipong.komin@gmail.com* ***Fax***: *+66 045288381;* ***Tel.*** *+66 0869931918*

ABSTRACT

We present a capping scheme for hybrid quantum-mechanical (QM/MM) calculations which is designed to reproduce the molecular structure, frontier bond potential, and spectroscopic properties for the quantum subsystem. An optimization of capping atom potentials is capable to reduce the perturbations of the electronic structure which are normally caused by a traditional link atoms between quantum and classical regions. In a previous study [J. Chem. Theory Comp., 5, 1490-1498 (2009)], we proposed analytic effective core potentials to replace the boundary atom on the active part of QM/MM method with a small set of adjustable parameters by means of variational perturbation theory. In the present study, our unique form of designed capping atom has been extended a suitable penalty functional including orbital information. Such theoretical models can be applied to reproduce the electronics structure of covalent bonds replaced with a capping pseudo potential atom in a wide range, such as C-C, C-N, C-O bonding. We demonstrate the efficiency of our optimized potentials for a series small molecules to structural and energetic results in the context of ground and excited properties such as protonation energies, optimized geometries, NMR chemical shifts and UV/Vis absorption. Our optimized QM/MM capping potentials are another step toward a realistic first principles prediction of spectroscopic parameters in complex chemical environments using a hybrid QM/MM calculations.

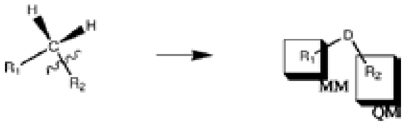

Figure 1. An illustration of the QM/MM partitioning. Cleavage of covalent bonds replace with a capping pseudo potential atom.

Keywords: Computational Material Science, NMR, QM/MM, TDDFT.

REFERENCES

1. S. Komin and D. Sebastiani, *J. Chem. Theory Comput*, 2009, **Volume 5**, 1490-1498.
2. Von Lilienfeld-Toal, I. Tavernelli, U. Rothlisberger and D. Sebastiani, J. Chem.Phys., 2005, 014113, 122.

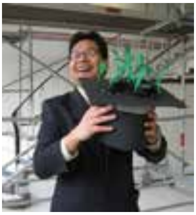	2004 – 2009:	Ph.D. in Chemistry at the Max-Planck Institute for Polymer Research, Mainz. Thesis title: Spectroscopic Properties from Hybrid QM/MM Molecular Dynamics Simulation.
	2005:	Three-month reasearch stay at the Swiss Federal Institute of Technology EPF Lausanne, Swizerland.
	2001 – 2003:	Physics studies at Chiangmai University. M.Sc. in Physics
	1994 – 1998:	Physics studies at Khonkaen University. B.Sc.(honors) in Physics

PFD -I- 5

Hybrid Design for Advanced Magnetic Recording Media: Combining Exchange Coupled Composite Media with Coupled Granular Continuous Media

Phanwadee. Chureemart[1], Richard Evan Evans[2], Roy Chantrell[2], Pin-Wei Huang[3], Kangkang Wang[3], Ganping Ju[3], and JessadaChureemart[1,C]
[1] *Computational and Experimental Magnetism Group, Department of Physics, Mahasarakham University, Mahasarakham, 44150, Thailand.*
[2]*Department of Physics, University of York, York, YO10 5DD, United Kingdom*
[3]*Seagate Technology, Fremont, CA, USA*

[C] ***E-mail**: jessada.c@msu.ac.th; **Tel.** +66 8 3018 6776*

ABSTRACT

Hard disc drives with high areal density and the low cost are a significant requirement in the marketplace. In order to achieve the required high capacity, the key factor to fulfil this aim is the reduction of the grain size as much as possible while sustaining a sufficiently large signal to noise ratio (SNR) and thermal stability of written information withstanding the demagnetizing field for 10 years [1]. There are several alternative approaches to overcome these limitations such as heat-assisted magnetic recording [2], microwave assisted magnetic recording [3] and bit pattered media [4]. Unfortunately, there are several limitations of these novel technologies which are not only a new design of write head but also the nano fabrication process for industry. Therefore, new designs of conventional perpendicular recording media (PRM) are still the favoured option and perpendicular magnetic recording remains the only technology currently used in hard disk drive. Recently, a new design of hybrid granular recording media [5-7] has been introduced, combining the advantages of exchange coupled composite (ECC) media with coupled granular continuous (CGC) media called hybrid ECC/CGC media to improve the performance of recording media in order to achieve an areal density beyond 1 Tbit/in^2 in conventional perpendicular recording. At present, the studies of the reversal process of such a complex structure as hybrid ECC/CGC media are lacking due to the complex ultra-thin multilayer design and are still required in experiment and theory. In order to deeper understand the magnetization reversal mechanisms behind the complex structure of PRM and also take full advantage of this media, an atomistic spin dynamics simulation is used to investigate theoretically the magnetic properties and the magnetization reversal behaviour for a composite media design. This model allows to investigate the effect of the magnetostatic interaction and inter/intra layer exchange coupling for realistic system. The composite granular medium investigated consists of hard and soft composite layers in which the grains are well segregated with a continuous layer capping layer deposited to provide uniform exchange coupling as fig.1 a). We present a detailed calculation aimed at revealing the reversal mechanism. In particular, the angular dependence of the critical field is investigated to understand the switching process as shown in fig.1 b). The calculations show a complex reversal mechanism driven by the magnetostatic interaction. It is also demonstrated, at high sweep rates consistent with the recording process, that thermal effects lead to a significant and irreducible contribution to the switching field distribution.

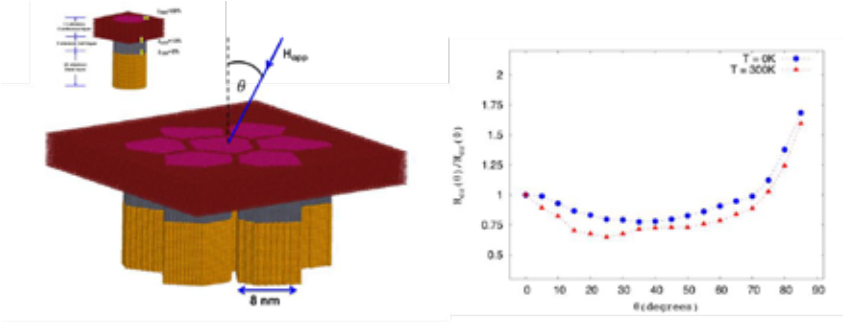

a)

b)

Figure 1. a) the few grains structure for ECC/CGC media and b) variation of the normalized critical field as a function of angle including demagnetizing field at 0 K and 300 K

Keywords: Switching field, the critical field, and magnetisation reversal behaviour.

REFERENCES

1. S. Charap, P.-L. Lu, and Y. He, IEEE Transactions on Magnetics 33, 978 (1997).
2. R. Rottmayer, S. Batra, D. Buechel, W. Challener, J. Hohlfeld, Y. Kubota, L. Li, B. Lu, C. Mihalcea, K. Mountfield, K. Pelhos, C. Peng, T. Rausch, M. A. Seigler, D. Weller, and X. Yang, IEEE Transactions on Magnetics 42, 2417 (2006).
3. J. G. Zhu, X. Zhu, and Y. Tang, IEEE Transactions on Magnetics 44, 125 (2008).
4. B. D. Terris and T. Thomson, Journal of Physics D: Applied Physics 38, R199 (2005).
5. T. P. Nolan, B. F. Valcu, and H. J. Richter, IEEE Transactions on Magnetics 47, 63 (2011).
6. K. K. Tham, S. Saito, D. Hasegawa, N. Itagaki, S. Hinata, S. Ishibashi, and M. Takahashi, Journal of Applied Physics 112, 093917 (2012).
7. J. Chureemart, P. Chureemart, J. Pressesky, T. Nolan, and K. O'Grady, IEEE Transactions on Magnetics 49, 3592 (2013).

	Dr. Jessada Chureemart had the scholarship to study Bachelor degree and Master degree under the program of the Development and Promotion of Science and Technology Talents (DPST) Thailand. He received his Bachelor of Physics from Khon Kaen University and his Master of Physics from Chulalongkorn University Thailand. He also had the Royal Thai government scholarship to study Master degree and PhD degrees at United Kingdom. He received MSc and PhD in Physics from the department of Physics at University of York (UoY) in 2013. Since returning to his post as Assistant Professor at Mahasarakham University (MSU) in Thailand, he has continued his research with UoY on the use of computational models to investigate the properties of materials with applications in magnetic recording under many collaborative projects with Seagate projects, DPST fund and the Thailand research fund (TRF). Now he has been awarded the status of Honorary Visiting fellow in the Department of Physics at the University of York, UK.

PFD
-I-
6

Spin Transport in Read Elements via Spin Accumulation Model

Jessada Chureemart[1], **Roy Chantrell**[2], **and** **Phanwadee Chureemart** [1,C]
[1] Department of Physics, Mahasarakham University, Mahasarakham, Thailand
[2]Department of Physics, University of York, York, United Kingdom Thailand

[C] ***E-mail***: *phanwadee.c@msu.ac.th*

ABSTRACT

The GMR and TMR investigations lead to a significant improvement in the potential applications in data storage technology such as readers in hard disk drives and spintronic devices. Spin torque induced magnetisation switching is a possible technique to control and manipulate the orientation of the magnetisation. This phenomenon provides a new concept for the development of advanced MRAM, nonvolatile logics and readers in hard disk drives. It has opened up the possibility to achieve a smaller reader subsequently leading to increases in the areal density in the hard disk drives. It is important to understand the physics behind the operation of readers which enables us to design them appropriately. Computational models of read sensors are generally based on micromagnetic approaches. Although successful, it is limited in a number of ways which makes the formalism inappropriate for the investigation of a number of factors which will become increasingly important with further scaling of device dimensions. Interestingly, the atomistic simulation of magnetic system increasingly becomes an essential tool in understanding the complex behaviour of the magnetic system such as the diffuse interface while the micromagnetic models cannot deal with this problem.

The physics of the STT phenomenon can be described in terms of a spin accumulation, which interacts with the local magnetic moments via a quantum mechanical exchange interaction. In general, the standard micromagnetic approach is extensively used to describe the STT effect via the spin torque coefficients: μx and βx. These coefficients describe the adiabatic and non-adiabatic contributions to STT. Their values are taken as an unknown constant but the magnitude of βx is still a matter of discussion. we study theoretically the spin-transfer torque acting on the magnetization when injecting polarised conduction electrons into a magnetic system. The spin accumulation is calculated self-consistently and naturally includes the adiabatic and non-adiabatic contributions, which depend on the rate of change of magnetization in relation to the spin diffusion length.

We propose a theoretical model to study the spin transport, particularly the interfacial resistance in a noncollinear system with a diffuse interface. The realistic interface region arising from the sputtering process is first modeled by using Fick's law. Subsequently, the spin transport behavior can be determined via a generalized spin accumulation model taking into account spin dephasing. Our model is able to deal with the magnetic system with arbitrary orientation of magnetization by employing the transform matrix approach. The model is used to investigate spin accumulation in a bilayer consisting of a non-magnet. It is

shown that that the interfacial resistance strongly depends on the relative orientation of magnetization as it decreases with increasing the angle between magnetizations. Influence of interdiffusion, spin current density and spin polarization on GMR are also investigated. We found that the interdiffusion of FM-NM interface giving rise to large spin scattering enhances GMR as demonstrated in Fig. 1. In addition, high MR output can be achieved by using materials with high spin polarization. The results demonstrate that the proposed model is able to calculate magnetoresistance for real devices and useful for device design.

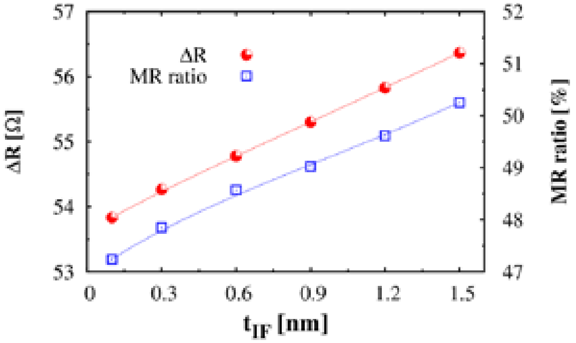

Figure 1. Resistance change and MR ration of the reader as a function of interface thickness

Keywords: spin torque, spin transport, reader.

	Dr Phanwadee Chureemart received her B. Eng. from Khon Kaen University, Khon Kaen, Thailand, and her M. Eng. in electrical engineering from Kasetsart University, Thailand. Then she was a MSc and PhD graduate of the Department of Physics at University of York, UK. Her PhD was of high quality; she was awarded the Anglo-Thai Society prize for best thesis in fundamental science in 2013. Since returning to her post as Assistant Professor at Mahasarakham University (MSU) in Thailand she has continued collaborating with UoY on the development of theoretical models of magnetic materials at the atomistic level including the effects of spin transport under many collaborative projects: A Samsung project on MRAM, Seagate projects and a collaborative project under the Newton fund (IAPP). Now she has been awarded the status of Honorary Visiting fellow in the Department of Physics at the University of York, UK.

PFD -I- 7	CMS Software and Computing: From RAW Data to Physics Results

Norraphat Srimanobhas[1,C]
[1]*Department of Physics, Faculty of Science, Chulalongkorn University, Bangkok, Thailand*

[C] ***E-mail**: norraphat.srimanobhas@cern.ch; **Fax**: +66 2 253 1150; **Tel.** +66 2 218 7693*

ABSTRACT

High energy experimental particle physics community has been produced the world's largest datasets for decades. At CERN Large Hadron Collider (LHC), the Compact Muon Solenoid (CMS) experiment has been collected the data from proton collisions with the rate of 1 kHz. The data has been reconstructed and analyze together with the Monte Carlo samples. Physicists around the world analyze this data to search for new physics, for examples, supersymmetric particles or dark matter, or to precisely measure the known physics parameters, for examples, top quark mass or cross-sections of standard model processes. In this talk, we will discuss the CMS computing system, starting from RAW data to physics results, and challenges in software and computing developments of CMS and high energy physics community.

Keywords: Large Hadron Collider, Compact Muon Solenoid, LHC, CMS.

Currently, I am the lecturer at the Department of Physics, Faculty of Science, Chulalongkorn University. My research interest includes “Searching for magnetic monopole with Compact Muon Solenoid (CMS) detector", “Searching for new physics using monojet signal at the LHC and future collider”. For the responsibility of Compact Muon Solenoid (CMS) operation, I was a convener (2014-2016) of the Physics Data-Monte Carlo Validation (PdmV) team, under the Physics Performance and Dataset (PPD) group. I also gave short lectures in Physics Analysis Tools (PAT) for CMS in several countries, including India, Oman, and Taiwan. In addition to researches mentioned above, I have responsibilities in the particle physics community in Thailand which includes (i) installation the CMS Tier-2 center in the collaboration of Chulalongkorn University, and the National Electronics and Computer Technology Center (NECTEC), and (ii) selection and training of Thai candidates in the CERN summer student, high school student, and teacher programs.

**PFD
-I-
8**

Bloch Spectral Functions of Palladium-Doped Iron Telluride from KKR-CPA Calculations

Teparksorn Pengpan
Department of Physics, Faculty of Science, Prince of Songkla University,
Hat Yai, Thailand 90112

***E-mail**: teparksorn.p@psu.ac.th; **Fax**: +66 0 7428 8751; **Tel.** +66 0 7455 8849*

ABSTRACT

The Korriga-Kohn-Rostoker method with coherent potential approximation (KKR-CPA) is one of the effective methods for investigating electronic structure and magnetic properties of a crystal that pertain impurity, vacancy and disorder [1-3]. In this talk, the calculated results by KKR-CPA on electronic structures such density of states (DOS) and Bloch spectral functions (BSF) of palladium-doped iron telluride ($Fe_{1-x}Pd_xTe$, $x = 0.70$, 0.80, 0.92 and 1.00) [4] which belong to the class 11 of iron-based superconductors [5-6] will be presented. As an example, DOS and BSF at Fermi surface of $Fe_{0.3}Pd_{0.7}Te$ for majority and minority spins are shown in Figure 1.

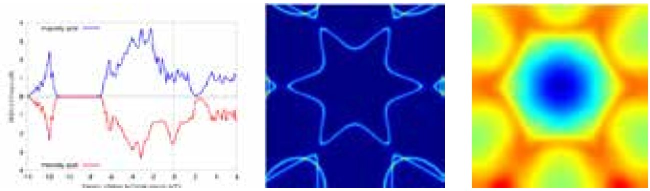

Figure 1. Total density of states (left) and Bloch spectral functions at Fermi surface of $Fe_{0.3}Pd_{0.7}Te$ for the majority (center) and minority (right) spins in the plane $k_z = 0$.

Keywords: Bloch Spectral Functtion, Cohenrent Potential Approximation, Iron-based Superconductors.

REFERENCES

1. Wiendlocha, B., *Phys. Rev. B*, 2013, **88** (20), 205205(7).
2. Akai, H., *J. Phys. Condens. Mater.*, 1989, **1** (43), 8045-64.
3. Gomi, H., Hirose, K., Akai., H., and Fei, Y., *Earth Planet. Sci. Lett.*, 2016, **451** (1 October 2016), 51-61.
4. Karki, A. B., Garlea, O., Custelcean, R., Stadler, S., Plummer, E. W., and Jim, R., *Proc. Natl. Acad. Sci. USA*, 2013, **110** (23), 9283-8.
5. Hosono, H. and Kuroki, K., *Physica C*, 2015, **514** (15 July 2015), 399-422.
6. Wen, H.-H. and Jim, R., *Annu. Rev. Condens. Matter. Phys.*, 2011, **2**, 121-40.

	Dr. Teparksorn Pengpan received his Ph. D. from University of Florida, Gainesville, USA, in 2000. At present, he is an associate professor at Prince of Songkla University. His current research interest is in condensed matter physics and quantum optics.

PFD
-I-
9

Predicting the High-Pressure Phases of Materials Using Evolutionary Algorithm

Komsilp Kotmool[C]
Department of Physics, Mahidol Wittayanusorn School, Nakhon Pathom, Thailand

[C] ***E-mail***: *kkotmool@mwit.ac.th;* ***Fax***: *+66 2 849 7102;* ***Tel.*** *+66 2 849 7218*

ABSTRACT

Evolutionary algorithm is an appropriate method used for predicting the crystal structures of materials at high pressure. By using USPEX code (Universal Structure Predictor: Evolutionary Xtalloraphy) interfacing with available *ab initio* computational codes (i.e. VASP, CASTEP, and Quantum Espresso), the novel structures of some materials (i.e. metal tetraborides and thallium) have been predicted at high pressure. The candidates from searching have been re-optimized with accurate criteria of calculation. Also the related properties of them would be demonstrated. For metal tetraborides consisting of FeB_4 and OsB_4, the semiconductor phases of both materials have been predicted at practical pressures. The predicted phases also exhibit hard/superhard materials and have large incompressibility. For thallium, a distorted face-centered cubic phase has been proposed at 80 GPa. This prediction has been confirmed by using an angle dispersive X-ray diffraction technique. The calculations suggest that s–p mixing states and the valence-core overlapping of 6s and 5d states play the most important roles for the phase transitions along the pathway h.c.p →f.c.c. →b.c.t.

Keywords: Evolutionary algorithm, Phase transition, metal tetraboride and thallium

REFERENCES

1. Kotmool, K., Chakraborty, S., Bovornratanaraks, T., and Ahuja, R., *Sci. Rep.*, 2017**, 7**, 42983.
2. Kotmool, K., Li, B., Chakraborty, S., Bovornratanaraks, T., Mao, H.K., and Ahuja, R., *PNAS*, 2016, **113**(40), 11143-11147.
3. Kotmool, K., Bovornratanaraks, T., Pinsook, U., and Ahuja, R., *J. Phys. Chem. C.*, 2016**, 120**, 23165-23171.
4. Kotmool, K., Kaewmaraya. T., Chakraborty, S., Anversa, J., Bovornratanaraks, T., *et al. PNAS*, 2014, **111**(48), 17050-17053.

	I am a physics teacher at Mahidol Wittayanusorn School (MWITS) and a member of the Extreme Conditions Physics Research Laboratory (ECPRL), Chulalongkorn University (CU), and Thailand. I earned my Ph.D. (physics) from CU under supervision of Assoc. Prof. Bovornratanaraks, T. and Prof. Ahuja, R. (Uppsala University). My research focuses on materials under extreme conditions and their related properties, including hardness, band structures, and superconductivity.

PFD
-I-
10

Current Computational Technique in High Energy Physics

Piti Ongmongkolkul[1]
[1] *Mahidol University International College(MUIC),*

[1] ***E-mail*** *piti.ong@mahidol.ac.th*

ABSTRACT

High Energy Physics is one of the most data intensive sciences. Over the years, many physics experiment collect a huge amount of data. For example, total amount data of BaBar experiment from October 1999 to April 2008 is 2.8 Petabytes. LHC experiment collects data on the order of 10 Petabytes per years. These data are raw sensor data, which will need to be processed into physical quantities. This requires serious computational power. Moreover, analysing high-energy physics data typically involve finding event of interest among all the background; for example, Higgs Boson decays among all the other more common background events. We aim to give an overview of the current computational technique and the challenge in high energy physics experiment.

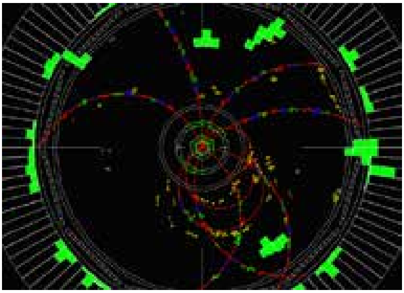

Figure 1. Particle Detector Response for an Event.

Keywords: Computational Science, Computational Conferences, High Energy Physics, Machine Learning.

Piti is a full-time lecturer at Mahidol University International College. He got is Ph.D in Physics from California Institute of Technology. He regularly teaches Physics, Math, and Computer Science. His current interest is in physics, health data, education and medical instrument.

CHE
-I-
1

Computational Approach to Design of Non-Platinum Catalyst for Oxygen Reduction Reaction: Boron Nitride with Gold

Tetsuya Taketsugu[1,2,C], **Andrey Lyalin**[2], **Min Gao**[1], **and Kohei Uosaki**[3]
[1] *Department of Chemistry, Hokkaido University, Sapporo 060-0810, Japan*
[2] *Global Research Center for Environment and Energy based on Nanomaterials Science (GREEN), National Institute for Materials Science (NIMS), Tsukuba 305-0044, Japan*

[C] ***E-mail****: take@sci.hokudai.ac.jp;* ***Fax&Tel.****: +81 11 706 3535*

ABSTRACT

Oxygen reduction reaction (ORR) is a key process in fuel cells, and the most efficient catalysts for ORR are based on platinum. Since platinum is a noble and rare metal, there are growing a lot of interests to develop alternative catalysts. Recently we theoretically demonstrated that hexagonal boron nitride (h-BN), which is catalytically inert insulator with a wide band gap, can be functionalized and act as an electrocatalyst for ORR. Such functionalization can be achieved by the nitrogen doping or deposition of the BN nanosheets on some transition metals [1,2]. Following theoretical suggestions, catalytic activities of h-BN on Au electrodes were examined experimentally [3]. The overpotential for ORR at Au electrode was reduced by ca. 270 mV by spin coating of the dispersion of liquid exfoliated BN nanosheet, proving the theoretical prediction. The present study demonstrates the possibility to functionalize inert materials to become ORR catalysts, opening new ways to design effective Pt-free catalysts for fuel cells based on materials never before considered as catalysts [4,5]. In our previous works, however, ORR on the terrace of BN/Au proceeds only via the 2e$^-$ mechanism with reduction of OOH* intermediate to H_2O_2, while the 4e$^-$ process is not favorable energetically due to stability of OOH* towards dissociation into OH* and O* on BN/Au(111) [3]. The stability of OOH* towards dissociation results from the weak adsorption of O* atom on BN/Au(111). Thus, providing sites for stabilization of oxygen would promote the effective 4e$^-$ pathway of ORR with formation of H_2O. Then, we demonstrate theoretically that gold nanoparticles (Au-NP) supported on BN/Au can provide such active sites for oxygen adsorption. Theoretical analysis of a free energy profile along the reaction pathway is performed for a planar Au_8 cluster which mimics very small and flexible Au-NP. It is demonstrated that OOH* dissociation is promoted at the perimeter interface between the Au-NP and BN/Au surface opening the 4e$^-$ pathway for ORR [6]. Therefore, the increase in the perimeter interface area between the supported Au-NP and the surface would result in increase of the ORR activity. Such increase in the perimeter interface can be achieved by decrease in size of Au-NP. Finally, it is also demonstrated that BN/Au can be utilized as catalysts for hydrogen evolution reaction [7].

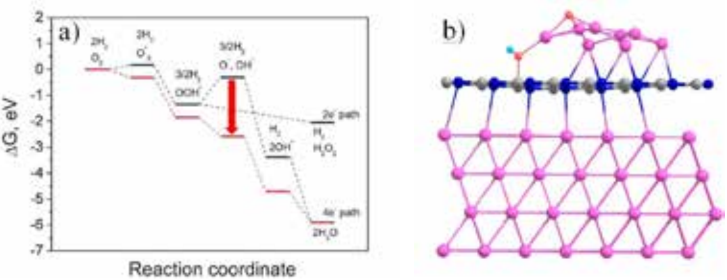

Figure 1. (a) Energy diagrams for ORR at BN/Au(111) (black) and Au_8@BN/Au(111) (red) electrodes and (b) optimized geometry of dissociated OOH on Au_8@BN/Au(111).

Keywords: Computational Design, Catalysts, Oxygen Reduction Reaction, Hydrogen Evolution Reaction, Boron Nitride

REFERENCES

1. A. Lyalin, A. Nakayama, K. Uosaki, and T. Taketsugu, *Phys. Chem. Chem. Phys.*, **15** 2809 (2013)
2. A. Lyalin, A. Nakayama, K. Uosaki, and T. Taketsugu, *J. Phys. Chem. C*, **117**, 21359 (2013).
3. K. Uosaki, G. Elumalai, H. Noguchi, T. Masuda, A. Lyalin, A. Nakayama, and T. Taketsugu, *J. Am. Chem. Soc.*,**136**, 6542 (2014).
4. M. Gao, M. Adachi, A. Lyalin, and T. Taketsugu, *J. Phys. Chem. C*, **120**, 15993-16001 (2016).
5. A. Lyalin, M. Gao, and T. Taketsugu, *Chem. Rec.*, **16**, 2324-2337 (2016).
6. K. Uosaki, G. Elumalai, H. C. Dinh, A. Lyalin, T. Taketsugu, and H. Noguchi, *Scientific Reports*, **6**, 32217 (2016).
7. G. Elumalai, H. Noguchi, A. Lyalin, T. Taketsugu, K. Uosaki, *Electrochemistry Communications*, **66**, 53-57 (2016).

	Tetsuya Taketsugu received his Ph.D. degree in theoretical chemistry from the University of Tokyo in 1994, and became Assistant Professor at the University of Tokyo in 1995. In 1999, he moved to Ochanomizu University as Associate Professor, and in 2005, he has become Professor of quantum chemistry group in Hokkaido University. His research interests focus on the development of new methodology to explore potential energy surfaces and reaction dynamics, as well as theoretical approach to design novel catalyst.

CHE
-I-
2

Mechanisms of C-O Bond Activation and Oxygen Activation: Density Functional Study

Panida Surawatanawong,[1,C] Taveechai Wititsuwannakul,[1] Surawit Visitsatthawong,[1] Boodsarin Sawatlon,[1] Pirom Chenprakhon,[2] Yuthana Tantirungrotechai,[3] and Pimchai Chaiyen[4]

[1]*Department of Chemistry and Center of Excellence for Innovation in Chemistry, Faculty of Science, Mahidol University, Rama VI Rd, Bangkok 10400, Thailand.*
[2]*Institute for Innovative Learning, Mahidol University, Bangkok 10400, Thailand*
[3]*Department of Chemistry, Faculty of Science and Technology, Thammasat University, Pathum Thani, Thailand.*
[4]*Department of Biochemistry and Center of Excellence in Protein Structure and Function, Faculty of Science, Mahidol University, Rama VI Rd, Bangkok 10400, Thailand.*

[C] ***E-mail**: panida.sur@mahidol.edu; **Tel.** +66 0 2201 5137*

ABSTRACT

We performed density functional calculations to give insights into the mechanisms of two important processes: C-O bond activation and O_2 activation. In the first process, C−O bond activation of aryl ethers attracts substantial interest as it is significant for lignin degradation. Nickel complex with N-heterocyclic carbene (Ni-SIPr) has been shown to selectively catalyze C−O bond hydrogenolysis of aryl methyl ether to obtain arene and alcohol as the only products. Our study showed that the C−O bond oxidative addition is the rate-determining step and *tert*-butoxide base could play a role to assist with the formation of Ni(SIPr)(η^2-PhOMe), the catalytically active species. Moreover, the β-H transfer from the methoxy to the phenyl group on Ni-SIPr after the C-O bond oxidative addition is essentially not a stepwise β-H elimination as generally perceived, but rather a concerted process that occurs *via* σ-complex-assisted metathesis (σ-CAM). This leads to benzene elimination before H_2 binding, in accordance with the isotope labeling experiment. In the second process, oxygen activation by flavin-dependent enzymes, which leads to oxidation and oxygenation reactions, is one of the most challenging issues in flavoenzymology. Density functional calculations and transient kinetics were performed to investigate the mechanism of oxygen activation in the oxygenase component (C_2) of *p*-hydroxyphenylacetate 3-hydroxylase (HPAH). We found that the protonation of dioxygen by His396 *via* a proton-coupled electron transfer mechanism is the key step in the formation of the triplet diradical complex of flavin semiquinone and •OOH. This complex undergoes intersystem crossing to form the open-shell singlet diradical complex before it forms the closed-shell singlet C4a-hydroperoxyflavin intermediate (C4aOOH). Notably, the reaction is nearly barrierless. The existence of a positively charged general acid at the position optimized for facilitating the proton-coupled electron transfer has emerged as an important catalytic feature for the oxygen activation process in flavin-dependent enzymes.

Keywords: C−O bond activation, nickel, N-heterocyclic carbene, oxygen activation, flavin, density functional theory

REFERENCES

1. Wititsuwannakul, T.; Tantirungrotechai, Y.; Surawatanawong*, P. *ACS Catal.* 2016, **6**, 1477.
2. Sawatlon, B.; Wititsuwannakul, T.; Tantirungrotechai, Y.; Surawatanawong*, P. *Dalton Trans.,* 2014, **43**, 18123.
3. Visitsatthawong, S.; Chenprakhon, P.; Chaiyen, P.; Surawatanawong*, P. *J. Am. Chem. Soc.,* 2015, **137**, 9363.
4. Wongnate†, T.; Surawatanawong†, P.; Visitsatthawong, S.; Sucharitakul, J.; Scrutton, N. S.; Chaiyen, P. *J. Am. Chem. Soc.*, 2014, **136**, 241.

PANIDA SURAWATANAWONG, Texas A&M University at College Station, USA (Ph.D., 2009), Max Planck Institute for Bioinorganic Chemistry, Germany (Postdoctoral Research Fellow, 2010), Mahidol University, Thailand (Lecturer, 2011-2012) (Assistant Professor, 2013-Present). Research Interest: Computational Chemistry / Catalysis / Organometallic Chemistry.

CHE
-I-
3

Recent Advances in the Determination of Structure and Bonding of Elemental Clusters

Minh Tho Nguyen

Division of Quantum Chemistry, Department of Chemistry, KU Leuven
Celestijnenlaan 200F, B-3001 Leuven, Belgium

***E-mail**: minh.nguyen@kuleuven.be. **Tel.** +32-16-32-7361*

ABSTRACT

Clusters of the elements are characterized by structural richness, unexpected stability and unusual bonding patterns. In connection with the theme of conference on computational approaches to novel materials, we briefly present our recent results in the search for the most thermodynamically stable structures of elemental clusters (genetic search, quantum chemical computations, molecular dynamics simulations…).
Subsequently some novel aspects of structural motifs of the pure and doped boron, silicon and silver clusters are presented. Although a cluster basically differs from a classical compound by its structure and chemical bonding, the aromatic character of a cluster can be established.
The clusters found exhibit a variety of motifs and shapes including the circular disk, the bowl, the cube, the hollow cylinder, the fullerene-type, cage, buckyball... For each shape, an aromatic character can be defined. These aromatic characters can be regarded, for the time being, as non-classical as they do not follow the conventional electron counting rules (refs 1-9).
Some possible applications of small pure and doped clusters in catalysis of simple chemical reactions such as the CO_2, methanol… decompositions, will also be presented.

Keywords: Clusters; Elemental Clusters; Boron Clusters; Silicon Clusters; Silver Clusters; Non-classical Structures;, Non-classical Aromaticity.

REFERENCES

1. Tai, T. B.; Ceulemans, A.; Nguyen, M. T. *Chem. Eur.* J. 2012, **18**, 4510.
2. Tai, T. B.; Havenith, R. W. A.; Teunissen, J.; Ahmet, D.; Hallaert, S.; Nguyen, M. T.; Ceulemans, A. *Inorg. Chem.* 2013, **52**, 10595.
3. Arvanitidis, A.; Tai, T. B.; Nguyen, M. T.; Ceulemans, A. *Phys. Chem. Chem. Phys.* 2014, **16**, 18311.
4. Tai, T. B.; Duong, L. V.; Pham, H. T.; Mai, D. T. T.; Nguyen, M. T. *Chem. Commun.* 2014, **50**, 1558.
5. Pham, H. T.; Duong, L. V.; Tam, N. M.; Pham-Ho, M. P.; Nguyen, M. T. *Chem. Phys. Lett.*, 2014, **608**, 295; *Chem. Phys. Lett.* 2014, **608**, 255; *Chem. Phys. Lett.* 2014, **595**, 271.
6. Muya, J. T.; Nguyen, M. T.; Ceulemans, A. *Annual Reports in Computational Chemistry*, 2015, **11**, 147.
7. T. B. Tai, M. T. Nguyen, M. T. *Phys. Chem. Chem. Phys.* 2015, **17**, 13672; *Chem. Commun.* 2015, **51**, 7677; 2016, **52**, 1653.

8. H. T. Pham, H. T.; Lim, K. N.; Havenith, R. W. A.; Nguyen, R. W. A. *Phys. Chem. Chem. Phys.*, 2016, **18**, xxxx; H. T. Pham, H. T.; Nguyen, M. T. *Phys. Chem. Chem. Phys.*, 2015, **17**, 17566.
9. Tam, N. M.; Nguyen, M. T. *Phys. Chem. Chem. Phys.* 2015, **17**, 3000; 2014, **16**, 19470.
10. Pham, H. T.; Nguyen, M. T. *J. Phys. Chem. A* 2017, **121**, 5056.
11. Nguyen, M.T.; Kiran, B. Editors: *Clusters: Structure, Bonding and Reactivity*, 2017, Springer.
12. Nhat, P. V.; Si, N. T.; Leszczynski, J; Nguyen, M. T. *Chem. Phys.* 2017, 492, 140.
13. Duong, L. V.; Nguyen, M. T. *Phys. Chem. Chem. Phys.* 2017, **19**, 14913.
14. Ferrari, P.; Nguyen, M. T.; Janssens, E. *Chem. Eur. J.* 2017. **23**, 4120.
15. Hang, T. D.; Nguyen, H. T.; Nguyen. M. T. *J. Phys. Chem. C* 2016, **120**, 10442.
16. Nhan. P. L.; Nguyen, M. T. *J. Phys. Chem. A* 2017, **121**, 1940.

	Minh Tho Nguyen was born and grew up in Quang Nam, Viet Nam. He survived the war and arrived in Belgium to pursue his chemical education at the Universite catholique de Louvain (Ph. D. degree in 1980). He received in 1985 a Doctor of Science (D. Sc.) degree of the National University of Ireland (Dublin). After carrying out for several years postdoctoral research in different countries, he was appointed associated professor at University of Groningen, The Netherlands. He returned to Belgium in 1990, for good, joining first the FWO-Vlaanderen as a research director, and then KU Leuven as a full professor of chemistry. His research interest lies in the discovery of new compounds and novel chemical phenomena using quantum chemical methodologies. His group publishes extensively on the issues related to the gas phase atmospheric and pre-biotic compounds, polymers with interesting opto-electronic properties, biomolecules and proteins for treatment of diseases and to a variety of elemental clusters. He is teaching courses on molecular spectroscopy, chemical kinetics and computational chemistry.

CHE
-I-
4

Theoretical Study of Frustrated Lewis Pair for Activation of Stable Chemical Bonds

J. Hasegawa[1,C], **M. Ohbo**[1], **Y. Hoshimoto**[2], **and S. Ogoshi**[2]
[1] *Instituite for Catalysis, Hokkaido University, Japan*
[2]*Division of Applied Chemistry, Graduate School of Engineering, Osaka University, Japan*

[C] ***E-mail****: haesgawa@cat.hokudai.ac.jp;* ***Fax & Tel.****: +81 11 706 9145*

ABSTRACT

Activation of stable chemical bonds is one of the central topics in organic chemistry and catalytic chemistry. Transition metals are commonly used for the catalysts. However, metal-free organic compounds also showed the H-H activation capability [1]. Lewis acid and base usually quench and make a stable chemical bond. When sterically bulky groups hinder the formation of the chemical bond, the Lewis pair is frustrated and affords to break stable bonds in small molecules. This frustrated Lewis pair (FLP) has been applied to hydrogenation catalysts for alkene and alkynes, and has been recognized as an important chemical concept [2].

In this presentation, we present our recent computational study on the mechanism of the dihydrogen activation by the LP (Figure 1) developed by the experimental co-workers [3]. One of the important issues in the FLP area is regeneration of active species from LP. In the LP shown below, the bulky substituents in the phosphine oxide group interact with the $B(C_6F_5)_3$ group to make a meta-stable van der Waals complex. This metastable state corresponds to the FLP state which can accommodate H_2 in a void space between carbene and the $B(C_6F_5)_3$ groups, which can proceed to the H_2 cleavage.

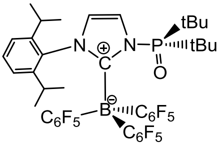

Figure 1. Phosphine oxide substituted LP that can be activated to FLP [3]

Keywords: Frustrated Lewis Pair, Computational Chemistry, Catalystic Chemistry

REFERENCES

1. Welch, G. C., San Juan, R. R., Masuda, J. D., and Stephan, D., *Science*, 2006, **314**, 1124-1126.
2. Stephan, D. and Erker, G., *Angew. Chem. Int. Ed.*, 2015, **54**, 6400-6441.
3. Hoshimoto, Y., Kinoshita, T., Ohashi, M., and Ogoshi, S., *Angew. Chem. Int. Ed.* 2015, **54**, 11666-11671.

	1970: Born in Japan, 1998: Ph. D. at Kyoto University (KU), 1999: Assistant professor, 2008: Lecturer, 2011: Associate Professor at KU, 2012-: Professor at Catalysis Research Center (Institute for Catalysis since 2015) at Hokkaido University. Research area: Quantum Chemistry, Catalytic Chemistry. 2009: Young Scientist Award from the Japan Society for Molecular Science, 2011: QSCP Promising Scientist Award from Centre de Mecanique Ondulatoire Appliquee, 2013: Asian Rising Star Lecturer at the 15- th Asian Chemical Congress.

CHE
-I-
5

Substitution Effect in the Reaction Rate of Criegee Intermediates with Water Vapor

Kaito Takahashi [1,C]
[1]*Institute of Atomic and Molecular Sciences, Academia Sinica,*
No. 1, Roosevelt Rd., Sec. 4, Taipei, 10617, Taiwan

[C] ***E-mail**: corresponding author email;kt@gate.sinica.edu.tw*
***Fax**: +886 223620200; **Tel**. +886 223668237*

ABSTRACT

Due to its fast reaction rate with SO_2, carbonyl oxides or Criegee intermediates (CIs) are thought to be important oxidizing agents in the atmosphere. However, in highly humid atmospheric conditions, some CIs react with water vapor to form hydroperoxy alcohols. Since these alcohols do not react with SO_2, this reaction of CI with water decreases the ability for CIs to act as oxidizing agents in the atmosphere. In this study, we examine the substituent dependence in the CI's reactivity toward water vapor. Starting from the simplest CI: CH_2OO, we calculated for CH_3CHOO, CH_3CH_2CHOO, and $(CH_3)_2COO$. Furthermore, to clarify the effect of unsaturated carbon bonds, we have also calculated $CH_2CHCHOO$ as well as CHCCHOO. Since the CIs that are obtained from the ozonolysis of biogenetic alkenes include unsaturated carbon bonds, we think the systematic study on these C3 CI will provide a good estimate for the CIs in the atmosphere. We performed *ab initio* calculations and obtained the bimolecular rate coefficients between CIs and H_2O as well as $(H_2O)_2$. The energies were calculated with QCISD(T)/CBS//B3LYP/6-311+G(2d,2p) and the partition functions were estimated with anharmonic vibrational corrections by using the second-order perturbation theory.

As can be seen from the results given in Figure 1, *syn*-substituted CIs (CIs with alkyl groups in the same direction as the OO bond) are less reactive toward water monomer than *anti*-substituted one. Therefore, this characteristic allows *syn*-substituted CIs to survive in high humidity.

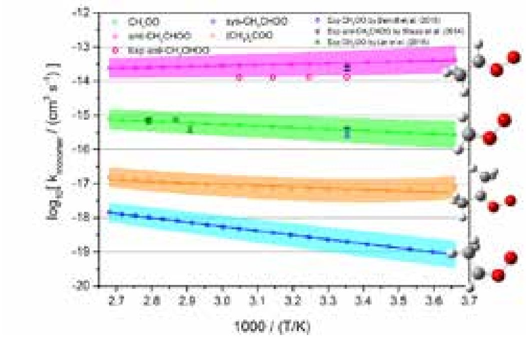

Figure 1. Arrhenius plot of CI+H_2O reaction

Keywords: carbonyl oxide reaction, water, ab initio

REFERENCES

1. Yin, C., and Takahashi, K. *Physical Chemistry Chemical Physics, 2017, DOI: 10.1039/c7cp01091e*
2. Lin, L.-C. et al. *Physical Chemistry Chemical Physics, 2016,* **18**, 28189 - 28197.
3. Lin, L.-C. et al. *Physical Chemistry Chemical Physics, 2016,* **18**, 4557-4568.

	Kaito Takahashi is a Japanese theoretical chemist working as an associate research fellow at the Institute of Atomic and Molecular Sciences, Academia Sinica (IAMS, AS) Taiwan. In 2005, he obtained his Ph.D. from Keio University under the tutelage of Prof. Satoshi Yabushita. After four years of postdoctoral fellow research under Prof. Rex. T. Skojde, he started his lab at IAMS in 2009. His scientific interest for the past few years has been to theoretically understand properties that control reactions and to simulate vibrational, photodetachment, and X-ray absorption spectra.

CHE
-I-
6

Theoretical Approaches for Improving Overall Performances of Dye-Sensitized Solar Cells

Jyh-Chiang Jiang, **Santhanamoorthi Nachimuthu**, **Wei-Chieh Chen**
Department of Chemical Engineering, National Taiwan University of Science and Technology, Taipei, Taiwan, ROC

E-mail:*jcjiang@mail.ntust.edu.tw*; ***Fax***: *+886 2 27376653*; ***Tel.*** *+886 2 27376644*

ABSTRACT

In the 21st century, Dye-sensitized solar cells (DSSCs) have been considered as an alternative to the conventional silicon-based devices in the generation of energy. The overall photovoltaic performance of DSSCs depends on many factors, such as molecular design of the dyes, dye adsorption characteristics on the semiconductor surface and dye regeneration mechanism. Thus, we aimed to improve the efficiency by considering the above factors using state of the art theoretical tools. In designing efficient sensitizer, we have proposed a design strategy and identified the suitable electron donors and acceptors and its effects on overall optoelectronic properties. In addition, finding an ideal adsorption configuration for a dye on the semiconductor surface is an important task. We also investigated the different adsorption configurations of designed model dyes on TiO_2 anatase (101) surface. Moreover, the influence of cyano group in the anchoring part of dye on its adsorption stability and the overall photovoltaic properties such as open circuit voltage, electron injection ability to the surface are reported. Furthermore, understanding the regeneration mechanism of an oxidized dye with redox couples is most significant in improving the efficiency of dye-sensitized solar cells (DSSCs). We also proposed a new regeneration mechanism for organic dyes by assuming the probability of two-electron injection from the stable dye-iodide intermediate complex and reported their UV-vis absorption spectra. In summary, we have explored all the possible ways to improve the overall photovoltaic performance of DSSC by means of designing efficient sensitizers, identifying the appropriate dye adsorption configurations and refining dye regeneration mechanism.

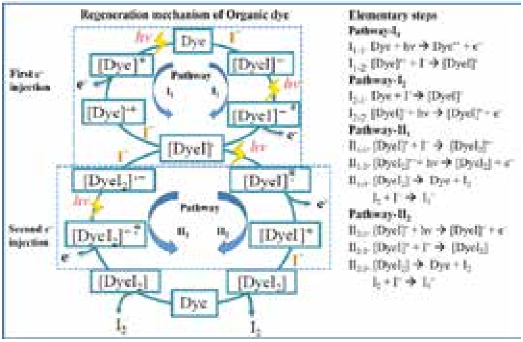

Figure 1. **Proposed mechanisms for the photo-oxidized dye regeneration**.

Keywords: DSSCs, TiO_2, anchoring, regeneration mechanism.

Jyh-Chiang Jiang graduated from National Taiwan University in 1986 with a B.S. in Chemistry and received his PhD in Chemistry in 1994 from the National Taiwan University. Jiang joined the faculty of National Taiwan University of Science and Technology (NTUST) in 2001. In 2010 he was full Professor in Chemical Engineering Department. Dr. Jiang is Executive Supervisor of the Taiwan Theoretical and Computational Science Association from Sept. 2014. He was the coordinator of NSC- computational chemistry group during Nov. 2009 ~Feb. 2013.

He focuses on the theoretical and computational chemistry study of the heterogeneous catalysis, optoelectronic materials and Li ion batteries. He has worked extensively in the development of combined electronic structure and kinetics methods for simulating processes that involve the reaction mechanisms of H_2 production, Hydrogen storage, NH_3 oxidation on metal oxide surfaces. Dr. Jiang has also involved in High throughput screening of many new materials for Li ion batteries based on quantum mechanics calculation. In addition, he has been active for many years in design of the optoelectronic materials for DSSCs using quantum mechanics simulation.

CHE
-I-
7

Catalytic Reactions at the Liquid/Metal-Oxide Interface: Role of the Acid-Base Sites

Akira Nakayama[1,2,C], **Masazumi Tamura**[2,3], **Ken-ichi Shimizu**[1], **and Jun-ya Hasegawa**[1]
[1] *Institute for Catalysis, Hokkaido University, Kita 21 Nishi 10, Kita-ku, Sapporo 0010021,Japan*
[2] *JST PRESTO, 4-1-8 Honcho Kawaguchi, Saitama 332-0012, Japan*
[3] *Department of Applied Chemistry, Graduate School of Engineering, Tohoku University,*
6-6-07 Aoba, Aramaki, Aoba-ku, Sendai 980-8579, Japan

[C] ***E-mail**: nakayama@cat.hokudai.ac.jp;* ***Fax**: +81 11 706 9145;* ***Tel.** +81 11 706 9145*

ABSTRACT

A detailed understanding of the interface between liquid and metal-oxide is fundamental due to its relevance to the broad range of physicochemical phenomena and also technological applications such as heterogeneous catalysis. Chemical reactions occurring at the liquid/metal-oxide interface are very complex, and the probing of the microscopic nature of the interface still remains a formidable task for experiments. In this work, we perform the first-principles molecular dynamics simulations for the liquid/metal-oxide interface and investigate the acid-basis character of the metal-oxide and also the structural and dynamical properties of solvent molecules. In particular, we focus on the catalytic reactions at the water/CeO_2 and methanol/CeO_2 interface since the CeO_2 surface has received considerable attention in recent years due to its broad scientific and technological importance.

We will present the following topics:

(1) First-principles molecular dynamics simulations at the water/CeO_2 surface.
(2) Substrate-specific adsorption of 2-cyanopyridine and hydration by water on CeO_2 explored by the free energy calculations.
(3) Self-assembled hybrid catalysis of 2-cynopyridine and CeO_2 and formation of strong base sites at the interface.
(4) Reaction mechanism for direct synthesis of dimethyl carbonate (DMC) from methanol and CO_2 over CeO_2.

Keywords: Ceria, Acid-Base Catalysis, First-Principles Simulation

REFERENCES

1. M. Tamura, K. Sawabe, K. Tomishige, A. Satsuma, and K. Shimizu, ACS Catal. **5**, 20 (2015).
2. M. Tamura, R. Kishi, Y. Nakagawa, and K. Tomishige, Nat. Commun. **6**, 8580 (2015).
3. Y. Yoshida, Y. Arai, S. Kado, K. Kunimori, and K. Tomishige, Catal. Today **115**, 95 (2006).

	1996	Bachelor of Engineering; Department of Applied Chemistry,School of Engineering, University of Tokyo
	2001	Ph.D.; Department of Chemical System Engineering, Graduate School of Engineering, University of Tokyo
	2001-2005	Postdoctoral Research Associate; Department of Chemistry,University of Illinois at Urbana-Champaign
	2005-2013	Assistant Professor; Department of Chemistry, Faculty of Science, Hokkaido Univerisity
	2013-2015	Associate Professor; Catalysis Research Center, Hokkaido University
	2015-	Associate Professor; Institute for Catalysis, Hokkaido University
	2016-	PRESTO Researcher, JST

CHE
-I-
8

Electronic Coupling and Rates for Singlet Fission

Chao-Ping Hsu
128 Academia Road, Sec. 2, Institute of Chemistry, Academia Sinica, Taipei, 11529, Taiwan

***E-mail**: cherri@sinica.edu.tw; **Fax**: +886 2 27831237; **Tel.** +886 2 27898658*

ABSTRACT

In the simulation of dynamics with curve-crossing, the states involved are close in energy, and the Born-Oppenheimer approximation breaks down. The dynamics is better described with diabatic states, which generally require additional conditions in their definition and description. Even though diabatic states are originally defined as the eigenstates of the kinetic energy operator, they are over-determined for systems with more than two atoms [1]. Thus, an alternative definition is necessary. Diabatic states are often defined as a state that retains certain key properties when the system moves along the reaction coordinate [2]. For example, the generalized Mulliken-Hush scheme, a useful method for for electron transfer, retains the dipole moment in the diabatic states [3]. The fragment excitation difference scheme is a similar method for energy transfer problems, in which the excitation population is localized to each fragment [4].

With a singlet exciton split into two triplet excitons, singlet fission has a great potential to increase the efficiency of solar cells. The Fragment Spin Difference (FSD) scheme was generalized to calculate the singlet fission coupling. Without manually including the CT components, the largest coupling strength obtained was 14.8 meV for two pentacenes in a crystal structure, or 33.7 meV for a transition-state structure, which yielded singlet fission lifetime of 239 or 37 fs, generally consistent to experimental result (80 fs). We found that the charge on one fragment in the S1 diabatic state correlates well with FSD coupling, indicating the importance of the CT component. The FSD approach is a useful first-principle method for singlet fission coupling, without the need to include the CT component explicitly [5]. Further implementation for spin-completeness or a Restrictive Active Space (RAS) excitation improves the quality of excited states. The results predict well for a set of experimentally studied intramolecular singlet fission and triplet-triplet annihilation rates.

Keywords: Singlet fission, Triplet-triplet annihilation, electronic coupling

REFERENCES

1. Mead, C. A.; Truhlar, D. G. J. Chem. Phys. 1982, **77**, 6090.
2. Kryachko, E. S.; Yarkony, D. R. Int. J. Quant. Chem. 2000, **76**, 235.
3. Cave, R. J.; Newton, M. D. Chem. Phys. Lett. 1996, **249**, 15.
4. Hsu, C.-P. Acc. Chem. Res. 2009, **42**, 509.
5. Yang, C.-H.; Hsu, C.-P. J. Phys. Chem. Lett. 2015, **6**, 1925.

	Chao-Ping Hsu obtained her B. S. and M.Sc. degrees in Chemistry in 1990 and 1992, both from National Taiwan University. She obtained her Ph.D. degree in Chemistry in 1998, from California Institute of Technology. She was a Miller Fellow in University of California, Berkeley. In 2002, she became an Assistant Research Fellow in the Institute of Chemistry, Academia Sinica, where she was promoted to Associate Research Fellow and Research Fellow in 2007 and 2013, respectively.

CHE
-I-
9

Functional Organic Materials for Optoelectronic Devices

Vinich Promarak
Department of Materials Science & Engineering, School of Molecular Science & Engineering,
Vidyasirimedhi Institute of Science and Technology (VISTEC), Wangchan, Rayong, 21210 Thailand

***E-mail**: vinich.p@vistec.ac.th; **Fax**: +66 33 014445; **Tel.** +66 33 014150*

ABSTRACT

In my talk, firstly I will give a brief introduction of our research team and a summary of our research interests and results. I will then focus on the two main topics of our research in the field of organic electronics namely dye-sensitized solar cells (DSSCs) and organic light-emitting diodes (OLEDs). In DSSC, an improvement of the performance of the organic dyes as sensitizers for DSSC by fine tuning the chemical structures will be presented. A series of organic dipolar compounds forming D-D-π-A type of dyads bearing carbazole-carbazole and carbazole-diphenylamine as D-D moieties, number of linearly connected arylene groups as central π-conjugation bridges (π), acrylic acid, a cyanoacrylic acid and a fused cyanoacrylic acid as anchoring groups (A) were designed, synthesized and investigated. In OLED, a molecular design of novel non-doped solution-processed hole-transporting light-emitting materials based on triarylamine and carbazole derivatives for single-layer solution processed OLEDs will be reported. The structure-property relationships of these materials obtaining from experimental and state-of-the-art theoretical calculations will be discussed.

Keywords: Organic materials, Optoelectronic devices, Theoretical calculations.

REFERENCES

1. N. Prachumrak, T. Sudyoadsuk, A. Thangthong, P. Nalaoh, S. Jungsuttiwong, R. Daengngern, S. Namuangruk, P. Pattanasattaya, V. Promarak, *Mater. Chem. Front.*, 2017, **1**, DOI: 10.1039/C6QM00271D.
2. T. Keawin, R. Tarsang, K. Sirithip, N. Prachumrak, T. Sudyoadsuk, S. Namuangruk, J. Roncali, N. Kungwan, V. Promarak, S. Jungsuttiwong, *Dyes Pigm.*, 2017, **136**, 697-706.
3. D. Muenmart, N. Prachumrak, R. Tarsang, S. Namuangruk, S. Jungsuttiwong, T. Sudyoadsuk, P. Pattanasattayavong, V. Promarak, *RSC Adv.*, 2016, **6**, 38481–38493.
4. A. Thangthong, N. Prachumrak, T. Sudyoadsuk, S. Namuangruk, T. Kaewin, S. Jungsuttiwong, N. Kungwan, V. Promarak, *Org. Electron.*, 2015, **21**, 117–125.
5. K. Sirithip, N. Prachumrak, R. Rattanawan, T. Keawin, T. Sudyoadsuk, S. Namuangruk, S. Jungsuttiwong, V. Promarak, *Chem.-Asian J.*, 2015, **10**, 882-893.
6. A. Thangthong, N. Prachumrak, S. Saengsuwan, S. Namuangruk, T. Keawin, S. Jungsuttiwong, T. Sudyoadsuk, V. Promarak, *J. Mater. Chem. C*, 2015, **3**, 3081-3086.

Vinich Promarak received his Ph.D. in 2002 from Oxford University, UK. He is currently a full Professor in Chemistry at VISTEC. His research interests involve around "high-tech" organic materials that can be used in applications such as organic light-emitting diode (OLED), perovskite/dye-sensitized solar cells (DSSC/PSC), bulk heterojunction solar cell (OPV), sensor, optical switch, organic field-effect transistor (OFET). To date, he has co-authored more than 115 peer-reviewed papers, and his publications have been cited over 2500 times with current H-index of 29 (Google Scholar).

CHE -I- 10

Multi-scale Modeling and Simulation for Gas-Phase Chemistry and Materials Design: Computational Tools and Applications

Lam K. Huynh
Department of Applied Chemistry, International University,
Vietnam National University - HCMC
Quarter 6, Linh Trung, Thu Duc District, Ho Chi Minh City, Vietnam

***E-mail**: hklam@hcmiu.edu.vn;* ***Fax**: +84-8 3724.4271;* ***Tel.** +84-8 2211.4046 (Ext. 3233)*

ABSTRACT

Computational modeling and simulation have served not only as a powerful post-facto tool for validating existing principles and knowledge but also a strong predictive tool in the discovery of new knowledge in science and engineering. Recent advances in information technology, algorithm, and scientific methods, which allow faster and more accurate calculations for more realistic systems, have laid a solid foundation for bridging the time and length scale from fundamental science to real engineering challenges. In this talk, a demonstration on how to bridge fundamental chemistry/physics and reaction engineering modeling/simulation will be presented in two domains: *(1) gas-phase chemistry* and *(2) catalysts/materials design (complex chemical processes on surfaces)*. In gas-phase chemistry, examples for understanding and modeling atmospheric chemistry and low-temperature combustion of hydrocarbon/alternative fuels will be discussed in detail. Then, the demonstration on how to design better catalysts for complex chemical systems will be presented. To facilitate the multiscale applications, main features of our in-house computational tools, namely *MultiSpecies-MultiChannel (MSMC)*[1] for complex gas-phase systems and *Surfkin*[2] for gas-surface reactions, will be introduced. New methodologies and approaches (e.g., machine learning) for such interests will be also discussed.

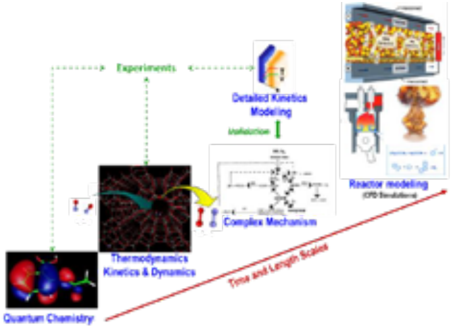

Figure 1. Multiscale approach from fundamental chemistry and physics to reactor modeling and simulation.

Keywords: Multiscale, Modeling, Simulation, Gas-phase Chemistry, Materials Design, Thermodynamics, and Kinetics.

REFERENCES

1. Duong, M. V.; Nguyen, H. T.; Truong, N.; Le, T. N. M.; Huynh, L. K. *International Journal of Chemical Kinetics* 2015, **47** (9), 564-575.
   Website: https://sites.google.com/site/msmccode/
2. Le, T. N.; Liu, B.; Huynh, L. K. *Journal of Computational Chemistry*, 2014, **35** (26), 1890-1899.

	Lam K. Huynh earned his Ph.D. in physical chemistry at the University of Utah (Utah, USA). After working as a Postdoctoral Associate at the University of Michigan (Ann Arbor, Michigan, USA) and the Colorado School of Mines (Colorado, USA), he joined the International University, VNU-HCM as a faculty member since 2010. He has been interested in multiscale interdisciplinary modeling and simulation of complex chemical systems with the focus on combustion of alternative fuels and materials design. He has also worked on scientific software development on high-performance computing (HPC) platform.

CHE
-I-
11

The Role of the Chemical Environment in Simulations of Photoactive Organic Materials

**Viktor Laszlo, Keenan Komoto, Natalya Garcia, Zoe Pollard,
Khoa Le, Alessandro Banducci, Alyssa Goodey, and Tim Kowalczyk**
*Department of Chemistry, Advanced Materials Science & Engineering Center,
and Institute for Energy Studies, Western Washington University, Bellingham, WA 98225, USA*

E-mail: *Tim.Kowalczyk@wwu.edu;* ***Fax***: *+1 360 650 6562;* ***Tel.*** *+1 360 650 6622*

ABSTRACT

In the design of organic materials that selectively absorb, manipulate, and emit visible light, molecular simulations offer mechanistic insights that are difficult to glean from experiment. The complex chemical environments in which these materials operate afford opportunities to fine-tune photophysical properties but also present obstacles to high-throughput virtual screening. In this context, multiscale models that couple a quantum mechanical description of the chromophore to a classical description of the molecular environment are valuable, but errors from the approximations they introduce can be difficult to quantify. Here we share insights gleaned from developing and applying approximate excited-state molecular simulations[1,2] to predict the effects of local chemical environments on the absorption, charge and energy transfer, and emission properties of selected organic chromophores. We employ multiscale models rooted in excited-state density functional theory (DFT) and DFTB to study dye-assisted photosensitization of singlet oxygen and to rationalize changes in the photophysics of chromophores in constrained environments.[3,4] Solvatochromic shifts obtained from a quantum mechanical treatment of the chromophore and its surroundings highlight the importance of the chromophore's local environment in the selection of a suitable computational model.

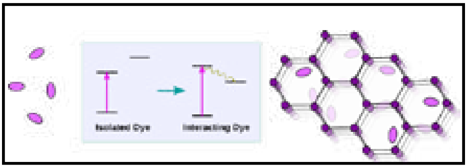

Figure 1. Embedding and encapsulation of organic chromophores alter their photoactivity.

Keywords: excited states, density functional tight binding, solvatochromism, singlet oxygen.

REFERENCES

1. Kowalczyk, T; Le, K.; Irle, S. *J. Chem. Theory Comput.* 2016, **12** (1), 313-323.
2. Komoto, K. T.; Kowalczyk, T. *J. Phys. Chem. A* 2016, **120** (41), 8160-8168.
3. Laszlo, V.; Kowalczyk, T. *J. Mater. Chem. A* 2016, **4** (27), 10500-10507.
4. Garcia, N.; Kowalczyk, T. *in preparation*.

Tim Kowalczyk is a computational materials scientist and an Assistant Professor at Western Washington University with joint appointments in Chemistry, Materials Science, and Energy Studies. Dr. Kowalczyk earned a B.S. in chemistry and mathematics from the University of Southern California and a Ph.D. in physical chemistry from MIT. Following a JSPS Postdoctoral Fellowship at Nagoya University, in 2014 he joined the faculty of WWU, where he is currently the Snohomish PUD Professor of Energy Studies.

CHE
-I-
12

Reactivity of Gold Clusters in the Regime of Structural Fluxionality

Min Gao[1,C], **Andrey Lyalin**[2], **Satoshi Maeda**[1,2] **and Tetsuya Taketsugu**[1,2]
[1]*Department of Chemistry, Faculty of Science, Hokkaido University, Sapporo060-0810, Japan*
[2]*Global Research Center for Environment and Energy based on Nanomaterial Science (GREEN), National Institute for Material Science (NIMS), 1-1 Namiki, Tsukuba 305-0044, Japan*

[C] ***E-mail****: gaomin@sci.hokudai.ac.jp;* ***Fax****: +81 11 7063821;* ***Tel****: +81 11 7063821*

ABSTRACT

Catalysis by nanoscaled particles (nanocatalysis) is one of the most exciting fields of modern nanoscience. The enormous interest in nanocatalysis is stipulated by the fact that the catalytic activity of nanoparticles is strongly dependent on their size, structure, morphology, charge state, type of the support material, etc., and hence can be controlled and tuned by these factors. However, despite intensive theoretical and experimental studies, the clear understanding of the morphology effects in nanocatalysis is still lacking. Metal clusters are structural flexible, which leads that they can possess different geometrical structures and different reactivity for the same sized cluster. This property makes the investigation of catalytic activity for metal clusters relatively difficult. Recently, we proposed a novel effective strategy for a systematic search of single bond activation reaction by small metal clusters. [1-3] This approach is based on the global reaction route mapping [4] technique by using the artificial force-induced reaction method. [5] The results demonstrated that the most stable structure of metal clusters are not always highly reactive and the most stable adsorption configurations of reactants on metal clusters do not necessarily lead to the low-energy dissociation pathways (Figure 1). Therefore, in order to investigate the activity of metal clusters, the contribution of all the possible reaction sites and low-energy isomers are highly required.

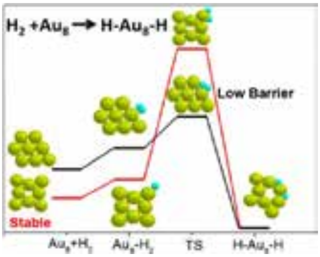

Figure 1. Reaction Scheme of H_2 dissociation paths on Au_8

Keywords: Metal Cluster, Catalytic Activity, Isomers

REFERENCES

1. M. Gao, A. Lyalin, S. Maeda, and T. Taketsugu, *J. Chem. Theo. Comp.,* 2014, **10**, 1623-1630.
2. M. Gao, A. Lyalin, M. Takagi, S. Maeda, and T. Taketsugu, *J. Phys. Chem. C*, 2015, **119**, 11120-11130.
3. M. Gao, D. Horita, Y. Ono, A. Lyalin, S. Maeda, and T. Taketsugu, *J. Phys. Chem. C*, 2017, **121**, 2661-2668.
4. S. Maeda, Y. Harabuchi, Y. Sumiya, M. Takagi, M. Hatanaka, Y. Osada, T. Taketsugu, K. Morokuma and K. Ohno, (see: http://grrm.chem.tohoku.ac.jp/GRRM/index_e.html [accessed on March 3, 2016], GRRM14
5. S. Maeda, Y. Harabuchi, M. Takagi, T. Taketsugu and K. Morokuma, *Chem. Rec.,* 2016, **16**, 2232−224.

	Min Gao was born in Shandong, China, in 1986. She received her Ph.D. degree in physical chemistry in 2012 from Hokkaido University under the supervision of Prof. Tetsuya Taketsugu. She then continued her research into catalytic reactions as a postdoctoral fellow until 2015. In 2016, she became an Assistant Professor in the Quantum Chemistry Group at Hokkaido University. Her research interests include the theoretical design of catalysts and mechanistic study of catalytic reactions.

CHE -I- 13

Theoretical Study on Enantioselective Hydrosilylation of Styrene Catalyzed by Palladium with Helical Poly(quinoxaline-2,3-diyl)s Chiral Phosphine Ligand

Manussada Ratanasak[1], **Michinori Suginome**[2], and **Jun-ya Hasegawa**[1,C]
[1] *Institute for Catalysis, Hokkaido University, Kita 21, Nishi 10, Sapporo, Hokkaido, Japan*
[2] *Department of Synthetic Chemistry and Biological Chemistry, Graduate School of Engineering, Kyoto University, Katsura, Nishikyo-ku, Kyoto, Japan*

[C] ***E-mail:*** *hasegawa@cat.hokudai.ac.jp;* ***Fax & Tel.*** *+81-11-706-9145*

ABSTRACT

The first theoretical study on the catalytic active site of single-handed helical poly(quinoxaline-2,3-diyl)s (PQXs) bearing chiral (*R*)-2-butoxymethyl ligand for the enantioselective palladium catalyzed asymmetric hydrosilylation of styrene reaction has been performed. Initially, we have calculated electronic circular dichroism spectra (ECD) of the right-handed polymer ligand (P) and the left-handed polymer ligand (M) helices of 21 mers using simplified Tamm-Dancoff approximation (sTDA) approach [1] compared with experiment [2]. Our computational results were able to successfully reproduce the experimental CD spectra. Then, the Chalk-Harrod and the Modified Chalk-Harrod mechanisms have been investigated by DFT calculations. The results concluded that this reaction proceeds through the Chalk-Harrod mechanism. Moreover, the palladium catalyst with presence of *R* and *S* chiral ligands have been examined. Our results indicated that steric effects have played an important role in defining the regio-, stereo-, and enantioselective. Moreover, the helix stability of four systems (P*S*, P*R*, M*S*, M*R*) were studied by ONIOM2 (ωB97XD/6-31G(d), SDD(Pd) // PM6) calculations. Our results in line with the experiment finding which revealed that P helix gave an enantioenriched hydrosilylation product with the *S* configuration and M helix gave the *R* product selectively [3].

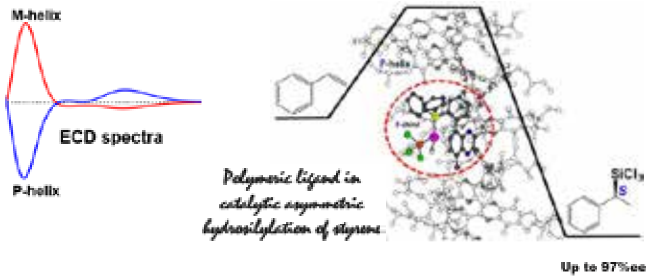
M-helix
ECD spectra
P-helix
P-helix
Polymeric ligand in catalytic asymmetric hydrosilylation of styrene
SiCl3
S
Up to 97%ee

Keywords: hydrosilylation, polymer chiral catalyst, palladium, ECD spectra, enantioselective

REFERENCES

1. Grimme, S., *J. Chem. Phys.,* 2013, **138**, 244104.
2. Yamada, T., Nagata, Y., and Suginome, M., *Chem. Commun.,* 2010, **46**, 4914-4916.
3. Yamamoto, T., Yamada, T., Nagata, Y., and Suginome, M., *J. Am. Chem. Soc.,* 2010, **132**, 7899.

	Manussada Ratanasak received her M.Sc. in Physical Chemistry from Chulalongkorn University in 2004 under supervision of Prof. Sirirat Kokpol. After that, she was an assistant researcher at computational chemistry unit cell. Then, she works at company as technician support for Accelrys software. And then, she returned to study Ph.D. and graduated Ph.D. program in Nanoscience and Technology, Graduate School at Chulalongkorn University in 2016 under Assoc. Prof. Vudhichai Parasuk. Currently, she is a posdoctoral researcher at Institutue for Catalysis, Hokkaido university with Prof. Jun-ya Hasegawa since April 2016. Her research interests are in the domain of computational studies of transition states in asymmetric catalysis, chiral polymer-based catalyst, and catalyst design.

BIO -I- 1

Self-Organizing Structures of Proteins by a Coarse-Grained Model

R.B. Pandey
Department of Physics and Astronomy
University of Southern Mississippi, Hattiesburg, MS 39406-5046, USA

E-mail: *ras.pandey@usm.edu; Telephone: +1 601 266 4485*

ABSTRACT

How a protein moves, relaxes and conform into a stable configuration has been a subject of continued interest for decades. Yet, a complete understanding of protein folding remains an open question from a first principle approach primarily due to inaccessible time scale. Some degree of approximation is therefore unavoidable in almost all models involving atomistic details to coarse-grained (CG) descriptions. Coarse-graining procedures generally involves simplifying structural details, devising interaction potentials, exploring the phase space selectively, resorting to efficient and effective methods, etc. Using a coarse-grained approach with reduced degrees of freedom and incorporating knowledge-based (e.g. NMR and X-ray crystallography structures of proteins from PDB) data ensembles in a phenomenological potential, we investigate the conformational dynamics of proteins. Examples include intrinsically disordered proteins such as histones (H3.1, H2AX) and Alpha-Synuclein (ASN), amyloid Lysozyme, and membrane proteins (e.g. hHv1, corA). A number of local and global physical quantities are analyzed including contact map, energy and mobility profiles, mean square displacement of protein, its radius of gyration, structure factor etc.

Structure and dynamics of H3.1 and H2AX are studied as a function of temperature and in implicit and explicit solvent. Several interesting observations are made [1] such as continuous conformational transition from globular to random coil in H3.1 to non-monotonic thermal response in H2AX. Alpha-synuclein is linked to such neurodegenerative diseases as Parkinson's disease (PD) and Alzheimer disease via toxic clumping into amyloid fibrils. Structure and dynamics of ASN is investigated as a function of temperature. Based on the mobility profile, we are able to identify [2] three distinct segment of ASN along its contour, i.e. sluggish N-terminal and C-terminal (least mobile) separated by the central region, the non-amyloid component (NAC) with higher mobility. Contact profile shows that the probability of intra-chain residue aggregation (clumping) is higher in the N-terminal region than the C-terminal with least aggregation in the NAC region. Variation of the radius of gyration (R_g) with the temperature is consistent with the finding of Allison et al. [3]. Estimate of the effective dimension (D) of the protein structure is consistent with the estimates reported by Uversky et al. [4]. Self-organizing dynamics of lysozymes (an amyloid protein) is investigated in detail [5] as function of temperature and protein concentration (effect of crowding) and made several interesting observations. For example, the dynamics of an isolated lysozyme is ultra-slow (quasi-static) at low temperatures and becomes diffusive asymptotically on raising the temperature. In contrast, the presence of interacting proteins leads to concentration induced protein diffusion at low temperatures and concentration-tempering sub-diffusion at high temperatures.

Investigations of the thermal response of membrane proteins (corA, hHv1) have been initiated recently and made some interesting observations already. For example, the inner (icorA) and outer (ocorA) segments of the transmembrane corA protein exhibit [5] asymmetrical thermal response to its conformations. Very recently, conformational response of the transmembrane segments of a voltage-gated human proton channel (hHv1) is also examined and find contradictory thermal response in native phase and high temperature denatured phase.

Keywords: coarse-grain model, computer simulations, proteins

Acknowledgement: RBP acknowledges generous support from the Chulalongkorn University where some of the recent work is performed in our on-going collaboration with the research group of Prof. Pornthep Sompornpisut. Warm hospitality of the Chemistry Department at the Chulalongkorn University is gratefully acknowledged.

REFERENCES

1. Fritsche, M., Pandey, R.B., Farmer, B.L., and Heermann, D.W. *PLoS One* 2013, **8**, e64507-1-e64507-6
2. Mirau, P., Farmer, B.L., and Pandey, R.B., *AIP Advances* 2015, **5**, 092504-1 - 092504-9.
3. Allison, J. R., Varnai, P., Dobson, C. M., and Vendruscolo, M. *J. Am. Chem. Soc.* 2009, **131**, 18314-18326.
4. Uversky, V.N., Li J., Souillac P., Doniac S., Jakes R., Goedert M., and Fink A.L., *J. Biological Chem.* 2002, **277**, 11970-11978.
5. Pandey, R.B., Farmer, B.L., Bernard S. Gerstman, B.S., *AIP Advances* 2015, **5**, 092502-1 - 092502-12.
6. Kitjaruwankul, S., Khrutto, C., Sompornpisut, P., Farmer, B.L., and Pandey, R.B. *J. Chem. Phys.* 2016, **145**, 135101-1 - 135101-7.

	After Ph.D. from IIT Roorkee in 1981, Prof. Pandey started at the North Carolina State University as a visiting assistant professor before his postdoctoral work at Cologne University, University of Cambridge, University of Georgia (1983-1985). He became assistant professor at the Jackson State University in 1985 and moved to University of Southern Mississippi where he is professor of physics is for about 30 years (1988-current). His research spans over a wide range of application of statistical physics (transport and flow of fluid in porous media, polymer chains, sol-gel, interface and roughness, nano-bio-composites, protein). He has published over 150 papers in refereed journals. He is an academic editor of AIP Advances (American Institute of Physics) and has served in many committees (panel for research funding, program review, promotion etc.). He has visited many institutions and collaborated with numerous research groups around the world. He is currently visiting Department of Chemistry at the Chulalongkorn University.

BIO
-I-
2

pKa Prediction in Biological Systems Based on the Statistical Mechanics Theory of Liquids

Norio Yoshida[1,C]
[1] *Department of Chemistry, Graduate School of Science, Kyushu University,
744 Motooka, Nishiku, Fukuoka, Japan*

[C] ***E-mail***: *noriwo@chem.kyushu-univ.jp;* ***Fax***: *+81 92 802 4133;* ***Tel.*** *+81 92 802 4133*

ABSTRACT

There are three universal molecular-processes observed in life phenomena, namely self-organization, molecular recognition, and chemical reaction. All these processes in living system do not work spontaneously in the condition in which the molecules are isolated in vacuum. It means water plays essential role in the processes. Therefore, to consider the processes, the theory should describe the solvent environment properly. Recently, we developed the methods to tackle the biological processes in water based on the statistical mechanics theory of liquids which is referred as three-dimensional reference interaction site model (3D-RISM) theory.[1,2] The 3D-RISM theory and its extended versions are successfully applied various chemical and biological processes in solution.

One of the most important processes in biological systems is a proton transfer reaction, namely protonation and de-protonation processes. The protonation state sometime determines the reactivity of enzyme, the structural stability, solubility of molecule and so forth. Therefore, the development of the methods to predicting the protonation states is highly desired.

In this talk, we review our recent studies on the p*K*a change of drug molecule in solution and the development of the method for p*K*a prediction based on the 3D-RISM-SCF theory.

Changes in the p*K*a of *p*-carboxybenzeneboronic acid (PCBA) upon complex formation with monosaccharide are considered by using the 3D-RISM-SCF theory. The p*K*a of PCBA is lowered through complex formation, which is consistent with experimental observations. (Figure 1.) Free energy component analysis of the dissociation reaction was performed to investigate the details of the contribution to the p*K*a shift. The magnitudes of the changes in both the electronic energy and the solvation free energy were smaller for the PCBA-complex than for PCBA. These smaller changes can be attributed to the delocalization of the excess charge and to a reduction of the solvent-accessible area near the boric acid group because of the steric bulk of the monosaccharide.

In the above study, we used a simple scheme to adjust overestimated computed p*K*a values. The corrected values worked well in our investigation; however, accurate p*K*a prediction is essential, and an elaborated method beyond the simple empirical correction used above is highly anticipated. Therefore, we proposed an efficient algorithm to predict p*K*a a value of dissociative amino acid in the protein based on the 3D-RISM-SCF theory. In the method, p*K*a value of amino acids is evaluated using least square fitting using parameters determined for small reference molecules, which is analogue of the method proposed by Matsui et al.[5] Using this scheme, we can obtain a semi-quantitative p*K*a value of specific chemical groups, like COOH, NH_3^+, and so on. We estimate p*K*a value of amino acid (Asp,

Glu, Lys, Cys, Try, His and Ser) with parameters. The results quantitatively agree with the experimental results.

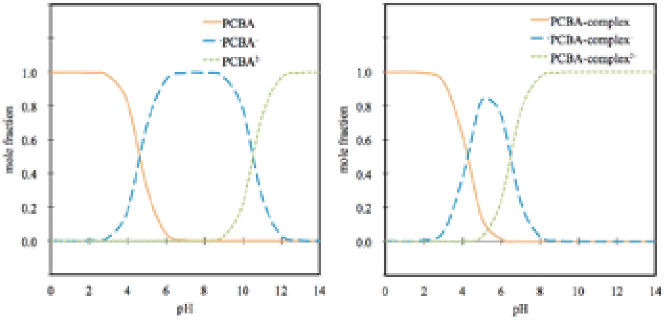

Figure 1. **p*K*a shift of PCBA by the complex formation with monosaccharide.**

Keywords: p*K*a, 3D-RISM-SCF theory, Molecular orbital method, Solvent effects.

REFERENCES

1. Yoshida, N., Nishiyama, K., *Handbook of Computational Chemistry*, Leszczynski et al. (eds.), Springer 2016
2. Yoshida, N., Imai, T., Phongphanphanee, S., Kovalenko, A., Hirata, F., *J. Phys. Chem. B., feature article*, 2009, **113**, 873-886.
3. Seno, Y., Yoshida, N., Nakano, H., *J. Mol. Liquids*, 2016, **217**, 93-98.
4. Kasai, Y., Matsui, T., Shigeta, Y., Yoshida, N., Nakano, H., *In preparation*.
5. Matsui, T., Baba, T., Kamiya, K., Shigeta, Y., *Phys. Chem. Chem. Phys.*, 2012, **14**, 4181-4187

Norio Yoshida is an associate professor of Kyushu University. He graduated as a Ph.D. from Kyoto University in 2003 with a Ph.D. thesis on the electronic structure theory of solvated molecules. His research interest includes theory of solvent effects on electronic structure of molecule and molecular thermodynamics in solution.

BIO
-I-
3

Simulational Studies of Aβ Amyloid Fibrils by Equilibrium and Nonequilibrium Molecular Dynamics Method

Hisashi Okumura[1,2,C]
[1] *Institute for Molecular Science, Okazaki, Japan*
[2] *The Graduate University for Advanced Studies, Okazaki, Japan*

[C] ***E-mail**: hokumura@ims.ac.jp; **Fax**: +81 564 55 7277; **Tel.** +81 564 55 7025*

ABSTRACT

Amyloids are insoluble and misfolded fibrous protein aggregates and associated with more than 40 serious human diseases. For example, amyloid-β fibrils (Aβ) are known to be associated with the Alzheimer's disease. We performed molecular dynamics (MD) simulations of Aβ fibrils in explicit water. We discovered that molecular structure is different between two ends: The two β-sheets β1 and β2 are close to each other. On the other hand, at the odd end the Aβ peptide fluctuates more and takes an open form, too [1]. Our theoretical prediction was proved by experiment after our MD simulations. We also performed nonequilibrium molecular dynamics simulations of an Aβ fibril in explicit water under supersonic wave to mimic some experimental reports that cavitation disrupts amyloid fibrils [2]. We found that when the pressure was decreased to a negative value, a bubble formation was observed. When the pressure was increased to a positive value, water molecules attacked the hydrophilic residues, the bubble collapsed, and the fibril was disrupted.

Keywords: Molecular Dynamics, Amyloid Fibril.

REFERENCES

1. H. Okumura and S. G. Itoh, *Sci. Rep.* **6** (2016) 38422 (9 pages).
2. H. Okumura and S. G. Itoh, *J. Am. Chem. Soc.* **136** (2014) 10549-10552.

Hisashi Okumura was born in 1975 and got his Ph.D. degree from Faculty of Science and Engineering, Keio University. He moved to University of Tokyo as a postdoctoral fellow of the Japan Society for the Promotion of Science for Young Scientists. He then moved to Institute for Molecular Science as a research associate. After he worked at Rutgers University in USA, got his present position of associate professor at Institute for Molecular Science.

BIO
-I-
4

Computer-Aided Drug Discovery: From Small Compounds to Protein Inhibitors Against Tyrosine Kinase of EGFR

Kiattawee Choowongkomon[1,C], Napat Songtawee[2], Leucha Tabtimmai[1], Siriluk Ratanabunyong[1], Bundit Booyarit[1],Orathai Sawadeechaikul[3],Ninnutt Moonrin[1], Wanwimon Mokmark[1], and Prapasiri Suphakun[1]

[1]*Department of Biochemistry, Faculty of Science, Kasetsart University, 50 Ngam Wong Wan Rd, Bangkok, Thailand*
[2] *Department of Clinical Chemistry, Faculty of Medical Technology, Mahidol University, Nakhon Pathom, Thailand*
[3]*Institute of Food Research and Product Development, Kasetsart University, 50 Ngam Wong Wan Rd, , Bangkok, Thailand*

[C] ***E-mail**: fsciktc@ku.ac.th; **Fax**: +66 2 561 5555; **Tel.** +66 8 5555 1480*

ABSTRACT

Computational studies are an essential part of research in Biochemistry today. The goal of theoretical investigation of biochemical processes is to gain a deeper insight into the molecular mechanism behind the process of study. It can further be used to predict the results of experiments. Protein Bioinformatics is a useful technique to understand biochemical processes of proteins on various levels including protein modeling, protein docking, and protein molecular dynamics. In our group, we focus on the anticancer targeted protein, the epidermal growth factor receptor (EGFR). This protein plays a crucial role in cellular signaling pathways that regulates key functions, especially proliferation. The EGFR abnormalities have been associated with several types of human cancer. Nowadays, there are cancer-treated drugs that inhibit the activity of tyrosine kinase (TK) domain of EGFR – a signaling part of this protein. However, each drug specifically treats with each cancer type and some tumor patients have resisted to those drugs. A discovery of better new efficient inhibitors is extremely needed. The virtual screening of compound databases, engineering peptide inhibitors, and screening nanobody library against EGFR-TK have been used to discover new inhibitors. These inhibitors including compounds, peptides, and nanobodies were tested on enzymatic inhibiting assay and non-small cell lung cancer cells, A549. Furthermore, the molecular dynamics simulation has been applied for the complex of the EGFR-TK with inhibitors and their asymmetric homodimer and heterodimer dimers to understand the molecular interaction.

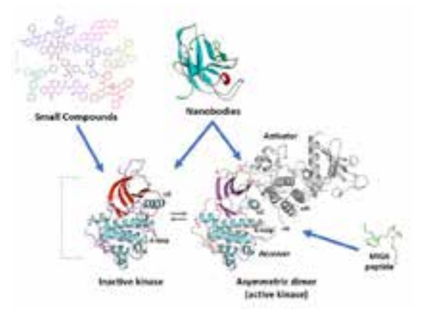
Small Compounds
Nanobodies
Activator
Inactive kinase
Receiver
MIG6 peptide
Asymmetric dimer
(active kinase)

Figure 1. Three inhibitors against tyrosine kinase of EGFR: small compounds, engineering MIG6 peptides, and nanobodies

Keywords: Computational Science, Computational Conferences.

REFERENCES

1. Choowongkomon, K., Sawatdichaikul, O., Songtawee, N., Limtrakul, J., Molecules, 2010, 15, 4041-4054
2. Sawatdichaiku O., Hannongbua S., Sangma C., Wolschann P., and Choowongkomon K., J Mol Model, 2011, 17, 1-14.
3. Songtawee N, Gleeson MP, Choowongkomon K. J Mol Model, 2013 ,19(2), 497-509.
4. Moonrin N; Songtawee N; Rattanabunyong S; Chunsrivirot S; Mokmak W; Tongsima S, Choowongkomon K., *BMC Bioinfor*., 2015, 16(1),103.
5. Songtawee, N.; Bevan, D.R.; Choowongkomon, K., *J. Mol. Graph. Model.,* 2015, 58, 16-29.

	Associate Professor at Department of Biochemistry, Faculty of Science Kasetsart University, Bangkok, Thailand. Graduated Ph.D. from Cell Physiology Program at Department of Cell Physiology and Biophysics, Case Western Reserve University, Ohio, USA. Interesting in drug discovery against virus and cancer by using computational biochemistry.

BIO
-I-
5

Enzyme Catalysis that Paves the Way for S-Sulfhydration *via* Sulfur Atom Transfer

Gou-Tao Huang[1] **and Jen-Shiang K. Yu**[1,2,C]
[1] *Department of Biological Science and Technology, National Chiao Tung University,*
No.75 Po-Ai St, Hsinchu City 300, Taiwan
[2] *Institute of Bioinformatics and Systems Biology, National Chiao Tung University,*
No.75 Po-Ai St, Hsinchu City 300, Taiwan

[C] ***E-mail**: jsyu@mail.nctu.edu.tw;* ***Fax**: +886 3 5729288;* ***Tel.** +886 3 5729287*

ABSTRACT

Mercaptopyruvate sulfurtransferase (MST) catalyzes sulfur transfer from mercaptopyruvate to sulfur acceptors, and the initial step of the catalytic reaction is the formation of cysteine persulfide via the S-sulfhydration of the corresponding cysteine residue in the active site. Mechanism of sulfur transfer for S-sulfhydration is generally anticipated to proceed through the transfer of the SH group (Nu−SH••••$^-$S−R → Nu$^-$••••HS−S−R), and the other route involves the sulfur atom (S^0) transfer occurring between two sulfhydryl anions (Nu−S$^-$••••−S−R → Nu$^-$••••−S−S−R) and is considered electrostatically unfavorable. In the enzyme system of human MST (PDB code: 4JGT), theoretical calculations at the level of ONIOM(M06-2X:Amber99sb) demonstrate that the S^0 transfer is more kinetically favorable than the SH transfer. The Ser250 residue of the Ser250/His74/Asp63 triad around the active site first deprotonates the sulfhydryl group of the mercaptopyruvate substrate to initialize the S^0 transfer, and additionally stabilizes the product in the form of pyruvate enolate with hydrogen-bond interactions. An electrostatic-interaction model is concluded to account for the S^0 transfer: the relatively electron-rich region of the S^0 atom being transferred interacts with its surrounding NH/OH groups of the Cys248-Gly249-Ser250-Gly251-Val252-Thr253 (CGSGVT) loop, which structurally orients the electron-deficient region of the S^0 atom facing toward the lone-pair electrons of the sulfhydryl anion of Cys248. Analyses of electrostatic potentials and frontier orbitals exhibit that the specific conformation of this CGSGVT loop not only stabilize the sulfhydryl/persulfide anions of the Cys248 residue, but is also able to enhance the electrophilicity of the persulfide anion. The S^0 transfer which is seldom regarded possible is hence, facilitated by both of the triad and the loop effects of the catalytic enzyme. The specificities that MST binds mercaptopyruvate while rhodaneses (*a.k.a.* thiosulfate sulfurtransferases) bind thiosulfates, are also explained by the simulations.

Keywords: Mercaptopyruvate sulfurtransferase, Persulfidation, Rhodanese.

REFERENCES

1. Huang, G.-T., and Yu, J.-S.K., *J. Phys. Chem. B*, 2016, **120**(20), 4608-15.

	Experiences: Professor (2016 –), associate professor (2012–2016), assistant professor (2007–2012), National Chiao Tung University, Taiwan Research area of interest: Enzymetic catalysis, Computational Chemistry, Theoretical coordination chemistry

BIO
-I-
6

Oligomerization Pathway of Amyloid-B Fragments Studied by the Hamiltonian Replica-Permutation Method

Satoru G. Itoh[1,2,C]
[1] *Department of Theoretical and Computational Molecular Science, Institute for Molecular Science, Okazaki, Aichi, Japan*
[2] *Department of Structural Molecular Science, The Graduate University for Advanced Studies, Okazaki, Aichi, Japan*

[C] ***E-mail**: itoh@ims.ac.jp; **Fax**: +81 564 55 7025; **Tel.** +81 564 55 7465*

ABSTRACT

The amyloid-β peptides (Aβ) form amyloid fibrils which are associated with Alzheimer's disease. It is necessary to clarify the oligomerization process of Aβ in order to understand the amyloid fibril formation process and to find a remedy for Alzheimer's disease. To investigate the oligomerization process of Aβ, we applied the Hamiltonian replica-permutation method (HRPM) [1-3] to Aβ fragments, Aβ(29-42) peptides, in explicit water solvent. Aβ(29-42) consists of the residues 29 to 42, which correspond to the transmembrane domain of Aβ. The length of Aβ after residue 29 is a critical determinant of the amyloid formation rate. Moreover, this fragment forms amyloid fibrils by itself. HRPM combines the advantages of RPM and the Hamiltonian replica-exchange method (HREM). RPM is a better alternative to REM. In RPM, temperature permutations among more than two replicas are performed with the Suwa-Todo algorithm. In HREM, by exchanging the parameters that are related only to limited degrees of freedom, the number of replicas can be decreased in comparison with REM. In our presentation, we will introduce HRPM and show the oligomerization process of Aβ(29-42) [4].

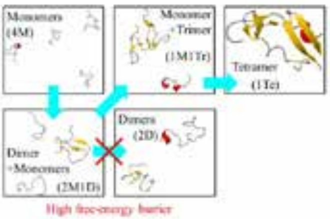

Figure 1. Tetramer formation pathway of Aβ fragments.

Keywords: Amyloid-beta peptides, Molecular dynamics simulation, Generalized-ensemble algorithm.

REFERENCES

1. S. G. Itoh and H. Okumura, *J. Chem. Theory Comput.* 2013, **9**, 570-581.
2. S. G. Itoh and H. Okumura, *J. Comput. Chem.* 2013, **34**, 2493-2497.
3. S. G. Itoh and H. Okumura, *J. Phys. Chem. B* 2014, **118**, 11428-11436.
4. S. G. Itoh and H. Okumura, *J. Phys. Chem. B* 2016, **120**, 6555-6561.

Satoru G. Itoh, Ph.D.
Assistant Professor
Institute for Molecular Science, Japan
Birth Year: 1978
Education: 2005 Ph.D. School of Physical Sciences, The Graduate University for Advanced Studies
Area of research: Computational biophysics

BIO
-I-
7

Reaction Model for Circadian Rhythm of Kai System Considering Elementary Processes

Shin-ichi Koda and Shinji Saito
Institute for Molecular Science, Okazaki, Aichi, Japan
The Graduate University for Advanced Studies, Okazaki, Aichi, Japan

E-mail: *shinji@ims.ac.jp,* ***Tel:*** *+81-564-55-7300*

ABSTRACT

A circadian rhythm is a biological endogenous oscillation of approximately 24 hours widely seen from prokaryotes to higher organisms. The simplest circadian clock is found in cyanobacteria whose oscillation consists of only three proteins, KaiA, KaiB, and KaiC.[1] More interestingly, it was discovered from an in-vitro experiment the circadian rhythm of phosphorylation of KaiC in the presence of KaiA, KaiB, and ATP.[2] Because of the simplicity of Kai system, various experimental studies have been performed to examine structures and functions of Kai system after the reconstruction experiment. As a result, it was revealed that the circadian rhythm is due to the phosphorylation cycle of S431 and T432 in the so-called CII domain in KaiC, induced by the interactions of KaiA and KaiB.[3] It was also recently reported that the ATPase activity in another domain, called CI domain, in KaiC is proportional to the frequency of phosphorylation cycle.[4] In addition to experimental studied, theoretical studies have been conducted to understand the circadian rhythm of Kai system[5]. In almost all theoretical studies, however, only the phosphorylation states of S431 and T432 have been considered and, but the ATP hydrolysis reactions in KaiC have not been considered explicitly. Here we present a simple but semi-quantitative reaction model, which can successfully reproduce not only the circadian rhythm but also several other experimental results of Kai system.[6]

Keywords: Circadian rhythm, reaction model, Kai system, phosphorylation, ATP hydrolysis

REFERENCES

1. Ishiura M., et al., *Science*, 1998, **281**, 1519-1523.
2. Nakajima M., et al., *Science*, 2005, **308**, 414-415.
3. Nishiwaki T., et al., *EMBO J.*, 2007, **26**, 4029-4037.
4. Abe J., et al. *Science*, 2015, **348**, 312-316.
5. For example, Phong C., et al., *Proc. Natl. Acad. Sci. U.S.A.*, 2013, **110**, 1124-1129.
6. Koda S., & Saito S., to be submitted.

Shinji Saito received his B.S. and M.E. from Keio University and Kyoto University. He got his Ph.D. from The Graduate University for Advanced Studies in 1995. He joined Nagoya University as a research associate in 1994 and became an associate professor in 1998. He has been a professor in Institute for Molecular Science (IMS) since 2005. He has been the chair of Department of Theoretical and Computational Molecular Science (since 2012) and the director of Research Center for Computational Science (since 2011) in IMS.

His research interest is theoretical analyses of hierarchical and heterogeneous dynamics and of properties, functions, and reactions in condensed phase systems e.g., liquids, glasses, and proteins.

BIO
-I-
8

Computational Design of Protein Inhibitor for Dengue Envelope Protein

Vannajan Sanghiran Lee [1]
[1] *Department of Chemistry, Centre of Theorectical and Computational Physics (TCP), Faculty of Sciecne, University of Malaya, 50603 Kuala Lumpur, Malaysia,*

***E-mail**: vannajan@gmail.com; **Tel.** +6016 320 8906 **Fax**: +603 7967 4193*

ABSTRACT

Designed Ankyrin Repeat Proteins (DARPins) are one of the most studies repeat proteins and has demonstrated antiviral property towards HER2 and HIV. It encourages exploration on existed DARPins for their potential in replacing monoclonal antibody to bind with DIII dengue virus. The presentation will cover the engineered of DARPIN under molecular docking and long time scale Molecular Dynamics (MD) simulations for refinement. Docked complexed of DARPins and DIII are generated through HADDOCK [1,2]. MMGBSA protocol using the MD trajectories collected is further decomposed on a per residue basis to reveal the binding affinity. Site-directed mutagenesis under SAAMBE [3] and BeAtMuSiC [4] web server were selected on randomized residue in ankyrin which does not disturb the structural framework. ΔΔG is predicted for each replacement. Dissecting the interactions mediated between DIII and DARPins permit a better understanding on rational computational protein/peptide design.

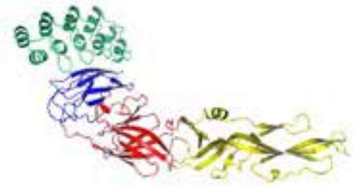

Figure 1. DARPins (green) bound to Domain III Dengue Envelope Protein.

Keywords: Protein engineering, Molecular dynamics, DARPins, Peptide, Computational site-directed mutagenesiss.

REFERENCES

1. Zundert, G.C.P Van., Rodrigues, J.P.G.L.M., Trellet, M., and Schmitz, C., J. Mol. Biol., 2016, 428(4), 720–5.
2. Vries, S.J. De., Dijk, M. Van., and Bonvin, A.M.J.J., Nat. Protoc., 2010, 5(5), 883–97.
3. Petukh, M., Dai, L., Alexov, E., Int. J. Mol. Sci., 2016, 14(4), 547.
4. Dehouck, Y., Kwasigroch, J.M., Rooman, M., and Gilis, D., Nucleic Acids Res., 2013, 41, 333–9.

Dr. V. S. Lee received her BSc (1994) in Chemistry from Chiang Mai University, Thailand and PhD (2001) in Pharmaceutical Sciences and Physical Chemistry from University of Missouri-Kansas City, USA under the scholarship from the Institute of Promotion and Development Science and Technology Project, Thailand. Her present research interest includes computer-aided molecular modeling, bioinformatics and computational chemistry using Molecular Dynamics (MD), Monte Carlo Simulations (MC) and Quantum Mechanics (QM), particularly in protein design and modification for Dengue and HIV-1 research.

BIO
-I-
9

Databases in Chemistry and Biology

Peter Wolschann[1,2*]
[1]*Institute of Theoretical Chemistry, University of Vienna, A-1090, Vienna, Austria*
[2] *Department of Pharmaceutical Technology and Biopharmaceutics, Faculty of Life Sciences, University of Vienna, A-1090, Vienna, Austria*

***E-mail**: karl.peter.wolschann@univie.ac.at **Tel.** +43(1) 4277 52772*

ABSTRACT

Modern scientific research creates big amount of information and in many cases the corresponding data are collected in proper databases. Many of these data banks are freely accessible via internet and are extensively used by many researchers. The retrieval of data sets of interest is enabled by fast algorithms as well as by convenient software packages for subsequent evaluation and detailed analysis of the own, experimentally obtained data. Two different data banks together with subsequent software packages will be introduced. 13C NMR spectra are characterized by a relatively large chemical shift dispersion and depend on a limited number of molecular properties. Therefore, this type of spectra is rather convenient for the application of computational data storage. The CSEARCH database, developed by Wolfgang Robien (University of Vienna) contains some 700,000 13C NMR spectra. Due to very sophisticated search algorithms the identification of compounds by their 13C NMR spectrum is fast and of high accuracy. Moreover, the content of the database allows the prediction of NMR- spectra of new compounds and vice versa creating structure proposals from their 13C NMR spectral data. In biology, biochemistry and pharmaceutical drug design the Protein Data Bank is a well-known source of structures of proteins, nucleic acids and carbohydrates together with organic and inorganic ligands. The combination with databases of drug-like compounds (in the particular case the ZINC data base with be described) a screening for substances fitting to a binding pocket can be performed to obtain lead candidates for further drug finding. The program package LigandScout developed by Thierry Langer (University of Vienna) allows a fast and efficient virtual screening procedure of large data sets.

A.Univ.Prof.Dr.Peter Wolschann is a professor at Institute of Theoretical Chemistry, and Department of Pharmaceutical Technology and Biopharmaceutics, Faculty of Life Sciences, University of Vienna. He has more than 199 publications in internationally well-known impact factor journals on his credit. Current research interests lied in the field of Computational Biochemistry. In particular, Molecular Modeling on Cyclodextrin Inclusion Complexes and Membrane Proteins (GPCR and Ion channels), Drug Design and Database screening, Structure-Activity Relationships and Hydrogen Bonding interaction. The professional activities are lecture about spectroscopy, molecular modeling, drug design at University of Vienna (Austria), Taschkent University (Uzbekistan), Kasetsart University and Chulalongkorn University (Thailand).

BIO
-I-
10

Molecular Insight of Recombinant Interleukin-18 as a Model for Functional Protein Design

Jirakrit Saetang [1], Aekkachai Puseenam [2], Niran Roongsawang [2], Supayang Piyawan Voravuthikunchai [3], Surasak Sangkhathat [1,4] and Varomyalin Tipmanee [1,C]

[1] Department of Biomedical Sciences, Faculty of Medicine, Prince of Songkla University, Songkhla, Thailand

[2] Microbial Cell Factory Laboratory,Bioresources Technology Unit, National Center for Genetic Engineering and Biotechnology, National Science and Technology Development Agency, Pathum Thani, Thailand

[3]Department of Microbiology, Natural Product Research Center of Excellence, Faculty of Science, Prince of Songkla University, Songkhla, Thailand

[4] Department of Surgery, Faculty of Medicine, Prince of Songkla University, Songkhla, Thailand

*[C] **E-mail**: tvaromya@medicine.psu.ac.th ; **Tel.** +66 7 445 1180*

ABSTRACT

In recent years, cytokine-mediated therapy, one of immunotherapy approach, has emerged as further advance alternative in cancer therapy. Interleukin-18 (IL-18) has exhibited interesting anti-cancer properties especially when combined with IL-12. We successfully engineered IL-18 in order to improve its activity using single point mutagenesis using both bioinformatics via interaction-based analysis as well as protein expression in yeast system. The engineered protein also known as a recombinant protein synthesized from *Pichia pastoris*, was purified, and then measured the activity by treating with the NK-92MI cell line to evaluate interferon-γ (IFN-γ) stimulation. Some recombinant IL-18 exhibits significantly higher activity with respect to wild-type interleukin-18, ranging from a factor of 4 up to 16. Furthermore, molecular dynamics studies have played an essential role as a molecular microscopy to elucidate the IL-18 structure and provide a molecular insight of a recombinant IL-18. Our findings could provide the combinatorial approach between computer-aided method (structure prediction, *in silico* mutagenesis and molecular dynamics simulation) and experiments (cloning, mutagenesis and protein expression) to design a functional protein with a desirable activity so that it can enhance some disease-preventive characteristics such as anti-cancer or slowing cancer progression.

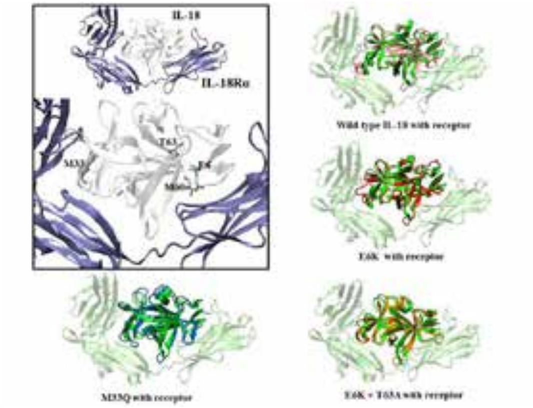

Figure 1. Model of recombinant IL-18's with its counterpart receptor

Keywords: Interleukin-18, Cytokine-mediated therapy, Molecular dynamics, Immunotherapy

REFERENCES

1. Saetang, J., Puseenam, A., Roongsawang, N., Voravuthikunchai, S.P., Sangkhathat, S., and Tipmanee, V., *PLoS One*, 2016, **11**(8), e0160321.
2. Sutsumi, N., Kimura, T., Arita, K., Ariyoshi, M., Ohnishi, H., Yamamoto, T., et al., *Nat. Commun.*, 2014, **5,** 5340.
3. Kato Z, Jee J, Shikano H, Mishima M, Ohki I, Ohnishi H, et al. *Nat. Struct. Biol.*, 2003, **10,** 966–71.

Dr Varomyalin Tipmanee had read PhD in Chemistry under a supervision of Prof Dr Jochen Blumberger at Darwin College, Cambridge. In September, 2012 Dr Tipmanee got a position in Department of Biomedical Sciences, Faculty of Medicine, Prince of Songkla University and his current research is based on a molecular dynamics simulation of protein structure and a virtual screening of some active molecules, such as active anti-cancer compounds, active compounds/proteins against drug-resistant bacteria, and disease-related enzyme.

BIO
-I-
11

The Vitality of Swivel Domain Motion in Performance of Enzyme I of Phosphotransferase System; A Comprehensive Molecular Dynamics Study

Gul Sanober[1], Saad Raza[1], Thanyada Rungrotmongkol[2,3] and Syed Sikander Azam[1*]
[1] *Computational Biology Lab, National Center for Bioinformatics, Quaid-i-Azam University Islamabad, Islamabad 45320, Pakistan*
[2] *Structural and Computational Biology Research Group, Department of Biochemistry, Faculty of Science, Chulalongkorn University, Bangkok 10330, Thailand*
[3] *Ph.D. Program in Bioinformatics and Computational Biology, Faculty of Science, Chulalongkorn University, Bangkok 10330, Thailand*

[C] ***E-mail**: syedazam2008@gmail.com , ssazam@qau.edu.pk* ***Tel.*** *+925190644130*

ABSTRACT

Enzyme I (EI) of bacterial phosphotransferase system is involved in the first step of the carbohydrate metabolism pathway. Due to its importance in bacterial survival and low similarity with human proteins, EI is an attractive drug target. With the aid of Computer Aided Drug Designing tools, we studied EI of Staphylococcus epidermidis, which recently adopted itself as a major etiological agent in discerning the cause of multi-drug resistant nosocomial infections of implanted medical devices. Due to a non-existent crystal structure, a high quality homology model of EI is predicted. Molecular docking analysis of potential inhibitors into the active site of the protein is performed and the best inhibitor is selected with according to the highest GoldScore (76.53). The protein-ligand complex was conducted through a 100 ns MD simulation. The trajectory analysis reveals that the N-terminal domain (EIN) and the P-His domain residues exhibited the greatest conformational changes whilst the active site shows minimum residual fluctuations and is considered as the most stable domain. The rigid body motions of EIN and P-His domain are recorded to be at their highest during the 35th and 83rd ns with highest RMSD values. Despite the highly flexible 'personality' of EI, the ligand remains tightly associated with the active site residues. The current lead compound holds potential as an effective drug against S. epidermidis which could be further tested in clinical settings. The dynamic nature of EI disclosed via MD simulation, can be further explored to understand the molecular kinetics of chemical reactions involved in the dedicated role of the protein would assist in better design of drugs in future.

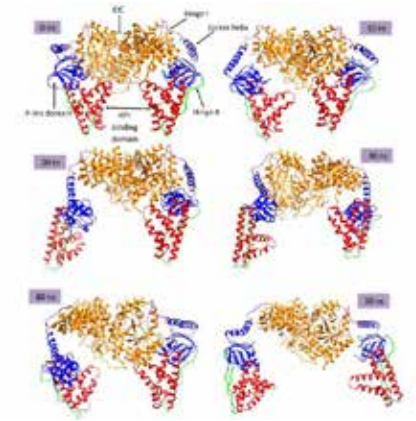

Figure 1. The screen shots of S. epidermidis EI at 0 ns, 10 ns, 20 ns, 30ns, 60ns, and 90 ns. The orange shows the EIC, red represents the EIN and P-His domain is shown in blue. The hinge I and hinge II are represented by green and purple, respectively.

Keywords: Molecular Dynamics Simulation; Enzyme I; Phosphotransferase system of S. epidermidis; EI protein dimerization; hinge movement; swivel domain motion.

	Dr. Sikander has more than 50 publications in internationally well-known impact factor journals on his credit. He has accomplished his Ph.D from the University of Innsbruck, Austria, in the field of Theoretical and Computational Chemistry on an Austrian Scholarship. He is an Ernst Mach Fellow and won international grants from International Foundation for Science and PakUS STCP Program. Current research interests lied in the field of Computational Biochemistry. In particular, Molecular Docking and Molecular Dynamic (MD) Simulations of proteins for understanding structural and dynamical aspects of the biological system. He attended and organized various national and international conferences and head of a computational biology lab at the National Centre for Bioinformatics which helps to maintain the synergistic relationship with the experimental research work carried out on various proteins at the resource lab of the institute.

BIO
-I-
12

Sequencing Data Deluge: Thailand Challenges in Big Data Analytics

Supasak Kullawonganunchai[1], Chumpol Ngamphiw[1], Sissades Tongsima[1*]
[1] *Bioinformatics Laboratory, Genome Technology Research Unit, National Center for Genetic Engineering and Biotechnology (BIOTEC), National Science and Technology Development Agency (NSTDA), Thailand Science Park, Pathum Thani, Thailand 12120*

[*] ***E-mail**: sissades@biotec.or.th; Tel. +66 2 564-6700*

ABSTRACT

About 30 years ago, DNA sequencing with a bold idea of analyzing the entire human genome was considered a breakthrough in modern biological science. With the advent of high throughput sequencing technologies as well as high competition in this business, the cost of sequencing has been reduced dramatically, supporting scientists to better our understanding of living organisms. Various DNA applications to predict traits are being introduced to markets. These include breed improvement via marker assisted selection (MAS) in plants and animals or checking a person DNA for potential risk of having adverse drug reaction. The once breakthrough technology is now accessible through various competitive sequencing service providers which have brought genome sequencing to the cusp of common DNA testing practice. The amount of sequencing data and their generation rate would surely fit the definition of big data, yet with some unwelcoming twists. Unlike other big data that have been constantly collected over accessing the Internet, DNA sequencing data are rather private, requiring reliable curator(s) and policy makers to manage. Such data will be generated by both local laboratory and some service providers. Nonetheless, large amount of data cannot be moved around efficiently. Current (decent) cloud computing services are available outside Thailand, making it very difficult to address both aforementioned issues. Even though there are some standard analytics to process the data, these analytics are not so straightforward that map-reduce paradigm can be easily deployed.

Sissades Tongsima received his Ph.D. in Computer Science and Engineering in 1999 from the University of Notre Dame, Indiana, USA. He is currently a principal researcher and the head of bioinformatics laboratory, National Center for Genetic Engineering and Biotechnology (BIOTEC). He has published his works in international scientific journals; some of which were highlighted in the Asia-Pacific International Molecular Biology Network (AIMB-N). He has served as an executive committee of the Asia Pacific Bioinformatics Network (APBioNet). He is also an associate editor of the Journal of Human Genetics (JHG).

CSE
-I-
1

AI in Practice: Applications & Challenges

Zong-Yao Chen
Acer Incorporated, Taipei, Taiwan

***E-mail**: gene.chen@acer.com*

ABSTRACT

In the consumer market, Acer is already a well-known brand name by its versatile PC /laptop offerings and StarVR, a joint venture between Acer and Starbreeze Sweden. In recent years, Acer also devoted its pioneering R&D resource on Artificial Intelligent filed with many investments and efforts.

Though the future of Artificial Intelligence will definitely change the way we live, however, during converting AI to real-life applications, Acer's team notice that many challenges arise.

For instance, which is more important for deep learning: Model or data? Accordingly to our experience, we would say that "the data". Sure, Yann LeCun and Geoffrey Hinton et al. have proved the deep neural network can work very well so far, we are eternally grateful and we should. But the problems of data still need to be solved in practice - how should we get the data – the labeled data which we care about? Generative Adversarial Networks, GAN can be a good solution in the future, but so far, GAN has a lot of limitations and it is not yet mature enough. So, what should we do now? In some cases, we use the traditional computer vision methodology to generate the simulation data for deep learning model, and in other cases we use other ways to generate or obtain the training data of deep learning model. It may not be fancy but can work fine to solve real world problem.

	Zong-Yao Chen obtained his Ph.D in Information Management from National Central University, Taiwan in 2015. His experiences are in the areas of project consultant of science & technology policy research and information center (information system development). For now, he is a senior project engineer at Acer Incorporated (Taipei, Taiwan).

CSE
-I-
2

Deep Learning on Hybrid GPU Cluster/Volunteer Computing

Ekasit Kijsipongse [1,C], and **Suriya U-ruekoran** [1]
[1] *NECTEC, National Science and Technology Development Agency (NSTDA),*
111 Thailand Science Park, Pathum Thani, Thailand

[C] ***E-mail**: ekasit.kijsipongse@nectec.or.th;* ***Tel.*** *+66 2564 6900*

ABSTRACT

Deep learning is a very computing intensive and time-consuming task which sophisticated models need amount of computing resource much greater than a single machine can afford. It normally requires GPU clusters to reduce the training time of a deep learning model from days to hours. However, building large dedicated GPU clusters is not always feasible or even effective for most organizations due to the cost of purchasing, operation and maintenance while the systems are not fully utilized all the time. In this regard, volunteer computing can address this problem as it provides additional computing resources at less or no cost. This work presents the hybrid cluster and volunteer computing platform that scales out the training task on GPU clusters into volunteer computers, which the owners contribute the unused computing resources to help in training a deep learning model. The challenge is to align the differences between GPU cluster and volunteer computing systems so as to ensure the scalability transparency. We validate the proposed work with sample cases.

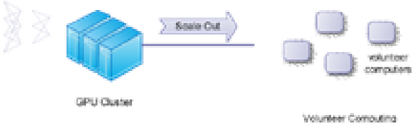

Figure 1. Deep Learning on Hybrid GPU Cluster/Volunteer Computing

Keywords: Deep Learning, Cluster Computing, Volunteer Computing

REFERENCES

1. Anderson D., Boinc: A system for public-resource computing and storage, *Proceedings of the 5th IEEE/ACM International Workshop on Grid Computing*, 2004.
2. Lud¨ascher B., Altintas I., Berkley C., Higgins D., Jaeger E., Jones M., Lee
3. E., Tao J., and Zhao Y., Scientic workow management and the kepler system: Research articles, *Concurr Comput : Pract Exper*, 2006, 18(10):1039-1065.
4. Chilimbi T., Suzue Y., Apacible J., and Kalyanaraman K., Project adam: Building an ecient and scalable deep learning training system, *Proceedings of the 11th USENIX Conference on Operating Systems Design and Implementation (OSDI)*, 2014.
5. Coates A., Huval B., Wang T., Wu D., Catanzaro B., and Ng A., Deep learning with COTS HPC systems, *Proceedings of the 30th International Conference on Machine Learning (ICML)*, 2013.
6. Torque resource manager, http://www.adaptivecomputing.com/products/open-source/torque/

Ekasit Kijsipongse is a researcher at the National Electronics and Computer Technology Center (NECTEC), Thailand. He received his Ph.D. in computer science from Mahidol University in 2009. His research interests include distributed and parallel systems, as well as grid and cloud computing. He is currently working on high performance big data analytics.

CSE
-I-
3

Climate Change Projections Using Statistical Downscaling

Waranyu Wongseree
Department of Electrical and Computer Engineering, Faculty of Engineering,
King Mongkut's University of Technology North Bangkok, Bangkok, Thailand

***E-mail**: waranyu.wongseree@gmail.com; **Fax**: +66 2 585 7350; **Tel.** +66 2 555 2000 x8421*

ABSTRACT

Statistical downscaling is a technique to correct biases and downscale climate variable output of general circulation model (GCM) onto higher spatial resolution for regional climate impact studies. Linear and non-linear statistical downscaling techniques have been used to determine relationship between GCM outputs and observed data during 1970-2005. The performance of statistical downscaling methods is compared in terms of the correlation between the estimated and observed data. The result indicated that non-linear statistical downscaling models provide better results to capture intensity, duration and frequency of climate change signals. These imply non-linear statistical downscaling offers more accurate climate projections at the local scale.

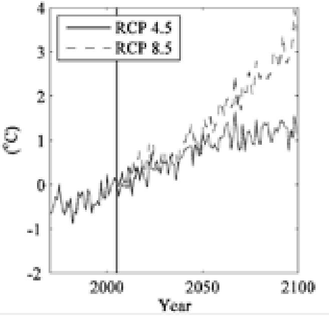

Figure 1. Temperature Change compare to 2005

Keywords: Climate Change, Statistical Downscaling, Machine Learning.

REFERENCES

1. Haylock, M. R., Cawley, G. C., Harpham, C., Wilby, R. L. and Goodess, C. M., *Int. J. Climatol.*, 2006, **26**, 1397–1415.
2. Hempel, S., Frieler, K., Warszawski, L., Schewe, J., and Piontek, F., *Earth Syst. Dynam.*, 2013, **4**, 219–236.
3. Stoner, A. M. K., Hayhoe, K., Yang, X. and Wuebbles, D. J., *Int. J. Climatol.*, 2013, **33**, 2473–2494.
4. Donat, M.G., L.V. Alexander, H. Yang, I. Durre, R. Vose, J. Caesar., *Amer. Meteor. Soc.*, 2013, **94**, 997–1006.

Asst. Prof. Dr. Waranyu Wongseree interests in the areas of machine learning for high-dimensional data and their applications to a variety of challenging problems, including climate modeling, bioinformatics and non-intrusive load monitoring.

CSE
-I-
4

On the Fine Tuning CNN with Pretrained Networks

Chantana Chantrapornchai[1,C]
[1] *Department of Computer Engineering, Faculty of Engineering*
Kasetsart University, Bangkok, Thailand, 10900

[C] ***E-mail**: fengcnc@ku.ac.th*

ABSTRACT

Currently, convolutional neural network (CNN) is a common network for deep learning. Such a network has been utilized for the classification, segmentation, and recognition recently. In this paper, we demonstrate an approach to build the CNN model based on existing ones. Many referenced CNN models were built with large training sets such as AlexNet, GoogLeNet, VGG, SqueezeNet etc. It is believed that several front layers are usually common since they are used to recognize low-level features for image processing while latter layers depend on specific classification task. Thus, existing network weights can be utilized for some front layers while later layers new weights can be learned. Such an approach is also called transfer learning or sometime called fine tuning [5]. The results of fine tuning depend on many factors such as the similarity of new data sets and original data set, the size of data sets, the network architectures, network parameters and others. Table 1 summarizes the performance of fine tuning each net on this data set. It shows the maximum accuracy and minimum loss values obtained in 100,000 iterations. SqueezeNet gives the best performance. It is interesting that its modification from AlexNet can lead to speedup the convergence to high accuracy.

Table 1. Accuracy and loss of fine tuning on LFW.

Net name	Iterations	Accuracy	Loss value
CaffeNet	2,000	0.999	0.0021
AlexNet	12,000	0.997	0.0412
GoogLenet	16,000	0.985 (loss3/top1)	-
ResNet10 (from scratch)	100,000	0.039	8.4531
VGG16	60,000	0.00048	8.6568
SqueezeNet	1,000	1	0.0201

Keywords: Deep learning, Transfer learning, CNN, Fine tuning.

	Chantana Chantrapornchai obtained her B.S. degree from Thammasat University of Thailand in 1991 in Computer Science. She graduated from Northeastern University at Boston, College of Computer Science, in 1993 and University of Notre Dame, Department of Computer Science and Engineering, in 1999, for her Master and Ph.D degrees respectively. She was an associated professor of Dept. of Computing, Faculty of Science, Silpakorn University, Thailand. Currently, she is an associated professor of Department of Computer Engineering, Faculty of Engineering, Kasetsart University, Bangkok, Thailand. Her research interests include parallel processing, GPUs applications (esp. deep learning and semantic query processing), fuzzy and embedded systems, and architecture synthesis.

ORAL PRESENTATION ABSTRACTS

PFD -O- 1

A Variable Multiquadric Shape Parameter in the Dual Reciprocity Boundary Element Method for Convection-Diffusion Problems

Krittidej Chanthawara[1,C], **and Sayan Kaennakham**[2]

[1]Department of Mathematics, Faculty of Science, UbonRatchathani Rajabhat University,
UbonRatchathani, Thailand, 34000.
[2]School of Mathematics, Institute of Science, Suranaree University of Technology, NakhonRatchasima,
Thailand, 30000.

*[C] **E-mail** : krittidej.kku@gmail.com; **Fax**: +66 45-352070; **Tel.** +66 0819992258*

EXTENDED ABSTRACT

Keywords: Multiquadric, Variable Shape Parameter, Convection-Diffusion.

INTRODUCTION

In addition to those well-known traditional numerical methods; finite difference method (FDM), finite element method (FEM), and finite volume method (FVM), Brebbia[1] proposed an alternative method known as 'Boundary element method (BEM)' and it's been drawing attention of both scientists and engineers ever since. Along its' path of development over the years many additional methods have also been invented and developed to strengthen its effectiveness. One of which is that known as the Dual Reciprocity BEM (or DRBEM) where the whole process is divided into two parts: complementary solutions of its homogeneous form and the particular solutions of the inhomogeneous counterpart. In the process of calculating using BEM the so-called Radial Basis Function (RBF) is known to play a very crucial rule in approximating the unknown. Amongst the most popular choices of RBFs, the so-called 'Multiquadric' is known to lead to satisfactory results when a proper value of parameter is given. The main task for researchers is then to provide means of choosing the optimal, if possible, value of this variable. In this paper, we propose a new form of Multiquadric shape parameter and tested it out with convective-diffusive types of problems.

PROPOSED APPROACH

DRBEM starts with considering the Poisson Equation $\nabla^2 u = b$ whose the solution can be expressed as $u = u_h + \hat{u}$. The approximation of b is carried out as a linear combination of interpolation functions in the following form;.

$$b_i(x,y) \approx \sum_{j=1}^{N+L} \alpha_j f_{ij}(x,y)$$

If there are N boundary nodes and L internal nodes, there will be $N + L$ interpolationfunctions,f_j,and consequently $N + L$ particular solutions, $\hat{u}_j$. The particular solution, $\hat{u}_j$, and the interpolation function, f_j, are linked through the relation.

$$\nabla^2 \hat{u}_j = f_j$$

Where $f_j(r,\varepsilon)=\sqrt{\varepsilon_j^2+r^2}$ is the Inverse Multiquadratic (IMQ) RBF with C being its shape function or parameter, normally ‘ad-hoc’ defined.
With more mathematical processes, the final form of solution can be written as follows;

$$u_i = -\sum_{k=1}^{N} H_{ik} u_k + \sum_{k=1}^{N} G_{ik} q_k = \sum_{j=1}^{N+L} \alpha_j \left(c_i \hat{u}_{ij} + \sum_{k=1}^{N} H_{ik} \hat{u}_{kj} - \sum_{k=1}^{N} G_{ik} \hat{q}_{kj} \right)$$

In this work, we are proposing a new variable shape parameter where both linear and exponential manners are taken into consideration, expressed as in equation (1).

$$\varepsilon_j = (1-\zeta)\left[\varepsilon_{\min}^2\left(\frac{\varepsilon_{\max}^2}{\varepsilon_{\min}^2}\right)^{\zeta}\right]^{\frac{1}{2}} + \zeta\left[\varepsilon_{\min} + \left(\varepsilon_{\max} - \varepsilon_{\min}\right)\zeta\right] \qquad (1)$$

Where $\zeta = \dfrac{j-1}{N-1}$ and $j=1,2,\ldots,N$. The automatically self-adjusted parameter ζ is introduced and act as a weight function leading ε_j to equal to the exponential manner when $j=1$. This weight then sets ε_j to become its linear mode when $j=N$.

RESULTS

To demonstrate how effective of the proposed variable, let us consider a 2D convection-diffusion problem in steady state, as given and studied in Gu and Liu [2]. The governing equation is expressed as follows;

$$L(u) = \mathbf{v}^T \cdot \nabla u - \nabla^T(\mathbf{D}\nabla u) + \beta u - q(\mathbf{x}) = 0$$

The computational domain is taken to be $(x,y) \in \Omega = [0,1]\times[0,1]$, and the coefficients are $\mathbf{D} = \begin{bmatrix} \gamma & 0 \\ 0 & \gamma \end{bmatrix}$, $\mathbf{v} = \{3-x, 4-y\}$, and $\beta = 1$ in which γ is a given constant of diffusion coefficient. The boundary conditions are set with $u=0$ on all four sides. The exact solution for this problem is given as $u(x,y) = \sin(x)\left(1-e^{-\frac{2(1-x)}{\gamma}}\right)y^2\left(1-e^{-\frac{3(1-y)}{\gamma}}\right)$.

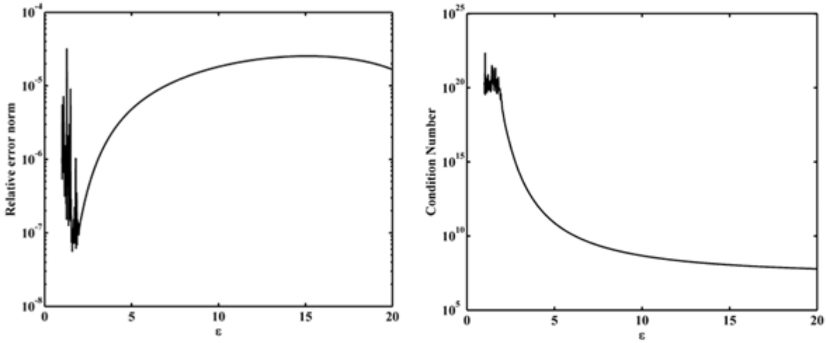

Figure1. left) Relative error norm and right) condition number; obtained from using the propose variable

REFERENCES

1. Brebbia, C.A. and Butterfield, R.L., *Applied Mathmatical Modelling*, 1978, **2**(2), 132-134.
2. Gu, Y.T. and Liu, G.R., *Comput. Mech.*, 2006, **38**, 171-182.

PFD -O- 2 Insight into the Interaction of 8-oxo-dG and DNA Aptamer by Molecular Dynamics Simulation for the Application in Biosonsor

Churtpong Choodet[1,C] **and Theerapong Puangmail**[1]
[1]*Department of physics, Faculty of Science, Khon Kaen University, Khon Kaen, Thailand*

[C] ***E-mail***: *c_churtpong@kkumail.com;* ***Tel.*** *+66 856367365*

ABSTRACT

Aptamers are oligonucleotide molecule (DNA or RNA) that binds to a specific target molecule. They are typically around 15-60 nucleotide bases. Due to a specific binding of the target molecule and DNA aptamer, they are widely used to detect biomarker. 8-oxo-2'-deoxyguanosine (8-oxo-dG) is the biomarker that indicates the risk of cancer such as bile duct cancer. In this work, the interaction between DNA aptamer and 8-oxo-dG was studied by molecular dynamics simulation. It was found that 8-oxo-dG changes the structure of the aptamer from random coil to G-quadruplex. The effect of 8-oxo-dG concentration on the change of the DNA structure was also elucidated. Our simulation results are useful for the development of high selectivity and low limit of detection of the biosensors.

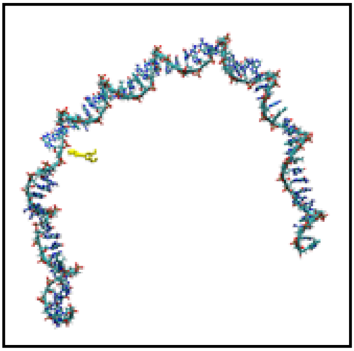

Figure 1

Keywords: Aptamers, G-quadruplex, 8-oxo-dG.

REFERENCES

1. Keefe, A. D., et al. (2010). "Aptamers as therapeutics." Nat Rev Drug Discov 9(7): 537-550.
2. Finkel, T., et al. (2002). "What is oxidative stress." *Japan Medical Association* 45(7): 271–276.
3. Wang, J.-C., et al. (2014). "An ultrasensitive label-free assay of 8-hydroxy-2′-deoxyguanosine based on the conformational switching of aptamer." Biosensors and Bioelectronics 58: 22-26.

PFD
-O-
3

Effect of Size, Shape and Surface Charge on Cellular Uptake of Gold Nanoparticles

Noppamas Yolai[1,C], **Todsaphon Lunnoo**[1], **Jirawat Assawakhajornsak**[1] **and**
Theerapong Puangmali [1,2]
[1] *Department of Physics, Faculty of Science, Khon Kaen University, Khon Kaen, 40002, Thailand*
[2]*Nanotec-KKU, Center of Excellence on Advanced Nanomaterials for Energy Production and Storage,*
Khon Kaen University, 40002,Thailand

[C] ***E-mail****: noppamas_yolai@kkumail.com;* ***Tel.*** *+66 845488488*

ABSTRACT

Gold nanoparticles (AuNPs) have been widely used in biomedical applications, such as photothermal therapy and targeted drug delivery, owing to their unique optical property. To apply AuNPs in biomedical applications, the cellular uptake of AuNPs is a significant factor to be determined. However, the molecular-level mechanism of the cellular uptakes cannot be observed by experiment. Herein, we studied, based on coarse-grained molecular dynamics simulations, the interactions between the realistic plasma membrane and AuNPs with different sizes, shapes and surface charges. The studied shapes include nanohexapod, nanorod and nanocage. For the size effect, the AuNPs entered the PM by direct translocation within 175 ns. For the shape effect, we found that AuNPs with similar size were taken up about the same simulation time. More interestingly, most AuNPs cause inter-pore formation on the PM during the internalization. It was, however, found that after the AuNPs have been internalized, the PM healed itself relying on the size and shape of the AuNPs. This may provide the information to design a proper nanocariers with a high uptake and low cytotoxicity for in vivo applications.

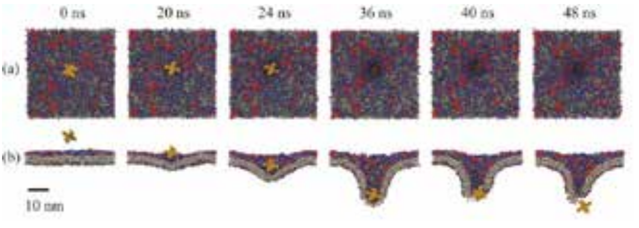

Figure 1. Snapshots of cellular uptake of gold nanohexapod, (a) top view and (b) side view.

Keywords: Gold nanoparticles, Realistic plasma membrane, Coarse-grained, Molecular dynamics simulations**.**

REFERENCES

1. Huang, X., M. A. El-Sayed. Journal of Advanced Research. 2010, **1**(1), 13-28.
2. Wang, Y., et al. Acs Nano. 2013, **7**(3), 2068-2077.
3. Gupta R. and Rai B. Journal of Physical Chemistry B. 2016, **120**(29), 7133-7142.

PFD
-O-
4

Empirical Tight-Binding Calculation of Electronic Structure of Mn-Doped ZnS Nanocrystals

Rutchapon Hunkao[1], Sujin Suwanna[1] and Worasak Sukkabot[2,C]

[1]Optical and Quantum Physics Laboratory, Department of Physiscs, Faculty of Science, Mahidol University,Bangkok,10400 Thailand
[2]Department of Physics, Faculty of Science, Ubon Ratchathani University, Ubon Ratchathani 34190, Thailand

*[C] **E-mail**: w.sukkabot@gmail.com; **Fax**: +66 4 528 8381; **Tel.** +66 8 8013 7387*

EXTENDED ABSTRACT

Keywords: Mn-doped ZnS nanocrystal, photoluminescence, tight-binding calculation.

INTRODUCTION

ZnS is a luminescent material that has been used for many applications, such as light-emitting diodes (LEDs), electroluminescence devices, flat panel displays, sensors, lasers, infrared windows, solar cells, bio-devices, and other optoelectronic devices. Its absorption and photoluminescence (PL) emission spectra can be tuned with particle size and doping materials. By doping Mn into ZnS nanocrystals, the luminescence efficiency enhances and the lifetime shortens in comparison with those of the bulk material [2, 4]. The main aim of the present work is to study the effects of Mn doping into ZnS nanocrystals, in particular the electronic structure, using empirical tight-binding calculations.

PROPOSED APPROACH

In the present study, the $sp^3d^5s^*$ tight-binding model with first-nearest neighbor interaction is used in conjunction with the spin-orbital coupling to simulate the electronic wave functions and associated energies in Mn-doped ZnS nanocrystals. The carrier wave function is given by a linear combination of atomistic orbitals α localized on each atom β as defined by

$$\varphi = \sum_{\beta=1}^{N}\sum_{\alpha=1}^{20} c_{R,\alpha}\, \phi_{\alpha}(\vec{r} - \vec{R}_{\beta})$$

where N is the total number of atoms. To obtain the single-particle spectra, the empirical tight-binding Hamiltonian H_{TB} is diagonalized numerically, where

$$H_{TB} = \sum_{\beta=1}^{N}\sum_{\alpha=1}^{20} \varepsilon_{\beta\alpha} c^{\dagger}_{\beta\alpha} c_{\beta\alpha} + \sum_{\beta=1}^{N}\sum_{\alpha=1}^{20}\sum_{\alpha'=1}^{20} \lambda_{R\alpha\alpha'} c^{\dagger}_{\beta\alpha} c_{\beta\alpha'} + \sum_{\beta=1}^{N}\sum_{\beta'=1}^{N}\sum_{\alpha=1}^{20}\sum_{\alpha'=1}^{20} t_{\beta\alpha,\beta'\alpha'} c^{\dagger}_{\beta\alpha} c_{\beta'\alpha'}$$

In the description of H_{TB}, the operator $c^{\dagger}_{\beta\alpha}$ $(c_{\beta\alpha})$ creates (annihilates) the particle on the orbital α of atom β. Results from our program are validated with those from others and experiment.

RESULTS AND DISCUSSION

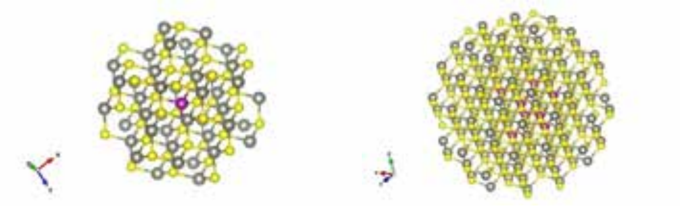

Figure 1. ZnS nanocrystals of different sizes (left: 1.6 nm, right 2.6 nm) with 1% Mn-doped. Mn, Zn and S atoms are displayed in purple, yellow and grey, respectively.

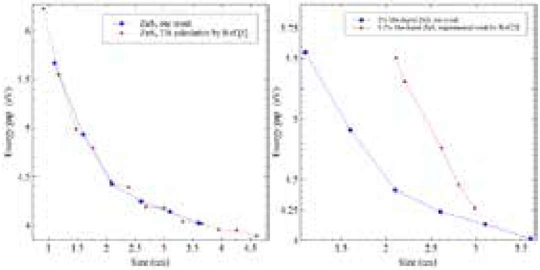

Figure 2. (left) Comparison of energy gap of ZnS (without doping) with other simulation results, and (right) of 1% Mn-doped ZnS with experimental results from Ref. [2].

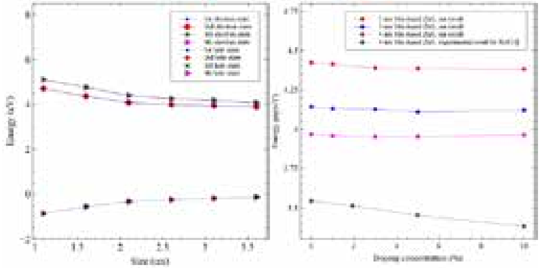

Figure 3. (left) Electron and hole energies of 1% Mn-doped ZnS are shown. (right) Effect of doping concentration on energy gaps, compared with experimental results. In the left panel, first four states of holes have nearly same energies, whereas those of electrons split into two levels. In the right panel, the energy gap decreases as doping increases.

ZnS nanocrystal are constructed to be a spherical shape with zincblende structure, and Mn atoms are substitutional doped at the central site as shown in figure 1, following an observation from experiment [1]. Our simulation results of energy gap agree well with those from Ref. [3], see figure 2 (left), which implies that our simulation program is reliable, and benchmarks the results. Furthermore, for 1% Mn-doped ZnS, our results show the same trend with experimental results, as shown in figure 2 (right). The calculated energies of the first four lowest electron states and highest hole states are shown in figure 3 (left). The dependence of electron and hole energies on the nanocrystal size is due to the quantum confinement effect. As evident in figure 3 (right), the effects of Mn doping concentration on the ZnS energy gap, from 0% to 10%, decrease the energy gap, with the effects more pronounced in smaller nanocrystal sizes. This is consistent with experimental results showing that photoluminescence peaks slightly shift to a higher wavelength, or lower energy gap, with increasing doping concentration. Other electronic properties such as the density of states are also investigated.

CONCLUSION

We have performed empirical tight-binding calculation of the electronic structure of Mn-doped ZnS nanocrystals. Our simulations are benchmarked consistently with other simulation and experimental results. As such, we can use our tight-binding model to further investigate other electronic and optical properties of Mn-doped ZnS nanocrystals.

REFERENCES

1. V. Albe, C. Jouanin, and D. Bertho, Phys. Rev. B, **57** (15), 8778-8781.
2. R. K. Chandrakar, R.N. Baghel , V.K. Chandra , and B.P. Chandra, Superlattices and Microstructures, **86** (2015), 256-269.
3. P. E. Lippens and M. Lannoo, Phys. Rev. B, **39** (15), 10935-10942.
4. V. D. Mote, Y. Purushotham, B. N. Dole, Cerâmica, **59** (2013), 395-400.

PFD -O- 5

The Scattering of Electromagnetic Waves from the Two-Layer Sphere When Outer Layer Has Variable Refractive Index: Shape Resonance

Umaporn Nuntaplook[1,C]
[1] *Department of Mathematics, Faculty of Science, Mahidol University, Bangkok, Thailand*

[C] ***E-mail**: umaporn.nun@mahidol.ac.th; **Fax**: +66 2 201 5343; **Tel.** +66 9 5759 6931*

EXTENDED ABSTRACT

Keywords: Computational results, shape resonance, variable refractive index.

INTRODUCTION

Although the concept of morphology-dependent resonances (MDRs) has been applied for the electromagnetic scattering by spherical structured media with a constant or piecewise constant refractive index in each layer, it is not useful in many general scatters that have variable refractive index profiles. Moreover, many interesting phenomena, such as invisibility, come from the position of the resonances in the electromagnetic scattering. Therefore, it is necessary to investigate the resonance locations for the more complicated structured media. In this paper, we apply the technique of so-called MDRs by [1] to investigate the resonance formulations of the scattering of electromagnetic waves from two-layer spheres when outer layer has a variable refractive index, $n(r)$.

PROPOSED APPROACH

The most common approach to this problem is based on solving the following second-order, linear differential equations for the radial Debye potential, for both transverse electric (E_l) and transverse magnetic modes (M_l):

$$\frac{d^2E_l}{dr^2}+\left\{{n_2}^2-\frac{l(l+1)}{r^2}\right\}E_l=0,$$

$$\frac{d^2M_l}{dr^2}-\frac{2}{n_2}\frac{dn_2}{dr}\frac{dM_l}{dr}+\left\{{n_2}^2-\frac{l(l+1)}{r^2}\right\}M_l=0,$$

where l is the angular momentum, and the radius $r \geq 0$.

We use the technique by [1,2] to solve the differential equations for the radial Debye potential in a model of two-layer sphere embedded in an infinite uniform particle, regions 1, 2, and 3, respectively as the radial coordinate increases away from zero. The inner layer has radius a, the outer layer has radius b, the center is at origin of the coordinate system. The refractive index in region 1, $0 \leq r \leq a$, is a constant, n_1. In region 2, $a \leq r \leq b$, the refractive index is defined as $n_2 = A(kr)^m$, where A and m are arbitrary constants. In region 3, outside the sphere, the refractive index is 1. The general solutions to this system obtained by the analysis in [3,4,5] used to derive *resonance* locations.

RESULTS

The derivation of the resonance formulation has been established. The numerical results have been generated for both modes. The result shown here is the typical resonance wave function for TM mode along with the potential function (dash line), where the refractive index $n_1 = 1.47, n_2 = 2(kr)^{-2}$, and the angular momentum $l = 40$. Obviously, the TM wave function shown in Figure 1 effectively trapped close to the surface of the inner sphere. More results can be found in the full paper.

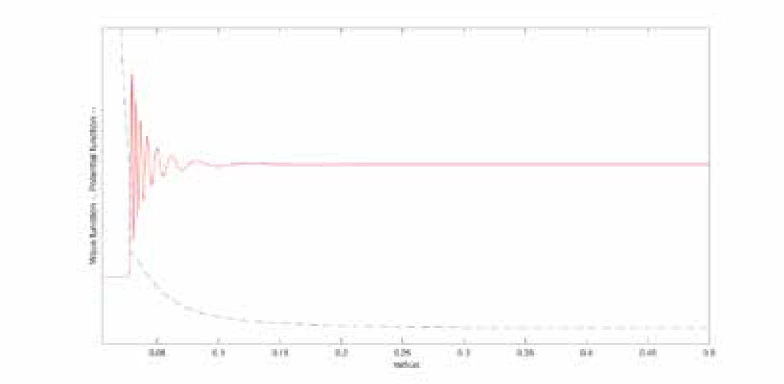

Figure 1: Radial wave function for TM resonance. The inner radius is $a = 0.02763707$ and the outer radius is 1.

REFERENCES

1. B. R. Johnson, Journal of the Optical Society of America A. 10, 343 – 352, 1993.
2. U. Nuntaplook, J. Adam, M. Pohrivchak, Light Scattering Reviews. 11, 339 – 361, 2016.
3. S. Levine, M. Kerker, ICES Electromagnetic Scattering; proceedings of the Interdisciplinary Conference held at Clarkson College of Technology, Potsdam, New York, 1962. Published by the MacMillan Company, pursuant to a special arrangement with Pergramon Press, Oxford, UK, 37 – 46, 1963.
4. E. Kamke, Differential gleichungen, Chelsea Publishing Co., New York. I, 440, 1948.
5. Y. Nomura, K. Takaku, Tohoku Research Institutes, Res. Inst. Elec. Comn. 7B, 107, 1955.

PFD -O- 6	Designing DNA-functionalized AuNP Dimer by Molecular Dynamics Simulation for the Application in Biosensor

Pakawat Toomjeen [1,C] **and Theerapong Puangmali**[1]
[1] *Materials Science and Nanotechnology Program, Department of Physics, Faculty of Science, Khon Kaen University, Khon Kaen, Thailand*

[C] ***E-mail****: pakawatt@kkumail.com;* ***Tel.*** *+66 8 83045625*

ABSTRACT

8-oxo-2'-deoxyguanosine (8-oxo-dG) is a biomarker of Cholangiocarcinoma or bile duct cancer [1] which is prevalently found in the northeastern Thailand. Thus, screening patients in the early state is essential. Colorimetric sensor based upon the aggregation of DNA-fuctionalized gold nanoparticle (AuNP) is a promising tool to screen patient. The working principle is based upon the assembly and disassembly of AuNP dimer. The color of the solution can be observed by naked-eyes. It is changed from blue to red once AuNP dimer is separated into a single AuNP. To gain high sensitivity, the interparticle of the dimer must be less than 1 nm [2]. In this work, we designed the sensor by molecular dynamics (MD) simulation. AuNP is functionalized with polyethylene glycol (PEG) and a single strand DNA (ssDNA). The formation of AuNP dimer is due to the complementary of ssDNA coated onto AuNP surface. The interparticle distance between AuNP dimer can be minimized by a structure of Y-shaped DNA duplex [3] by binding aptamer to each half of ssDNA. In the presence of 8-oxo-dG, the binding of 8-oxo-dG and its aptamer can be observed leading to the disassembly of AuNP dimer. Based on MD simulation, it was found that the density and molecular weight of PEG coated onto AuNP surface affect the interparticle distance. In addition, the interparticle distance is also dependent on the length of spacer between ssDNA and AuNP. In our design, a strategy to minimize the interparticle gap through the formation of AuNP dimer enables to increase the limit of detection of 8-oxo-dG. This biosensor is useful for screening and detecting the patients in the early state of cancer.

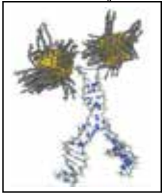

Figure 1. Strucuture of AuNP dimers though Y-shaped duplex

Keywords: Dimer, AuNP, 8-oxo-dG, Aptamer, Cholangiocarcinoma, Molecular dynamics

REFERENCES

1. Roszkowski, K., et al. (2011). *Oxidative damage DNA: 8-oxoGua and 8-oxodG as molecular markers of cancer.* Med Sci Monit **17**(6): Cr329-333.
2. Cha, H., et al. (2014). *Probing Quantum Plasmon Coupling Using Gold Nanoparticle Dimers with Tunable Interparticle Distances Down to the Subnanometer Range.* ACS Nano **8**(8): 8554-8563.
3. Guo, L., et al. (2013). *Oriented Gold Nanoparticle Aggregation for Colorimetric Sensors with Surprisingly High Analytical Figures of Merit.* Journal of the American Chemical Society **135**(33): 12338-12345.

PFD
-O-
7

A New Hybrid Radial Basis Function: The First Step Towards Numerically Solving Nonlinear PDEs

Nissaya Chuathong[1,C] **and Sayan Kaennakham**[2]
[1]*Faculty of Science, Environment and Energy, King Mongkut's University of Technology North Bangkok (Rayong Campus), Rayong 21120, Thailand*
[2]*School of Mathematics, Institute of Science, Suranaree University of Technology, Nakhon Ratchasima 30000, Thailand*
[2]*Center of Excellence in Mathematics, Bangkok 10400, Thailand*

[C] ***E-mail****: nissaya.c@sciee.kmutnb.ac.th email;* ***Tel.*** *+66 8 9678 9360*

EXTENDED ABSTRACT

Keywords: Hybrid Radial Basis Function, Collocation, Non-linear PDEs.

INTRODUCTION

Kansa's method is consist of several important components and one of which is the choice of the RBF used itself. The method represents the approximate solution $u(\mathbf{x})$ by the interpolation, using an RBF interpolation as $u(\mathbf{x}) = \sum_{j=1}^{N} c_j \varphi\left(\left\|\mathbf{x}-\mathbf{x}_j\right\|\right)$, with the usual Euclidean norm. Despite of the large number of researches devoting to finding an optimal RBF, it has been accepted that the most suitable RBF depends very much on the nature of the problem (with its conditions) at hand. Our previous study [3] focused on the effectiveness of several well-known and mostly-used RBFs for nonlinear class of PDE. In this work, it has been found that while Gaussion-RBF produces the reasonably worst results' quality, the so-called Cubic Matérn RBF type is found to yield the best results' quality for all test cases.

Recently, a new RBF which is a combination of Gaussian and Cubic type, has been invented and proposed by PK. Mishra et.al [4]. In this work, they attempted to alleviate the problem of ill-condition normally encountered when using Kansa' method, and the proposed combined RBF was applied in several benchmark scattered-data interpolation problems; 1D, 2D and 3D. This immediately prompts the question of applying this newly invented RBF to problems of solving PDE, particularly non-linear ones and this is our main objective of investigation.

PROPOSED APPROACH

As proposed and tested out with a series of numerical tests for 1D, 2D and 3D problems as well as synthetic and real geophysical data by PK. Mishra et.al [4] , here we expand their work to another challenging problem of solving non-linear PDEs. The hybrid RBF is of the following form;

$$\varphi\left(\left\|\mathbf{x}-\mathbf{x}_j\right\|\right) = e^{-(\rho\left\|\mathbf{x}-\mathbf{x}_j\right\|)^2} + \left\|\mathbf{x}-\mathbf{x}_j\right\|^3$$

This is referred to, hereafter, as **'Hyb'**. The first component, $e^{-(\rho\left\|\mathbf{x}-\mathbf{x}_j\right\|)^2}$ is Gaussian part which is shape parameter dependent while the Cubic part, $\left\|\mathbf{x}-\mathbf{x}_j\right\|^3$, does not contain any shape parameter term . This combination of RBF makes it `*Gaussian radial basis function with small cubic doping"* for large shape parameter whereas for small shape parameter, the cubic term dominates the kernel making it `Cubic radial basis function with small Gaussian doping'.

RESULTS

Example 1. The nonlinear PDE as given in GE. Fasshauer [5] on a square domain $0<x<1,\ 0<y<1$ is taken a look at. The governing equation is as follows; $-\varepsilon^2\nabla^2 u - u + u^3 = f$ with the boundary condition $u=0$ on $\partial\Omega$ and the right hand side of the equation is chosen from the analytical solution of form; $u(x,y)=\psi(x)\psi(y)$ with $\psi(t)=1+e^{-1/\varepsilon}-e^{-t/\varepsilon}-e^{(t-1)/\varepsilon}$, (x,y) denotes the Cartesian coordinate of $\mathbf{x}\in\sqcap^{2}$.

Table 1. Solutions comparison of the one abstained in this work against both alternative numerical work, WL [3], and the exact ones.

Point	WL[3]	Hyb	Exact
(0.2,0.6)	0.848346	0.87731258	0.846440
(0.4,0.2)	0.848346	0.87731258	0.846440
(0.4,0.4)	0.958317	0.92524858	0.958933
(0.4,0.6)	0.958317	0.92524858	0.958933
(0.6,0.2)	0.848346	0.87731258	0.846440

Example 2. The following nonlinear equation as given in Linesawat[6,7] is studied. The governing equation is as follows; $\Delta^2 u = 2u^3$ in a$(1,5)\times(1,5)$ domain with the Dirichlet boundary condition $u=-1/x$ on $\partial\Omega$. The analytical solution of the above problem is $u=-1/x$.

Table 2. Solutions comparison of the one abstained in this work against both alternative numerical work, Linesawat [7] , and the exact ones.

Point	Linesawat[7]	Hyb	Exact
(2,2)	-0.5047	-0.4751	-0.5000
(2,3)	-0.4993	-0.4767	-0.5000
(3,3)	-0.3358	-0.2008	-0.3333
(3,4)	-0.3290	-0.2237	-0.3333
(4,4)	-0.2290	-0.1545	-0.2500

REFERENCES

1. E. J. Kansa, Multiquadrics—a scattered data approximation scheme with applications to computational fluid-dynamics—I. Surface approximations and partial derivative estimates, Comput. Math. Appl, 19 (1990) 127-145.
2. S. A. Sarra and E. J. Kansa, Multiquadric radial basis function approximation methods for the numerical solution of partial differential equations, Adv. Comput. Math, 2 (2009).
3. N. Chuathong, S. Kaennakham and W. Toutip, "Numerical solutions of 2D nonlinear PDEs using Kansa's meshless method and the search for optimal radial basis function," Proceeding of 19th International Annual Symposium on Computational Science and Engineering. (Ubon Ratchthani university, Ubon Ratchathani, Thailand, 2015), pp. 13-15.
4. P. K. Mishra, S. K. Nath and M. K. Sen, A hybrid radial basis function for scattered data interpolation. Submitted to Elsevier, URL: sites.google.com/site/pankajkmishra01, (2015).

5. G. E. Fasshauer, Newton iteration with multiquadrics for the solution of nonlinear PDEs, Comput. Math. Appl, 43 (2002) 423-438.
6. S. Kaennakham, “The dual reciprocity boundary element method for two dimensional Burger’s equations using MATLAB,” Master Thesis, Khon Kaen University, 2004.
7. K. Linesawat, “The dual reciprocity boundary element method for nonlinear problems using compactly supported radial basis function,” Master Thesis, Khon Kaen University, 2010.
8. C. V. Pao, Block monotone iterative methods for numerical solutions of nonlinear elliptic equations, Numer. Math, 72 (1995) 239–262.

PFD -O- 8

Electrical Conductivity of Flexible PEDOT Thermoelectric Foams

Warittha Thongkham [1], **Charoenporn Lertsatitthanakorn** [1], **Paisan Khanchaitit** [2],
and Monrudee Liangruksa [2,C]
[1] *Energy Technology Division, School of Energy, Environment and Materials, King Mongkut's University of Technology Thonburi, 126 Pracha u-thit Road, Bangmod, Tungkru, Bangkok, Thailand*
[2] *NANOTEC, National Science and Technology Development Agency (NSTDA),*
111 Thailand Science Park, Pathum Thani, Thailand

[C] ***E-mail**: monrudee@nanotec.or.th; **Fax**: +66 2 564 6985; **Tel.** +66 2 654 7100*

EXTENDED ABSTRACT

Keywords: electrical conductivity, organic thermoelectrics, PEDOT: PSS, surfactant

INTRODUCTION

Thermoelectric devices are renewable energy source that can alter thermal energy or waste heat into electricity and vice versa. In this work, we build a composite organic thermoelectric, consisting of organic conductive films (poly(3,4-ethylenedioxythiophene): polystyrene sulfonate (PEDOT:PSS)), randomly scattered in the foam's structure, to perform as an electric-generating insulators. The electrical conductivity is one of the most important properties. Several models of the electrical properties of porous materials have been proposed[1-4]. One of widely-used approaches uses a tetrakaidecahedral unit-cell to represent an open-cell foam, and considers the current flow through the foam by assuming an electrical resistor network.[1-4] In this work, the new concept of organic thermoelectric employs a melamine foam as a scaffold for instant three-dimensional fabrication of PEDOT: PSS. The effects of anionic surfactant, sodium dodecyl sulfate (SDS), to the PEDOT: PSS film formation in the 3D melamine scaffold are performed by varying the amounts of surfactant in PEDOT: PSS solution from 0 to 5 wt%. The models are then developed and validated with the experimental results to obtain the relationship between the film formation and the electrical conductivity.

PROPOSED APPROACH

Electrical conductivity of foam structure, σ_f, can be calculated by using electrical resistance in each layer of tetrakaidecahedral unit cell[1, 2] written as:

$$\sigma_f = \frac{\sqrt{2}L}{2(R_A + R_B + R_C + R_D)}. \qquad (1)$$

where L is the ligament length and $R_{A,B,C,D}$ is the electrical resistivity in each unit cell layer.

In addition, it can predict from electrical equivalent circuit in a tetrakaidecahedral unit cell of foam structure.[3, 4] The electrical conductivity is the reciprocal of electrical resistivity that can be expressed as:

$$R = \frac{\rho L}{A} = \frac{L}{\sigma_f A}. \qquad (2)$$

where R is the total electrical resistivity from electrical circuit and A is the surface area.

The electric current direction can be considered via two paths including the direction from two opposite square faces, and the direction from two hexagonal faces.

Finally, the effective electrical conductivity, σ_{eff}, of the system is obtained by varying volume fraction, Φ_f of polymer thin films in the melamine foam scaffolds as follows:

$$\sigma_{eff} = \Phi_f \sigma_f . \tag{3}$$

RESULTS

The results were observed that the uniformity of thin films in microporous scaffold foam was enhanced when PEDOT:PSS solution was doped with SDS surfactant as shown in Fig. 1. The actual σ value of TE foam has increased approximately two orders of magnitude from the experiment data due to the air portion. The maximum electrical conductivity is around 50 S/cm with 3 wt% SDS doping corresponding to ~3.4 % of film volume fraction. Therefore, this study can help understand the role of film formation and predict the key parameters affecting the electrical conductivity in this thermoelectric porous structure.

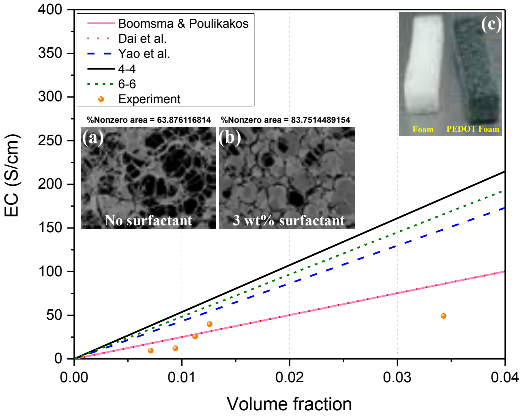

Figure 1. Comparison between experiment data and model prediction of σ_{eff} at different SDS contents. Inset (a), (b) are SEM images of PEDOT:PSS thin films coated on the foam network analyzed by Image J program and (c) is the photographs of foam with and without PEDOT:PSS.

REFERENCES

1. Z. Dai, K. Nawaz, Y. G. Park, J. Bock and A. M. Jacobi, *International Communications in Heat and Mass Transfer*, 2010, **37**, 575-580.
2. Y. Yao, H. Wu and Z. Liu, *International Journal of Thermal Sciences*, 2015, **97**, 56-67.
3. K. P. Dharmasena and H. N. G. Wadley, *Journal of Materials Research*, 2011, **17**, 625-631.
4. A. S. Zuruzi and K. S. Siow, *Electronic Materials Letters*, 2015, **11**, 308-314.

PFD
-O-
9

Designing Colorimetric Aptasensor Based on Disassembly of AuNP Dimers for Detection of Ochratoxin A

Witthawat Phanchai[1,C] **and Theerapong Puangmali**[1]
[1] *Materials Science and Nanotechnology Program, Department of physics, Faculty of Science, Khon Kaen University, Khon Kaen, Thailand*

[C] ***E-mail****: witthawat_p@kkumail.com;* ***Tel.*** *+66 952308778*

ABSTRACT

Ochratoxin A (OTA) is one of the abundant food-contaminating mycotoxins. On-side detection is vitally important. Colorimetric aptasensor based upon disassembly of aggregates of oriented gold nanoparticle (AuNP) dimer is a promising sensor for the on-side detection. The disassembly of the dimer, induced by OTA, leads to the change of the color of the solution which can be observed by naked-eyes. However, aptamer-OTA binding affinity is far from being fully understood. Herein, the molecular dynamics (MD) simulation was used to investigate the interaction of aptamer and OTA during binding. We studied (i) aptamer-OTA binding and (ii) developed aptasensor by MD simulations. The effect of the sequence of the DNA aptamer on the degree of binding was elucidated. The aptamer-OTA binding depends on the optimal sequence of aptamer and suitable conditions. Based on our computational simulation, we can provide the suitable condition for experimentalists to obtain the low limit of detection and high sensitivity. Additionally, our study also opens the door for the design of novel biosensors.

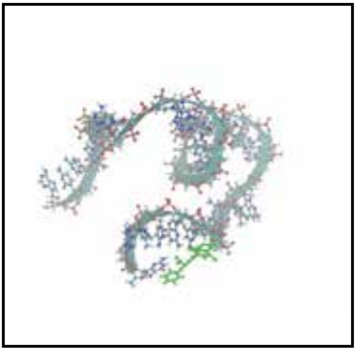

Figure 1. Aptamer-OTA binding affinity.

Keywords: Ochratoxin A, Aptamer, Dimer, AuNP, Biosensor, Molecular dynamics**.**

REFERENCES

1. Xiao, R., Wang, D., Lin, Z., Qiu, B., Liu, M., Guo, L., & Chen, G. (2015). Disassembly of gold nanoparticle dimers for colorimetric detection of ochratoxin A. Anal. Methods, 7(3), 842-845.

2. Motycka, J., Mach, P., Melichercik, M., & Urban, J. (2014). DFT and MD study of the divalent-cation-mediated interaction of ochratoxin A with DNA nucleosides. J Mol Model, 20(6), 2274.
3. Guo, L., Xu, Y., Ferhan, A. R., Chen, G., & Kim, D. H. (2013). Oriented gold nanoparticle aggregation for colorimetric sensors with surprisingly high analytical figures of merit. J Am Chem Soc, 135(33), 12338-12345..

PFD
-O-
10

Effect of Platinum Decorated Carbon Nanocones on Hydrogen Storage Reactions: Theoretical Study

Nuttapon Yodsin[1], Chompoonut Rungnim[2], Supawadee Namuangruk[2], and
Siriporn Jungsuttiwong[1,C]
[1] *Department of Chemistry, Faculty of Science, Ubon Ratchathani University, Ubon Ratchathani 34190, Thailand*
[2]*NANOTEC, National Science and Technology Development Agency (NSTDA),*
111 Thailand Science Park, Pathum Thani, Thailand

[C] ***E-mail**: siriporn.j@ubu.ac.th; **Fax**: +66-45-288379; **Tel.** +66-81-692-2125*

EXTENDED ABSTRACT

Carbon nanocones (CNC) are considered as an important material for the hydrogen storage. The hydrogen adsorption and storage on platinum (Pt)-decorated CNC (Pt-CNC) has been investigated by density functional theory (DFT). The severe curvature of CNC could bind the metal and hydrogen molecules through enhanced binding at the top section. In this work, we performed DFT studies of metal doped on single walled carbon nanocones (SWCNCs) as well as the H_2 adsorption capacity. In term of Pt doped various positions on pristine CNC, our calculations showed that Pt atom deposited on bridge site between pentagons. For the H_2 adsorption reaction, the H_2 adsorption energies on Pt-CNC were more favorable than that on pristine CNT due to the Pt atom served as the active site for H_2 adsorption. Moreover, we carried out the effect of shape of the CNC by varying number of pentagons from 1 to 6. As the Pt atom was the active site for H_2 adsorption, the maximum adsorption energy of hydrogen molecules on 4-pentagon pristine carbon nanocone (4CNC) can bind up to 2 hydrogen with the average adsorption energy of -0.47 eV/H_2 and bind up only one hydrogen with -0.56 eV/H_2 for 4-pentagon defective carbon nanocone (d4CNC) supporting material. Hydrogen spillover mechanisms on d4CNC were investigated by first-principles calculations. We found that this mechanism can enhanced hydrogen uptake up to 3 hydrogen molecules.

Keywords: Density functional theory (DFT); Hydrogen storage; Carbon nanocone (CNC); Platinum

INTRODUCTION

Owing to the population began to increase; the demand of energy is increasing as well. Subsequently, alternative energy has received considerable attentions such as wind energy, hydro energy, geothermal energy, solar energy and hydrogen energy. Among these, we are interested in hydrogen energy because it is clean energy, no harmful emission and renewable to use. Therefore, it is urgent to develop more effective materials for hydrogen adsorption. CNCs have become one of the most promising nanoscale materials since it can be first synthesized by using arc-discharge method without a catalyst in synthesis procedure.

PROPOSED APPROACH

The calculations were done, the geometry optimized structures and frontier orbital energy levels were calculated using the density functional theory (DFT) with hybrid functional of Becke's three parameter gradient-corrected exchange potential and the

Lee-Yang-Parr gradient-corrected correlation potential (B3LYP) combined with 6-31G(d,p) level of theory. Full optimization were investigated at the B3LYP level of theory by using the 6-31G(d,p) basis set and lanl2dz for platinum atom.

RESULTS

The carbon nanocones (CNCs) with different shape were investigated, we carried out the effect of shape of the CNC by varying number of pentagons from 1 to 6. The tip angles for 1-6 pentagon cones were shown in Figure.1. From optimized structures, the tip angle reduced when number of pentagon on CNC increased. In this work, our investigated cone angles of CNCs that are according to previous works. The most stable position on cone tip was bridge site between pentagons. According to pi-orbital axis vector (POAV) on the conical CNCs tips, the POAV analysis was the most agreement with binding energy. For H_2 adsorption, the maximum adsorption energy of hydrogen molecules on 4CNC can bind up to 2 hydrogen with the average adsorption energy of -0.47 eV/H_2 and bind up one hydrogen with -0.56 eV/H_2 for d4CNC supporting material. Hydrogen spillover mechanisms on d4CNC were investigated to enhanced hydrogen uptake up to 3 hydrogen molecules.

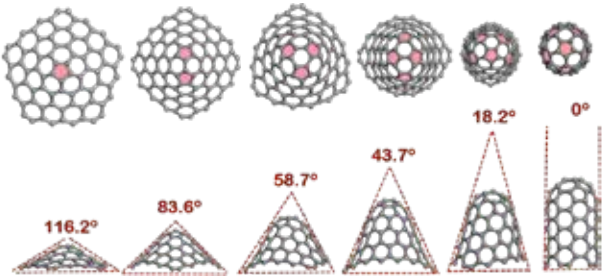

Figure 1. Optimized structures of six CNCs with one (1-CNC), two (2-CNC), three (3-CNC), four (4-CNC), five (5-CNC), and six (6-CNC) pentagons respectively.

REFERENCES

1. Harris, P. J. F.; Tsang, S. C.; Claridge, J. B.; Green, M. L. H. *Journal of the Chemical Society, Faraday Transactions* **1994**, *90*, 2799.

2. Sano, N.; Taniguchi, K.; Tamon, H. *The Journal of Physical Chemistry C* **2014**, *118*, 3402.

3. Karousis, N.; Suarez-Martinez, I.; Ewels, C. P.; Tagmatarchis, N. *Chemical Reviews* **2016**, *116*, 4850.

4. Liu, Y.; Brown, C. M.; Neumann, D. A.; Geohegan, D. B.; Puretzky, A. A.; Rouleau, C. M.; Hu, H.; Styers-Barnett, D.; Krasnov, P. O.; Yakobson, B. I. *Carbon* **2012**, *50*, 4953.

CHE
-O-
1

First-Principles Study of Sn-Doped V_2O_5 as Cathode Material of Li-Ion Batteries

Suwit Suthirakun[1,2,C], **Sirichok Jungthawan**[2,3], **and Sukit Limpijumnong**[3]
[1] *School of Chemistry, Institute of Science, Suranaree University of Technology, Nakhon Ratchasima, Thailand*
[2] *CoE-AFM SUT Center of Excellence in Advanced Functional Materials, Suranaree University of Technology, Nakhon Ratchasima, Thailand*
[3] *School of Physics, Institute of Science, Suranaree University of Technology, Nakhon Ratchasima, Thailand*

[C] ***E-mail**: suthirak@sut.ac.th; **Tel.** +66 4 4224 886*

EXTENDED ABSTRACT

Keywords: Li-ion batteries, Sn-doped V_2O_5, periodic DFT calculations, DFT+U method

INTRODUCTION

The development of novel cathode materials for Li-ion batteries can significantly enhance the overall performance of the batteries. Experiments find that Sn-doped V_2O_5 displays substantial enhancement of Li-ion storage capacity, kinetics, and cyclic stability when compare to that of stoichiometric V_2O_5 film.[1] Introducing small amount of Sn (5%) into the V_2O_5 film reduces the electrochemical reaction resistance, increases the electrochemical reaction reversibility, and improves Li-ion diffusivity.[1]

From a computational point of view, first-principles methods, in particular density functional theory (DFT), have been used as a tool to obtain better understanding of the atomic and electronic structures and intercalation behavior of cation insertion in the V_2O_5-based cathode materials.[2-4] We propose to use DFT+U to explore the roles of Sn-doping towards the improved electrochemical activity of V_2O_5 based cathodes. In particular, we aim at studying *(i)* the atomic and electronic structures of V_2O_5 cathode and *(ii)* the behavior of Li intercalation in the cathode material. We considered the low limit of 2.8% Sn concentration and dilute regime of Li intercalation in the bulk α-V_2O_5.

PROPOSED APPROACH

All calculations were carried out using spin-polarized DFT+U approach, $U_{3d}(V) = 4.0$ eV, with periodic supercell models implemented in the Vienna ab initio simulation package (VASP 5.3).[5] The exchange and correlation functional was approximated using the optimized non-local vdW-DF functional (modified versions of the vdW-DF of Dion et al.[6]) as implemented in VASP, where its original GGA exchange functional was replaced by an optimized Perdew-Burke-Ernzerhof (PBE) functional[7] to take into account the weak van der Waals attraction between V_2O_5 layers. We chose the ultra soft pseudopotential with projector augmented-wave (PAW) method[8] to describe the nuclei and core electronic states. The V $3s3p3d4s$, O $2s2p$, Sn $4d^{10}5s^{2}5p^{2}$, and Li $2s$ were treated as valence electrons where their wave functions were expanded in plane–waves with a cutoff energy of 400 eV for electronic structure calculations and geometry optimization.

In order to study the impact of Sn-doing toward the electrochemical performance of V_2O_5 cathode material, we first optimized lattice parameters and ion positions of the V_2O_5 unit cell using Monkhorst-Pack (MP) approach[9] with a dense k-point sampling of 5×11×11. The optimization was ceased when the calculated residual forces were lower than 0.02 eV/Å. The obtained unit cell was then used to construct a 1×3×3 supercell of $V_{36}O_{90}$ to further use for evaluation of Sn and Li insertions. Intercalation of metals, Li or Sn, into the V_2O_5 supercell were carried out where both lattice parameters and ion positions of the supercell were allowed to relax to examine the effect of metal-insertion to alterations of the V_2O_5 structure and lattice parameters. These calculations were carried out using MP k-point grid of 2×2×2 with the same convergence criterion to that of the optimization of unit cell. We have tried several inserted positions to ensure the most stable intercalated V_2O_5 structures.

To explore the electronic structures of stoichiometric and intercalated V_2O_5, we computed their projected density of states (PDOS) employing tetrahedron smearing method with Bloch corrections. The k-point grid of 2×2×2 was found to be sufficient for DOS calculations, using a denser 4×4×4 k-point results in a negligible difference of the produced DOS.

RESULTS

Computations reveal that Sn atoms prefer to occupy a channel between two V_2O_5 layers. The calculated electronic structure shows that the bonding interaction of Sn-V_2O_5 exhibits mixed ionic/covalent character. The inserted Sn atom donates two of its four valence electrons to the nearby V centers (ionic character) forming small polarons in the lattice whereas the other two electrons are shared with the surrounding oxygen atoms (covalent character). The mixed ionic/covalent bonding character of Sn-doped V_2O_5 plays an important role in enhancing Li intercalation in the material. Electron polarons generated from Sn-insertion increase number of charge carriers in the V_2O_5 lattice which could improve electronic conductivity of the material. Higher electronic conductivity could in turn lead to high diffusion kinetics of Li-ion in the V_2O_5-based cathode. Furthermore, co-existence of Sn-ion and small polarons in the V_2O_5 structure imposes geometrical constraint into the lattice which primarily affects behavior of Li intercalation. Favorable insertion sites of Li in Sn-doped V_2O_5 involve relatively low energies of polaron formation and high stabilities of Li-ion whereas the less stable configurations have adjacent polaronic sites on the same V_2O_5 layers which lead to high polaron formation energies. In addition to the insertion energies, we calculated diffusion barriers for Li-ion to further explore the intercalation behavior. The calculated diffusion barriers in conjunction with the insertion energies reveal that Sn-doping promotes Li-ion insertion by stabilizing the intercalated Li-ion while maintaining ion diffusion property. Nevertheless, trapping and blocking of ion diffusion path may be expected due to the presence of Sn in the V_2O_5 lattice.

REFERENCES

1. Li, Y. W.; Yao, J. H.; Uchaker, E.; Zhang, M.; Tian, J. J.; Liu, X. Y.; Cao, G. Z. *J. Phys. Chem. C* **2013**, *117*, 23507.
2. Scanlon, D. O.; Walsh, A.; Morgan, B. J.; Watson, G. W. *J. Phys. Chem. C* **2008**, *112*, 9903.
3. Carrasco, J. *J. Phys. Chem. C* **2014**, *118*, 19599.
4. Ma, W. Y.; Zhou, B.; Wang, J. F.; Zhang, X. D.; Jiang, Z. Y. *J. Phys. D: Appl. Phys.* **2013**, *46*, 105306.
5. Kresse, G.; Furthmüller, J. *Phys. Rev. B* **1996**, *54*, 11169.
6. Dion, M.; Rydberg, H.; Schroder, E.; Langreth, D. C.; Lundqvist, B. I. *Phys. Rev. Lett.* **2004**, *92*.
7. Perdew, J. P.; Burke, K.; Ernzerhof, M. *Phys. Rev. Lett.* **1996**, *77*, 3865.
8. Kresse, G.; Joubert, D. *Phys. Rev. B* **1999**, *59*, 1758.
9. Monkhorst, H. J.; Pack, J. D. Phys. Rev. B **1976**, 13, 5188.

CHE -O- 2	**Nitrous Oxide Decomposition over Cu-BTC Metal-Organic Frameworks: A DFT Study**

Yuwanda Injongkol[1,2], **Panisara Pensuk**[1], **Nutthakarn Aeimsa-ard**[1], **Piti Treesukul**[1],
Bundet Boekfa[1,2] **and Thana Maihom**[1,2,C]

[1]*Department of Chemistry, Faculty of Liberal Arts and Science, Kasetsart University, Kamphaeng Saen Campus, Nakhon Pathom 73140, Thailand*
[2]*Center for Advanced Studies in Nanotechnology for Chemical, Food and Agricultural Industries, KU Institute for Advanced Studies, Kasetsart University, Bangkok 10900, Thailand.*

[C] ***E-mail**: faastnm@ku.ac.th; **Tel.** +(66)34352259*

EXTENDED ABSTRACT

Keywords: Nitrous oxide, Decomposition, MOFs, Cu-BTC, M06-L functional.

INTRODUCTION

Nitrous oxide (N_2O) produced from motor vehicle exhausts and an industrial process is well known as an environmental pollutant. It is a strong greenhouse effect gas and also plays an important role in the destruction of the stratospheric ozone layer. The reduction of N_2O via catalytic decomposition therefore attractively challenge in terms of environmental problems [1]. In this work, we theoretically investigate the decomposition of N_2O to O_2 and N_2 on the Cu-BTC metal-organic frameworks that encloses coordinatively unsaturated site (CUS) active site [2] by employing DFT calculations with the M06-L functional.

PROPOSED APPROACH

The cluster model of Cu-BTC is illustrated in Figure 1b. The M06-L density functional [3] was used in all calculations. The basis set of 6-31G(d,p) was employed for O, N, C and H atoms, while the Cu and Fe atoms was described by the effective core potentials (ECP) [4]. Frequency calculations were performed at the same level of theory to ensure that each transition structure has only one imaginary frequency. All calculations were performed with the Gaussian 09 code [5].

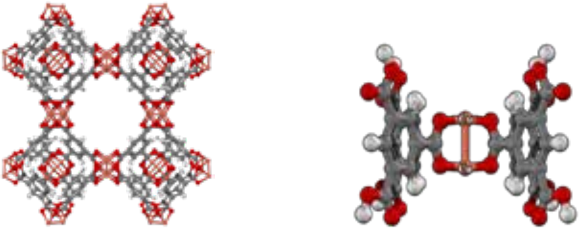
(a) (b)

Figure 1. Cu-BTC MOF Unit cell (a) and optimized structure of Cu-BTC model (b).

RESULTS

The N_2O decomposition is proposed to proceed in two steps (Figure 2a). In the first step, the N_2O N–O bond is broken to give the N_2 and oxygen deposited on Cu active site of Cu-BTC. This step is followed by the O-O bond formation to produce the O_2 and N_2 products. The first step is considered to be a rate determining step of the reaction with the higher activation energy barrier (67.6 kcal/mol) than the second one (36.6 kcal/mol). To understand the effect of MOF metals active site, we analyze the molecular electron transfers by using NBO method [6] during the N-O bond breaking state. We found electron transferred from the Cu active site to the anti-bonding of the N_2O molecule leading to a more positive charge of the Cu active site and also a more negative N_2O molecule. Moreover, we also compare the N-O bond breaking step on Cu-BTC to the same reaction step on Fe-BTC which is one paddlewheel MOF used in catalysis [7]. The activation energy for this step on Fe-BTC is found to be lower than that of on the Cu-BTC about 3 times (see Figure 2b). This is due to a larger charge transfer from the MOF to the N-O bond of the N_2O molecule in the Fe-BTC case (0.25*e* and 0.45*e* for Cu-BTC and Fe-BTC, respectively). This result shows that the charge transfer process is plays an important role for N-O bond breaking in the N_2O decomposition.

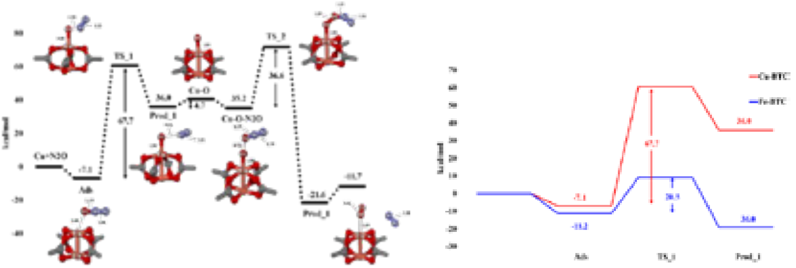

(a) (b)

Figure 2. Energy profile for the N_2O decomposition over Cu-BTC (a) and energy profiles comparism for the rate-determining step of the N_2O decomposition over Cu-BTC and Fe-BTC (b).

REFERENCES

1. Shelef, M., *Chem. Rev.* 1995, **95**, 209-225.
2. Chui, S. S. Y., Lo, S. M. F., Charmant, J. P. H., Orpen, A. G., and Williams, I. D., *Science* 1999, **19**, 1148-1150.
3. Zhao, Y. and Truhlar, D. G., *Acc. Chem. Res.* 2008, **41**, 157-167.
4. Dolg, M., Wedig, U., Stoll, H., and Preuss, H., *J. Phys. Chem.* 1987, **86**, 866-872.
5. M.J. Frisch et al., *Gaussian 09, revision c.01*; Gaussian, Inc.: Pittsburgh, PA, 2009.
6. Reed, A. E., Curtiss, L. A., and Weinhold, F., *Chem. Rev.* 1988, **88**, 899-926.
7. Riou-Cavellec, M., Albinet, C., Greneche, J-M., and Ferey, G. J., *Mater Chem* 2001, **11,** 3166-3171.

CHE
-O-
3

Influence of Metal Species in Porphyrin-base Metal-organic Frameworks on Carbon Dioxide Capture

Panchanit Piyakeeratikul[1], **Bundet Boekfa**[2], **Taweesak Pila**[3], **Sippakorn Wannakao**[1], **and Kanokwan Kongpatpanich**[1,C]
[1]*Department of Materials Science and Engineering, School of Molecular Science and Engineering, Vidyasirimedhi Institute of Science and Technology, Rayong, Thailand*
[2]*Computational Chemistry Laboratory, Department of Chemistry, Faculty of Liberal Arts and Science, Kasetsart University, Kamphaeng Saen Campus, Nakhon Pathom, Thailand*
[3]*Department of Chemical and Biomolecular Engineering, School of Energy Science and Engineering, Vidyasirimedhi Institute of Science and Technology, Rayong, Thailand*

[C] ***E-mail***: *kanokwan.k@vistec.ac.th;* ***Fax***: *+66 3 301 4445;* ***Tel.*** *+66 3 301 4154*

EXTENDED ABSTRACT

Keywords: Metal-organic framework, Porphyrin , CO_2 capture, DFT calculation.

INTRODUCTION

Accumulation of carbon dioxide (CO_2) from human activities has posed challenge to researchers for many decades to find out new technologies for CO_2 capture and utilization. Several porous materials have been developed for CO_2 capture at cryogenic temperature or at high pressure. However, it remains challenging to develop materials for CO_2 capture at ambient conditions (room temperature and atmospheric pressure) with high CO_2/N_2 selectivity. Metal-organic frameworks (MOFs), which are crystalline porous materials composed of metal ions and organic linkers, are particularly attractive for CO_2 separation and storage due to their large surface area, versatile framework topologies, and tunable chemical functionality.

Tuning of pore surface in MOF by functionalization with polar organic groups or open metal sites are the key strategies to improve CO_2 adsorption selectivity over N_2. Open metal sites in MOF are coordinatively unsaturated sites generated upon removal of weakly-coordinated solvent molecules from the metal centers. A recent report shows different metals influence on the CO_2 adsorption process.[1] However, these sites are generally air and moisture sensitive as the open metal sites are typically in low valence state or easy to interact with moisture resulting in several handling problems in practical applications. In recent years, incorporating Zr_6O_8 nodes in MOFs is found to largely improve the stability of MOF materials because of a strongly coordinated Zr-O bonds and high coordination number of Zr. However, use of Zr ions as metal nodes make the MOF structure lack of open metal sites and limit the choices of metal species in MOFs. Thanks to the diversification of organic ligands, porphyrin is interesting because structure of porphyrin has a free center site for metal ions to coordinate to form open metal sites in ligand. Therefore, metal centers in porphyrin-based ligands could be an effective strategy to obtain active units for CO_2 binding in MOFs.

Herein, we synthesize porphyrin-based MOFs by varying the metal center in porphyrin ligand (PCN-222-M, where M = transition metals) to study effect of metal on CO_2 capture at ambient conditions. Furthermore, density functional theory (DFT) calculation has been used to investigate the interaction between CO_2 and metal centers to explain the influence of metal species on CO_2 adsorption. The study would provide a guideline to design the suitable metal centers or metal complexes in the center of porphyrin ligands to enhance the adsorption and selectivity of CO_2.

PROPOSED APPROACH

M-PCN-222 samples were synthesized by solvothermal reaction of $ZrCl_4$ (75 mg), metallated tetrakis(4-carboxyphenyl)porphyrin or M-TCPP (50 mg) and benzoic acid (2700 mg) in *N,N'*-dimethyformamide (DMF) as modified from the literature.[2] All synthesized M-PCN-222 samples were characterized by power X-ray diffraction, elemental analysis and CO_2 adsorption experiments.

The cluster model of PCN-222 topology was obtained from the available crystallographic data of Fe-PCN-222. Other M-PCN-222 structures were created by substituting Fe with the desired metal species. High spin state provide the most stable structure for both Fe-PCN-222 and Mn-PCN-222. Various positions of CO_2 adsorbed on the clusters were studied. The clusters were optimized with M06-L functional. The C, O, N and H atoms were calculated with the 6-31G(d,p) level of theory while the transition metals were calculated with Stuttgart basis functional. All atoms were allowed to relax during structural optimization. All calculations were performed on the Gaussian 09 program.

RESULTS

We synthesized M-PCN-222 and evaluated CO_2 adsorption capacities up to an atmospheric pressure at 298 K. The preliminary results show that Mn-PCN-222 provides the highest CO_2 uptake. To clarify the effect of metal centers in porphyrin ligand on the CO_2 binding affinity, DFT calculation was conducted to calculate the heat of adsorption of CO_2 on M-PCN-222. The heat of adsorption values of Fe-PCN-222 from the calculation are compared with the values obtained from CO_2 adsorption experiments to validate the reliability of the cluster models. Optimized structures of $FeClC_{44}H_{28}N_4$ and $MnClC_{44}H_{28}N_4$ clusters representing the Fe-PCN-222 and Mn-PCN-222 clusters. The average Fe-N bond distance was 2.04 Å while the Fe-Cl bond distance was 2.29 Å compared well with our experimental data of 2.03 and 2.36 Å. For Mn-PCN-222, the average Mn-N bond distance was 2.04 Å while the Mn-Cl bond distance was 2.35 Å. The CO_2 adsorbed on Fe-PCN-222 (CO_2 @ Fe-PCN-222) and Mn-PCN-222 (CO_2 @ Mn-PCN-222) are shown in Figure 1. The CO_2 adsorbs on the metal clusters by oxygen atom with the intermolecular distances of O - - Fe and O - - Mn were 2.95 and 3.12 Å, respectively. The adsorption energies were calculated to be -5.0 and -5.9 kcal/mol, respectively.

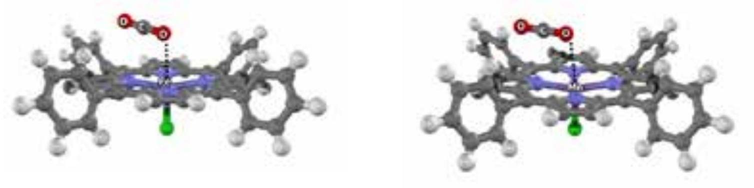

(a) (b)

Figure 1. Optimized structure for (a) CO_2 @ Fe-PCN-222 and (b) CO_2 @ Mn-PCN-222 with M06-L functional.

REFERENCES

1. Queen, W. L., Hudson, M. R., Bloch, E. D., Mason, J. A., Gonzalez, M. I., Lee, J. S., Gygi, D., Howe, J. D., Lee, K., Darwish, T. A., James, M., Peterson, V. K., Teat, S. J., Smit, B., Neaton, J. B., Long, J. R., Brown, C. M., *Chem. Sci.*, 2014, **5**(12), 4569-4581.
2. Feng, D., Gu, Z.-Y., Li, J.-R., Jiang, H.-L., Wei, Z., Zhou, H.-C., Angew. Chem. Int. *Ed.*, 2012, **51**(41), 10307-10310.

CHE
-O-
4

The Preparation of 5,7-Dihydroxy-4-Methylcoumarin via the Pechmann Reaction

Suwapich Pornsatitworakul[1,2], **Bundet Boekfa**[1,2C], **Thana Maihom**[1,2], **Piti Treesukol**[1,2],
Supawadee Namuangruk[3], **Suwatchai Jarussophon**[3], **Nongpanga Jarussophon**[1*] **and**
Jumras Limtrakul[4]
[1]*Department of Chemistry, Faculty of Liberal Arts and Science, Kasetsart University, Kamphaeng Saen Campus, Nakhon Pathom 73140, Thailand.*
[2]*Center for Advanced Studies in Nanotechnology for Chemical, Food and Agricultural Industries, KU Institute for Advanced Studies, Kasetsart University, Bangkok 10900, Thailand.*
[3]*National Nanotechnology Center (NANOTEC), National Science and Technology Development Agency (NSTDA), Pathum Thani 12120, Thailand.*
[4]*Department of Materials Science and Engineering, Vidyasirimedhi Institute of Science and Technology, Rayong 21210, Thailand.*

[C] ***E-mail****: bundet.b@ku.ac.th, faasnpj@ku.ac.th;* ***Tel.*** *+66 8 6555 4089*

EXTENDED ABSTRACT

Keywords: Coumarin, Pechmann reaction, DFT, M06-2X, NMR

INTRODUCTION

Coumarin, an important natural compound from the plants in families of Rutaceae and Umbelliferia, has shown the evidence for the laser activity and medical usage [1]. The Pechmann reaction is one of the important coumarin synthesis methods [2]. Previously, we combined experimental and theoretical method to study the production of 7-Hydroxyl-4-methyl coumarin from resorcinol and ethyl acetoacetate [3]. In this work, we studied Pechmann reaction between ethyl acetoacetate and benzene-1,3,5-triol using sulfuric acid as catalysts by both experiment and theory. The detailed mechanism was investigated by density functional theory calculations. The relative energies, structure of adsorption, transition state, and intermediate were also elucidated.

PROPOSED APPROACH

Pechmann reaction between ethyl acetoacetate and benzene-1,3,5-triol using the sulfuric acid as catalyst has been studied by density functional theory, the M06-2X functional. The structures were optimized with 6-31G(d,p) and the energies were corrected with 6-311+G(2df,2p). Transition states were located using the Berny algorithm and only one imaginary frequency which correspond to the reaction pathway were checked. All calculations were performed using Gaussian 09 program.

For experimental section, the reaction of benzene-1,3,5-triol (20 mmol) and ethyl acetoacetate (20 mmol) with sulfuric acid (1.0 mL) were performed in 50 mL round-bottom flask under controlled pH, time and temperatures. The crude products were collected by vacuum filtration and the crystal was washed with cold DI water. The reaction product was characterized by the TLC technique, IR and NMR spectroscopy.

RESULTS

Pechmann reaction between ethyl acetoacetate with benzene-1,3,5-triol using sulfuric acid was proposed to be three-step reaction: transesterification, intramolecular hydroxylalkylation, and dehydration, as shown in scheme 1. The calculated reaction pathway with relative energies was described shown in figure 1.

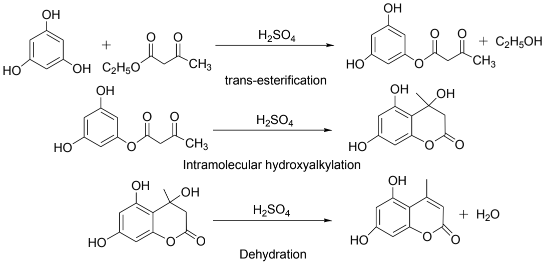

Scheme 1

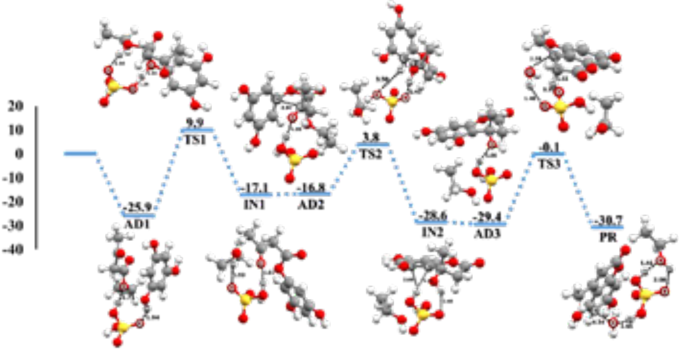

Figure 1. Reaction Pathway of Pechmann reaction for 5,7-dihydroxy-4-methyl coumarin calculated by M06-2X/6-311+G(2df,2p)//M06-2X/6-31G(d,p) level of calculation.

In the experimental part, 5,7-dihydroxy-4-methylcoumarin was synthesized from benzene-1,3,5-triol and ethyl acetoacetate via Pechmann reaction. Several experiments were performed under identical condition but different temperatures. Percent yield of 5,7-dihydroxy-4-methylcoumarin was increased up to 80% without minor product.

REFERENCES

1. Sethna SM, Shah NM. *Chem Rev* 1945, **36**, 1.
2. Pechmann Hon V. *Berichte der deutschen chemischen Gesellschaft* 1884, **17**, 929.
3. Pornsatitworakul S, Boekfa B, Maihom T, Treesukol P, Namuangruk S, Jarussophon S, Jarussophon N, Limtrakul J, *Chemical Monthly* 2017, DOI s00706-017-1962-4

CHE
-O-
5

A DFT Study of Volatile Organic Compounds Adsorption on Transition Metals Doped Single Vacancy Graphene

Preeyaporn Poldorn[1], **Manaschai Kunaseth**[2], **Siriporn Jungsuttiwong**[1,C]
[1]*Department of Chemistry, Faculty of Science, Ubon Ratchathani University,*
Ubon Ratchathani, Thailand
[2]*National Nanotechnology Center (NANOTEC), National Science and Technology Development*
Agency (NSTDA), Pathumthani, Thailand

[C] ***E-mail**: siriporn.j@ubu.ac.th;* ***Fax**: +66-45-288379;* ***Tel.** +66-81-692-2125*

EXTENDED ABSTRACT

The aim of this work is to investigate the adsorption of volatile organic compounds (VOCs) on transition metal (TM) doped single vacancy graphene (SDG) by using density functional theory (DFT) calculation. To facilitate the adsorption of VOCs under ambient conditions, various TM species such as Pd, Pt, Ag and Au were decorated on the SDG surface to increase the efficiency of adsorbent. Adsorption energies were calculated for organosulfur (thiophene), organonitrogen (pyrrole, and pyridine), organooxygen (furan) and benzene. Calculation results showed that the Pd, Pt, Au and Ag clusters were suitable for decorating SDG surface, which cloud be adsorbed stably on the surface. In case of VOCs adsorption, the adsorption strength of VOCs adsorption especially pyridine on the TM cluster doped SDG surface were Pt_4 (-2.11 eV) > Pd_4 (-2.05 eV) > Ag_4 (-1.53 eV) > Au_4 (-1.87 eV). Our study had indicated that TM doped SDG was a suitable adsorbent material for VOCs removal and provides a key insight into the fundamentals of VOCs adsorption on carbon-based adsorbent.

Keywords: DFT, single vacancy graphene, adsorption and volatile organic compound.

INTRODUCTION

Volatile organic compounds (VOCs) are the major pollutants in the atmosphere. There are many sources releasing them such as motor vehicles and chemical plants[1,2]. Some VOCs are hazardous to human health and cause harm to the environment. Combustion, adsorption, bio-filtration, biodegradation and catalytic oxidation are processes that used for removing VOCs. Carbon-based materials such as activated carbons have been widely used as adsorbents for removing a large amount of VOCs. However, adsorption efficiency of these materials are limited. Therefore, improvement of VOCs adsorbent is beneficial and challenging.

PROPOSED APPROACH

All of the calculations were performed using density functional theory (DFT) via the Dmol3 program package in Materials Studio 5.5[3]. The main calculations are conducted with the generalized gradient approximation (GGA) with a PW91 exchange-correlation functional, which is more suitable for adsorption energy calculation than the local density approximation. A Monkhorst–Pack mesh k-points grid of 7×7×1 is used to simplify the Brillouin zone and the real space cutoff radius is maintained as 4.5 Å.

RESULTS

We investigated the adsorption of benzene, furan, thiophene, pyrrole, and thiophene VOCs on to TM-doped SDG, both TM atom tetramer TM clusters (TM = Pd_4-B, Pt_4-A, Au_4-B, andAg_4-B) as adsorbents. Adsorption energies of VOC/TM atom-doped

SDG surface fall in the range −0.94 to −2.23 eV. VOCs have stronger interactions with TM-clusters doped SDG than they do with single TM atoms on SDG. Decreasing adsorption strength is in order of Pt_4-A > Pd_4-A > Au_4-B > Ag_4-B**.** We found that pyridine adsorbs well on all TM-cluster doped SDG adsorbents, especially for Pt_4-A doped SDG, which has the greatest adsorption energy of −2.11 eV[4].

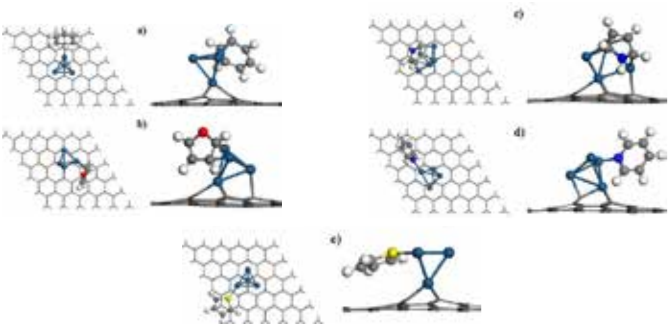

Figure 1. VOCs adsorption on TM-cluster doped SDG (a) benzene, (b) furan (c) pyrrole(d) pyridine and (e) thiophene.

REFERENCES

1. Kamal, M. S.; Razzak, S. A.; Hossain, M. M. *Atmospheric Environment* **2016**, *140*, 117.
2. Brunchi, C. C.; Castillo Sanchez, J. M.; Stankiewicz, A. I.; Kramer, H. J.; Vlugt, T. J. *Industrial & Engineering Chemistry Research* **2012**, *51*, 16697.
3. Delley, B. *The Journal of chemical physics* **1990**, *92*, 508.
4. Kunaseth, M.; Poldorn, P.; Junkeaw, A.; Meeprasert, J.; Rungnim, C.; Namuangruk, S.; Kungwan, N.; Inntam, C.; Jungsuttiwong, S. *Applied Surface Science* **2017**, *396*, 1712.

CHE
-O-
6

A Theoretical Study of Small Schiff Base Complexes with Heavy Metal

Kunanon Chattrairat[1] , **Piyawan Leepheng**[2], **Songwut Suramitr**[3] **and Darinee Phromyothin** [1,2, C]
[1] *College of Nanotechnology, King Mongkut's Institute of Technology Ladkrabang,*
Chalongkrung Rd., Ladkrabang, Bangkok, Thailand 10520
[2]*Nanotec-KMITL Center of Excellence on Nanoelectronic Devices, King Mongkut's Institute of*
Technology Ladkrabang, Chalongkring Rd., Ladkrabang, Bangkok, Thailand 10520
[3]*Department of Chemical, Faculty of Science, Kasetsart University, Ladyao, Chatuchak, Bangkok,*
Thailand 10900

[C] ***E-mail**:* darinee.ph@kmitl.ac.th *;* ***Fax**: +66 2 329 8265 ext 3034 ;* ***Tel.** +66 2 329 8000*

EXTENDED ABSTRACT

Keywords: DFT calculation, Schiff base, Heavy metal detection.

INTRODUCTION

Heavy metal ions from industry are highly dangerous for humans. The major threat of heavy metal ions is mercury (Hg^{2+}) owing to high toxicity even at very low concentrations[1-3]. Lead (Pb^{2+}) also has high toxicity, the excessive of it leads to headaches, irritability and memory problems[3]. Copper (Cu^{2+}) and cobalt (Co^{2+}) is toxic as well. It is a neurotoxic that linked to physical and psychiatric symptoms[4]. The detection has desired to measure them. So, the one way that is low cost and less time consuming is computational method. For example, Density Functional Theory (DFT) calculation was used to determine the derivative Schiff base complex with heavy metal ions[5]. In this work, the molecular structure was designed and calculated the probability of it to interact with heavy metal ions. The heavy metal ions which used in this work are Hg^{2+}, Pb^{2+} and Cu^{2+}. DFT method was used to optimize and calculate the structures and complexes using B3LYP/6-311G(d,p) method for C, N, H, S and O atom and LANL2DZ basis set for heavy metal ions. The optical properties, binding energies and electron distribution were analyzed. The mechanism of interaction was also investigated.

PROPOSED APPROACH

Quantum chemical calculation was investigated the structure geometry and electronic properties. The structure of Schiff base molecule was designed owing to simple synthesis. DFT was used to optimize the derivative Schiff base structure with B3LYP/6-311G(d,p) method. Then the optimization of complexes were calculated by B3LYP/6-311G(d,p) method for C, N, H, S and O atom and LANL2DZ basis set for heavy metal ions (Hg^{2+}, Pb^{2+} ,Cu^{2+} and Co^{2+}). Then, TD-DFT was used to determine the transition state of complexes. Finally, the electronic properties, binding energies and electron distribution were studied.

RESULTS

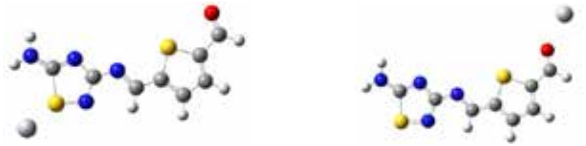

I II

Figure 1. Proposed interacting site between Schiff base molecule and metal ion (I) Sulfur position (II) oxygen position

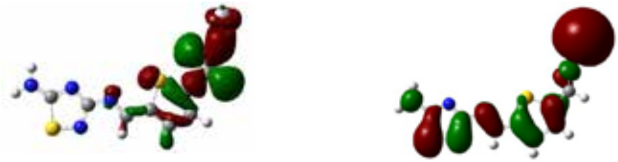

HOMO LUMO

Figure 2. Electron distribution of Schiff base complexs with Hg^{2+} at O site

All structures were optimized by DFT using Gaussian09 suite. The positions which interact with heavy metal ions (Hg^{2+}) were varied by S site and O site as show in Fig. 1(I) and 1(II), respectively. Interacting at oxygen position presented lower binding energy than the sulfur position which was implied that O site of Schiff base interacts with Hg^{2+} by LMCT transition. Considering the electronic properties, HOMO and LUMO were presented electron distribution of complex which Hg^{2+} interact to O site at HOMO state and LUMO state, respectively. The result indicates that the transfer of the electron from derivative Schiff base to Hg^{2+}. Further work, the optical properties binding energies and mechanism of all complexes were investigated.

REFERENCES

1. Bernhoft, R.A., *Mercury toxicity and treatment: a review of the literature.* J Environ Public Health, 2012. **2012**: p. 460508.
2. Suresh, M., et al., *Fluorescent and Magnetic Mesoporous Hybrid Material: A Chemical and Biological Nanosensor for Hg(2+) Ions.* Sci Rep, 2016. **6**: p. 21820.
3. Avuthu, S.G.R., et al., *A Screen Printed Phenanthroline-Based Flexible Electrochemical Sensor for Selective Detection of Toxic Heavy Metal Ions.* IEEE Sensors Journal, 2016. **16**(24): p. 8678-8684.
4. Pal, A., *Copper toxicity induced hepatocerebral and neurodegenerative diseases: an urgent need for prognostic biomarkers.* Neurotoxicology, 2014. **40**: p. 97-101.
5. Jafari, M., et al., *DFT studies and antioxidant activity of Schiff base metal complexes of 2-aminopyridine. Crystal structures of cobalt(II) and zinc(II) complexes.* Inorganica Chimica Acta, 2017. **462**: p. 329-335.

CHE-O-7

Binding Mode Study of Genistein in Complex with Estrogen Receptor Beta by Computational Methods

Supawadee Sainimnuan[1,2], **Warabhorn Boonyarat**[1,2], **Autchara Namkhaw**[1,2],
Supa Hannongbua[1,2] **and Patchreenart Saparpakorn**[1,2]*
[1]*Department of Chemistry, Faculty of Science, Kasetsart University, Bangkok 10900, Thailand*
[2]*Center for Advanced Studies in Nanotechnology for Chemical, Food, and Agricultural Industries, Kasetsart University, Bangkok 10900, Thailand*
E-mail: fscipnsk@ku.ac.th; **Fax: +66 2 579 3955; **Tel.** +66 2 562 5555*

EXTENDED ABSTRACT

Estrogen receptors beta (ERβ) is highly expressed in the hippocampus and cerebral cortex, which is part of the brain associated with learning and creating memory formation. ERβ has become the focus of investigation as a potential drug target for using in the prevention and treatment of Alzheimer's disease (AD). In this work, genistein (GEN) in complex with ERβ is used to study the binding mode using molecular dynamics simulations. 100 ns of MD simulations were performed in GROMACS 5.0 program. From the results, MD simulations reveals the stabilized complex structure after 30 ns and key amino acids for the binding are also investigated. Conformations of 30-100 ns MD trajectories are further clustered based on their conformations. The first conformational cluster posed the highest contribution of the conformations from MD trajectories is selected for analyzing the binding interaction of genistein. The H-bond interactions to amino acids in the binding pocket are Met295, Leu298, Glu305, Leu339, Met340, Leu343, Arg346, Phe356, Ile376, His475, and Leu476. Information from the study can indicate the structural effect of GEN during the binding and can use for further analysis in order to improve the activity of this derivative.

Keywords: Alzheimer's disease (AD); genistein (GEN); Estrogen receptors beta (ERβ); Molecular dynamics simulations (MD)

INTRODUCTION

The estrogen is a group of steroid hormones in females, most of which were synthesized in the gonad and secreted into the bloodstream in order to control the operation of target organs by active through the estrogen receptors (ERs). The main functions of estrogen related to the reproductive system and the operation of the nervous system include the protection and treatment of nerve cells. There are classified into two groups of estrogen receptors, referred to as α and β forms. All of them, they have functions and expression in the different organs. Estrogen receptors alpha (ERα) is expressed in neurons of the cholinergic basal forebrain bundle, which is a part of the brain associated with emotional behavior. While estrogen receptors beta (ERβ) is highly expressed in the hippocampus and cerebral cortex, which is part of the brain associated with learning and creating memory formation. Estrogen receptors beta (ERβ) has become the focus of investigation as a potential drug target in this research and we attempt to study the estrogen receptors beta (ERβ) for use in the prevention and treatment of Alzheimer's disease (AD).

PROPOSED APPROACH

For starting conformation, the crystal structure of genistein in complex with estrogen receptors beta (PDB code: 1X7J) was taken from Protein Data Bank. The molecular dynamics simulations for 100 ns were then performed by using GROMACs program. Octahedron box, SPC water models and the Amber99SB protein, nucleic AMBER94 force field were used.

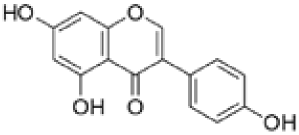

Figure1. Structure of genistein (IC_{50} = 0.0789 µM)

RESULTS

After 30 ns of MD trajectories, the low fluctuation with the RMSD value of 1 Å is found. Conformations of 30-100 ns of MD trajectories were further investigated the number of hydrogen bonds of inhibitor interacted to amino acids in the binding pocket and root mean square fluctuation (RMSF) of amino acids along the simulations. From the results, hydrogen bond interactions between the inhibitor and amino acids in the binding pocket are found. The average number of hydrogen bond interactions is 3.2. RMSF of backbone amino acids in MD trajectories is investigated for the fluctuation of amino acids in the binding pocket. Most of amino acids reveal low fluctuation with the RMSF less than 1 Å. A cluster posed the high contribution of the conformations from MD trajectories was further selected for analyzing the binding interaction to amino acids in the binding site. Genistein revealed H-bond interactions to amino acid in the binding pocket which are Met295, Leu298, Glu305, Leu339, Met340, Leu343, Arg346, Phe356, Ile376, His475, and Leu476.

REFERENCES

1. Ashley C.W.Pike et al., *The EMBO Journal*, 1999, **18 (17)**, 4608-4618.
2. Eric S. Manas et al., J. *Am. Chem. Soc.,* 2004, **126**, 15106-15119.
3. Eric S. Manas., Zhang B. Xu., Rayomand J. Unwalla., and William S. Somers., *Structure*, 2004, **12**, 2197–2207.
4. Zhu Tian et al., *Neural Regen Res*, 2013, **8(5)**, 420–426.
5. Jung Hoon Lee et al., *Mol Neurobiol*, 2014, **49**, 39-49.
6. Liqin Zhao., Sarah K. Woody., Anindit Chhibber., *Ageing Research Reviews*, 2015, **24**, 178–190.
7. Olaf J. Rolinski., Thorben Wellbrock., David J. S. Birch., and Vladislav Vyshemirsky., *J. Phys. Chem. Lett*, 2015, **6**, 3116-3120.

BIO
-O-
1

Backward Bifurcation of SEIR Epidemic Model with Treatment Function

Sasiporn Rattanasupha[1,C] **and Settapat Chinviriyasit**[2]
[1] *Department of Mathematics, Faculty of Science, King Mongkut's University of Technology Thonburi, Bangkok 10140, Thailand*
[2] *Department of Mathematics, Faculty of Science, King Mongkut's University of Technology Thonburi, Bangkok 10140, Thailand*

[C] ***E-mail**: sasipornoh22@gmail.com;* ***Tel.*** *+66 8 1845 ext. 0841*

EXTENDED ABSTRACT

Keywords: Backward Bifurcation, SEIR Epidemic Model, Treatment Function.

INTRODUCTION

Mathematical model of epidemiology is the modelling of an infectious diseases which has been used to predict the transmission dynamics of the infectious diseases in the host population[1-2]. In epidemic model, the treatment is an important method to control or decreasing the spread of diseases [3-6]. In this work, SEIR epidemic model with treatment function is proposed to investigate the effect for treatment of infectious on the disease spread. The model compounds with 4 individuals: Susceptible (*S*), Exposed (*E*), Infected (*I*) and Recovered (*R*) as shown in the following,

$$\begin{aligned}
\frac{dS}{dt} &= A - \beta SI - \mu S \\
\frac{dE}{dt} &= \beta SI - (\mu + \varepsilon)E \\
\frac{dI}{dt} &= \varepsilon E - (\mu + \gamma + d)I - \frac{rI}{1+\alpha I} \\
\frac{dR}{dt} &= \gamma I - \mu R + \frac{rI}{1+\alpha I}
\end{aligned} \tag{1}$$

where A is the recruitment rate, β is the infection rate, μ is the natural death rate, ε is the progression rate to symptom development (the rate at which an infected individual becomes infectious per unit time), γ is the removal rate (the rate at which an infectious individual recovers per unit time), d is the disease-related death and $T(I)$ is the treatment rate function. The treatment function is defined by $T(I) = \frac{rI}{1+\alpha I}$ where r is the cure rate, α is present to measure the extent of the effect of there being a delay in the treatment of infection.

PROPOSED APPROACH

Since the first three equations of the system (1) do not contain the variable R. Thus the system (1) is analyzed in the SEI variables. The equilibrium of the system are established by setting the derivative term equal to zero. The model has equilibrium points:

(I) Disease-free equilibrium (DFE) , $X_0 = \left(S^0, E^0, I^0\right) = \left(\frac{A}{\mu}, 0, 0\right)$

(II) Endemic equilibrium (EE) , $X^* = \left(S^*, E^*, I^*\right)$,

$$S^* = \frac{A}{\beta I^* + \mu} \quad , \quad E^* = \frac{\beta A I^*}{(\mu+\varepsilon)(\beta I^* + \mu)} \quad \text{and} \quad aI^{*2} + bI^* + c = 0$$

where

$$\begin{aligned} a &= \alpha\beta(\mu+\varepsilon)(\mu+\gamma+d) \\ b &= \beta(\mu+\varepsilon)(\mu+\gamma+d+r) + \alpha\mu(\mu+\varepsilon)(\mu+\gamma+d) - \varepsilon\beta\alpha A \\ c &= \mu(\mu+\varepsilon)(\mu+\gamma+d+r)(1-R_0) \end{aligned}$$

and $R_0 = \dfrac{\varepsilon\beta A}{\mu(\mu+\varepsilon)(\mu+\gamma+d+r)}$ is the basic reproductive number.

It indicates that the possibility of backward bifurcation exist in the system when $R_0 < 1$.

RESULTS

Observe that the backward bifurcation will take place when the effect of the infected being delayed for treatment (α) becomes stronger than some level. Thus, α is one of the factors which lead to the backward bifurcation and the following theorem is established.

Theorem 1 When $\alpha > \alpha_0$ then system has a backward bifurcation at $R_0 = 1$,

where $\alpha_0 = \dfrac{\beta(\mu+\gamma+d+r)}{\mu r}$

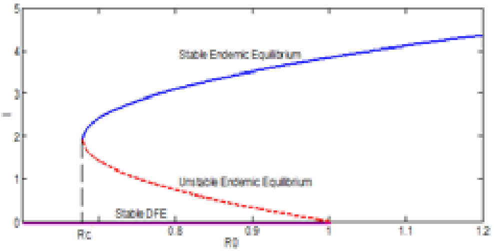

Figure 1. Backward bifurcation of the model.

The numerical solutions in Figure 1 are illustrated backward bifurcation of the model when $A = 10, \beta = 0.05, \mu = 0.2, \varepsilon = 1.2, \gamma = 0.4, d = 0.2, r = 2, \alpha = 1.5$

Conclusion, the basic reproduction number below one is not enough condition to eradicate the disease and also depend on the value of the effect of the infected being delayed for treatment.

REFERENCES

1. Arino, J., Brauer, F., van den Driessche, P., Watmough, J., and Wu, J., J. *Thero.Biol*., 2008, **253**(1), 118-130
2. Ruan, S., Wang, W., *J. Differ. Equations*, 2003, **188**, 135-163.
3. Zhou, X., Cui, J., *Commun. Nonlinear Sci. Numer. Simulat*, 2011, **16**, 4438-4450.
4. Zhang, X., Liu, X., *J. Math. Anal. Appl* , 2008, **348**, 433-443.
5. Hu, Z., Liu, S., Wang, H., *Nonlinear Anal. Real World Appl.*, 2003, **9**, 2302-2312.
6. Zhang, J., Jia, J., Song, X., *Scientific World J.*, 2014,1-11.

BIO
-O-
2

In Vitro and *In Silico* Studies of Chalcone as a New Anticancer Drug Candidate Against a Cancer Target Protein

Kanyani Sangpheak[1], Chompoonut Rungnim[3], Warinthon Chavasiri[4], Peter Wolschann[5,6], Monika Muller[5], and Thanyada Rungrotmongkol[2,C]

[1] Program in Biotechnology, Faculty of Science, Chulalongkorn University, Bangkok 10330, Thailand.
[2] Structural and Computational Biology Research Group, Department of Biochemistry, Faculty of Science, Chulalongkorn University, Bangkok 10330, Thailand.
[3] Nanoscale Simulation Laboratory, National Nanotechnology Center, National Science and Technology Development Agency, Pathum Thani, 12120, Thailand
[4] Natural Products Research Unit, Department of Chemistry, Faculty of Science, Chulalongkorn University, Bangkok 10330, Thailand.
[5] Department of Pharmaceutical Technology and Biopharmaceutics, University of Vienna, Vienna 1090, Austria
[6] Institute of Theoretical Chemistry, University of Vienna, Vienna 1090, Austria

[C] ***E-mail**: thanyada.r@chula.ac.th; **Tel:** +66 2218 5426**; Fax:** + 66 2218 5418.*

EXTENDED ABSTRACT

Keywords: Chalcone, Target drugs, Anticancer, Docking, MTT assay

INTRODUCTION

Cancer is one of the most serious diseases in the world with number of deaths up to 8.2 million in 2012 (World Cancer Report, 2014). Current cancer treatments including surgery and chemotherapy are associated with severe side effects; hence development of drugs with no or less side effects and great selectivity is of prime concern. Target therapy has become potential and popular for cancer treatment because of improved effectiveness and less harm to normal cells. Several kinds of molecular targets have been focused in recent years and one of them is topoisomerase II (TOP2). Chalcone (1,3-diphenyl-2-propen-1-one), is a phenolic compound abundant in edible plant and is considered to be TOP2 inhibitor. Natural and synthetic derivatives of chalcones have been reported to influence several biological activities including anti-proliferative, antioxidant and anti-inflammatory activities. Especially the anticancer activities against various cancer cell lines such as breast (MCF7) [1, 2], cervical (HeLa) [3], lung (A549) [4] cancer cell lines have been reported.

PROPOSED APPROACH

1. Computational methods

1.1 Docking studies

Screening of potent chalcone against target proteins was carried out by a docking procedure using the CDOCKER module. The structures of 47 chalcone derivatives were designed. The all of chalcones and commercial drug were created and optimized. The crystal structure of target protein was downloaded from RSCB Protein Data Bank. The 47 chalcones were docked into the active and binding sites of target protein. The chalcones with the three lowest interaction energies were synthesized and examined the cytotoxicity with cancer cell lines.

2. Experimental approach

2.1 Cytotoxicity assay

The cell viabilities of three cancer cell lines (HT-1376, HeLa, MCF-7) exposed to three chalcones derivatives were evaluated by MTT assay. The 100 µL cell lines were seeded into 96-well plates and incubated for 24 hours under normal culture conditions. By the following day, test compounds at various concentrations (100, 50, 25, and 12.5 µM) were added into wells and incubated for another 24 hours. Afterwards, MTT solution was added to each well and incubated at 37°C for 2 hours, then reaction was stopped by 100 µL of DMSO. The absorbance was measured at 570 nm using a microplate spectrophotometer system. The percentage of cell viability in each compound was calculated, and the IC_{50} values were determined in comparison with untreated controls using Table Curve 2D program version 5.01.

RESULTS

The screening of chalcones for synthesis was guided by docking of all designed chalcones into the ATP-binding site of TOP2α as a target enzyme for anticancer agents. The binding affinities between chalcone and TOP2α were indicated by the ligand-protein interaction energy. The known anticancer drug (salvicine) was used to the reference for prediction the possible binding of designed chalcones. As results the docked chalcone **3c**, **3d** and **3f** showed the third rank lowest interaction energies with the values of -61.08, -60.68 and -59.27 kcal/mol, respectively, that were slightly lower than salvicine (-58.72 kcal/mol). In comparison to the experimental IC_{50} values of the three chalcones against the HT-1376, HeLa and MCF-7 cancer cell lines, it is clearly seen that the chalcone 3d showed a high cytotoxicity with IC_{50} of 10 ± 1 µM on HT-1376, 3 ± 3 µM on HeLa and 21 ± 6 µM on MCF-7. Nonetheless, the cytotoxicity of salvicine on three cancer cell lines is needed to fulfill the screening process.

REFERENCES

1. Chauhan, S.S., et al., Synthesis of novel β-carboline based chalcones with high cytotoxic activity against breast cancer cells. *Bioorganic & medicinal chemistry letters* 2014, **24** (13), 2820-2824.
2. Potter, G., P. Butler, and E. Wanogho, Substituted chalcones as therapeutic compounds 2001, *Google Patents*.
3. Vogel, S., et al., Natural and non-natural prenylated chalcones: synthesis, cytotoxicity and anti-oxidative activity. *Bioorganic & medicinal chemistry* 2008, **16** (8), 4286-4293.
4. Warmka, J.K., et al., Inhibition of mitogen activated protein kinases increases the sensitivity of A549 lung cancer cells to the cytotoxicity induced by a kava chalcone analog. *Biochemical and biophysical research communications* 2012, **424** (3), 488-492.

BIO -O- 3

Enantioselectivity and Enzyme-Ligand Docking Studies of pfDHFR and Cycloguanil Compounds

Suriyawut Kulatee[1], **Pisanu Toochinda**[1], **and Luckhana Lawtrakul** [1,C]
[1] *School of Bio-Chemical Engineering and Technology, Sirindhorn International Institute of Technology, Thammasat University, Pathum Thani, 12121 Thailand*

[C] ***E-mail**: luckhana@siit.tu.ac.th; Fax: +66 2 986 9112~3; Tel. +66 2 986 9103~5 ext. 2301*

EXTENDED ABSTRACT

Keywords: Chiral compounds, Antimalarial drugs, Docking model, Protein-ligand interaction.

INTRODUCTION

Plasmodium falciparum Dihydrofolate Reductase (pfDHFR) is the target of antifolate antimalarial drugs [1]. The mutation reduces the inhibiting activity of antimalarial drugs including Cycloguanil (Cyc). To tackle this problem, Cyc derivatives were designed. The design can increase the inhibiting activity of Cyc derivatives with inhibition constant in the nanomolar level [2]. Unfortunately, there is no report on the drug's property towards inhibiting potential against pfDHFR (*R* and *S* enantiomer). This is important because stereochemistry plays an important role in the drug design and the responses of the drug to the body [1, 3-5]. In this study, theoretical investigation of enantioselective enzyme-ligand binding interaction between 24 enantiomeric Cyc derivatives and wild-type pfDHFR and mutant-type pfDHFR were investigated via molecular docking.

PROPOSED APPROACH

The methodology discussed involves two sections consisting of molecular construction of ligands (Cyc derivatives) and pfDHFR enzymes. Three-dimensional structures of 24 Cyc derivatives were constructed and their geometry were optimized at HF/6-31G (d,p) calculations via GaussView05 and Guassian09 software package, respectively. The crystal structure of wild-type and mutant-type pfDHFR were downloaded from RSCB Protein Data Bank (PDB ID: 3UM8 and 3UM6 respectively [6]). Water molecules were removed and hydrogen atoms were added to the host molecules via Discovery Studio 4.0. Molecular docking of wild-type and mutant-type of pfDHFR with 24 enantiomeric Cyc compounds were carried out using AutoDock 4.2.6 software package. All rotatable bonds within Cyc compounds were allowed to be freely flexible during the docking simulations, whereas enzyme structures were fixed as the rigid macromolecule. Gasteiger charges were assigned for the system. The Lamarkian Genetic Algorithm was used at 100 dockings for each Cyc compounds. The grid size of 0.375 Å spacing was set at specified grid points of 60 points in x-y-z directions. Other parameters were run at the program's default settings. Clusters obtained from Autodock calculations are then compared to pfDHFR-Cyc interactions available in the crystal structures [6]. The best-fit configuration with the lowest binding energy was selected from each of Cyc compounds for further analysis.

RESULTS

Molecular docking results with best-fit configuration shown similar binding interactions as the crystal structures. Fig.1 shows the superposition of Cyc derivatives in *R* and *S* configuration on its parent Cyc structure. A thorough analysis predicts Asp54 to be the characteristic hydrogen bond. Cys15 and Thr185 are binding interactions observed apart from the reference structure. Molecular docking of 24 enantiomeric Cyc compounds with wild-type and mutant-type of pfDHFR indicates the preferential binding of one enantiomeric form over the other form. This work also include the discussion regards to the effects of chlorine substitution at *meta* and *para* position of the phenyl ring on the overall binding activity between ligand-host interaction, the effect of substituent bulkiness on the binding activity between ligand-host interaction and the comparison of experimental data obtained from reference literature versus computational molecular docking data.

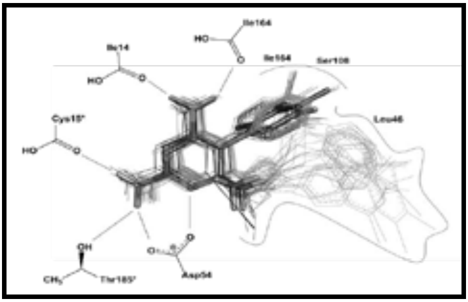

Figure 1. Superposition of Cyc derivatives with inhibitor template; Cyc (stick model). Cyc derivatives in *R* and *S* configuration are shown as stick model as light grey lines and dark grey lines respectively. The best-fit configurations have similar hydrogen bonding interactions as the reference structure. Hydrogen bonding and hydrophobic interactions are viewed as straight lines and curve lines respectively.

REFERENCES

1. Nguyen L.A., H. He, and C. Pham-Huy. *Int. J. Biomed. Sci.,* 2006, **2**, 85-100.
2. Kamchonwongpaisan S., et al*., J. Med. Chem.*, 2004, **47**, 673-680.
3. McConathy J. and M.J. Owens. *Prim. Care Companion J. Clin. Psychiatry,* 2003, **5**, 70-73.
4. Kubinyi H., *J. Braz. Chem. Soc.,* 2002, **13**, 717-726.
5. Sekhon B.S., *J. Mod. Med. Chem.,* 2013, **1**, 10-36.
6. Vanichtanankul J., et al., *Antimicrob. Agents Chemother.,* 2012, **56**, 3928-3935.

ACKNOWLEDGEMENT

The authors gratefully acknowledge the financial support provided by Thai Government Research Fund Contract No. 34/2560.

BIO
-O-
4

Molecular Modelling of 5-Lipoxygenase Enzyme with Antiasthmatic Substances from Plai

Kulpavee Jitapunkul[1], **Orapan Poachanukoon**[2], **Supa Hannongbua**[3], **Pisanu Toochinda**[1], **and Luckhana Lawtrakul** [1,C]

[1] *School of Bio-Chemical Engineering and Technology, Sirindhorn International Institute of Technology, Thammasat University, Pathum Thani, 12121, Thailand*

[2] *Center of Excellence for Allergy, Asthma and Pulmonary diseases, Faculty of Medicine, Thammasat University, Pathum Thani, 12121, Thailand*

[3] *Department of Chemistry, Kasetsart University, Chatuchak, Bangkok, 10900, Thailand*

[C] ***E-mail****: luckhana@siit.tu.ac.th;* ***Tel.*** *+66 2 986 9009 ext. 2301*

EXTENDED ABSTRACT

Keywords: Molecular Dynamics Simulation, Asthma, Ligand-Protein Interaction.

INTRODUCTION

In 2014, The Global Asthma Network reported that approximately 334 million people suffered from asthma[1]. In general, asthma drug (inhaled corticosteroids) is used to control symptoms until it reach resting-state. By using inhaled corticosteroids, the long-term side effects may occur. However, the corticosteroids are still used in asthma treatment due to their low market price. Therefore, the development for alternative asthma drugs with lower price and less side effects are necessary[2-3]. In the past decade, there are many studies aimed to study about anti-leukotriene substances in order to use them as alternative asthma drugs. Some are used in clinical practice for curing asthma such as Zileuton (ZYFLO CR®)[4]. Nevertheless, those medications have lower efficacy than corticosteroids and contain many side effects[5]. Plai or *Zingiber cassumunar Roxb.* is a herb found in the South East Asia region. The major bioactive components of this plant are Compound D {(E)-4-(3',4'-dimethoxyphenyl)but-3-en-2-ol} and DMPBD {(E)-1-(3',4'-dimethoxyphenyl)-butadiene}, which have antiasthmatic activities[6]. Unfortunately, their mechanisms are not fully understood. The possible target for these substances is 5-Lipoxygenase enzyme (5-LO) because the constriction and inflammation of guinea pigs airways can be reduce by 5-LO inhibition[7]. Thus, molecular modelling approaches are used to investigate ligand-protein complexes in order to suggest opportunities for using Compound D and DMPBD as the novel antiasthmatic drugs in comparison with 5-LO natural substrate (arachidonic acid, AA) and asthma drug (Zileuton).

PROPOSED APPROACH

1. *Molecular preparation and optimization*

AA structure was extracted from x-ray structure downloaded from RCSB protein data bank (PDB ID: 3V99). Zileuton, Compound D, and DMPBD molecules were constructed by GaussView05 program. Then, perform structural optimization by density functional theory (DFT) at B3LYP/6-31G (d,p) level by using Gaussian09 program for all ligands. However, the x-ray of substrate-bound 5-LO structure (PDB ID: 3V99) is not complete. Thus, the complete x-ray structure of substrate-free 5-LO was downloaded (PDB ID: 3O8Y) in order to use it as host for molecular modelling simulations.

2. *Molecular docking calculations*

Molecular dockings were performed using the AutoDock 4.2 software package. All torsional angles within ligands were set free to perform flexible ligand docking. Gasteiger charges were assigned for all molecules. The Lamarckian Genetic Algorithm was used at 100 dockings for each ligand. All other parameters were run at program's default settings.

3. *Molecular dynamics (MD) simulations*

MD simulations were performed with AMBER force field in AMBER12 program. The stable prediction of 5-LO complex systems from molecular docking are solvated with a periodic truncated octahedral water box. Each of 5-LO system was started from a temperature of 0 K and gradually heated up to 300 K over 20 ps with constant volume. The whole system was equilibrated for 20 ns at 300 K and 1 atm (isothermal–isobaric ensemble, NPT) with 2 fs time steps. Several thermodynamic properties can be extracted from the output files. In addition, the free binding energy estimation by MM/GBSA (Molecular Mechanics Generalized Born Surface Area) method is used to calculate the binding energy between each ligand and specific amino acid residues of 5-LO.

RESULTS

MD simulations showed that Zileuton, Compound D, and DMPBD are possible to bind at substrate (AA) binding site of 5-LO (Figure 1). AA and Zileuton have similar binding mode with different binding affinity. The hydroxyl group of AA and Zileuton occur two hydrogen bonds with Leu420 and Ala424. Even though Compound D and DMPBD binding at the same catalytic site but molecular interactions with each amino acid residues are different. The binding energy of 5-LO with AA (-48.21 kcal/mol) is much lower than binding with Zileuton (-29.40 kcal/mol), Compound D (-26.83 kcal/mol) and DMPBD (-29.15 kcal/mol) due to the van der Waals interaction between its hydrocarbon chain with many amino acid residues. The overall structures of 5-LO complexed with each ligands are very similar (RMSD 1.66 Å -1.79 Å) which indicated that the 5-LO enzyme has the same dynamics motion even though it was binding with different ligands. This also support our assumption that Compound D and DMPDB are competitive inhibitors, same as Zileuton. The binding affinities of Compound D and DMPBD on 5-LO enzyme also reveal the opportunities for using them as the novel antiasthmatic drugs.

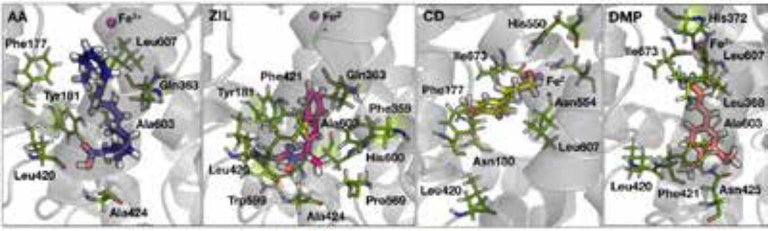

Figure 1. 5-LO binding site and interacting amino acid residues from MD models at 19 ns. 5-LO structure shown as ribbon. The amino acid residues shown as stick models. Arachidonic acid (AA), Zileuton (ZIL), Compound D (CD) and DMPBD (DMP) shown as blue, magenta, yellow, and pink stick models, respectively.

REFERENCES

1. Asher, I. & Pearce, N., *J. Tuberc. Lung Dis.*, 2014, **18**, 1269-1278.
2. Pandya, D., Puttanna, A. & Balagopal, V., *Open Respir. Med. J.*, 2014, **8**, 59-65.
3. Luhadia, S. K., *J. Assoc. Physicians India*, 2014, **62**, 38-40.

4. O'Byrne, P. M., *Can. Respir. J.*, 1998, **5** (Suppl A), 64a-70a.
5. Werz, O. & Steinhilber, D., *Pharmacol. Ther.*, 2006, **112**, 701-718.
6. Panichyupakaranunt, P. & Latae, L., *J. Thai Tradit. Altern. Med.*, 2013, **11**, 123-137.
7. Jeenapongsa, R., Yoovathaworn, K., Sriwatanakul, K. M., Pongprayoon, U. & Sriwatanakul, K., *J. Ethnopharmacol.*, 2003, **87**, 143-148.

BIO
-O-
5

Effects of Incorporating Genetic Models into a Genetic Programming Tree Ensemble for Genetic Association Studies

Pawanrat Aksornsingchai[1], Kittipat Jutawongcharoen[1], Waranyu Wongseree[1],
Nachol Chaiyaratana[1,2], and Damrongrit Setsirichok[1,C]
[1] *Department of Electrical and Computer Engineering, Faculty of Engineering,*
King Mongkut's University of Technology North Bangkok, Bangkok, Thailand
[2] *Division of Molecular Genetics, Department of Research and Development,*
Faculty of Medicine Siriraj Hospital, Mahidol University, Bangkok, Thailand

[C] ***E-mail**: d.setsirichok@gmail.com; **Fax**: +66 2 585 7350; **Tel.** +66 2 555 2000 ext. 8421*

EXTENDED ABSTRACT

Keywords: Case-Control Study, Ensemble of Classifiers, Genetic Association Study, Genetic Programming, Random Forest, Single Nucleotide Polymorphism.

INTRODUCTION

With the completion of the Human Genome Project, it is now possible to locate over 3,000,000 single nucleotide polymorphisms (SNPs), which are common genetic markers, in the human genome [1]. This poses one of the biggest challenges for genetic epidemiologists, which is to identify SNPs that are associated with complex diseases [2]. Nowadays, a genetic association study is treated as the first step to identify the causes of a complex disease of interest. In a population-based study, case-control samples are drawn from a population where SNP information is then extracted through genotyping. The difference between genotypic distribution among case samples and that among control samples usually signifies that SNPs are associated with the disease. In other words, the study aims to identify informative SNPs among available SNPs that lead to case-control classification [3].

From a pattern recognition viewpoint, the identification of informative SNPs can be treated as an attribute selection problem. This means that all three attribute selection approaches—filter, wrapper and embedded approaches—are suitable for the task [4]. Among the embedded techniques, a technique which is proven to be highly capable of identifying informative SNPs is a random forest (RF) [5]. RF was successfully applied to a number of genetic association studies which cover the presence of epistasis or gene-gene interactions and genetic heterogeneity where the same disease is caused by multiple independent genetic factors [6, 7].

Although RF is a suitable technique for genetic association studies, it is impossible to directly incorporate genetic models into RF. Therefore, it is interesting to study the effects of incorporating genetic models into a tree ensemble. One possibility is to use genetic programming (GP) to generate each tree in the ensemble. GP is a variant of genetic algorithm that is specifically designed to evolve a tree [8]. Each GP tree therefore inherits an ability to perform stochastic attribute selection. A genetic model, a genetic-Boolean model or a Boolean function, which can be chosen from a predefined set, is assigned to each non-leaf node in a GP tree. A benchmark experiment in which both RF and GP tree ensemble (GPTE) are used as classifiers where selected attributes are subsequently compared would provide an answer to the question regarding the necessity of genetic models.

PROPOSED APPROACH

GPTE was benchmarked against RF in a simulation trial involving penetrance-based two-locus disease models M1, M7, M97 and M170 [9]. They represent a jointly recessive model, a single-locus recessive model, a semi-pure epistasis model and a pure epistasis model, respectively. The interesting differences between penetrances of disease-predisposing and protective genotypes were 0.2, 0.4, 0.6, 0.8 and 1.0. Each simulated dataset consisted of 20 unlinked SNPs where a disease model was present. The allele frequencies of both causative SNPs were 0.5 while the minor allele frequencies (MAFs) of the remaining SNPs were between 0.05 and 0.5. The dataset consisted of 400 balanced case-control samples. All SNPs in control samples were in Hardy-Weinberg equilibrium. One hundred independent datasets for each simulation setting were generated by genomeSIM [10]. The number of output SNPs and the number of correctly-identified causative SNPs reported by the algorithm were used as the performance indicators [11, 12]. A paired t-test was applied to results obtained for each simulation setting to assess the significance of difference in algorithm performance.

RESULTS

The number of output SNPs reported by GPTE was not different from that reported by RF in the majority of simulation settings. Similarly, the number of correctly-identified causative SNPs reported by GPTE was not different from that reported by RF when there is a large difference between penetrances of disease-predisposing and protective genotypes. However, GPTE was capable of reporting more correctly-identified causative SNPs when the difference between penetrances of disease-predisposing and protective genotypes is small ($p < 0.05$). This suggests that incorporating genetic models into a tree ensemble is required for the latter scenario, which closely resembles to that in genetic association studies.

REFERENCES

1. Bentley, D. R., *Med. Res. Rev.*, 2000, **20**(3), 189–96.
2. Heidema, A. G., Boer, J. M. A., Nagelkerke, N., Mariman, E. C. M., van der A, D. L., and Feskens, E. J. M., *BMC Genet*., 2006, **7**, 23.
3. Ziegler, A. and König, I. R., *A Statistical Approach to Genetic Epidemiology*, 2nd ed., Wiley-Blackwell, Weinheim, 2010.
4. Saeys, Y., Inza, I., and Larrañaga, P., *Bioinformatics*, 2007, **23**(19), 2507–17.
5. Breiman, L., *Mach. Learn.*, 2001, **45**(1), 5–32.
6. Lunetta, K. L., Hayward, L. B., Segal, J., and van Eerdewegh, P., *BMC Genet.*, 2004, **5**, 32
7. Meng, Y. A., Yu, Y., Cupples, L. A., Farrer, L. A., and Lunetta, K. L., *BMC Bioinformatics*, 2009, **10**, 78.
8. Koza, J., *Genetic Programming: On the Programming of Computers by Means of Natural Selection*, MIT Press, Cambridge, 1992.
9. Li, W. and Reich, J., *Hum. Hered.*, 2000, **50**(6), 334–49.
10. Dudek, S. M., Motsinger, A. A., Velez, D. R., Williams, S. M., and Ritchie, M. D., *Proceedings of the Pacific Symposium on Biocomputing 2006*, Edited by Altman, R. B., Dunker, A. K., Hunter, L., Murray, T., and Klein, T. E., World Scientific, Singapore, 2006, 499–510.
11. Wongseree, W., Assawamakin, A., Piroonratana, T., Sinsomros, S., Limwongse, C., and Chaiyaratana, N., *BMC Bioinformatics*, 2009, **10**, 294.
12. Setsirichok, D., Tienboon, P., Jaroonruang, N., Kittichaijaroen, S., Wongseree, W., Piroonratana, T., Usavanarong, T., Limwongse, C., Aporntewan, C., Phadoongsidhi, M., and Chaiyaratana, N., *SpringerPlus*, 2013, **2**, 230.

BIO
-O-
6

Incorporating a Genetic Model into a Logistic Regression Model Improves SNP Selection by Lasso for Genetic Association Studies

Damrongrit Setsirichok[1,C], **Waranyu Wongseree**[1], **and Nachol Chaiyaratana**[1,2]
[1] *Department of Electrical and Computer Engineering, Faculty of Engineering,*
King Mongkut's University of Technology North Bangkok, Bangkok, Thailand
[2] *Division of Molecular Genetics, Department of Research and Development,*
Faculty of Medicine Siriraj Hospital, Mahidol University, Bangkok, Thailand

[C] ***E-mail**: d.setsirichok@gmail.com; **Fax**: +66 2 585 7350; **Tel.** +66 2 555 2000 ext.8421*

EXTENDED ABSTRACT

Keywords: Case-Control Study, Genetic Association Study, Lasso, Logistic Regression, Single Nucleotide Polymorphism.

INTRODUCTION

Genetic association studies focus on the identification of genetic markers including single nucleotide polymorphisms (SNPs) that are associated with complex diseases. Family-based and population-based studies aim to identify common disease alleles among related and unrelated individuals, respectively [1]. From a classification viewpoint, a population-based study is essentially an attribute selection problem. In other words, the study attempts to select SNPs that can be used to classify case-control samples from affected and unaffected individuals. Many regression analysis with attribute selection methods are suitable for the task. They include a least absolute shrinkage and selection operator (lasso) [2] and an elastic net (EN) [3]. Lasso exploits an l_1 penalty during the optimisation of a logistic regression model's coefficients, which leads to the attribute selection capability. In contrast, EN exploits a combined l_1/l_2 penalty. Lasso is suitable when attributes are uncorrelated while EN is suitable when attributes are correlated.

The logistic regression model's parameters that represent the coefficients for SNPs should be zero if these SNPs are not associated with the disease. Nonetheless, the possibility of irrelevant SNPs having non-zero coefficients exists. Hence, it is necessary to determine whether each non-zero coefficient is crucial for the classification capability of the logistic regression model. Recently, a method for determining statistical significance of coefficients in a logistic regression model was proposed [4].

With the availability of regression analysis with attribute selection methods and how to determine the statistical significance of a logistic regression model's coefficients, it is possible to apply the aforementioned methodology to population-based association studies. There are two possible strategies: direct application of the methodology and incorporating a genetic model into the logistic regression model [5] prior to the application of the methodology. These two strategies are the interest of this article. Since the candidate gene approach to genetic association studies mainly focuses on selection of unlinked SNPs, lasso was chosen for this study.

PROPOSED APPROACH

A logistic regression model with an incorporated genetic model was compared with a standard logistic model in a simulation trial. Lasso was used to obtain the logistic regression models' parameters. Each simulated dataset consisted of 20 unlinked SNPs where two SNPs were causative SNPs. Both causative SNPs were governed by one of four penetrance-based two-locus disease models: M1 (a jointly recessive model), M7 (a single-locus recessive model), M97 (a semi-pure epistasis model) and M170 (a pure epistasis model) [6]. The differences between penetrances of disease-predisposing and protective genotypes in each disease model were 0.2, 0.4, 0.6, 0.8 and 1.0. The minor allele frequencies of irrelevant SNPs were between 0.05 and 0.5 while the allele frequencies of both causative SNPs were 0.5. The dataset consisted of 400 balanced case-control samples in which all causative SNPs in control samples were in Hardy-Weinberg equilibrium. genomeSIM [7] was used to generated 100 independent datasets for each simulation setting. The interesting performance indicators were the number of selected SNPs and the number of correctly-identified causative SNPs in the logistic regression model [8, 9]. The significance of difference between the numbers of SNPs in the logistic regression models was assessed through a paired *t*-test.

RESULTS

The number of selected SNPs in the logistic regression model with an incorporated genetic model was either similar to or higher than that in the standard logistic regression model in every simulation setting. On the other hand, the numbers of correctly-identified causative SNPs in the logistic regression model with an incorporated genetic model and standard logistic regression model were similar in two scenarios. These are the scenarios when the disease model is M7, and when the disease model is M1 and the difference between penetrances of disease-predisposing and protective genotypes is large. The logistic regression model with an incorporated genetic model contained more correctly-identified causative SNPs in the remaining scenarios ($p < 0.05$). This suggests that incorporating a genetic model into a logistic regression model is important for detecting informative SNPs in genetic association studies.

REFERENCES

1. Ziegler, A. and König, I. R., *A Statistical Approach to Genetic Epidemiology*, 2nd ed., Wiley-Blackwell, Weinheim, 2010.
2. Tibshirani, R., *J. R. Stat. Soc. Ser. B-Methodol.*, 1996, **58**(1), 267–88.
3. Zou, H. and Hastie, T., *J. R. Stat. Soc. Ser. B-Stat. Methodol.*, 2005, **67**(2), 301–20.
4. Lockhart, R., Taylor, J., Tibshirani, R. J., and Tibshirani, R., *Ann. Stat.*, 2014, **42**(2), 413–68.
5. Cordell, H. J., *Hum. Mol. Genet.*, 2002, **11**(20), 2463–8.
6. Li, W. and Reich, J., *Hum. Hered.*, 2000, **50**(6), 334–49.
7. Dudek, S. M., Motsinger, A. A., Velez, D. R., Williams, S. M., and Ritchie, M. D., *Proceedings of the Pacific Symposium on Biocomputing 2006*, Edited by Altman, R. B., Dunker, A. K., Hunter, L., Murray, T., and Klein, T. E., World Scientific, Singapore, 2006, 499–510.
8. Wongseree, W., Assawamakin, A., Piroonratana, T., Sinsomros, S., Limwongse, C., and Chaiyaratana, N., *BMC Bioinformatics*, 2009, **10**, 294.
9. Setsirichok, D., Tienboon, P., Jaroonruang, N., Kittichaijaroen, S., Wongseree, W., Piroonratana, T., Usavanarong, T., Limwongse, C., Aporntewan, C., Phadoongsidhi, M., and Chaiyaratana, N., *SpringerPlus*, 2013, **2**, 230.

BIO
-O-
7

Pushing The Limits of Detection of Weak Binding Using Fragment Based Drug Discovery: Identification of New Cyclophilin Binders

Charis Georgiou[1,2,C], **Malcolm Walkinshaw**[2], **and Julien Michel**[1]
[1] *EaStCHEM School of chemistry, University of Edinburgh, Joseph Black Building, David Brewster Road, Edinburgh, Scotland, EH9 3FJ*
[2] *Institute of Structural and Molecular Biology, The University of Edinburgh, Edinburgh, EH9 3JR*

[C] ***E-mail**: Charis.Georgiou@ed.ac.uk;*

EXTENDED ABSTRACT

Keywords: PPIases, cyclophilin inhibitors, fragment based drug discovery, free energy calculations, protein – ligand X-ray crystallography

INTRODUCTION

Fragment based drug discovery (FBDD) is an increasingly popular and successful method to identify novel small-molecule drug candidates. One of the limitations of the approach is the difficulty of accurately characterizing weak binding events, and there is a need for pushing the limits of detection of weak binding to broaden the scope of FBDD. On the other hand, rapid developments in computational chemistry during the past decades let to the use of molecular simulations and free energy calculations as part of the structure-based drug design process, to complement the experimental approaches.[1] This research was focused on the combination of biophysical measurements and molecular simulation methods to characterize weak Cyclophilins (Cyps) binders present within a library of small fragments.

Cyclophilins (Cyp) are proteins able to catalyze the interconversion of trans/cis isomers of proline and belong to the peptidyl-prolyl isomerases family (PPIase).[2] In addition to their PPIase activity, Cyps have diverse biological roles and have been implicated in a number of different diseases such as HIV-1, HCV and neurodegenerative diseases such as Parkinson's and Alzheimer's.[3] Although several Cyp inhibitors have been reported in the literature, none are able to inhibit with high specificity specific Cyp isoforms. Yet it is necessary to produce chemical probes with high binding specificity in order to elucidate the biological roles of different Cyp isoforms and to pave the way for the next-generation Cyp drugs with reduced side-effects.

PROPOSED APPROACH

To facilitate the development of isoform-specific Cyp ligands, we pursue detailed studies of Cyp dynamics and binding thermodynamics using molecular simulations, biophysical assays and protein X-ray crystallography. Research efforts were initially focussed on the identification of novel Cyp inhibitors using X-ray crystallographic studies and Surface Plasmon Resonance (SPR) experiments on fragments from an in-house bespoke library of small compounds. To further examine the binding of these fragments to cyclophilins, identify interactions with the proteins and explain specificity trends from SPR and X-ray results, molecular dynamics (MD) simulations and free energy calculations were pursued. Models of apo and holo Cyps in complex with fragments that we had experimentally tested were set up using the Amber, AmberTools and FESetup software.[4,5] Free energy calculations were performed using the multistate bennett acceptance ratio (MBAR) technique with the Sire/OpenMM softwares.[6,7]

RESULTS

The combined data from SPR, X-ray crystallography measurements and MD simulations provides solid evidence that several, structurally novel fragments from the present in-house bespoke library interact with Cyp surfaces with dissociation constants in the low millimolar range.

Binding free energies computed via molecular dynamics simulations were able to reproduce the preference for the binding of the fragments in distinct Cyp pockets and binding affinity estimated from MD were in line with the range inferred from SPR analysis. Additionally, analysis and visualisation of MD trajectories for selected fragments proved to be a rich source of structural insights. These simulations revealed different poses that several fragments can adopt in the binding site of Cyp and these data could be used to assist model refinement process of X-ray diffracted crystals as also as a guidance for fragment growing strategies.

Furthermore, the binding modes of the various fragments from the present library in the active site of Cyp, were found to be remarkably similar to compounds recently reported in the literature.[8,9] Renewed chemistry efforts to merge the presently disclosed fragments with the scaffold from the lead series of previously published compounds may produce superior ligands for further drug development or in vivo investigations.

REFERENCES

1. Michel, J. *Phys. Chem. Chem. Phys.* **2014**, *16* (10), 4465–4477.
2. Davis, T. L.; Walker, J. R.; Campagna-Slater, V.; Finerty, P. J.; Finerty, P. J.; Paramanathan, R.; Bernstein, G.; Mackenzie, F.; Tempel, W.; Ouyang, H.; Lee, W. H.; Eisenmesser, E. Z.; Dhe-Paganon, S. *PLoS Biol.* **2010**, *8* (7).
3. Fliri, H. *Drug Target Review*. January 2016.
4. D.A. Case, J.T. Berryman, R.M. Betz, D.S. Cerutti, T.E. Cheatham, III, T.A. Darden, R.E. Duke, T.J. Giese, H. Gohlke, A.W. Goetz, N. Homeyer, S. Izadi, P. Janowski, J. Kaus, A. Kovalenko, T.S. Lee, S. LeGrand, P. Li, T. Luchko, R. Luo, B. Madej, K.M. Merz, D. M. Y. and P. A. K. University of California: San Francisco 2014.
5. Loeffler, H. H.; Michel, J.; Woods, C. *J. Chem. Inf. Model.* **2015**, *55* (12), 2485–2490.
6. Woods, C.; Calabro, C.; Michel, J. www.siremol.org www.siremol.org (accessed Apr 29, 2016).
7. Eastman, P.; Pande, V. *Comput. Sci. Eng.* **2010**, *12* (4), 34–39.
8. Gelin, M.; Delfosse, V.; Allemand, F.; Hoh, F.; Sallaz-Damaz, Y.; Pirocchi, M.; Bourguet, W.; Ferrer, J.-L.; Labesse, G.; Guichou, J.-F. *Acta Crystallogr. Sect. D* **2015**, *71* (8), 1777–1787.
9. Ahmed-Belkacem, A.; Colliandre, L.; Ahnou, N.; Nevers, Q.; Gelin, M.; Bessin, Y.; Brillet, R.; Cala, O.; Douguet, D.; Bourguet, W.; Krimm, I.; Pawlotsky, J.-M.; Guichou, J.-F. *Nat. Commun.* **2016**, *7*, 12777.

CSE
-O-
1

The Numerical Solution of Fractional Angiogenesis Problem by Meshless Local Petrov-Galerkin Method

Kunwithree Phramrung [1,C], **Anirut Luadsong** [1,2], **and Nitima Aschariyaphotha** [2]
[1]*Department of Mathematics, Faculty of Science, King Mongkut's University of Technology Thonburi (KMUTT), Bang Mod, Thung Khru, Bangkok 10140, Thailand*
[2]*Ratchaburi Learning Park, King Mongkut's University of Technology Thonburi (KMUTT), Rang Bua,Chom Bueng, Ratchaburi 70150, Thailand*

[C] ***E-mail**: kunwithree.kp@mailkmutt.ac.th;* ***Fax**: +66 2 428 4025;* ***Tel.** +66 9 9097 5232*

EXTENDED ABSTRACT

Keywords: Keller-Segel model, angiogenesis, Caputo and Fabrizio, MLPG method.

INTRODUCTION

In the recently years, chemotaxis has attracted significant interest due to its critical role in a wide range of biological phenomena. Chemotaxis is the oriented movement of the bacteria in response to gradients of the concentration of the chemical signal substance in their environment. In 1953, Patlak proposed the first mathematical modelling of chemotaxis. In 1970, Keller and Segel proposed a chemotaxis model to describe the aggregation process of cellular slime mold by chemical attractions. In this paper, we will explore example of problems for which the Keller-Segel model [4], angiogenesis, has been used to describe the evolution of a system in which organisms respond to chemicals in their environment [7].

PROPOSED APPROACH

The model proposed by Levine et al. [5] was extended to the concept of the differential equation by using the fractional order derivative without singular kernel [3].

$$\frac{\partial^{\alpha}\eta(\mathbf{x},t)}{\partial t^{\alpha}}=D\frac{\partial}{\partial x}\left(\eta\frac{\partial}{\partial x}\ln\left(\frac{\eta}{\tau}\right)\right), \tag{1}$$

$$\frac{\partial^{\alpha}c(\mathbf{x},t)}{\partial t^{\alpha}}=\frac{\lambda_1\eta v}{1+\upsilon_1 v}, \tag{2}$$

$$\frac{\partial^{\alpha}v(\mathbf{x},t)}{\partial t^{\alpha}}=\frac{-\lambda_1\eta v}{1+\upsilon_1 v}, \tag{3}$$

$$\frac{\partial^{\alpha}f(\mathbf{x},t)}{\partial t^{\alpha}}=\frac{-\lambda_2 cf}{1+\upsilon_2 v}+\beta f\left(f_M-f\right)\eta . \tag{4}$$

where v is the concentration of tumor angiogenesis factors, c is the concentration of proteolytic enzymes, η is the density of endothelial cells, f is the density of fibronectin and $\mathbf{x}\in\Omega,\ t>0,\ \Omega\in\Re^{d},\ d=1,2,3,\ldots$. The approximation solutions of the angiogenesis model for the spatial discretization used the MLPG [1, 6]. In the MLPG method, the moving Kriging interpolation is employed to construct the shape function which has the Kronnecker delta property. And the Dirac delta function is applied in the local weak form as the test functions.

$$A\frac{d^{\alpha}U}{dt^{\alpha}}+B(U)U=0 \tag{5}$$

where $A=\left[A_{ij}\right]_{N\times N};\ A_{ij}=\phi_j(x_i)=\begin{cases}0;\ i\neq j\\ 1;\ i=j\end{cases},\ B(U)=\begin{bmatrix}B_{11} & 0 & 0 & 0\\ 0 & 0 & B_{23} & 0\\ 0 & 0 & B_{33} & 0\\ 0 & 0 & 0 & B_{44}\end{bmatrix},$

$$B_{11}=\left[-\phi_j(x_i)D\frac{\partial^2}{\partial x^2}\left(\ln\left(\frac{\eta}{\tau}\right)\right)-\phi_{j,x}(x_i)D\frac{\partial}{\partial x}\left(\ln\left(\frac{\eta}{\tau}\right)\right)\right]_{N\times N},\ B_{23}=\left[-\phi_j(x_i)\frac{\lambda_1\eta}{1+\upsilon_1 v}\right]_{N\times N},$$

$$B_{33}=\left[\phi_j(x_i)\frac{\lambda_1\eta}{1+\upsilon_1 v}\right]_{N\times N},\ B_{44}=\left[\phi_j(x_i)\frac{\lambda_2 c}{1+\upsilon_2 v}-\phi_j(x_i)\beta(f_M-f)\eta\right]_{N\times N},U=\left[\hat{H}\ \ \hat{C}\ \ \hat{V}\ \ \hat{F}\right]^T,$$

$$\hat{H}=\left[\hat{\eta}_1\ \ \hat{\eta}_2\ \ \ldots\ \ \hat{\eta}_N\right]^T,\hat{C}=\left[\hat{c}_1\ \ \hat{c}_2\ \ \ldots\ \ \hat{c}_N\right]^T,\hat{V}=\left[\hat{v}_1\ \ \hat{v}_2\ \ \ldots\ \ \hat{v}_N\right]^T,\hat{F}=\left[\hat{f}_1\ \ \hat{f}_2\ \ \ldots\ \ \hat{f}_N\right]^T.$$

For the temporal discretization used implicit finite difference method [2, 8]. The grid points in the time interval $[0,T]$ are labeled $t_i=i\Delta t+t_0$ where $i=0,\ 1,\ 2,\ \ldots,\ N$. At the time level n ,

$$U^n=G^n\left(d_0U^0+\sum_{j=1}^{n-1}(d_j-d_{j-1})U^j\right)\tag{6}$$

where $\sigma=1-\exp\left[-\alpha\frac{\Delta t}{1-\alpha}\right],\ k=-\alpha\frac{\Delta t}{1-\alpha},\ d_j=\exp[(n-j-1)k]-\exp[(n-j)k]$ and

$$G^n=\left(\sigma I+\frac{\alpha\Delta t}{M(\alpha)}B^n\right)^{-1}.$$

RESULTS

The numerical results were compared with integer order differential equations to confirm the accuracy and effectiveness of the proposed method. We conclude the results of a numerical experiment conducted by from Figures (a)-(d) show the approximation of the system obtained numerically. The initial condition on the tumor angiogenesis factors of the numerical experiment are set by Levine et al.

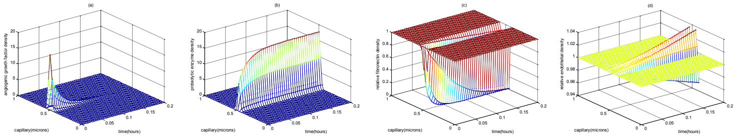

Figure (a) Evolution of the growth factor decay. (b) Evolution of the protease. (c) Evolution of fibronectin decay. (d) Evolution of the endothelial cells.

REFERENCES

1. Atluri, S. N. and Shen, S., *Computer Modeling in Engineering & Sciences, 2002b*, **3** (1), 11–51.
2. Atangana, A. and Alkahtani B. S. T., *Advances in Difference Equations*, 2016, **1** (156).
3. Caputo, M. and Fabrizio, M., *Progress in Fractional Differentiation and Applications,* 2015, **1** (2), 73-85.
4. Keller, E. F. and Segel, L. A., *Journal Theory Biology*, 1970, **26**, 399–415.
5. Levine, H. A., Sleeman, B. D., and Nilsen-Hamilton, M., *Journal of Mathematical Biology*, 2001, **42** (3), 195-238.
6. Phaochoo, P., Luadsong, A., and Aschariyaphotha, N., *Springer Plus*, 2016, **5**, 305.
7. Ritter, L. R., *A Short Course in the Modeling of Chemotaxis*, 1^{sd} ed., Texas A & M University, Texas, 2004, 36-52.
8. Thamareerat, N., Luadsong,A., and Aschariyaphotha, N., *Advances in Difference Equations*, 2017, **1** (74).

CSE
-O-
2

The Meshless Local Petrov-Galerkin Method for Solving the Black-Scholes-Schrodinger Model

Naravadee Nualsaard[1,C], **Anirut Luadsong**[1,2], **Nitima Aschariyaphotha**[2]
[1] *Department of Mathematics, Faculty of Science, King Mongkut's University of Technology Thonburi (KMUTT),126 Pracha-utid Road, Bangkok 10140, Thailand*
[2] *Ratchaburi Learning Park, King Mongkut's University of Technology Thonburi (KMUTT), Rang Bua, Chom Bueng, Ratchaburi 70150, Thailand*

[C] ***E-mail**: naravadee401@gmail.com; **Fax**: +66 24284025; **Tel.** +66 0817345895*

EXTENDED ABSTRACT

Keywords: Black-Scholes-Schrodinger model, Meshless local Petrov-Galerkin method, Moving Kriging interpolation, Arbitrage, Option pricing, Quantum mechanics, θ-weighted method**.**

INTRODUCTION

Black–Scholes model is proposed by Black and Scholes (1973) [2]. This model cannot explain some conditions such as the effects of arbitrage on the option pricing dynamics. Haven E. (2002) [5] presented that an arbitrage is a necessary condition of the Black–Scholes model in a more general of quantum physics. Contreras, M., et al. (2010) [4] propose the new Black-Scholes-Schrodinger model which can be described the Black-Scholes model with the arbitrage possibility in the sense of the Schrodinger equation. The meshless local Petrov-Galerkin (MLPG) method was first discovered by Atluri and Zhu (1998) [1]. Phaochoo P., et al. (2016) [6] present a numerical study of the European option by the meshless local Petrov-Galerkin (MLPG) method with moving kriging interpolation. In this paper, the meshless local Petrov-Galerkin (MLPG) method is applied for solving the new Black-Scholes-Schrodinger model.

PROPOSED APPROACH

The new Black-Scholes-Schrodinger model which can be described the Black-Scholes model with the arbitrage possibility in the sense of the Schrodinger equation is proposed by [4].

$$\frac{\partial\psi(x,t)}{\partial t}+\frac{1}{2}\sigma^2\frac{\partial^2\psi(x,t)}{\partial x^2}+v(x,t)\left(\frac{\partial\psi(x,t)}{\partial x}-\psi(x,t)\right)=0\ ,(x,t)\in\mathbb{R}^+\times[0,T] \qquad (1)$$

where t is time variable, $\psi(x,t)$ is wave function, $v(x,t)$ is the potential energy, σ is the volatility of underlying asset price and T is the expiration date. For solving the new Black-Scholes-Schrodinger model, the MLPG method is used for spatial discretization. In MLPG method, the shape function is constructed by the moving kriging interpolation and the Kronecker delta function is chosen as the test function in each sub-domain for simplifying the equation.

$$A\frac{d\Psi}{dt}=B\Psi \qquad (2)$$

where $A=\left[A_{ij}\right]_{N\times N}$; $A_{ij}=\phi_j(x_i)$

$$B=\left[B_{ij}\right]_{N\times N};\ B_{ij}=-\frac{1}{2}\sigma^2\phi_{j,xx}(x_i)-v(x_i,t)\left(\phi_{j,x}(x_i)-\phi_j(x_i)\right)$$

$$\Psi=\left[\hat{\psi}_1\ \hat{\psi}_2\ldots\ \hat{\psi}_N\right]^T$$

for $i=1,2,\ldots,N$ and $j=1,2,\ldots,N$.

While, the θ-weighted method is chosen for the temporal discretization. The nodal points in the time interval [0,*T*] are given by $t_n = n\Delta t, n = 0,1,2, \ldots$

$$(I - \theta\Delta tB)\Psi^{n+1} = [I + (1-\theta)\Delta tB]\Psi^n \qquad (3)$$

where $\Psi^n = \left[\hat{\psi}_1\ \hat{\psi}_2 \ldots \hat{\psi}_N\right]^T$

N is the total number of nodal points.

B is the discretization matrix for the space of linear differential operator.

I is the identity matrix.

RESULTS

The results are presented in figures 1-2. Figure 1 shows a wave function which is solved by MLPG method. In figure 2, option price is solved by MLPG method and semi-classical method. From the numerical experiment, results from MLPG method are agreed to semi-classical solution.

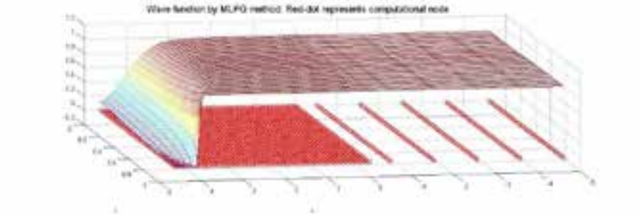

Figure 1. The wave function is solved by MLPG method.

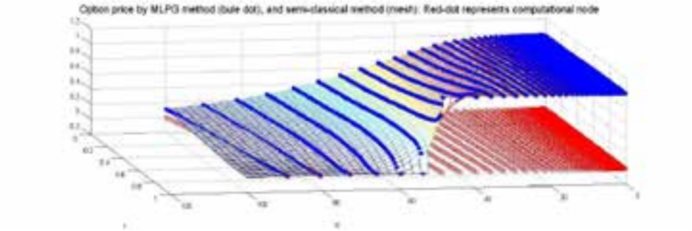

Figure 2. The option price is solved by MLPG method and semi-classical method.

REFERENCES

1. Atluri, SN. and Shu, T., *Computational Mechanics*, 1998, **22**, 117-127.
2. Black, F. and Scholes, M., *Journal of Political Economy*, 1973, **81**(3), 637-654.
3. Contreras, M., Montalva, R., Pellicer, R., and Villena, M., *PhysicaA*, 2010, **389**, 3552-3564.
4. Contreras, M., Pellicer, R.,Villena, M., and Ruiz, A., *PhysicaA*, 2010, **389**, 5447-5459.
5. Haven, E., *PhysicaA*, 2002, **304**, 507-524.
6. Phaochoo, P., Luadsong, A., and Aschariyaphotha, N., *SpringerPlus*, 2016, **5**(305), 1-14.

CSE
-O-
3

Spinner: Failure Detection and Recovery Software in Software Define Network

Chinnawat Nualta[1], **Chanon Taupachit**[1], **and Supakit Prueksaaroon** [1,C]
[1]*Department of Electrical and Computer Engineering, Faculty of Engineering, Thammasat University, Bangkok, Thailand*

[C] ***E-mail****: psupakit@engr.tu.ac.th;* ***Tel.*** *+66 8 4088 9437*

EXTENDED ABSTRACT

Keywords: Software define network, Failure detection and recovery.

INTRODUCTION

Cloud computing provider dealing with thousand of nodes and network switches. The link or node failures happen regularly. Enterprise provider needs an intelligent network capability to detect any malfunctions and establish an alternative path to support by network operation center (NOC). Recently, Software-Defined Networking (SDN) is an industry movement for building programmable networks that are elastic and reach to market requirement. SDN refers to the use as standards-based infrastructure, because it enables the modern network switches and routers to management and operation on data plane functions directly. SDN is concepts that separate network sub-system into 2 parts. The first part called control plane that function to control traffic flow and policies. The second part called data plane performs the packet forwarding. Instead, a centralize management, often referred to as the SDN controller, performs the control plane functionality from center, i.e. monitoring, policies, access control list, and devices configuration. Most advantage of the central controller point introduced in SDN is its enable network monitor for performance, functionality and reprogram when necessary. SDN controller can observe entire network health per-flow characteristics, such as throughput, delay and packet loss [1]. The standard of SDN based on OpenFlow specification. Openflow use the flow table matching technique. The flow tables consist of rules of every package that are running on the same domain. The most important work of NOC is to maintain end-to-end connectivity between nodes. Hence, when a link down, the controller detect automatically and reconfigure new network paths to restore or maintain end-to-end connectivity for all paths. However, the recovery period of a broken path includes the detection time, path re-computation time, and deploy new configuration to all data plane devices by the controller. In this work, we propose *Spinner*, Openflow management software based on OpenDaylight [2]. The OpenDaylight, largest open source SDN controller, is a highly available, modular, extensible, scalable and multi-protocol controller built for SDN development on modern heterogeneous multi-vendor networks. OpenDaylight provides a service platform that allows users to write an application that easily work across a wide variety of devices. Spinner provides automate link failure detection based on nodes periodic probing and reroute mechanism of traffic flows with shortest path algorithm. The enhanced control offered by Spinner aligns well with Cloud computing providers. Due to scale on dynamic resources and variety of user requirement, cloud computing require efficient mechanism to rapidly and efficiently management. As a result, Spinner software prototype provides well responsible for point-to-point link failure detection and recovery.

PROPOSED APPROACH

Spinner provides mechanisms to perfrom link failure detection and automatic path recovery using shortest path algorithm, without requiring command from SDN controller. Spinner develops based on Python and OpenDaylight controller. The REST API is used to communication between controller and Spinner. Spinner downloads the real time information from OpenDaylight and calculated the cost of every link in the system to generate the link state of all nodes. The JSON file was used as standard document. The features implemented by Spinner are consisted of link cost calculation, and automatic rerouting with shortest path algorithm. The diagram of Spinner is depicted in Figure 1.

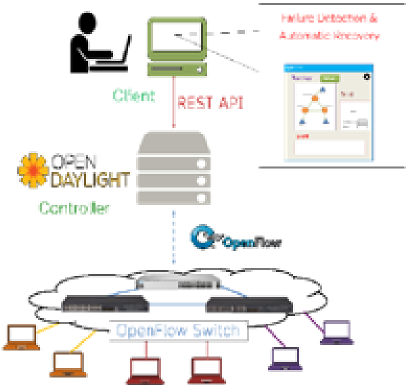

Figure 1. An example figure.

RESULTS

This paper we have presented Spinner, a failure detection and recovery in SDN that provides a fully programmable to application developers and support for cloud datacentre. Spinner has been implemented with OpenDaylight. Spinner has tested in the real environment. The prototype has plan to validation in the enterprise cloud provider.

REFERENCES

1. N. L. M. van Adrichem, C. Doerr, and F. A. Kuipers, *"Opennetmon: Network monitoring in openflow software-defined networks,"* Network Operations and Management Symposium (NOMS), 2014 IEEE.
2. J. Medved, R. Varga, A. Tkacik and K. Gray, "OpenDaylight: Towards a Model-Driven SDN Controller architecture," *Proceeding of IEEE International Symposium on a World of Wireless, Mobile and Multimedia Networks 2014*, Sydney, NSW, 2014, pp. 1-6. doi: 10.1109/WoWMoM.2014.6918985
3. C. Cascone, D. Sanvito, L. Pollini, A. Capone, and B. Sanso, *"Fast Failure Detection and Recovery in SDN with Stateful Data Plan," International Journal of Network Management*, 2017, **Volume** 27, Issue 2, doi: 10.1002/nem.1957.

CSE
-O-
4

System Tuning for Energy Efficient Big Data Infrastructure

Soratouch Pornmaneerattanatri[1,C] **and Putchong Uthayopas**[1]
[1] *Department of Computer Engineering, Faculty of Engineering, Kasetsart University, Bangkok, Thailand*

[C] ***E-mail***: *soratouch.p@ku.th, putchong@ku.th; Tel.* *+66852201444*

EXTENDED ABSTRACT

Keywords: Big Data, Energy Efficient, Green IT, Performance Tuning.

INTRODUCTION

Big Data is an emerging area of applying complex data analytic to a massive number of data. Big Data has a broad application in science, engineering, business, financial, and industrial application. For a massive multi-terabyte dataset, a Big Data platform consists of hundreds of computing servers and middleware such as spark or Hadoop are used for the processing. One of the major operation cost for such a large infrastructure is energy cost. In this paper, various approaches of system tuning of Big Data infrastructure is proposed. This enables the big data platform to achieve the results with much less time and energy. Hence, the total operation cost is substantially reduced for an organization that depends on large-scale Big Data analytic for their strategic advantages.

PROPOSED APPROACH

To reduce energy consumption for big data platform, there are many system parameters involved such as CPU, Memory, I/O and Storage speed. The main concept is to focus on a few behaviors of the system. For each computer, the system has two energy consumption components. The first component is a baseline energy consumption, this component will consume energy around 5-20% based on the hardware configuration, the baseline energy consumption caused by every hardware and CPU operating in "idle" state without any workload. When the processing start, CPU need more energy to operate in higher frequency state, energy consumption is then increased. This energy consumption component caused by CPU running in working mode at the higher frequency. Overall energy consumption caused by the baseline component, working component, and the execution time of the process. These 3 components must be tuned to reduce the energy consumption.

First, we can start by the CPU tuning methods. The frequency of CPU can be adjusted to a higher frequency which will lower the execution time but increase the energy consumption. With the right balance, the saving can be achieved. There are parameters in Hadoop configuration regarding the CPU adjustment. The default value is not matched with every CPU and workload so the tuning of this parameter can result in an energy reduction. Second, we can add more memory to the system. This will help decrease execution but increase energy consumption for each memory module that is inserted into the system. In the past, memory size is very small, therefor, part of storage is used as memory paging. By disable the paging with the right amount of memory, the execution time and energy consumption can be reduced.

Third, can change normal hard disk drive to solid state drive to increase the rate of storage read and write. This will substantially decrease the execution time and energy consumption of the system. There are many parameters that needed to be explored in tuning Hadoop for energy consumption reduction.

RESULTS

The proposed method has been tested on a cluster of PC using CPU Intel i5-3330, 8 gigabytes of memory, 1 terabytes of storage, an operating system is Linux Centos 7, Java version 1.7 and Hadoop version 2.6.5. The result of experiments shows in the graph below.

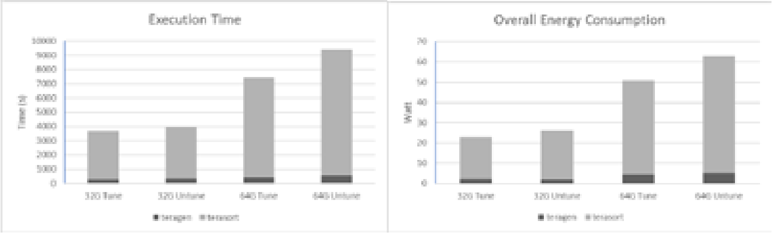

Figure 1. The experimental result

From this graph, the result shows that tuning system is better than untune system by 320 seconds or 5.20 minutes in execution time from 32 gigabytes case and even different in 64 gigabytes case by 1961 seconds or 32.41 minutes. This can save energy in 32 gigabytes case is 3 Watt per hour and in 64 gigabytes case is 12.2 Watt per hour.

REFERENCES

1. LaValle, Steve, Eric Lesser, Rebecca Shockley, Michael S. Hopkins, Nina Kruschwitz, *Big Data, Analytics and the Path From Insights to Value*, MIT Sloan Management Review, 2011, **52** (2), 21-32.
2. White Tom, *Hadoop: The definitive guide*, O'Rilly Media, Inc., 2012.
3. Jeffrey Dean, Sanjay Ghemawat, *MapReduce: simplified data processing on large clusters* , Communications of the ACM, 2008, **51** (1), 107-113.

CSE
-O-
5

Application of Intensified Current Search to Design Optimal PIDD^2 Controller for BLDC Motor Speed Control with Back EMF Detection

Danupon Kumpanya[1,C], **and Chookiat Kiree**[2]
[1]*Department of Electrical Engineering, Faculty of Engineering and Architecture,*
Rajamangala University of Technology Suvarnabhumi (RUS), Suphanburi 72130, Thailand
[2]*Department of Electrical, Saraburi Technical College, Saraburi 18000, Thailand*

[C]***E-mail**: kdanupon@yahoo.com;* ***Fax**: +66 3 5434 014;* ***Tel.** +66 8 1850 3236*

EXTENDED ABSTRACT

Keywords: BLDC Motor, PIDD^2 Controller, Intensified Current Search, Back EMF Detection.

INTRODUCTION

Design and implementation of the BLDC motor drive by PIDD^2 (proportional plus integral plus derivative plus double-derivative) controller [1] based on TMS320F28335 DSP board [2] interfacing to MATLAB/SIMULINK [3] is proposed in this paper. In order to obtain the optimal PIDD^2 controller, the intensified current search (ICS) is one of the newest and most efficient methods. The ICS is firstly proposed in 2014 [4] for solving engineering optimization problems. Algorithms of the ICS are inspired and conceptualized from the electric current flowing through electric network. With both diversification and intensification properties, the ICS has been successfully applied to many engineering problems [4],[5]. The ICS is applied to achieve the optimal tracking and regulating responses. The trapezoidal Back EMF waveforms are modeled as a function of rotor position, while the switching function concept is adopted to model the voltage source inverter (VSI). In this work, the tabu search (TS) [6],[7] is conducted to design the PIDD^2 controller for comparison in simulation results. By the proposed experimentation, speed and current waveforms of the controlled system can be easily obtained.

PROPOSED APPROACH

The plant model, $G_p(s)$, of the BLDC in the third-order transfer function form stated in Eq.(1) was obtained from metaheuristic identification by the ICS [5], while the PIDD^2 controller model, $G_c(s)$, is theoretically expressed in Eq. (2), where K_P, K_I, K_D, and K_{DD} are the proportional, integral, derivative, and double-derivative gains.

$$G_p(s) = \frac{0.04421}{5.423\times10^{-9}s^3 + 5.936\times10^{-6}s^2 + 0.001618s + 0.03683} \tag{1}$$

$$G_c(s) = K_P + \frac{K_I}{s} + K_D s + K_{DD}s^2 \tag{2}$$

Algorithms of the ICS can be represented by some movements over 3-D search space as visualized in Figure 1. The proposed ICS-based PIDD^2 controller design is shown in Figure 2, where $C(s)$ and $R(s)$ stand for obtained and desired responses. The objective function $f(\cdot)$, summation of a sum-squared error between $C(s)$ and $R(s)$, is set for minimization. The $f(\cdot)$ will be fed back to the ICS in order to obtain an appropriate PIDD^2 parameters, i.e. K_P, K_I, K_D, and K_{DD}, giving a satisfactory response. For comparison, results obtained by the ICS will be compared to those obtained by the tabu search (TS), one of the widely used single-solution based metaheuristic optimization techniques.

RESULTS

As simulation results, it was found that the ICS can provide optimal parameters of PIDD^2 controller giving more satisfied system response than the TS. This can be observed by the system responses without and with PIDD^2 controller designed by the TS and ICS as depicted in Figure 3. The proposed ICS-based PIDD^2 controller design approach is suitable to design an optimal PIDD^2 controller for the BLDC motor.

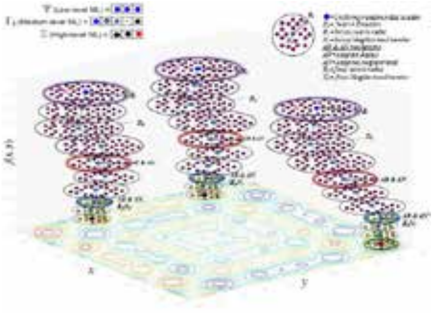

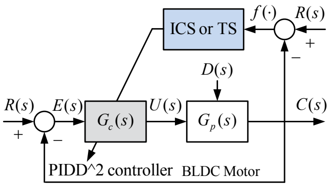

Figure 1. Some movements of the ICS. **Figure 2. ICS-based PIDD^2 controller design.**

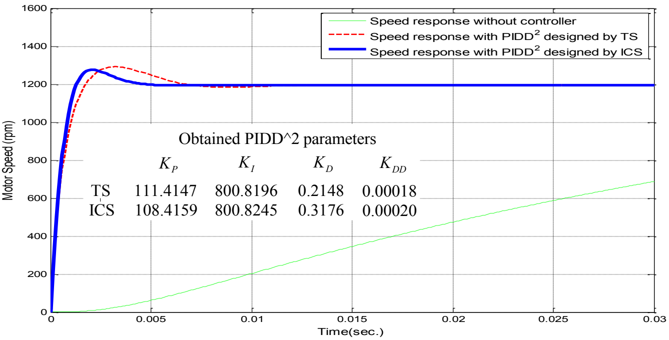

	K_P	K_I	K_D	K_{DD}
TS	111.4147	800.8196	0.2148	0.00018
ICS	108.4159	800.8245	0.3176	0.00020

Figure 3. Results of PIDD^2 controller design for BLDC motor speed control system.

REFERENCES

1. Ki-Chang Lee, Yeon-Ho Jeong, Dae-Hyun Koo and Hyeong Joon Ahn, “Development of a radial active magnetic bearing for high speed turbo-machinery motors,” *SICE-ICASE, International Joint Conference 2006*, 18–21 Oct. 2006,1543–1548.
2. Texas Instruments, *TMS320F28335, Digital Signal Controller*, 2007.
3. MATLAB/SIMULINK User’s Guide, *The Math Works Inc.*, Natick, MA, 1998.
4. Nawikavatan, A., Tunyasrirut, S. and Puangdownreong, D., “Application of intensified current search to optimum PID controller design in AVR system,” *AsiaSim-2014*, 2014,255–66,.

5. Nawikavatan, A., Tunyasrirut, S., and Puangdownreong, D., "Optimal PID controller design for three-phase induction motor speed control by intensified current search," *The 19th International Annual Symposium on Computational Science and Engineering (ANSCSE19)*, 2015,104–109.
6. Glover, F., Tabu search - part I, *ORSA Journal on Computing*, 1989, 1(3),190–206.
7. Glover, F., Tabu search - part II, *ORSA Journal on Computing*, 1990, 2(1),4–32.

CSE
-O-
6

Express Lane Services on Software-Defined Networks

Peeranon Wattanapong [C], **Kittipat Jutawongcharoen, and Vara Varavithya**
Department of Electrical and Computer Engineering, Faculty of Engineering, King Mongkut's University of Technology North Bangkok, Bangkok, Thailand

[C] ***Email**: w.peeranon@gmail.com; **Fax**: +66 2 585 7350; **Tel**. +66 2 555 2000 ext.8421*

EXTENDED ABSTRACT

Keywords: Computer network, software define network, on demand services.

INTRODUCTION

The main objective of express lane services is to provide high bandwidth connections for research and education institutes. Current bandwidth offered by ISPs cannot effectively serve the demands from researchers. Providing dedicated services and quality of services between two end points involves complex system configuration. Based on these requirements, a research and education network has to support on-demand high speed networks. SDN concept [1] offers additional flexibilities in managing network. In this work, we present the integrations of software defined network (SDN) and L2-VPN networks to create a new high performance services. The NetFPGA [2] cards are deployed as the SDN switches and the RYU [4] is implemented as a controller. The system can allocate resources by sending commands to set the designated flows at the SDN switches via OpenFlow protocol [2, 3].

PROPOSED APPROACH

Users in the express lane system are classified into three groups, namely audience, member, and administrator. As shown in Figure 1 (a), the use cases are assigned to each group. The system administrator responsible for managing users and approving service requests as well as monitoring system operations. In creating service request, a member user has to provide [Src_MAC, Dest_MAC, Start_Time, End_Time] to the system. The service duration is specified by Start_Time and End_Time. Accordingly, the user can configure both communication end points and using high speed connection within the requested period. The mapping between a user request and SDN flow specification for each switch is generated by the express lane system and then communicate with the SDN controller, as shown in Figure 1 (b). Express lane architecture is shown in Figure 2. The system consists of five components, the express lane system, an SDN overlay network, a research DMZ, the SDN controller, and SDN switches. The SDN overlay network is considered as the high bandwidth network infrastructure which is an overlay network

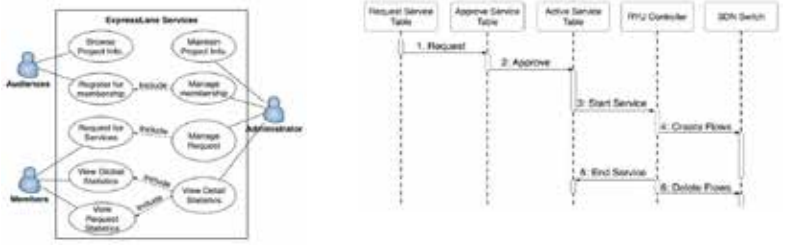
ExpressLane Services
Browse Project Info.
Maintain Project Info.
Audiences
Register for membership
include
Manage membership
Administrator
Request for Services
include
Manage Request
View Global Statistics
include
View Detail Statistics
Members
View Request Statistics
include
Request Service Table
Approve Service Table
Active Service Table
RYU Controller
SDN Switch
1. Request
2. Approve
3. Start Service
4. Create Flows
5. End Service
6. Delete Flows

(a) (b)

Figure 1. (a) Use case diagram for express lane services (b) Sequence diagram specifying the express lane service approval and operational process.

over research and education network, the UniNet in our case. The overlay network is supported by underlining MPLS network where traffic engineering policy is imposed. The RYU controller was selected in our works. The RYU controller reads the request and generate respective entries in the participated SDN switches.

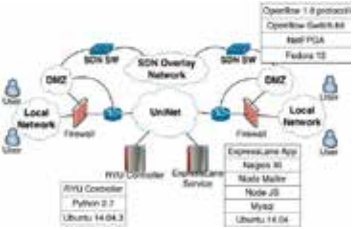
Openflow 1.0 protocol
Openflow Switch
NetFPGA
Fedora 13
SDN SW
SDN Overlay Network
SDN SW
DMZ
DMZ
User
Local Network
User
Firewall
UniNet
Firewall
Local Network
User
User
RYU Controller
ExpressLane Service
RYU Controller
Python 2.7
Ubuntu 14.04.3
ExpressLane App
Nagios XI
Node Mailer
Node JS
Mysql
Ubuntu 14.04

Figure 2. Express lane architecture. Software architecture diagrams are shown for SDN Switch, Controller, and Express Lane Service.

RESULTS

The system were deployed on 7 nodes in the UniNet which operated in the real environment. The service request, [00:23:ae:9c:89:f9, 00:26:5a:7c:03:af, 08:00 10-10-2016, 12:00 10-10-2016], was submitted to the system. After the service was approved, the RYU controller create the flow and send to respective switches. Example of SDN flows based on Openflow version 1.0 are shown below.

[cookie= 0, duration= 2s, table_id= 0, priority= 32768, n_packets= 22, n_bytes= 1320, idle_timeout=0, hard_timeout=600, in_port=1, dl_dst=00:23:ae:9c:89:f9]

[cookie= 0, duration= 5s, table_id= 0, priority= 32768, n_packets= 0, n_bytes= 0 idle_timeout=0, hard_timeout=600, in_port=4, dl_dst=00:26:5a:7c:03:af]

Figure 3 (a) shows bandwidth results obtained from the real experiment. The bandwidth result is about 500 Mbps which is much higher than bandwidth obtained from shared campus environment. The ping results is shown in Figure 3 (b)

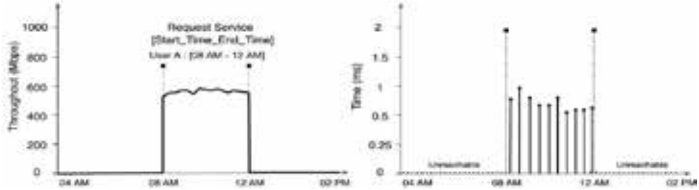

(a) **(b)**

Figure 3. Experimental results, the express lane request was created between 8:00-12:00 am.The bandwidth performance is shown in (a) and the connectivities between end points using ping command is depicted in (b)

REFERENCES

1. N. McKeown, T. Anderson, H. Balakrishnan, G. Parulkar, L. Peterson, J. Rexford, S. Shenker, and J. Turner, *OpenFlow: Enabling innovation in campus networks*, SIGCOMM Comput. Commun. Rev., **38**(2), 2008, 69–74.
2. J.Naous, D.Erickson, G. Adam Covington, G.Appenzeller, N.McKeown, *Implementing an OpenFlow switch on the NetFPGA platform*, ANCS '08 Proceedings of the 4th ACM/IEEE, ACM, USA, 2008.
3. *OpenFlow Switch Specification Version 1.0.0* [Online], Available: http://archive.openflow.org/documents/openflow-spec-v1.0.0.pdf.
4. *Using OpenFlow 1.3 RYU SDN Framework: RYU project team* [Online], Available: https://osrg.github.io/ryu-book/en/Ryubook.pdf.

CSE
-O-
7

Blood Vehicle Routing Network Using Artificial Chemical Reaction Optimization Algorithm

Kanon Sujaree[1,C]
[1] *Department of Industrial Engineering , Faculty of Engineer, Rajamangala University of Technology Rattanakosin Salaya, Thailand*

[C] ***E-mail***: *Kanon.suj@rmutr.ac.th;* ***Tel.*** *+66 8 6932 2033*

EXTENDED ABSTRACT

Keywords: Artificial Chemical Reaction Optimization Algorithm, Blood Vehicle Routing, Design of experiment, Factorial design

INTRODUCTION

The National Blood Center (NBC) has been established by Thai Red Cross. There is only one in Bangkok. For eleven places in the regional areas call Regional Blood Centers (RBCs) as follows Chiang Mai, Phitsanulok, Nakhon Sawan, Khonkaen, Ubon Ratchathani, Ratchaburi, Chonburi, Prachuap Khiri Khan, Phuket and Songkhla. Both NBC and RBCs donate blood and screening after that transfer blood to the required from hospitals. The blood screening process consists of blood clotting and blood screening with Hepatitis A and C, Syphilis, and HIV. All blood is separated in the form of red blood cells. Donor Red Cells maintain 21-42 days depending on the type of red blood cells. Plasma (Single Donor Plasma) is about 1 year at low temperature and platelet (Single Donor Platelets) is about 5 days. In figure 1, Focusing on Chiang Mai donation blood center (blue point) to support the hospitals (black points) in the northern Thailand. It is responsible for donating and delivering blood to hospitals in Chiang Mai, Chiang Rai, Phrae, Nan, Lam Pang, Lam Poon, Pha Yao and Mae Hong Son. The number of hospitals that deliver blood is 112 hospitals. The transportation cars were set the optimal temperature for blood storage and delivery schedule 3 days per times [1].

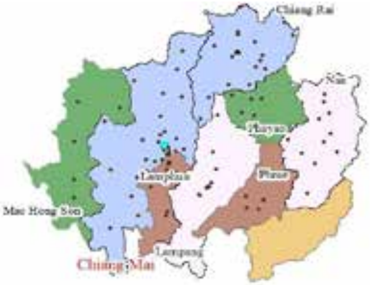

Figure 1. Chiang Mai donation blood center and responsible area

PROPOSED APPROACH

Blood vehicle routing is to minimize the distance to be considering blood resource and vehicle capacity limitation. The mathematical model and its notations for blood vehicle routing considered in this paper are these equations.

Indices:

Z	denotes total distances for vaccine cold chain network
i,j	denotes hospital i to hospital j
k	denotes blood vehicles k

Parameters:

d_{ij}	is distance from hospital i to hospital j
N	is number of hospitals
K	is number of blood vehicles
p	is hospital (1,2,3,…..N)
A	is blood group A
B	is blood group B
AB	is blood group AB
O	is blood group O
a_k	is capacity of blood vehicles k
q_i^A	is blood group A demand of hospital i
q_i^B	is blood group B demand of hospital i
q_i^{AB}	is blood group AB demand of hospital i
q_i^O	is blood group O demand of hospital i

Decision variables:

X_{ij}^k = 1 if vehicles k from hospital i to hospital j, otherwise 0

Y_i^k = 1 if blood load in vehicles k**,** otherwise 0

U_i^k is variable for protection cannot supply all hospitals

Objective function

$$Min\, Z = \sum_{k=1}^{K}\sum_{j=0}^{N}\sum_{i=0}^{N} d_{ij}X_{ij}^k + \sum_{k=1}^{K}\sum_{j=0}^{N}\sum_{i=0}^{N} d_{jl}X_{jl}^k \tag{1}$$

Representation by

$$\sum_{j=1}^{N} X_{oj}^k \quad \leq 1 \quad (K = 1,2,3,\dots \dots . . K) \tag{2}$$

$$\sum_{i=0}^{N} X_{ip}^k - \sum_{j=0}^{N} X_{pj}^k = 0 \;\; (p = 1 \dots N) \tag{3}$$

$$\sum_{k=1}^{K} Y_i^k \;\; = 1 \qquad (i = 1,2,3 \dots K) \tag{4}$$

$$\sum_{i=1}^{N} q_i^A\, Y_i^K \leq a_k^A \qquad (k = 1 \dots . K) \tag{5}$$

$$\sum_{i=1}^{N} q_i^B\, Y_i^K \leq a_k^B \qquad (k = 1 \dots . K) \tag{6}$$

$$\sum_{i=1}^{N} q_i^O\, Y_i^K \leq a_k^O \qquad (k = 1 \dots . K) \tag{7}$$

$$\sum_{i=1}^{N} q_i^{AB}\, Y_i^K \leq a_k^{AB} \quad (k = 1 \dots . K) \tag{8}$$

$$Y_i^k \;\leq\; \sum_{i=1}^{N} X_{ji}^k \;\; (i = 1 \dots . N), (k = 1 \dots . K) \tag{9}$$

$$\sum_{k=1}^{K}\sum_{i=0}^{N} X_{ij}^k \;\geq 1 \qquad (j = 1,2,3 \dots . N) \tag{10}$$

$$U_i^k \geq U_j^k + q_i - a_k + \left(a_k * \left(X_{ij}^k + X_{ij}^k\right)\right) - X_{ij}^k\left(q_i + q_j\right) \qquad (11)$$

$$U_i^k \leq a_k - X_{0i}^k\left(a_k - q_i\right) \qquad (12)$$

$$U_i^k \leq q_i + \sum_{j=1}^{N} q_j X_{ji}^k \qquad (13)$$

The Artificial chemical reaction optimization algorithm (ACROA) can be considered as a simulation of reactants in a vessel. Suppose a fixed volume vessel containing a spatially uniform mixture of N chemical reactants interacting through specific chemical reaction channels. Let $Ri(1 \leq i \leq N)$ be the list of chemical reactants, and suppose these reactants can interact through M specified chemical reaction channels. According to the above algorithm concept, the ACROA flow chart of which is depicted in Fig. 2 consists of the following five steps:

Step 1: Problem and algorithm parameter initialization.
Step 2: Setting the initial reactants and evaluation.
Step 3: Applying chemical reactions.
Step 4: Reactants update.
Step 5: Termination criterion check.

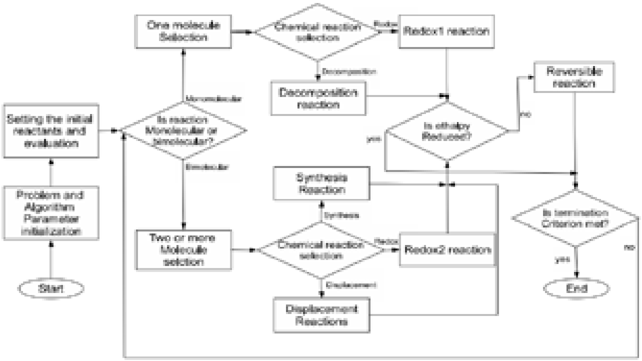
One molecule Selection
Chemical reaction selection
Redox
Redox1 reaction
Decomposition
Decomposition reaction
Reversible reaction
Monomolecular
Setting the initial reactants and evaluation
Is reaction Monomolecular or bimolecular?
no
yes
Is ethalpy Reduced?
Bimolecular
Synthesis Reaction
Problem and Algorithm Parameter initialization
Synthesis
Is termination Criterion met?
Two or more Molecule selection
Chemical reaction selection
Redox
Redox2 reaction
no
yes
Start
Displacement
End
Displacement Reactions

Figure 2. Flow chart of ACROA [2]

RESULTS

Nowadays, there are several factors impacted on the algorithm. The research objective is to find factors that influence with to find the objective function for the application. This paper has to use statistic of experimental theory to design the experiment in term of full factorial design 3 level [3]. The summary of the objective function obtained from Genetic Algorithm (GA), Cuckoo Search (CS) [4] and Artificial Chemical Reaction Optimization Algorithm (ACROA) is shown in Table 1. It can be seen that for small size problem GA, CS and ACROA were able to find the minimizing distance with 389 km. For medium size problem, both CS and ACROA once more produced minimizing distance lower than the GA (38 km). Whereas for large size problem, the best-so-far results obtained from ACROA was better than GA (136 km) and CS (4 km) respectively.

Table 1. Summary of the results obtained from GA, CS and ACROA

Problem size	Best-so-far solution		
	GA	CS	ACROA
Small size (26 hospitals)	389 (km)	389 (km)	389 (km)
Medium size (38 hospitals)	735 (km)	697 (km)	697 (km)
Large size (112 hospitals)	1968 (km)	1836 (km)	1832 (km)

REFERENCES

1. Chaiwuttisak P., Smith H., Wu Y., Potts C., *Lecture Notes in Management Science*, 2014, **6**, 23-31
2. Alatas.B, *Expert systems with application*, 2011, **38**(2011), 13170-13180
3. Montgomery DC, *Design & Experiment,* John Wiley and Sons, NY, 2001
4. Sujaree K , *1th RMUTP Engineering Conference*, 2016, **1**, 27-35

CSE
-O-
8

The Development of a VM Auto-Scaling Software for OpenStack Cloud

Krailerk Manopattanagorn[1,C] **and Putchong Uthayopas**[1]
[1] *Department of Computer Engineering, Faculty of Engineering, Kasetsart University, Bangkok, Thailand*

[C] ***E-mail***: *krailerkm@gmail.com, putchong@ku.th; Tel. +66814944962*

EXTENDED ABSTRACT

Keywords: OpenStack, Cloud Computing, Cloud Media Server, Auto-Scaling Software.

INTRODUCTION

Cloud computing system (Mell, P. and Grance, T., 2011) becomes an important platform for the next generation IT services. One of the main applications of a cloud system is to service the media downloading and media streaming to a massive number of users. As a number of users increases, an ability to automatically scale to match the user's demands becomes critical issues. In this paper, an implementation of a software called ***MASS (Media Auto-scale Streaming Service)*** is presented. This MASS software added an auto-scaling capability to the widely used OpenStack (V. K. Cody Bumgardner, 2016) open source cloud computing software. This software enables a developer to easily add a smarter auto-scaling policy to OpenStack Cloud.

PROPOSED APPROACH

The MASS software has been developed using Python 2.7 and OpenStack Mitaka. This software is an independent software that interface with OpenStack using OpenStack REST API. MASS communicate with Ceilometer to get the workload information.

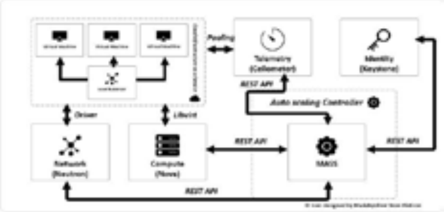

Figure 1. The interaction between MASS software and OpenStack components

As MASS start, a pool of resources will be created in OpenStack using API, then a set point of maximum workload and minimum workload will be set into Ceilometer. When the workload increases and exceeds the maximum set point, Ceilometer will report back as a notification to MASS. Upon receiving the notification, MASS will execute the workload scaling policy, then use OpenStack API to create a new VM to enable a workload sharing on more physical machines. If the workload decreases and becomes less than the minimum threshold, the notification will be sent to MASS. Upon receiving the notification, MASS will make a decision based on its policy and shutdown some VM to save the resources. The policy can be easily coded into the MASS system. Currently, the policy available is only the round-robin VM creation on the physical machine.

RESULTS

The test environment composed of a set of 7 computers. One computer is used as an OpenStack controller and 2 more are used as OpenStack compute nodes base on CPU Intel Q6600 2.4Ghz, Memory 6GB DDR2, HDD80GB SATA. The rest are used as load generator. The test has been conducted using Jmeter version 3.1 (B. Erinle, 2014) as the workload generator. The main load test computer base on CPU Intel I7-4700MQ 2.4Ghz, Memory 16GB DDR3, SSD240GB SATA installed with Windows 7 and two more load test slave base on CPU Intel E750 2.93Ghz, Memory 2GB DDR3, HDD160GB SATA for Jmeter used CentOS7. The rest is installed with Linux CentOS Version 7.2. The test configuration is as shown in Figure. 2. In this test, we pre-created 3 VM types; small size (s), medium size (M), and large size (L).

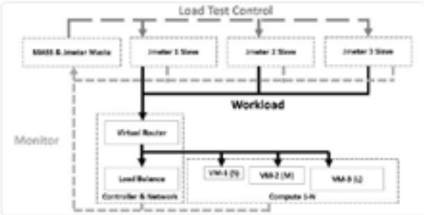

Figure 2. The test system configuration

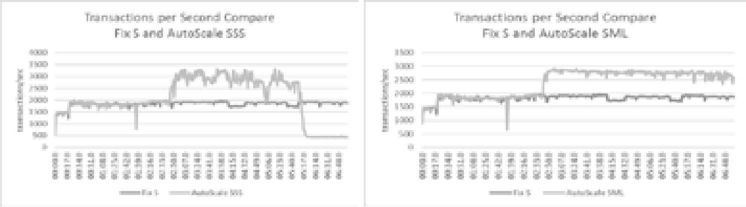

(a) (b)

Figure 3. The throughput comparison of (a) fixed small size VM and scaled small size VM (b) fixed small size VM and Scaled small/medium/large size VM

Figure 3 (a) shows the transaction rate using a single fixed small size VM compared with 3 auto scale VM of size S (SSS). At first, the transaction rate is equal. As more VM has been started, the transaction rate that the cloud can service increases about 30% because more VM and compute nodes has been employed. Figure 3 (b) shows that when VM size increases the service quality and scaling has also improved.

REFERENCES

1. Mell, P. and T. Grance, “The NIST Definition of Cloud Computing”, NIST Special Publication 800-145., 2011.
2. V. K. Cody Bumgardner, “OpenStack in Action”, Manning Publication Co., ISBN-13: 978-1617292163, 2016.
3. B. Erinle, “JMeter cookbook”, Packt Publication, Birmingham, U.K., 2014.

CSE
-O-
9

Mobile Dental Unit Using Computer Simulation Theory

Kanon Sujaree[1,C]
[1] *Department of Industrial Engineering, Faculty of Engineering, Rajamangala University of Technology Rattanakosin, Nakhon Prathom, Thailand*

[C] **E-mail**: *Kanon.suj@rmutr.ac.th;* **Tel.** *+66 8 6932 2033*

EXTENDED ABSTRACT

Keywords: computer simulation theory, mobile dental unit, simulation model

INTRODUCTION

Many people, especially those from lower socio-economic families, have limited access to dental care, transportation problems, and poor appointment attendance. Mobile dental clinics have been implemented in many communities to address these issues [1]. The services mainly focus on reaching every section of the community by catering troops and portable dental equipment to serve the basic oral health needs and taking the sophisticated oral health services, especially to the underserved population with free service of charge [2]. Because of a high number of patient rates per day, the aim of this study is to present the computer simulation modeling to design, create, and evaluate this complex system for effective, efficient, and optimized performance. The mobile dental chairs have been used in this project.

This unique project has been collaborated by the Thai government together with charitable organizations to provide comprehensive dental services including full or partial acrylic dentures, scaling, cleaning, filling, etc. The program provides diagnostic, preventive, and treatment procedures [1]. Each mobile clinic can serve around 600-1000 patients per day. In this study, the clinic is a royal dental project initiated by Princess Maha Chakri Sirindhorn and established in 1970. This is a successful collaboration between universities including Chiang Mai, Khon Kaen, Prince of Songkhla, Naresuan, Thammasat, and Srinakharinwirot universities. In addition, each region has its own University to be taking care. The operators helping in this project include 40 dentists, 40 dental assistants, and 40 coordinators [3].

PROPOSED APPROACH

One of the most popular and powerful software tools named Arena, Visio-compatible and flowcharting methodology for modeling dynamic processes has been applied in this study to mimic the behavior of a real-world system. The program provides users with enabling visualization of an entire system and statistics graphically displaying the status and performance of equipment [4]. One of the most important components of a mobile dental clinic is a comfortable ergonomic chair splitting itself into two sides, left and right sides, for filling and scaling, respectively. The mobile dental unit is diagrammed as shown in Figure 1.

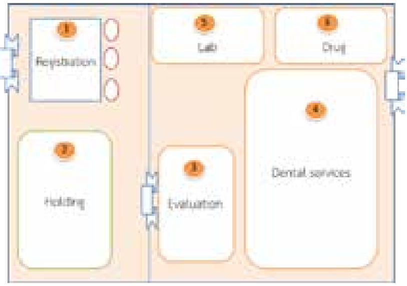

Figure 1. Mobile dental service diagram

The average waiting time of patients receiving the dental care can be defined mathematically as follows.

$$a^{td} = \frac{\rho/\mu}{1-\rho} \quad (1)$$

$$\rho = \frac{\lambda}{\mu} \quad (2)$$

a^{td} is an average waiting time of the patients.

ρ is a density of the services.

λ is an average rate of the arrival.

μ is an average rate of the services.

RESULTS AND DISCUSSION

This study presents the mobile dental clinic model simulated using Arena simulation software. The comparison has been made between the prototype together with the other three alternatives, which include 1) a reduction in the number of dentists who are responsible for the dental diagnostic unit from 13 to 17 pm and they were reallocated and assigned to a task at the dental service unit, 2) a reduction in the number of receptionists and coordinators by transferring 3 and 5 of them, respectively, to the dental denture unit, 3) a combination of the first and second scenarios with 100 replications using Arena simulation software. The simulation results show that the half-width was equal to 0.19 with around 10 replications. The average waiting times of the simulation is shown in Table 1.

Table 1. Patients' average waiting times (minutes)

Positions	Original	Scenario 1	Scenario 2	Scenario 3
Registration	2.23	2.98	3.24	3.24
Diagnose	5.48	6.23	5.48	6.84
Dental services	196	108	196	104
Denture	248	256	116	116
Drug	12.36	13.48	13.36	13.21
Summary	464.07	286.69	292.45	243.29
Percentage	-	-38.2%	-36.1%	-47.6%

REFERENCES

1. Douglass J.M., *Journal of public health dentistry*, 2005, **65**(2), 110-113.
2. Ganavadiya R., Chandrashekar B., Goel P., Hongal S. & Jain M., *Annals of medical and health sciences research*, 2014, **4**(3), 293-304.
3. Sujaree K., Watcharanad S., *1st RMUTP Engineering Conference*, 2016, **1**, 36- 44
4. Garrido J.M., *Object oriented simulation: A modeling and programming perspective,* Springer Science & Business Media, 2009, NY, 1-2

POSTER PRESENTATION ABSTRACTS

PFD -P- 1 Finite Volume Scheme with Weighted Average Flux for Wet and Dry Shallow Water Simulations

Lanchakorn Kittiratanawasin[1], **Montri Maleewong**[1,C], **Anand Pardhanani**[2]
[1]*Department of Mathematics, Faculty of Science, Kasetsart University, Thailand*
[2]*Department of Mathematics, Natural Sciences Division, Earlham College, U.S.A.*
[C] ***E-mail**: fscimtm@ku.ac.th ; **Fax**: +66- 2942-8038; **Tel.** +66-2562-5444 ext. 647023*

EXTENDED ABSTRACT

Keywords: shallow water, TVD, WAF, wet, dry, predictor, corrector

INTRODUCTION

The shallow water equations have a wide variety of applications in ocean and hydraulic engineering. Some examples include tides in oceans, moving waves in shallow beaches, and flood waves in rivers. Due to the nonlinear behavior of the hyperbolic equations, analytical methods are only successful in very special cases of flow. Efficient numerical methods are, therefore, crucially important for modeling realistic problems. In this study, a predictor and corrector method with TVD-WAF approximations for time integration in two dimensions on shallow water equation is proposed.

PROPOSED APPROACH

Unsteady two-dimensional open channel flow under hydrostatic pressure assumption can be described by the shallow water equations as

$$\frac{\partial U}{\partial t}+\frac{\partial F}{\partial x}+\frac{\partial G}{\partial y}=S(U) \qquad (1)$$

The predictor-corrector scheme is used for solving the shallow water equations (1). The total variation diminishing (TVD) criteria of weighted average flux (WAF) approximation [1,2]. is applied at the cell interfaces for calculating numerical flux. The scheme of predictor-corrector is illustrated on figure 1

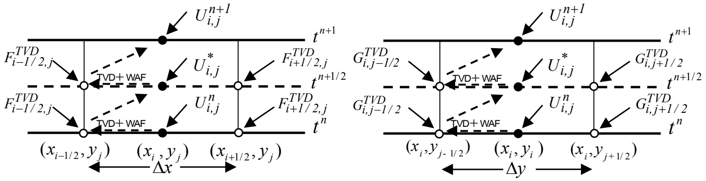
$U_{i,j}^{n+1}$
t^{n+1}
$F_{i-1/2,j}^{TVD}$
TVD+ WAF
$U_{i,j}^{*}$
$F_{i+1/2,j}^{TVD}$
$t^{n+1/2}$
$F_{i-1/2,j}^{TVD}$
TVD+ WAF
$U_{i,j}^{n}$
$F_{i+1/2,j}^{TVD}$
t^{n}
$(x_{i-1/2}, y_j)$
(x_i, y_j)
$(x_{i+1/2}, y_j)$
Δx
$U_{i,j}^{n+1}$
t^{n+1}
$G_{i,j-1/2}^{TVD}$
TVD+ WAF
$U_{i,j}^{*}$
$G_{i,j+1/2}^{TVD}$
$t^{n+1/2}$
$G_{i,j-1/2}^{TVD}$
TVD+ WAF
$U_{i,j}^{n}$
$G_{i,j+1/2}^{TVD}$
t^{n}
$(x_i, y_{j-1/2})$
(x_i, y_i)
$(x_i, y_{j+1/2})$
Δy

Figure 1 Computation diagram in the xt and yt planes: The main step begins by calculating numerical fluxes for the half time step using the TVD-WAF method, and then calculating $U_{i,j}^{*}$. Then the TVD-WAF method is applied again for

finding numerical fluxes at time, $t^{n+1/2}$ which are used to compute the solution for the next time step, $U_{i,j}^{n+1}$.

RESULTS

To show accuracy of scheme, we present results of applying our method to solve shallow flow problems in both wet and dry bed cases. The first three cases involve problems with frictionless and flat bottoms, while the last two cases involve source terms, to demonstrate the ability of the numerical scheme for handling more realistic situations.The following figure show a simulation of dam-break flow in diverging and converging channel. This test case is based on the experimental work presented by Bellos et al. [3]. The top view of this channel is shown in Fig. 2 and comparisons between numerical simulations and experimental data detected at sensors 1 is shown in Fig. 3.

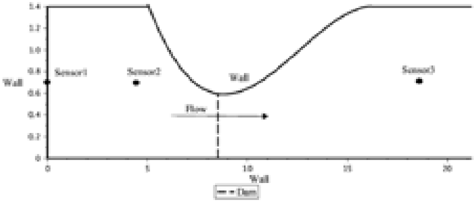

Figure 2 Dam-break flow diagram in diverging and converging channel.

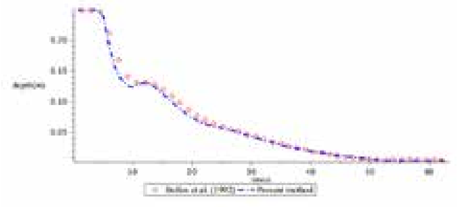

Figure 3 Comparison of water depth from experimental work and numerical simulations at location *x* =0 (sensor 1).

REFERENCES

1. E. Toro, Riemann problems and the WAF method for solving twodimensional shallow water equations, Philos. Trans. R. Soc. London Ser. A, 338 (1992) 43–68.
2. A. Harten, High resolution schemes flow hyperbolic conservation laws, J. Comput. Phys. 49 (1983) 357–393.
3. C. V. Bellos, J. V. Soulis, and J. G. Sakkas, Experimental investigation of two dimensional dam-break induced flows. *J. Hydraul. Res.*, 30(1):47–63, 1992.

PFD -P- 2

Image Processing for Astronomical Objects

Chewa Thassana[1,2,C] **and Wiraporn Maithong**[3]
[1] *Department of Physics, Faculty of Science and Technology, Rambhai Barni Rajabhat University*
41 M 5 T.Thachang, Muang District, Chanthaburi, Thailand
[2] *National Astronomical Research Institute of Thailand (Public Organization),Chiang Mai,Thailand*
[3] *Department of Physics and General Science, Faculty of Science and Technology,*
Chiang Mai Rajabhat University 202 Changpuerk Road, Muang District, Chiang Mai, Thailand

[C] ***E-mail***: *chewa.t@rbruac.th* , ***Fax***: *+6639471060;* ***Tel.*** *+66 39471060*

ABSTRACT

The image processing is a procedure to improve the photographic image quality. In this work, we study focusing on the improvement the image of astronomical objects, such as the Moon and a nebula, which were obtained using the CCD and the DSLR digital camera on December, 2016 at the Regional Observatory for the Public, Cha Cheong Sao, and Thailand. The image processing analysis showed that the finest conditions adjustment in each photographic objects.

Keywords: image processing, quality improvement, astronomical image.

**PFD
-P-
3**

Atomistic Simulation of Structural Evolution at Long Time Scales: Diffusion in the FCC NiAl System

Nuttapong La-ongtup[1] and Yuranan Hanlumyuang [1,C]

[1] *Department of Materials Engineering, Faculty of Engineering, Kasetsart University, Bangkok, Thailand*

[C] ***E-mail**: fengynh@ku.ac.th; **Fax**: +66 2 955 1811; **Tel.** +66 2 7970999 ext. 2119*

EXTENDED ABSTRACT

Keywords: Atomistic simulation, Long time scales evolution, Atomic diffusion

INTRODUCTION

Simulating long-time dynamical behaviour in materials has been a grand challenge in materials engineering. Despite its success in simulating dynamical evolution of atomic systems, it has been known that traditional molecular dynamics (MD) methods are inefficient for studying dynamics at the laboratory timescale. Autonomous basin climbing (ABC) method [1] offers a solution to this problem. The method aims at predicting atomic evolution by collecting activation energies of many reaction pathways of the potential energy surface of the system. In combination with the techniques of Kinetics Monte Carlo simulation (KMC) [2], atomic evolution at long time scales can be predicted. The combined ABC+E and KMC are applicable for a variety of materials problems such as diffusion, creep of material, migration of defect in structure, and surface growth, among others.

PROPOSED APPROACH

Our work is to evaluate the diffusivity in NiAl system, using ABC method. Most probable diffusion pathways will be determined. A nudged elastic band (NEB) method will be employed to obtain diffusion pathways and the corresponding activation barriers of all possible hopping processes. In combination with the techniques of Kinetic Monte Carlo (KMC), the hopping process will be chosen from all possible diffusion pathways with eligible probabilities under the standard KMC scheme. The change in atomic positions of each step will be presented as atomic diffusion trajectories. The tracer diffusion coefficient will be calculated as a function of temperature from the time evolution data of each atomic step. The simulation results will be compared to an experimental data.

RESULTS

The preliminary exploration of minimum energy pathways for solutes Al hopping in a Ni host lattice was calculated with an embedded-atom method (EAM) interatomic potential for the Ni-Al system [4]. The calculated hopping barrier is approximately 0.68 eV.

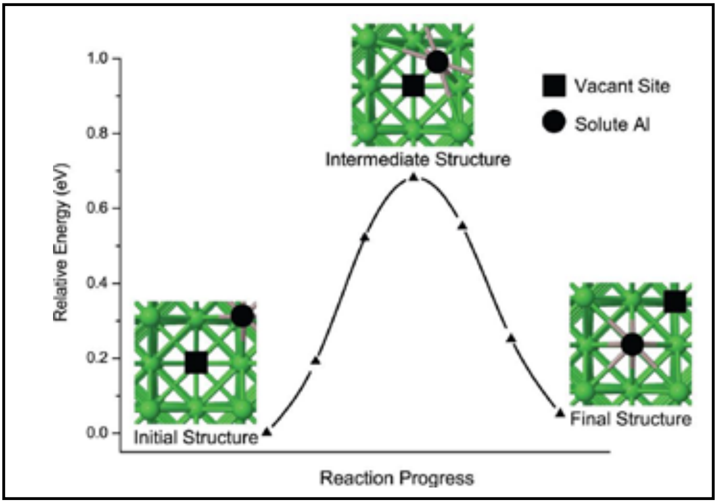

Figure 1. The minimum energy reaction pathway and structure of vacancy assisted Al diffusion in Ni host. Filled square and filled circle represent vacant site and solute Al respectively. The pathway was calculated by NEB method with the EAM potential.

REFERENCES

1. Kushima, A., X. Lin, J. Li, J. Eapen, J.C. Mauro, X. Qian, P. Diep and S. Yip., The Journal of Chemical Physics, 2009, **130** (22), 224504.
2. Voter, A.F., Radiation Effects in Solids, **235**, Springer, Dordrecht, 2007, 1-23.
3. Henkelman, G., B.P. Uberuaga and H. Jónsson, The Journal of Chemical Physics, 2000, **113**(22), 9901-9904.
4. G.P. Purja Pun and Y. Mishin, Philosophical Magazine, 2009, **89** (34), 3245-3267.

**PFD
-P-
4**

The Effects of Stone-Wales Defect on Quantum Capacitance in Carbon Nanotube

Sorasit Buapong[1] and Yuranan Hanlumyuang[1,2,C]
[1] *Department of Materials Engineering, Faculty of Engineering, Kasetsart University, Bangkok, Thailand*
[2] *Materials Innovation Center, Faculty of Engineering, Kasetsart University, Bangkok, Thailand*

[C] ***E-mail***: *yuranan.h@ku.th;* ***Fax***: *+66 2 955 1811;* ***Tel.*** *+66 9 6445 1330*

EXTENDED ABSTRACT

Keywords: Quantum capacitance, Carbon nanotube, Stone-Wale defect.

INTRODUCTION

Carbon nanotube (CNT) is an emerging material that demonstrate enhanced capacitance. An influencing parameter to the overall capacitance of a dielectric material is quantum capacitance, a quantum entity arisen from local interface charge density profile. The quantum capacitance (C_Q) is defined as a function of density of state at Fermi energy ($\rho_0(\varepsilon_F)$) and the length (L) of one-dimension system as

$$C_Q = e^2 \rho_0(\varepsilon_F) L \tag{1}$$

It is generally accepted that the quantity of capacitance depends on the sign of quantum capacitance. This perplexing property has led to a number of studies on the quantum capacitances in various materials. For example, there are studies on negative quantum capacitance of gate carbon nanotubes[1], the relationship of quantum capacitance and charge carrier density in graphene [2], and studies on Nitrogen doping of graphene [3]. In this work, the effects of Stone-Wales defect on quantum capacitance in carbon nanotube are studied. Defects in carbon nanotube are known to alter its properties noticeably.

PROPOSED APPROACH

1. Create a geometry of zigzag (10x0) carbon nanotube
2. Placing the modeled nanotube inside a calculation cell equipped with a Poisson solver. The source and drain of current are defined for simulating the quantum capacitance. The simulate geometry is shown in Figure 1 and the equation for solving the quantum capacitance is shown in (2)

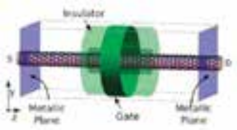

Figure 1. The simulated geometry consist of the zigzag (10x0) carbon nanotube inside the Poisson box, insulator, metallic plane and gate[4]

$$C_Q(n_1) = C_{ins,1}\left[\frac{\delta Q(n_{1,crit})}{\delta Q(n_1)} - 1\right]^{-1} \qquad (2)$$

Where $C_Q(n_1)$ is quantum capacitance at carrier density n_1. $\delta Q(n_1,\text{crit})$ is a total charge induced on carbon nanotube at critical value of the carrier density when complete screening observed. $\delta Q(n_1)$ is the total charge induced at each doping level of carrier density. $C_{ins,1}$ is the capacitance between carbon nanotube and insulator

3. Add a Stone-Wales defect to a middle of zigzag (10x0) carbon nanotube and compute the quantum capacitance of this defected nanotube

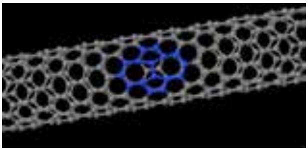

Figure 2. The Stone-Wales defect in simulated zigzag (10x0) carbon nanotube

4. Compare the quantum capacitances of zigzag (10x0) carbon nanotube and defective carbon nanotube

RESULTS

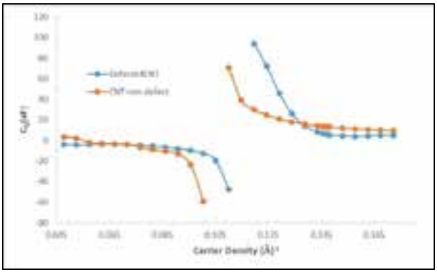

Figure 3. The effect of Stone-Wales defect on quantum capacitance

Figure 3 shows the effects of a Stone-Wales defect on quantum capacitance. The sign switching behavior of the nanotube is altered due to the influence of the defects on the Fermi level. Generally, a negative quantum capacitance enhances the overall capacitance. Our results demonstrate that Stone-Wales defects alter the quantum capacitance of the nanotube.

REFERENCES

1. Latessa, L., Pecchia, A., and Di Carlo, A., *PHYSICAL REVIEW B*, 2005, **72**, 035455-1-035455-5.
2. Dröscher, S., Roulleau, P., Molitor, F., Studerus, P., Stampfer, C., Ensslin, K. and Ihn, T., *APPLIED PHYSICS LETTERS*, 2010, **96,** 152104-1-152104-3.
3. Li Zhang, L., Zhao, X., Ji, H., D. Stoller, M., Lai, L., Murali, S., Mcdonnell, S., Cleveger, B., M. Wallace, R. and S. Ruoff, R.. *The Royal society of chemistry*., 2012.
4. Hanlumyuang, Y.,Li, X., and Sharma, *Phys.Chem.Chem.Phys*., 2014, **16**, 22962-22966.

PFD
-P-
5

Stellar Spectrum Analysis from eShel Spectroscope

Wiraporn Maithong[1,2,C], **Athipong Ngamjarurojana**[3], **and Chewa Thassana**[4]
[1] Department of Physics and General Science, Faculty of Science and Technology,
Chiang Mai Rajabhat University 202 Changpuerk Road, Muang District, Chiang Mai, Thailand
[2] National Astronomical Research Institute of Thailand (Public Organization),Chiang Mai,Thailand
[3] Department of Physics and Material Science, Faculty of Science, Chiang Mai University
239 Huay Keaw Road, Muang District, Chiang Mai, Thailand
[4] Department of Physic, Faculty of Science and Technology,Rambhai Barni Rajabhat University
41 M 5 T.Thachang, Muang District, Chanthaburi, Thailand

[C] ***E-mail****: wiraporn.m@gmail.com,* ***Fax****: +66 53 885 632;* ***Tel.*** *+66 8 1532 1299*

ABSTRACT

The classification of stars is classified the stars based on their spectral characteristics. The Harvard spectral classification uses the letters O, B, A, F, G, K, and M. The O type is the hottest stars and the M type is the coolest stars. In this work, the stellar spectrums in many types were observed by eShel spectroscope on April, 2016 at the Thai National Observatory (TNO), Chiang Mai, Thailand. The spectral line analysis showed that the wavelength which related to the elements in the star.

Keywords: Spectrum, Wavelength, Element.

CHE -P- 1

Effects of Different Proton Donor and Acceptor Groups on Excited-State Intramolecular Proton Transfers of Amino-type and Hydroxy-type Hydrogen-Bonding Molecules: Theoretical Insights

Narissa Kanlayakan[1], Khanittha Kerdpol[1], Chanatkran Prommin[1], Rusrina Salaeh[1], Warinthon Chansen[1], Chanchai Sattayanon[1], and Nawee Kungwan[1,C]
[1] *Department of Chemistry, Faculty of Science, Chiang Mai University,*
Chiang Mai 50200, Thailand

[C] ***E-mail**: naweekung@gmail.com email;* ***Tel.** +66 8 4828 3641*

EXTENDED ABSTRACT

Keywords: Excited-state intramolecular proton transfer, DFT, TD-DFT, Dynamic simulations, Hydrogen-bonding molecule.

INTRODUCTION

Bifunctional molecules with a strong intramolecular hydrogen bond connected by a proton donor (D:$-NH_2$, $-OH$) and a proton acceptor (A:$-O-$,$-N=$) can undergo excited-state intramolecular proton transfer (ESIPT) processes via the four-level photocycle, in which the tautomer emission gives a large red-shift with respect to the normal absorption (Stokes shift). This unique photophysical property caused by ESIPT reactions which are well accepted to be driven from significant changes in the acidity and basicity of the proton donor and acceptor moieties respectively, has attracted numerous studies in the past few decades owing to its various optoelectronic applications in bioimaging, chemical sensors, organic light-emitting devices, laser dyes, and molecular switches. The most of previous reports on ESIPT of H-bonding molecules have only dealt with their absorption and emission spectra as well as the chance of ESIPT occurrence affected by the OH-type and NH-type proton donating groups of phenyl moiety and proton acceptor groups on the benzothiazole, benzimidazole, and imidazo[1,2-a]pyridine backbones whereas the in-depth insights into the similarities and differences of both N-H and O-H proton donors on dynamics ESIPT process is still lacking. Therefore, in this study, we systematically investigated the different proton donor group of NH-type and OH-type on three different proton acceptor moieties: benzimidazole, benzothiazole and imidazo[1,2-a] pyridine giving six distinct compounds namely 2-(2′-aminophenyl)benzimidazole (APBI), HBI, 2-(2′-aminophenyl)benzothiazole (APBT), HBT,2-(imidazo[1,2-a]pyridine-2-yl) aniline (HNHPIP), and 2-(2′-hydroxyphenyl)imidazo[1,2-a]pyridine (HPIP). Main objectives are to shed light on the effect of different proton donor and proton acceptor moieties on the photophysical behaviors of all interested compounds in terms of H-bond strength, and PT process. This study is expected to provide the understanding of the photophysical behaviors driven by ESIPT of these NH-type and OH-type H-bonding systems.

PROPOSED APPROACH

The effect of proton donor namely NH-type and OH-type on the excited-state intramolecular proton transfer (ESIPT) of hydrogen-bonding (H-bond) molecules was investigated using the density functional theory (DFT) and time-dependent DFT (TD-

DFT), the structural and electronic properties as well as the potential energy surfaces along the proton transfer reaction in the ground and excited states of all compounds were analyzed. On-the-fly dynamics simulations on the first excited-state were further carried out for all compounds using in NEWTON-X interfaced with TURBOMOLE 6.3 program package to provide the important dynamic information on PT time and probability.

RESULTS

The important parameters on bond distances involving the intramolecular H-bond revealed that H-bonds of OH-type are stronger than those of NH-type and supported by the more red-shift of O−H vibrational mode in the excited-state. All simulated absorption peaks of all compounds are in consistent with experimental results. The potential energy surfaces along the PT reaction show that ESIPT of O-H type occurs with a small barrier or barrierless in the excited-state whereas those of N-H type have higher PT barrier except the one with stronger proton acceptor, resulting in a smaller barrier. The results of dynamic simulations are accordance with the potential energy surfaces in which the N-H type shows no PT in APBT but slow PT in APBI and fast PT in HNHPIP while O-H type (HBI, HBT and HPIP) exhibits ultrafast PT within 80 fs. Moreover, the occurrence of ESIPT process are strongly dependent with reaction energy and activation energy, in which the H-bond molecules with thermodynamically and kinetically favorable characters always provide the ESIPT. Therefore, the type of proton donor and proton acceptor of H-bond molecules is very important to hinder or effectively facilitate ESIPT process.

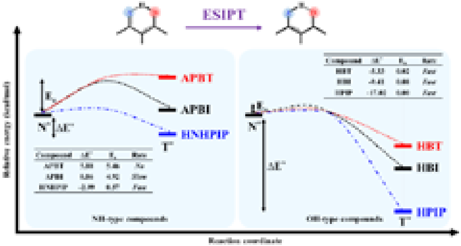

Figure 1. Thermodynamics and kinetics correlations for N-H type and O-H type for all compounds. Note that the potential energy curves drawn for the ESIPT reactions are only qualitative.

REFERENCES

1. Santra, S. and S.K. Dogra, *Chemical Physics*, 1998. **226**(3): p. 285-296.
2. Stasyuk, A.J., et al., *The Journal of Organic Chemistry*, 2012. **77**(13): p. 5552-5558.
3. Tseng, H.-W., et al., *The Journal of Physical Chemistry Letters*, 2015. **6**(8): p.1477-1486.

CHE
-P-
2

Structural Screening of Photoactive Covalent Organic Frameworks

Jack D'Amelio and Tim Kowalczyk
Department of Chemistry, Advanced Materials Science and Engineering Center, and Institute for Energy Studies, Western Washington University, Bellingham, WA 98225, USA

[C] ***E-mail***: *Tim.Kowalczyk@wwu.edu;* ***Fax***: *+1 360 650 2826;* ***Tel.*** *+1 360 650 6622*

EXTENDED ABSTRACT

Keywords: contact profiles, electronic couplings, steric interactions, singlet fission

INTRODUCTION

Two-dimensional covalent organic frameworks (COFs) form extended, porous molecular architectures which can be adapted for solar energy conversion applications by constructing the linker segments out of chromophores.[1,2] These structures, when vertically stacked and photoexcited, can facilitate the splitting of singlet excitons into two triplet excitons, a process called singlet fission.[3] We recently showed that the possibility of singlet fission occurring in these materials is strongly influenced by the angle between each layer's chromophore.[4] Designing a functionalized chromophore that reduces the linkers' range of rotation closer to an optimum angle is critical. In this work, we propose and implement a high-throughput virtual screening strategy for COF chromophore design based on a simple steric model of chromophore-chromophore interactions.

PROPOSED APPROACH

We explore the space of chemical substitutions for promising chromophore orientations between COF layers through the construction of contact profiles for a library of acene linker derivatives. Contact profiles are a graphical representation of the minimum distance between linkers in adjacent layers of the COF as one linker rotates with respect to the other. In this work, a combinatorially generated library of acene derivative linkers is generated using the SmiLib tool,[5] and contact profiles for these linkers are produced to identify linkers that are sterically locked at angles that produce greater electronic couplings between the chromophores. These electronic couplings, which govern the rate of singlet fission, are evaluated via constrained density functional theory (DFT).

RESULTS

Analysis of a library of procedurally generated functionalized linkers indicate that the orientations can be controlled by functionalization. The contact profiles demonstrate how asymmetric substitution of acenes affects the most favorable interchromophoric orientations. We have also established a proof-of-concept that electronic couplings along this same orientational degree of freedom can be correlated against the contact profiles to further optimize the chromophore design. Computational screening of COF linkers using this simple model can guide the identification, synthesis, and characterization of COFs supporting singlet fission.

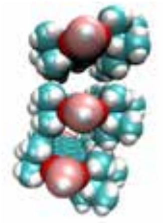

Figure 1. Steric clash of acene-COF linkers

REFERENCES

1. Addicoat, M. A.; Tsotsalas, M. *Front. Mater.* 2015, **4**, 00007.
2. Dogru, M.; Bein, Th. *Chem Commun*. 2014, **50**, 5531-5546.
3. Smith, M. B.; Michl, J. *Annu. Rev. Phys. Chem.* 2013, **64**, 361-386.
4. Laszlo, V.; Kowalczyk. T. *J. Mater. Chem. A* 2016, **4**, 10500-10507.
5. Schüller A.; Hähnke, V.; Schneider, G. QSAR Comb. Sci. 2007, 3, 407-410.

CHE -P- 3

Theoretical Studies of Excited State Proton Transfer of 2-Hydroxybenzaldehyde, 1-Hydroxy-2-naphthaldehyde, 1,8-Dihydroxy-2-naphthaldehyde, and Their Derivatives

Chanatkran Prommin [1], **Khanittha Kerdpol** [1], **Tinnakorn Saelee**[1] **and Nawee Kungwan** [1,C]
[1] *Department of Chemistry, Faculty of Science, Chiang Mai University,*
Chiang Mai 50200, Thailand

[C] ***E-mail**: naweekung@gmail.com; **Tel.** +66 8 48283641*

EXTENDED ABSTRACT

Keywords: Excited-State Intramolecular Single Proton Transfer, Excited-State Intramolecular Double Proton Transfer, DFT, TD-DFT.

INTRODUCTION

The excited state intramolecular single proton transfer (ESIntraSPT) is extensively investigated both experimental and theoretical studies due to its fundamental and important processes in chemistry and biology. The pre-requisite for ESIntraSPT is the presence of an intramolecular hydrogen bond between a proton donor and a proton acceptor in close proximity within a molecule. Besides molecules with ESIntraSPT, molecules having two proton donor sites and either with one or two proton acceptor sites connected by intramolecular hydrogen bond have emerged as a new interesting compound for undergoing the excited state intramolecular double proton transfer (ESIntraDPT) because of their dual emission with large Stokes shift. The applications of ESIntraSPT and ESIntraDPT molecules include laser dyes, fluorescence sensors, and molecular switches.

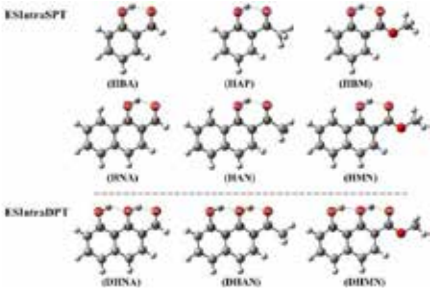

Figure 1. Ground-state optimized structures of HBA, HNA, DHNA, and their derivatives computed at B3LYP/TZVP level.

In this study, we investigate the ESIntraSPT in 2-hydroxybenzaldehyde, 1-hydroxy-2-naphthaldehyde and their derivatives, and ESIntraDPT in 1,8-dihydroxy-2-naphthaldehyde and its derivatives (shown in Figure 1) using density functional theory (DFT) and its time-dependent DFT (TD-DFT) at Becke's three-parameter hybrid functional and correlation functional of Lee-Yang-Parr (B3LYP) with TZVP basis set. Our results based on B3LYP/TZVP level are in good agreement with experiment data.

PROPOSED APPROACH

The ground state (S_0) geometries of all structures were optimized using DFT at B3LYP with TZVP basis set with constrained Cs symmetry in gas phase. The geometries of the excited state (S_1) were performed using TD-DFT at TD-B3LYP with the same basis set as in the S_0 state. All optimized structures were confirmed to be global minimum without an imaginary frequency. Further, vertical excitation energy calculations were carried out on the optimized S_0 and S_1 states. Frontier molecular orbitals (MOs), absorption spectra, and emission spectra as well as Infrared (IR) vibrational spectra were analyzed. Moreover, the S_0 and S_1 PECs involving PT coordinates were scanned by constrained optimizations with fixed O‒H distance 0.05 Å in step.

RESULTS

The results show that the ESIntraDPT molecules provide dual emission with large Stokes shift compared to those molecules having ESIntraSPT (Figure 2). Calculated absorption and emission spectra of ESIntraDPT molecules as depicted in Figure 3 are blue-shift when compared with those of the ESIntraSPT molecules. Moreover, when substituting $-CH_3$ and $-OCH_3$ to carbonyl group (C=O), the absorption spectra of both ESIntraSPT and ESIntraDPT molecules are red-shift because the resonance capacity of substituent increases compared with the molecules without substituent.

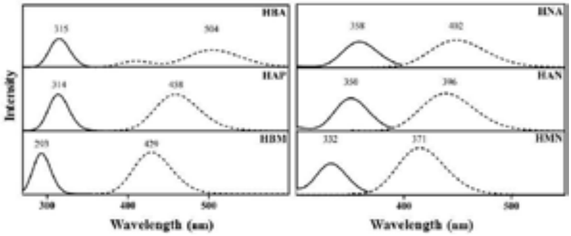

Figure 2. Calculated absorption (─) and emission (---) spectra of HBA, HNA and their derivative.

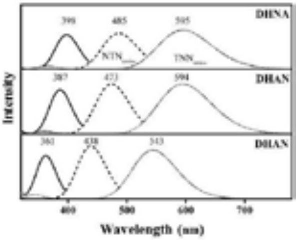

Figure 3. Calculated normal absorption (─), emission (---) of NTN form, and emission (···) of TNN form spectra of DHNA and its derivative.

REFERENCES

1. Tobita, S., Yamamoto, M., Kurahayashi, N., Tsukagoshi, R., Nakamura, Y., Shizaka, H., *Phys. Chem. A.*, 1998, **102**, 5206-5214.
2. Kwon, J. E., Park, S. Y., *Adv. Mater.*, 2011, **23**(32), 3615-3642.
3. Peng, C., Shen, J., Chem, Y., Wu, P., Hung, W., Hu, W., Chon., *Am. Chem. Soc.*, 2015, **137**, 349-57.
4. Serdiuk, I. E., Roshal, A. D., *Dyes Pigm.*, 2017, **138**, 223-244.
5. Julie, S., Tanja, B., Stefan, L., *Chem Phy Lett*, *2002*, **354**, 409-416.
6. Sankar, P., Sankarlal, A., Sudipta, D., Ajay, M, *J Mol Struc-Theochem*, 2007, **807**, 33-41.

CHE -P- 4

Theoretical Study of Different Donor and Acceptor-Type Effect in Push−Pull Porphyrin Dyes for Dye-Sensitized Solar Cells

Suparada kimchompoo[1] , **Siriporn Jungsuttiwong**[1,C]
[1]*Department of Chemistry, Faculty of Science, Ubon Ratchathani University, Warinchamrab, Ubon Ratchatani, 34190,Thailand.*

[C] ***E-mail:*** *siriporn.ubu@gmail.com*

EXTENDED ABSTRACT

Keywords: Dye sensitized solar cell, Density functional theory, porphyrin derivatives

INTRODUCTION

The issue environmental pollution and the consumption of the fossil fuels becoming the major point for sustainable development, so it has developed a new energy alternatives that are environmentally friendly. Dye-sensitized solar cells (DSSCs) have attracted much attention due to the advantages of low cost materials, low toxicity, simple fabrication procedure and relatively high efficiency. In this work, we used computational density function theory (DFT) and time- dependent density function theory (TD-DFT) to study the structure, absorption and electronic transition of porphyrin derivatives in dye-sensitized solar cell.

PROPOSED APPROACH

The geometries and electronic structures of porphyrin sensitizer were theoretical studied based on Kohn-Sham density functional theory (DFT). Beck's three parameter gradient-corrected hybrid functional and Lee-Yang-Parr correlation functional (B3LYP) with a 6-31G (d,p) basis set were used for fully geometry optimization The vertical excitation energies were investigated using time-dependent density functional theory (TD-DFT) on PBE0 functional. The solvent effect as well as the electrostatic solute-solvent interactions in dichloromethane (CH_2Cl_2) solvent was evaluated using conductor-like polarized continuum model (C-PCM) framework. All DFT and TD-DFT calculations were carried out using Gaussian09 program package. Moreover the electron injection mechanism from porphyrin dyes to the semiconductor was obtained by $(TiO_2)_{38}$ cluster model employing PBE functional with DNP basis set.

RESULTS

The absorption spectra of A0 displays an intensity B band at 427 nm and Q band at 687 nm and A1 displays an intense B band at 426 nm and red shift Q band to 698 nm. Moreover, the electron injection mechanism from porphyrin dyes to the semiconductor was obtained by using TD-CAM-B3LYP with the 6-31G(d,p) basis set, we found that two dyes binding to $(TiO_2)_{38}$ clusters,the HOMO of A0 and A1 are mostly distributed in the dye molecules while LUMO+21, LUMO+22 and LUMO+23 are mainly located on the $(TiO_2)_{38}$ clusters. The electron transfer from electron acceptor to the titaniumdioxide clusters, imply to the electron distributions in dyes

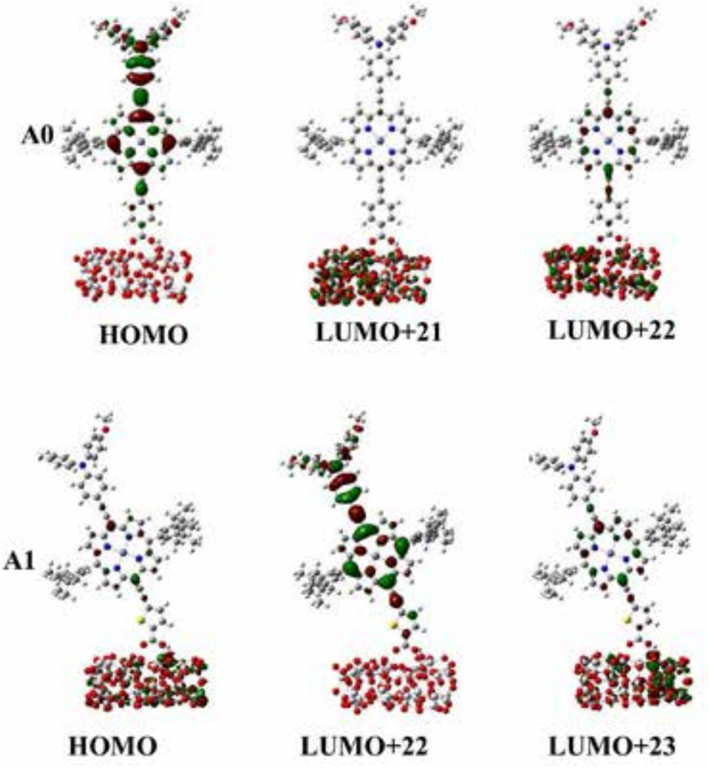

Figure 1. Molecular orbital spatial distributions of A0 and A1 after binding to $(TiO_2)_9$

REFERENCES

1. Chou, H.-H.; Reddy, K. S. K.; Wu, H.-P.; Guo, B.-C.; Lee, H.-W.; Diau, E. W.-G.; Hsu, C.-P.; Yeh, C.-Y., *ACS applied materials & interfaces* **2016,** *8* (5), 3418-3427.
2. Qian, X.; Lu, L.; Zhu, Y.-Z.; Gao, H.-H.; Zheng, J.-Y., *RSC Advances* **2016,** *6* (11), 9057-9065.
3. Kang, G.-J.; Song, C.; Ren, X.-F., *Molecules* **2016,** *21* (12), 1618.
4. Zhang, J.; Zhang, J.-Z.; Li, H.-B.; Wu, Y.; Geng, Y.; Su, Z.-M., *Physical Chemistry Chemical Physics* **2014,** *16* (45), 24994-25003.
5. Kang, G.-J.; Song, C.; Ren, X.-F., *Journal of Photochemistry and Photobiology A: Chemistry* **2017,** *333*, 200-207.

CHE
-P-
5

Theoretical Study on Effect of Auxiliary Acceptor In Novel D-π-A-π-A Featured Sensitizers for Dye-Sensitized Solar Cells

Ruangchai Tarsang[1,C], **Siriporn Jungsuttiwong**[2], **and Vinich Promarak**[3]
[1] *Department of Science and Mathematics, Faculty of Indrustry and Technology, Rajamangala University of Technology Isan Sakonnakhon Campus, Sakonnakhon, Thailand*
[2] *Department of Chemistry, Faculty of Science, Ubon Ratchathani University, Ubon Ratchathani, Thailand*
[3]*Department of Material Science and Engineering, School of Molecular Science and Engineering, Vidyasirimedhi Institute of Science and Technology, Rayong, Thailand*

[C] ***E-mail**: ruangchai.ta@rmuti.ac.th; **Fax**: +66 4277 2392; **Tel.** +66 8 6866 5485*

EXTENDED ABSTRACT

Keywords: Auxiliary acceptor, D-π-A-π-A sensitizers, dye-sensitized solar cells

INTRODUCTION

Dye-sensitized solar cells (DSSCs) have received great research attention in particular with the development of organic dyes as sensitizers for DSSCs. In the design of organic dyes, the common structure of organic dyes is composed of donor-π bridge-acceptor (D-π-A). In terms of dye development, organic sensitizers containing a D-A-π-A configuration have drawn special attention, in which being the role of an auxiliary acceptor. Recently, the newly synthesized organic dye **RK1** (see Fig. 1), which is new D-π-A-π-A based type organic sensitizer, showed a record of power conversion efficiency of 10.20%, which is the first time that exceeds the efficiency of 10.19% based on the standard **N719** dye under the same condition. This outstanding record for an organic based champion cell inspires us to find out newly potential candidates which can perform significantly better than **RK1** for further improvement of the power conversion efficiency. Therefore, this work provides a feasible strategy of molecular engineering by modifying the structure of the auxiliary acceptor units.

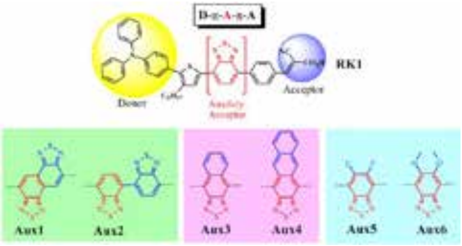

Figure 1. The molecular structures of RK1 and the newly designed dyes

PROPOSED APPROACH

The geometry structures of these newly designed dyes were fully optimized at the B3LYP level with 6-31G(d,p) basis set. The vertical excitation energy, electronic properties and optical absorption spectra were calculated by different XC functions, including CAM-B3LYP, in TDDFT calculations as implemented in Gaussian 09 program. The adsorption of dyes on a titanium dioxide surface was studied through using periodic DFT at the PBE functional with the DNP basis set as implemented in Dmol^3 module in Material Studio program package.

RESULTS

The calculated ground-state geometries of dyes showed that carbazole donor in **RK1** dye are non-planar, which can prevent the intermolecular aggregation. In addition, the dihedral angle between π - conjugated linker, auxiliary acceptor and electron withdrawing group display obvious co-planarity indicating the fast intramolecular charge transfer (ICT). Furthermore, replacing benzothiazole with different auxiliary acceptor had affected on co-planarity between adjacent π-conjugated units, especially **Aux3** and **Aux4**, which hamper the ICT. The simulated absorption spectra are shown in Fig.2. It is obvious that **Aux3** and **Aux4** cover the entire visible region with reduced intensity. It has been reported that low intensity leads to a decreasing LHE parameter. The maximum absorption peak of **Aux1** and **Aux2** are 495 and 489 nm, respectively, which exhibit a large redshift of 28 and 22 nm compared to **RK1** (467 nm). The calculated results of charge density difference (Δρ) and charge transfer distance (d^{CT}) were also confirmed a great ICT property for **Aux1** and **Aux2** dyes. After binding on TiO_2 surface, the calculated adsorption energies are in the range of -15.23 to -19.51 kcal mol^{-1}, indicating strong interactions between the dyes and the TiO_2. Finally, the electron injection process was evaluated, and showed the electrons delocalized predominantly from anchoring group to TiO_2 surface of **Aux2**-$(TiO_2)_{38}$ adsorption complex, which may improve the photo current as well as the conversion efficiency of the DSSCs cells. Considering the calculated results, the newly introduced auxiliary acceptor dye **Aux2** is promising candidate sensitizer for D-π-A-π-A organic dyes for DSSCs.

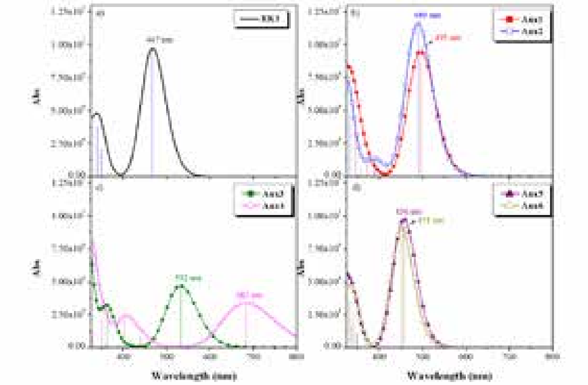

Figure 2. The calculated UV-Visible absorption spectra of all dyes by TD-CAM-B3LYP/6-31G(d,p) in CH_2Cl_2

REFERENCES

1. Joly, D. *et al*. *Scientific Reports*, 2014, **4**(4033), 1-7.
2. Cheng, J.-X. *et al*. *Dyes and Pigments* **2016,** 131, 134-144.
3. Fan, W. *et al*. *ChemPhysChem* **2012,** 13, (8), 2051-2060.

CHE
-P-
6

Theoretical Study on Electronic and Optical Properties of Polythiophene, Polyfuran,Polypyrrole and Their Derivatives as Light-Emitting Materials

Chattarika Sukpattanacharoen [1], **Khanittha Kerdpol**[1], **Tinnakorn Saelee**[1], **Rathawat Daengngern** [2]**and Nawee Kungwan**[1,C]
[1] *Department of Chemistry, Faculty of Science, Chiang Mai University,*
Chiang Mai 50200, Thailand
[2] *Department of Chemistry, Faculty of Science, King Mongkut's Institute of Technology Ladkrabang,*
Bangkok 10520, Thailand

[C] ***E-mail***: *naweekung@gmail.com;* ***Tel.*** *+66 8 4828 3641*

EXTENDED ABSTRACT

Keywords: Electronic and Optical Properties ; Optoelectronic devices ; Polythiophene (PTh), Polyfuran (PFu), Polypyrrole (PPy); Energy gaps ; Time-dependent density-functional theory ; OLED

INTRODUCTION

In areas of modern chemistry and physics, the electronic and optical properties of organic conjugated polymers (CPs) have been interested. CPs are a film of electroluminescent layer in device as organic light-emitting diodes (OLEDs). OLEDs are used to create many application such as digital display in television screens, computer monitors and mobile phones. The operation principle of OLEDs is shown in Figure 1 in which the two electrodes as function anode and cathode have been well developed. However, the suitable organic dyes as the emitting layer having hole-transporting and electron injection ability are still challenging research for OLEDs technology.

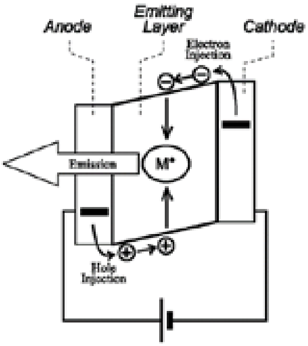

Figure 1. Operation principles of OLEDs.

In this work, the electronic and optical properties of the proposed molecules for being used as emitting layer possessing heterocyclic ring with different heavy atom such S-series, O-series and N-series (Figure 2) will be investigated using theoretical calculations with density functional theory (DFT) and time-dependent density functional theory (TD-DFT).

PROPOSED APPROACH

To first select the best method to investigate the electronic and optical properties, five different DFTs with various exchange-correlation functions (B3LYP, M06-2X, LC-BLYP, CAM-B3LYP, and ωB97X-D) with 6-311+G (d) basis set were performed and compared with available experimental data. The best suitable method in term of reproducing experimental data will be chosen to further study electronic and optical properties of S-series, O-series, and N-series. In addition, HOMO-LUMO gaps or energy gaps (E_{gap}), ionization potentials (IPs) and electron affinities (EAs), and electronic spectra (absorption and emission) for all series were calculated. All calculations were performed using the Gaussian09 program package.

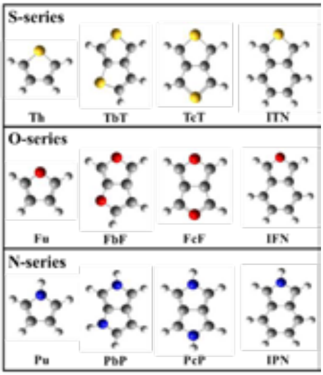

Figure 2. Geometric structure of S-series, O-series, and N-series

RESULTS

For overall performance of DFTs, in two hybrid functionals, the B3LYP (20% HF) method gave the best suitable E_{gap} close to experiment data than the M06-2X (54% HF) method. Whereas three long-rang-corrected functionals (LC-BLYP, CAM-B3LYP, and ωB97X-D) failed to reproduce the experimental data (Figure 3). Consequently, the B3LYP method with 6-311+G (d) basis set was chosen for investigating the electronic and optical properties of all studied molecules.

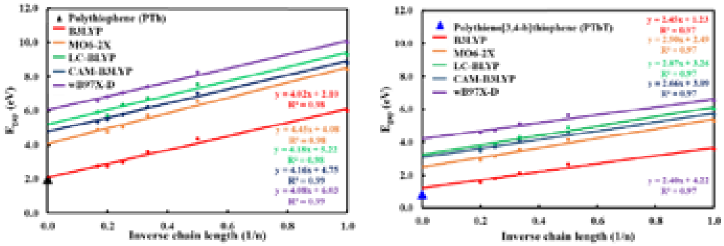

Figure 3. **The theoretical energy gaps, eV (*E*$_{gap}$) by several DFT method such as B3LYP, M06-2X, LC-BLYP, CAM-B3LYP, and ωB97X-D with 6-311+G (d) and experimental energy gaps, eV (*E*$_{gap}$) of PTh and PTbT.**

REFERENCES

1. J. H. Burroughs, D. D. C. Bradley, A. R. Brown et al., *Nature*, 1990, **347** (6293), 539–541.
2. Yakhanthip, T., Kungwan, N., Jitonnom, J., Anuragudom, P., Jungsuttiwong, and S., Hannongbua, S., *Int. J. Photoenergy*, 2011, **2011**, 570103-570109.
3. Rajendran, A., Tsuchiya, T., Hirats, S., and Iordanov, T. D., *J. Phys. Chem. A*, 2012, **116**, 12153-12162.

CHE
-P-
7

Theoretical Study on the Structural and Spectroscopic Properties of Cyanine Dyes as Fluorescent Dyes for DNA Detection

Malinee Promkatkaew [1,C], **Patchanee Tiemkeeree** [1], **Sakunrat Chansamon** [1],
Chanoknun Thakrabao [1], **and Songwut Suramitr** [2]

[1]*Faculty of Science at Sriracha, Kasetsart University Sriracha Campus, Chonburi, 20230 Thailand*
[2]*Faculty of Science, Kasetsart University, Bangkok, 10903 Thailand*

[C] ***E-mail**: sfscimlp@src.ku.ac.th; **Tel.** +66 3835 2812 ext.2798*

EXTENDED ABSTRACT

Keywords: Cyanine dyes, Fluorescent dyes, DNA detection, Density functional calculations (DFT), Time-dependent DFT (TD-DFT)

INTRODUCTION

Cyanine dyes present typical optical properties and act as the most important organic functional dyes in many processes of technological interest like sensitizers in photography, optical recording materials in laser disks, sensitizers in solar cells. A very attractive additional feature of cyanine dyes is the affinity for biological structures, especially DNA, which are characterized by large molar extinction coefficient, high fluorescence efficiency, large tunable range of maximum absorption wavelength, ease of synthesis and relatively high stability. Fluorescence technology is the most sensitive and easily available method to study intermolecular interactions and the transcriptional dynamics of the cell nucleus. Therefore, these dyes are suggested to be used as fluorescent probes of DNA, as exhibiting, a dramatic enhancement in fluorescence intensity upon binding to DNA[1]. The objective of this research is to design and develop new cyanine dyes as fluorescent dyes for DNA detection using the theoretical approaches. Structural, electronic, absorption and fluorescence properties of the cyanine dyes will be investigated using the DFT and TD-DFT levels of theory and examined the relationships between the experimental and theoretical data.

PROPOSED APPROACH

The series of sixteen new asymmetric monomethine cyanine dyes were synthesized and their spectral characteristics and interaction with double stranded DNA were investigated[2]. These cyanine dyes absorb in the region 453-519 nm and have high molar absorptivity in the range 37,900-93,100 L mol^{-1}cm^{-1}. It was found that four of the cyanine dyes (D9, D10, D12 and D16) were recommended as the most sensitive DNA labels. In this work, the cyanine dyes as fluorescent dyes for DNA detection were selected are showed in Table 1. The main computational efforts to simulate the absorption and fluorescence energy have been based on quantum chemistry calculations such as density functional theory (DFT) and a combination of time-dependent density functional theory (TD-DFT) with the B3LYP/6-311G(d,p) and polarizable continuum model (PCM) consisting of methanol[3]. The structures of cyanine dyes with/without ion were considered. Ground state and first-excited properties were calculated in order to investigate the absorption and fluorescence energy. All calculations will be performed using the Gaussian 09 suite of programs.

RESULTS

The molecular structure of four cyanine dyes with the experimental absorption maxima (λ_{max}) and extinction coefficients (ε) in methanol as fluorescent dyes for DNA detection are reported in Table 1. All structures were evaluated using an B3LYP/6-311G(d,p) method with a PCM solvent model consisting of methanol. As the results, cyanine dyes showed the corresponding results with the experimental absorption and fluorescence wavelength. D16 dye with the substitution groups as fluorobenzene and thiolane show the best absorption and fluorescence properties. This expect that this dye is suitable for use as non-covalent fluorescent DNA probes.

Table 1 The molecular structure of four cyanine dyes (D9, D10, D12 and D16) with the experimental absorption maxima (λ_{max}) and extinction coefficients (ε) in methanol.

	Structure	λ_{max} (nm) / ε (L $mol^{-1}cm^{-1}$)
D9	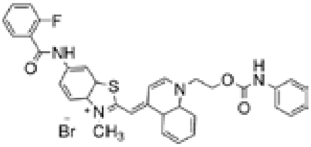	519 / 75,300
D10	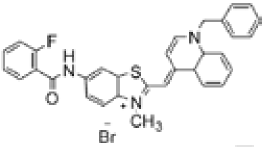	519 / 93,100
D12	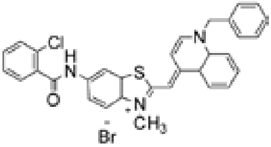	519 / 85,600
D16	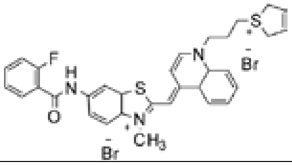	517 / 58,600

REFERENCES

1. Okoshi, M., Saparpakorn, P., Takada, Y., Hannongbua, S., and Nakai; H., *Bull. Chem. Soc. Jpn*., 2014, **87**, 267-273.
2. Kaloyanova, S., Trusova, V., M.; Gorbenko, G. P., and Deligeorgiev, T., *J. Photochem. Photobiol. A*, 2011, **217**, 147-156.
3. Promkatkaew, M., Suramitr, S., Karpkird, T., Ehara, M., and Hannongbua, S., *Int. J. Quan. Chem.*, 2013, **113**, 542-554.

CHE
-P-
8

Time-Dependent Density Functional Theory (TDDFT) Investigation on Electronic and Photophysical Properties of Derivatives of 3-Hydroxyflavone

Rusrina Salaeh[1], **Chanchai Sattayanon**[1], **and Nawee Kungwan**[1,C]
[1] *Department of Chemistry, Faculty of Science, Chiang Mai University, Chiang Mai 50200, Thailand*

[C] ***E-mail****: naweekung@gmail.com;* ***Tel.*** *+66 8 48283641*

EXTENDED ABSTRACT

Keywords: Electronic properties; 3-hydroxyflavone (3HF); Density functional theory (DFT); Time-dependent density functional theory (TDDFT)

INTRODUCTION

Excited state intramolecular proton transfer (ESIPT) plays an important role in a wide range of phenomena from biological to material science applications. Fluorophores containing ESIPT moieties can be potentially used in fluorescent probes because of their large Stokes shifts and four-level photocycle (**Figure 1**) to achieve population inversion. ESIPT processes occur in molecules featuring a strong intramolecular hydrogen bond between the proton donor (D) and the proton acceptor (A) moiety.

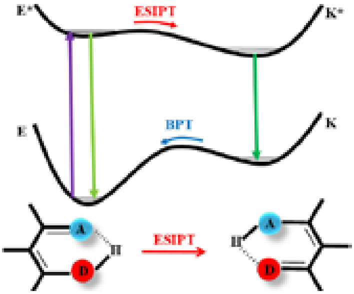

Figure 1. **Four-level photocycle.**

In this context, computational chemistry methods are valuable tools to explore the properties of these sensors providing the theoretical grounds to modify their structure. One of promising ESIPT probes is 3-hydroxylflavone. 3HF belongs to a group of flavonoids, which are responsible for the yellow color of petals. 3HF and its derivatives have been widely used in fluorescent probes. In this study, we systematically compared the effect of substitution on spectral characteristics of 3HF and its derivatives using theoretical calculations with density function theory (DFT) and its time-dependent DFT (TD-DFT). The following substituents placed to two positions (R_1, R_2) of 3HF to give 3HF derivatives as depicted in figure 2.

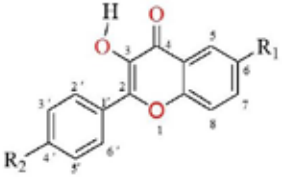

Figure 2. **Structure of 3HF and its derivative (R_1 and R_2 are substituent group)**

PROPOSED APPROACH

The enol absorption spectra of 3-hydroxyflavone (3HF) was computed by five different DFTs with various exchange-correlation functions (B3LYP, PBE0, LC-BLYP, CAM-B3LYP and ωB97XD) with 6-311+G(d, p) basis set to obtain the best suitable method compared with experimental data. After that the most suitable method will be utilized to study the effect of electron donating and withdrawing groups on the absorption properties of 3HF derivatives. All calculations were performed using Gaussian09 program package.

RESULTS

For all DFT functionals, hybrid functional PBE0 gave a better agreement to experiment data than B3LYP. For long-range-corrected hybrids, LC-BLYP provided a good agreement to experiment data whereas CAM-B3LYP and ωB97XD failed because their predicted wavelengths disagree with experimental results. From the results, LC-BLYP and PBE0 are suitable method, however, only one functional should be used due to cost-effective screening tool. Therefore, LC-BLYP and TD-LC-BLYP will be used to investigate electronic and photophysical properties of the 3HF derivatives. In addition, the nature of the excited state, the orbital transition from the highest occupied molecular orbital (HOMO) to the lowest unoccupied molecular orbital (LUMO) (HOMO→LUMO) is corresponded to π to π* transition.

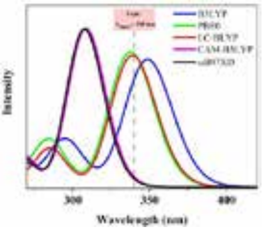

Figure 3. The maximum wavelengths (λ_{max}) of absorption spectra from the experimental data are shown in dashed lines.

REFERENCES

1. Kwon, J. E., Park, S. Y., *Adv. Mater.,* 2011, **23** (32), 3615-3642.
2. Gunduz, S., Goren, A. C., Ozturk, T., *Org. Lett.* 2012, **14** (6), 1576-1579.
3. Klymchenko, A. S.; Demchenko, A. P., *Phys.l Chem. Chem. Phys.* 2003**, 5** (3), 461-468;
4. Klymchenko, A. S., Duportail, G., Ozturk, T., Pivovarenko, V. G.; Mély, Y., Demchenko, A. P.,*Chemistry & Biology,* 2002**, 9** (11), 1199-1208.
5. Mandal, P. K.; Samanta, A., *J. Phys. Chem. A,* 2003**, 107** (32), 6334-6339

CHE
-P-
9

Aldol Condensation of Benzaldehyde and Acetophenone on Zirconium Based Metal-Organic Framework: A DFT Study

Worawaran Thongnuam[1,2], **Thana Maihom**[1,2], **Nongpanga Jarussophon**[1],
Piti Treesukol[1,2], **Kanokwan Kongpatpanich**[3] **and Bundet Boekfa**[1,2]*
[1]Department of Chemistry, Faculty of Liberal Arts and Science, Kasetsart University, KamphaengSaen Campus, NakhonPathom 73140, Thailand.
[2]Center for Advanced Studies in Nanotechnology and Its Applications in Chemical, Food and Agricultural Industries, Kasetsart University, Bangkok 10900, Thailand.
[3]School of Molecular Science and Engineering, Vidyasirimedhi Institute of Science and Technology, Rayong 21210, Thailand

*** E-mail**: *bundet.b@ku.ac.th* ***Tel.*** *+6686 555 4089*

EXTENDED ABSTRACT

Keywords: Aldol condensation, Metal-organic Framework, UiO-66-SO_3H, Benzaldehyde, Acetophenone

INTRODUCTION

Aldol condensation, which is an important reaction to form a carbon-carbon bond in organic synthesis, can be readily catalyzed by acids or bases. Several heterogeneous catalysts were used to study the aldol condensation reaction. The aldol condensation of benzaldehyde and acetophenone produces chalcone product. Chalcone is a versatile chemical which has several biological activities including anti-diabetic and anti-oxidant. This reaction has been demonstrated in the university laboratory as the chalcone in solid form is easy to be separated from the reaction solution.

Metal-organic Frameworks (MOFs) have been used in many applications such as gas storage, gas separation and catalysis. Several studies have demonstrated the potential uses of MOFs for heterogeneous catalysis. Zr-based MOFs [$Zr_6O_4(OH)_4(O_2C\text{-}C_6H_4\text{-}CO_2)_6$] (UiO-66) has pore dimension of in the range of 6-11 Å in its crystal structure. UiO-66 can be synthesized from $ZrCl_4$ and terephthalic acid by solvothermal method. Recently, we focus on the design of UiO-66 derivatives by functionalized the aromatic parts with several acidic groups to enhance the catalytic performance on the aldol condensation of acetone.

In this work, the reaction mechanism of the aldol condensation reaction of benzaldehyde and acetophenone on UiO-66-SO_3H catalysts (Scheme 1) has been calculated by density functional theory with the M06-L functional. The knowledge obtained from this study would be useful for further development of MOF-based catalysts for the condensation reaction and other acid- catalyzed organic transformations.

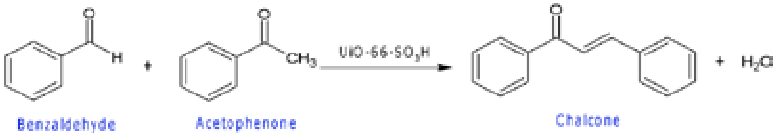

Scheme 1. The aldol condensation of benzaldehyde and acetophenoneon UiO-66-SO3H catalysts.

PROPOSED APPROACH

The density functional theory has been used to study the reaction mechanism of the aldol condensation of benzaldehyde and acetophenone on UiO-66-SO_3H catalysts. The $C_{162}H_{122}O_{67}SZr_{12}$ cluster, which is the model representing the entire structure of UiO-66-SO3H, has been calculated with ONIOM (M06-L:PM6) approach. Only the organic linker with a sulfonic acid group and adsorbed molecules was specifically calculated with the higher level of theory as the functionalized linkers act as active sites in the reaction. The remaining framework was treated with the lower level of theory to achieve reliable results with a reasonable computational time. The single point calculation at the M06-L functional for the whole cluster was used (M06-L//ONIOM(M06-L:PM6)) to obtain the accurate energy values. The C, H, O and S atoms were optimized with 6-31G(d,p) basis set and the Zr atoms were calculated with LANL2DZ. All calculations were performed with Gaussian 09 program.

RESULTS

The aldol condensation of benzaldehyde and acetophenone on UiO-66-SO_3H catalysts calculated with M06-L//ONIOM(M06-L:PM6) method was shown in Fig 1. The optimized transition states are shown in Fig 2. The first reaction step is the tautomerization of acetophenone to an enol product. As shown in Fig 2a, the reaction is a double-proton transfer. This step required activation energy of 14.9 kcal/mol. The required energy is lower than zeolite catalysts (16.6-24.9 kcal/mol). The second step is the aldol condensation with the activation energy of 3.7 kcal/mol with the C-C bond formation as shown in Fig 2b. The last step is the dehydration step. The transition state shows the C-H bond and C-O bond breaking (Fig 2c) with the activation energy of 30.8 kcal/mol. Chalcone and water are the products of this reaction.

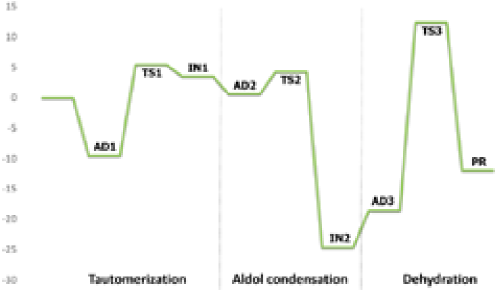

Fig 1. Energy pathway for the aldol condensation of benzaldehyde and acetophenone on UiO-66-SO_3H catalysts. Energies are in kcal/mol.

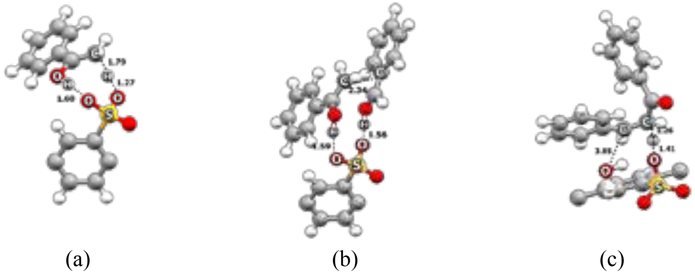

(a) (b) (c)

Fig 2. Optimized structures of the transition state complexes for the aldol condensation of benzaldehyde and acetophenone (a) TS1, (b) TS2 and (c) TS3. Distances are in Å.

Acknowledgements This work was supported by grants from the Thailand Research Fund (TRF), the Thailand Graduate Institute of Science and Technology (TGIST), and the Commission on Higher Education, Ministry of Education (the National Research University Project of Thailand-NRU, the National Center of Excellence for Petroleum, Petrochemical and Advanced Materials-NCE-PPAM) and the National e-Science Infrastructure Consortium. B.B. acknowledges the Thailand Research Fund (TRF). The support from Kasetsart Research and Development Institute (KURDI) and Graduate School Kasetsart University are also acknowledged.

REFERENCES

1. M. Kandiah, M.H. Nilsen, S. Usseglio, S. Jakobsen, U. Olsbye, M. Tilset, C. Larabi, E.A. Quadrelli, F. Bonino, K.P. Lillerud, *Chem. Mater.* 2010, **22**, 6632.
2. J. Hajek, M. Vandichel, B. Van De Voorde, B. Bueken, D. De Vos, M. Waroquier, V. Van Speybroeck, *J. Catal.* 2015, **331,** 1.
3. D. K. Mahapatra, V. Asati, and S. K. Bharti, *Euro. J. Med. Chem.* 2015, **92,** 839.

CHE
-P-
10

Carbon-Doped Boron Nitride Nanosheet: An Efficient Metal-Free Catalyst for Catalytic Oxidation of Carbon Monoxide

Sarinya Hussadee[1], Supawadee Namuangruk[2*], Nawee Kungwan[3], Siriporn Jungsuttiwong[1*]
[1]Department of Chemistry and Center of Excellence for Innovation in Chemistry, Faculty of Science, Ubon Ratchathani University, Ubon Ratchathani 34190, Thailand

[2]National Nanotechnology Center (NANOTEC), National Science and Technology Development Agency (NSTDA), Pathum Thani 12120, Thailand

[3]Department of Chemistry, Faculty of Science, Chiang Mai University, Chiang Mai 50200, Thailand

E-mail: siriporn.j@ubu.ac.th **Fax: +664 528 8379 **Tel.:** +664 535 3400 ext. 4510*

EXTENDED ABSTRACT

Keywords: CO oxidation, Boron Nitride Nanosheet

INTRODUCTION

CO gas can case harmful health when breathe much CO gas that oxygen in the blood is displaced effects by oxygen delivery to the heart and brain. To avoid the release of carbon monoxide into the atmosphere, CO is normally converted into carbon dioxide (CO_2). Although CO_2 is a greenhouse gas, which is responsible for global warming, however CO_2 is not hazardous for human health. Therefore the catalytic oxidation of CO became one of applications as control of environmentally-harmful pollutants.

PROPOSED APPROACH

The calculations were performed with the DMol3 in the Materials Studio 5.5. The Perdew−Burke−Ernzerhof (PBE) function within determination of the generalized gradient approximation (GGA) manages the exchang and correlations. The ionelectron interaction is employed effective core potentials and the doule numerical plus polarization (DNP). The Self-consistent field (SCF) calculation was carried on a convergence criterion of 10^{-6} au on the total energy, and the real space cutoff radius was 4.1 Å. A hexagonal 5x5 supercell were built 50 boron nitride units, including 25 B and 25 N atoms and and the Brillouin zone was sampled with 7x7x1 k-point grid in geometric optimization and search for the transition state (TS).

RESULTS

In summary, we investigate the possible reaction mechanism for CO oxidation on C-doped BN. The calculation results indicate that C-doped BN are investigated by replacement of B atom (C_BBN) that the interaction between C atom and associated N atoms is strongly couple with the 2p state of C and 2p state of N. The C-doped BN affect decrease of energy band gap (4.20 eV for C_NBN and 1.08 eV of C_BBN) smaller than h-BN surface (4.79 eV). Therefore, the small energy gap brings increased adsorption. As a result, the reaction of CO oxidation is considered following the Eley-Rideal (ER) pathway and the calculated energy barrier for $CO + O_2 \rightarrow CO_2 + O$ is 0.16 eV. The second reaction steps of $CO + O \rightarrow CO_2$ is 0.18 eV. From results of calculated the energy barrier, indicating it is much lower than that on the traditional noble metal catalysts.

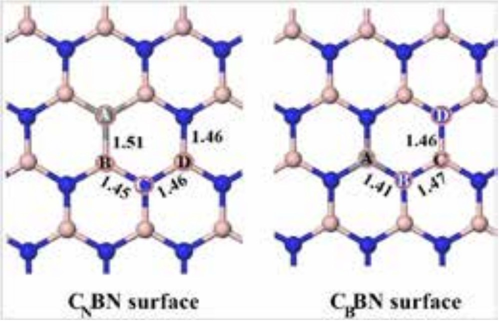

Figure 1. The adsorption sites are considered on C_NBN and C_BBN surface.

REFERENCES

1. Zhao, J.; Chen, Z. *The Journal of Physical Chemistry C* 2015, **119**, 26348-26354.
2. Lin, S.; Ye, X.; Huang, *J. Physical Chemistry Chemical Physics* 2015, **17**, 888-895.
3. Hashemzaei, M.; Barani, A. K.; Iranshahi, M.; Rezaee, R.; Tsarouhas, K.; Tsatsakis, A. M.; Wilks, M. F.; Tabrizian, *K. Environmental Toxicology and Pharmacology* 2016, **46**, 110-115.
4. Sinthika, S.; Vala, S. T.; Kawazoe, Y.; Thapa, *R. ACS Applied Materials & Interfaces* 2016, **8**, 5290-5299.

CHE-P-11

Confinement Effect on the Adsorption of Glucose, Hydroxymethylfurfural and Levulinic Acid on H-Zeolites (H-ZSM5, H-MOR and H-BEA)

Nattida Maeboonruan[1,2], **Thana Maihom**[1,2], **Piti Treesukol**[1,2] **Bundet Boekfa**[1,2C]

[1]Department of Chemistry, Faculty of Liberal Arts and Science, Kasetsart University, KamphaengSaen Campus, NakhonPathom 73140, Thailand.
[2]Center for Advanced Studies in Nanotechnology for Chemical, Food and Agricultural Industries, KU Institute for Advanced Studies, Kasetsart University,
Bangkok 10900, Thailand.

[C]***E-mail***: *bundet.b@ku.ac.th* ***Tel.*** *+6686 555 4089*

EXTENDED ABSTRACT

Keywords: glucose, hydroxymethylfurfural, levulinic acid, zeolite, ONIOM

INTRODUCTION

Zeolite is one among the most important heterogeneous catalysts. Many types of zeolite possess strong Brønsted acidity that enhances the catalytic activity. Well defined microporous structure makes zeolite the shape-selective catalyst for many reactions such as hydrocarbon cracking, isomerization and dehydration. The confinement effect of zeolite framework was originally introduced by Derouane and has been confirmed to have a prime effect on the adsorption and reaction occurring inside its framework.

Biomass energy is a novel renewable resource and has been increasing interested due to the environmental concern. D-glucose, which is the main component of cellulose, can be used to produce chemical substances such as levulinic acid via the dehydration reaction. Zeolite has been previously reported to be an effective catalyst for the dehydration reaction of glucose with high performance.

In this study, the adsorption of glucose, hydroxymethylfurfural and levulinic acid on on acidic zeolites (H-ZSM-5, H-MOR and H-BEA) were theoretically studied using the ONIOM (our own n-layered integrated molecular orbital and molecular mechanics) method. Understanding the zeolite framework effect in molecular level is the stepping stone to applications in biomass technology process.

PROPOSED APPROACH

Three 34T quantum clusters representing H-ZSM-5, H-MOR and H-BEA zeolites have been taken from their X-ray structures to cover the intersection cavity of the zeolites. Each model cluster was divided into two sub-regions according to the ONIOM method. The 5T high-level cluster representing the active region was treated with MP2 calculation while the 34T cluster representing the extended framework was calculated by density functional theory with M06-2X functional. All atoms were described by 6-31G(d,p) basis set. During the optimization only the 5T active region and the probe molecule were allowed to relax while the rest was kept fixed with its crystal structure. All calculations were performed using Gaussian 09 program.

RESULTS

The adsorption of glucose, hydroxymethylfurfural and levulinic acid on various proton zeolites (H-ZSM-5, H-MOR and H-BEA) were calculated with ONIOM 5T:34T (MP2:M06-2X) approach. Figs 1 shows the optimized structures of glucose on acidic zeolites. The adsorption energies were calculated and showed in table 1.

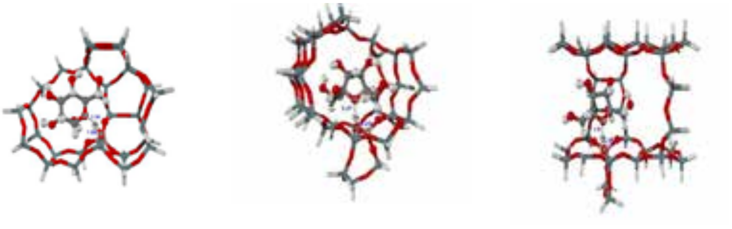

(a) (b) (c)

Fig 1. Glucose adsorbed on H-ZSM-5 (a), H-MOR(b) and H-BEA (c) zeolites (distances are in Å)

Table 1. The adsorption energies of Acetone, glucose (GLU), hydroxymethylfurural (HMF) and levulinic acid(LVA) (kcal/mol)

	MP2:M06-2X	High level	Low level
H-ZSM-5			
Acetone	-29.1	-19.0	-10.1
Glucose	-43.3	-18.1	-25.2
HMF	-37.7	-20.4	-17.3
LVA	-34.1	-22.4	-11.7
H-MOR			
Acetone	-27.7	-19.3	-8.4
Glucose	-35.6	-11.1	-24.5
HMF	-36.1	-18.4	-17.7
LVA	-26.0	-9.8	-16.2
H-BEA			
Acetone	-25.2	-18.5	-6.7
Glucose	-33.4	-16.2	-17.2
HMF	-26.0	-9.8	-37.8
LVA	-27.0	-21.5	-5.5

Acknowledgements This work was supported by grants from the Thailand Research Fund (TRF), the Thailand Graduate Institute of Science and Technology (TGIST), and the Commission on Higher Education, Ministry of Education (the National Research University Project of Thailand-NRU, the National Center of Excellence for Petroleum, Petrochemical and Advanced Materials-NCE-PPAM) and the National e-Science Infrastructure Consortium. B.B. acknowledges the Thailand Research Fund (TRF). The support from Kasetsart Research and Development Institute (KURDI) and Graduate School Kasetsart University is also acknowledged.

REFERENCES

1. Corma A, Canos, Iborra S, Velty A. *Chem. Rev.* 2007, 107, 2411.
2. Derouane EG, Chang CD. *Microporous Mesoporous Mater.* 2000, 35-36, 425.
3. Maeboonruan N, Maihom T, Poolmee P, Treesukol P, Boekfa B. *KMUNTNB.* 2017, DOI.

CHE
-P-
12

Dynamics simulations of ESIPT reactions of 2,5-bis(2'-benzoxazolyl)hydroquinone

Rathawat Daengngern [1,C], Rusrina Salaeh [2], Tinnakorn Saelee [2], Khanittha Kerdpol [2]
and Nawee Kungwan [2,C]
[1] *Department of Chemistry, Faculty of Science, King Mongkut's Institute of Technology Ladkrabang, Bangkok, Thailand*
[2] *Department of Chemistry, Faculty of Science, Chiang Mai University, Chaing Mai, Thailand*

[C] ***E-mail**: rathawat.da@kmitl.ac.th, naweekung@gmail.com; **Tel.** +66-2329-8400 ext. 345*

EXTENDED ABSTRACT

Keywords: ESIPT, 2,5-bis(2'-benzoxazolyl)hydroquinone, dynamics simulations.

INTRODUCTION

The excited-state intramolecular proton transfer (ESIPT) is one of the fundamental processes in chemistry and biochemistry due to its photophysical properties. The applications of ESIPT are found in many applications such as organic light emitting diodes, luminescent materials, and fluorescent probes. Most of the ESIPT processes occur in molecules having a strong intramolecular hydrogen bond between the acidic proton and the basic moiety and the suitable geometry such as 2,5-bis(2'-benzoxazolyl)hydroquinone (BBHQ). To provide more complete pictures of ultrafast PT of BBHQ, dynamics calculations are required to investigate whether PT occurs through single or double proton transfer as well as the potential energy surfaces.

PROPOSED APPROACH

All possible structures of BBHQ and its solvent clusters such as water were optimized at the using B3LYP/SVP level. These calculations were carried out using TURBOMOLE. Then, selected optimized geometries were used as initial geometries in dynamics photoexcitation using Newton-X interfaced with TURBOMOLE at TD-B3LYP/SVP level. Twenty-five trajectories as a representative set for each system were simulated using a time step of 1 fs with maximal duration of 500 fs. Furthermore, details of dynamics simulations were described by a statistical analysis.

RESULTS

The dynamics simulations of ESIPT of BBHQ and its solvent clusters have been performed on their lowest energy structures using time-dependent density functional theory (TDDFT) at TD-B3LYP/SVP level.

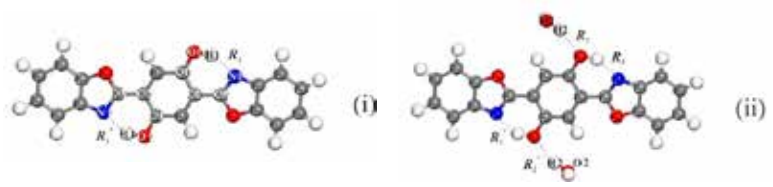

Figure 1. Optimized geometry of 2,5-bis(2'-benzoxazolyl) hydroquinone computed at B3LYP/SVP level. (i) isolated BBHQ and (ii) BBHQ with one water molecule

Our dynamics simulations showed that the intramolecular hydrogen bond N···H−O is strengthened in the excited state, which triggers driving force to effectively facilitate the proton transfer process through an intrinsic intramolecular hydrogen bond. There are two possible mechanisms of the ESIPT processes: *a*) single proton transfer and *b*) double proton transfer. The ESIPT mechanism of BBHQ systems elucidates that single proton transfer is more likely to take place in comparison with the double proton transfer reaction. Moreover, the competition between the formations of intermolecular and intramolecular hydrogen bons of water and BBHQ plays a role in lower the reaction.

REFERENCES

1. Daengngern, R., Prommin, C., Rungrotmongkol, T., Promarak, V., Wolschann, P., Kungwan, N. *Chem. Phys. Letts.*, 2016, **657**, 113.
2. Ernsting, N. P. *J. Phys. Chem.*, 1985, **89**, 4933.
3. Zhao, J., Chen, J., Liu, J., Hoffmann, M. R. *Phys. Chem. Chem. Phys.*, 2015, **17**, 11990.
4. Zhang, Y., Sun, M., Li, Y. *Sci. Rep.*, 2016, **6**, 25568.

CHE
-P-
13

Mechanistic Study of CO Oxidation by N_2O Over Ag_7Au_6 Cluster Investigated by DFT Methods

Yutthana Wongnongwa[1], **Supawadee Namuangruk**[2,C], **and Siriporn Jungsuttiwong**[1,C]
[1]*Department of Chemistry, Faculty of Science, Ubon Ratchathani University,*
Ubon Ratchathani, 34190 Thailand
[2]*NANOTEC, National Science and Technology Development Agency (NSTDA),*
111 Phahon Yothin Rd, Klong Luang, Pathumthani, 12120 Thailand

[C] ***E-mail****: supawadee@nanotec.or.th (S.N.) and siriporn.j@ubu.ac.th (S.J.)*

EXTENDED ABSTRACT

Keywords: Ag_7Au_6 alloy catalyst, CO oxidation, DFT.

INTRODUCTION

The poisonous gases that are produced during fuel combustion, transportation, and industrial processes are of concern for both health and environmental reasons. Among those gases are nitrous oxide (N_2O) and carbon monoxide (CO). These gases are among the most harmful gases emitted by automobile exhaust systems. The problems with N_2O are twofold: the gas is a significant contributor to global warming, with a global warming potential (GWP) that is 300 times greater than that of carbon dioxide (CO_2). It is also a precursor to NO, which is a major catalyst for stratospheric ozone depletion. The chemical transformations of N2O and CO to the non-harmful gases N_2 and CO_2 are thermodynamically favorable. However, the non-catalyzed reactions have high activation energies, which render them kinetically unfavorable.

PROPOSED APPROACH

Despite many contributions from experimental and theoretical studies on CO adsorption on varying Ag-Au clusters, the elementary reaction steps for reaction of N_2O with CO on the Ag_7Au_6 cluster have not yet been elucidated. Thus, a description of detailed reaction mechanisms at the atomic level is needed. On the basis of previous work, herein we present the results of DFT calculations performed to investigate the reaction mechanisms of CO oxidation by N_2O over the Ag_7Au_6 cluster following the two aforementioned steps, ($N_2O \rightarrow N_2 + O^*$) the reduction of N_2O to N_2 and ($O^* + CO \rightarrow CO_2$) the oxidation of CO to CO_2. We have studied the elementary reactions in detail and determined the influence of each atom in the cluster on the reactions. The understanding gained in the current study might be helpful in the development of active catalysts for N_2O and CO removal from automotive and other exhaust streams.

RESULTS

The Ag_7Au_6 structure (shown in Figure 1a) has C_{3v} symmetry and an Au surface-segregated hollow structure. The NBO analysis of Ag_7Au_6 cluster predicts atomic NPA charges as follow: +0.017e on the edge Au atoms, +0.230e on edge Ag atoms and −0.412e on the center Ag atom. This result indicates that the electron density on the edge Ag and Au atoms transfers to the center Ag atom. For the HOMO, the electron density is localized on the corner Au atoms, which suggests that these are active sites for adsorbing electrophile probe molecules (Figure 1b). On the other hand, the electron density of the LUMO is localized on the edge Ag atoms (Figure 1c). This indicates that these edge Ag atoms are actives site for the adsorption of nucleophilic probe molecules.

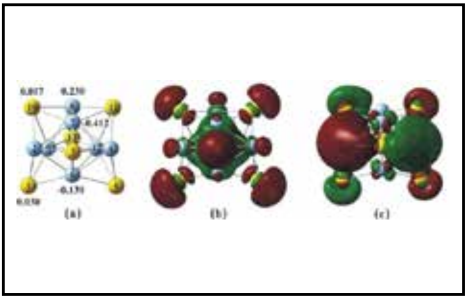

Figure 1 The structure and frontier molecular orbitals of the Ag_7Au_6 cluster: (a) the most stable configuration, (b) HOMO, and (c) LUMO of Ag_7Au_6 cluster.

REFERENCES

1. A. Ravishankara, J.S. Daniel, R.W. Portmann, *science*. 326 (2009) 123-125.
2. V. Blagojevic, G. Orlova, D.K. Bohme, *Journal of the American Chemical Society*. 127 (2005) 3545-3555.

CHE-P-14

Nitrous Oxide Decomposition with CO Reducing Agent over Oxotitanium Porphyrin: A Theoretical Study

Phornphimon Maitarad,[1] **Supawadee Namuangruk,**[2*] **Masahiro Ehara**[3*]
[1] *Research Center of Nano Science and Technology, Shanghai University, Shanghai 200444, P. R. China*
[2] *National Nanotechnology Center (NANOTEC), NSTDA, 111 Thailand Science Park, Pahonyothin Road, Klong Luang, Pathum Thani 12120, Thailand*
[3] *Institute for Molecular Science and Research Center for Computational Science, 38 Nishigo-naka, Myodaiji, Okazaki, 444-8585, Japan*

E-mail*: pmaitarad@shu.edu.cn (PM), supawadee@nanotec.or.th (SN) and ehara@ims.ac.jp (ME)*

EXTENDED ABSTRACT

Keyword: metal-porphyrin; N_2O decomposition; Reaction mechanism; Photocatalyst; Density functional theory

INTRODUCTION

To reduce the amount of N_2O concentration in the atmosphere, there are four types of several after-treatment technologies; *(i)* thermal decomposition, *(ii)* non-selective catalytic reduction, *(iii)* selective catalytic reduction, and *(iv)* direct catalytic decomposition (deN_2O).[1-4] The N_2O catalytic decomposition is one of the most promising methods for control of N_2O emissions, due to its simplicity, high efficiency, and low energy requirements. For this reason, significant research efforts have been lately focused on the development of novel catalytic materials for N_2O abatement.

PROPOSED APPROACH

In this project, we will systemically perform the theoretical calculations for N_2O direct decomposition reaction processes with CO catalyzed by the oxotitanium-porphyrin (TiO-por). The model of TiO-por was constructed and then optimized by using the density functional theory (DFT) based on the M06L functional[5,6] without any restrictions. The 6-31G(d,p) basis set was assigned to carbon, oxygen, nitrogen and hydrogen atoms and Dunning-Hay-Wadt with LANL2DZ was assigned to Ti transition metal. All calculations were carried out by using the Gaussian09 program package revision B01.[7]

RESULTS

We performed the DFT to investigate the N_2O reduction with CO agent catalyzed by TiO-por. There are two possible pathways: (1) Adsorption of N_2O followed by CO and (2) Adsorption of CO followed by N_2O. The N_2O was more likely to adsorb on TiO-por (**Path A**). In **Path B**, the higher barrier energy would limit the reaction to react. Therefore, the N_2O molecule was first decomposed on the TiO-por site yielding the N_2 and TiO_2-por, which was more active species for the CO oxidation (**Path A1**) than the 2ndN_2O (**Path A2**). So, in alternatively, the CO oxidizing agent played important role on catalyst regeneration step and its reaction was exothermic process.

Path	Main Reaction	Step	Energy (kcal/mol)
A	TiO-por + 1st N_2O	Adsorption	-4.64
		Transition state	48.29
		Product	-3.01
		Desorption N_2	2.44
B	TiO-por + CO	Adsorption	-3.07
		Transition state	>70**
		Product	23.26
		Desorption N_2	12.74
A1	TiO_2-Por +CO	Adsorption	-3.14
		Transition state	16.08
		Product	-89.12
		Desorption CO_2	5.16
A2	TiO_2-por + 2nd N_2O	Adsorption	-5.22
		Transition state	47.49
		Product	9.87
		Desorption N_2	4.72

** the transition state is not convergence

REFERENCES

1. Kapteijn, F.; Rodriguez-Mirasol, J.; Moulijn, J. A., Applied Catalysis B: Environmental 1996, 9 (1), 25-64.
2. Konsolakis, M., ACS Catalysis 2015, 5 (11), 6397-6421.
3. Liu, Z.; He, F.; Ma, L.; Peng, S., Catalysis Surveys from Asia 2016, 20 (3), 121-132.
4. V. Leont'ev, A.; A. Fomicheva, O. g.; V. Proskurnina, M.; S. Zefirov, N., Russian Chemical Reviews 2001, 70 (2), 91-104.
5. Zhao, Y.; Truhlar, D. G., Theoretical Chemistry Accounts 2008, 120 (1), 215-241.
6. Zhao, Y.; Truhlar, D. G., Journal of Chemical Theory and Computation 2011, 7 (3), 669-676.
7. Frisch, M. J.; Trucks, G. W.; Schlegel, *et al.* Gaussian 09, Revision B.01. Wallingford CT, 2009.

CHE
-P-
15

The Catalytic Reaction of Ethanol to Ethylene : a DFT Study

Saowalak Phikulthai[1,2], Yuwanda Injongkol[1,2], Chularat Wattanakit[3], Thana Maihom[1,2],Nongpanga Jarussophon[1], Bundet Boekfa[1,2] and Piti Treesukol[1,2*]

[1] Department of Chemistry, Faculty of Liberal Arts and Science, Kasetsart University, Kamphaeng Saen Campus, Nakhon Pathom 73140, Thailand.
[2] Center for Advanced Studies in Nanotechnology for Chemical, Food and Agricultural Industries, KU Institute for Advanced Studies, Kasetsart University, Bangkok 10900, Thailand.
[3] Department of Chemical and Biomolecular Engineering, School of Energy Science and Engineering, Vidyasirimedhi Institute of Science and Technology, Rayong 21210, Thailand.

[*] ***E-mail**: faasptt@ku.ac.th **Tel.*** +6689-798-5952

EXTENDED ABSTRACT

Keywords: Biomass, ethanol, ethylene, M06-2X, NBO analysis

INTRODUCTION

Biomass has become an interesting research issues due to the environmental concern. Bio-ethanol produced by fermentation of biomass product such as sugar and wood-wastes is one of the most important renewable energy sources. Thailand, which is the top-three sugar-export country, has a stimulus package to increase value of sugar by converting it to ethanol fuel. Nevertheless, ethanol can be catalytic converted to much more valuable products for chemical industrial. The most important product would be ethylene, which is currently used as raw materials for the polyvinyl chloride (PVC) production. The dehydration reaction of ethanol to ethylene is shown below:

$$C_2H_5OH \quad \rightarrow \quad C_2H_4 + H_2O \qquad \text{---(1)}$$

Several catalysts can be used in this dehydration reaction. The acidic catalysts such as sulfuric acid and phosphoric acid have been widely used in the production of ethylene. At low temperature, the side reaction is possible as shown below:

$$2\ C_2H_5OH \quad \rightarrow \quad (C_2H_5)_2O + H_2O \qquad \text{---(2)}$$

In this study the dehydration of ethanol to ethylene was studied at molecular level. The proposed mechanism was examined by Density functional theory with the hybrid M06-2X functional. The Natural Bond Orbital (NBO) analysis was applied to the adsorption step.

PROPOSED APPROACH

The dehydration reaction has been studied by computational chemistry. Effect of sulfuric concentration has been determined by vary ethanol: sulfuric ratio from 1 to 3. Structures of all related species were optimized by DFT methodology with M06-2X functional and 6-31G(d,p) basis set. Transition states were located by using the Berny algorithm and each optimized TS was confirmed by its single imaginary frequency that corresponded to the reaction pathway. The adsorption structures were analyzed by NBO method. All calculations were performed using Gaussian 09 program.

RESULTS

The dehydration reaction of ethanol to ethylene catalyzed by sulfuric acid was examined by M06-2X functional. The calculated energy pathway was shown in figure 1. The transition state with some selected distances are shown in figure 2. Activation energies for the reaction with the ethanol: sulfuric ratio varied from 1 to 3 were 53.1, 51.3 and 55.2 kcal/mol, respectively. For the interaction of one- and two ethanol molecules with the sulfuric acid, electron transfer from the lone pair electron of oxygen of ethanol to the antibonding of O-H bond of sulfuric acid was found to be important (E2 = 50.0 and 100.2 kcal/mol, respectively). In case of 3 ethanol molecules, the protonated form of ethanol was found and electron transfer from the lone pair of oxygen atoms to the antibonding of O-H bond was even more important (E2 = 98.2 and 87.3 kcal/mol).

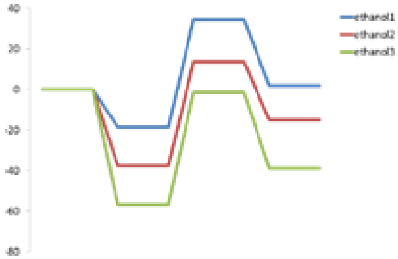

Fig 1. Energy profiles for the dehydration of ethanol to ethylene with different number of ethanol molecules determined by M06-2X/6-31G(d,p) level of theory. Energies are in kcal/mol.

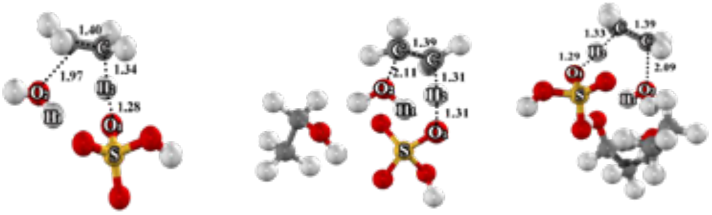

(a) (b) (c)

Fig 2. Optimized structures of the transition state complexes over sulfuric acid for (a) one ethanol molecule, (b) two ethanol molecules and (c) three ethanol molecules at M06-2X/6-31G(d,p) level of theory. Distances are in Å.

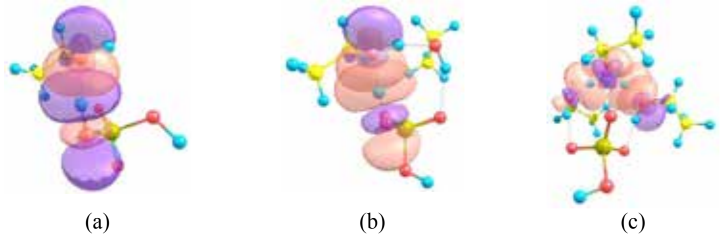

Fig 3. The Natural Bond Orbital Analysis of adsorption complexes over sulfuric acid for (a) one ethanol molecule, (b) two ethanol molecules and (c) three ethanol molecules at M06-2X/6-31G(d,p) level of theory.

Acknowledgements This work was supported by grants from the National Research Council of Thailand (NRCT), the Thailand Research Fund (TRF), Thailand Graduate Institute of Science and Technology (TGIST), and the Commission on Higher Education, Ministry of Education (the National Research University Project of Thailand-NRU, the National Center of Excellence for Petroleum, Petrochemical and Advanced Materials-NCE-PPAM) and the National e-Science Infrastructure Consortium. P.T. acknowledges the NRCT and B.B. acknowledges the TRF. The support from Kasetsart Research and Development Institute (KURDI) and Graduate School Kasetsart University are also acknowledged.

REFERENCES

1. Ezinkwo GO, Tretyakov VP, Aliyu A, Llolov AM. *ChemBioEng Rev* 2014, **5**, 194.
2. Braskem SA, *J. Marcomolecule Sci* 2009, **49**, 79.
3. Zhang M, Yu Y, *Ind. Eng. Chem. Res.* 2013, **52**, 9505.

CHE
-P-
16

The Conversion of Methane to Methanol over the $[Cu\text{-}O\text{-}Cu]^{2+}$/ZSM-5 Zeolite: a Density Functional Theory Study

Wasinee Panjan[1,2], **Jakkapan Sirijaraensre** [1,3,C], **and Jumras Limtrakul** [4]
[1]*Department of Chemistry, Faculty of Science and NANOTEC Center for Nanoscale Materials Design for Green Nanotechnology, Kasetsart University, Bangkok, Thailand*
[2]*Maejo University Phrae Campus, Phrae, Thailand*
[3]*Center for Advanced Studies in Nanotechnology and Its Applications in Chemical, Food and Agricultural Industries, KU Institute for Advanced Studies, Kasetsart University, Bangkok, Thailand*
[4]*Department of Materials Science and Engineering, School of Molecular Science and Engineering, Vidyasirimedhi Institute of Science and Technology, Rayong, Thailand*

[C] ***E-mail***: *fscijkp@ku.ac.th;* ***Fax***: *+66 2 562 5555 ext 2176;* ***Tel.*** *+66 8 9005 3470*

EXTENDED ABSTRACT

Keywords: Methane, Methanol, Cu-ZSM-5, ZSM-5, Zeolite, DFT.

INTRODUCTION

With continuously lessening reserves of crude oil, natural gas, which consists primarily of methane, is attracting increasing attention as an important source of clean fossil energy and as a feedstock for chemicals. As a feedstock, methane can be converted to chemicals by an indirect route which involves multiple steps via the formation of synthesis gas (a mixture of CO and H_2). From syngas, a variety of products can be obtained directly via the Fischer-Tropsch synthesis. Alternatively, syngas can also be converted first to methanol and then from methanol to chemicals using technologies such as methanol-to-olefin, methanol-to-gasoline. However, the synthesis gas production is strongly endothermic and requires a lot of thermal energy. As a result, the most expensive step in process is synthesis gas generation, which accounts for 60% of the capital cost of the process. The direct oxidation of methane to methanol at the low temperature would therefore be a highly attractive industrial process. The process chemistry of direct methane to methanol conversion have been proposed continuously. The ion-exchanged Cu/ZSM-5 zeolite is found to be an efficient catalyst that is able to catalyze the partial oxidation of methane.[1] The unique reactivity of Cu/ZSM-5 zeolite in CH_4 oxidation to CH_3OH has been related to extra-framework binuclear oxygen-containing Cu complexes.[2,3] Despite the large number of studies, a clear connection between the local structure of zeolite and the active Cu-O-Cu species in C-H bond activation has not been unambiguously established. In this work, the conversion of methane to methanol over the $[Cu\text{-}O\text{-}Cu]^{2+}$/ZSM-5 zeolite was studied by means of density functional theory calculations.

PROPOSED APPROACH

The 12T ZSM-5 zeolite cluster model was used in this study. The geometry of this cluster was taken from the crystal structure of ZSM-5. The Si atoms at the edge of the cluster were terminated by the H atoms with the Si–H bond length of 1.47 Å along the direction of the crystallographic Si–O bonds. Two silicon atoms were substituted with two aluminium atoms at T12 and T9 positions.[4] The modelled active site of Cu-ion-exchanged ZSM-5 zeolite as shown on Fig. 1, was composed by a positive di-cupper center $[Cu\text{-}O\text{-}Cu]^{2+}$ inserted in part of the zeolite framework (Z^{2-}). During the geometry optimization, all atoms of the 12T cluster, with the $[Cu\text{-}O\text{-}Cu]^{2+}$ and the adsorbing molecules were allowed to relax. The terminated H atoms of the structure were kept fixed. The M06-L meta-GGA functional was used since it has been shown to give accurate results in the literatures. Basis set at the 6-31G(d,p) was used for non-metal atoms and the LANL2DZ effective core potential (ECP) was used the Cu atom. Transition state structures were confirmed by normal mode analysis, revealing one imaginary frequency that corresponds to the reaction coordinate. All calculations were carried out using the Gaussian 09 package.

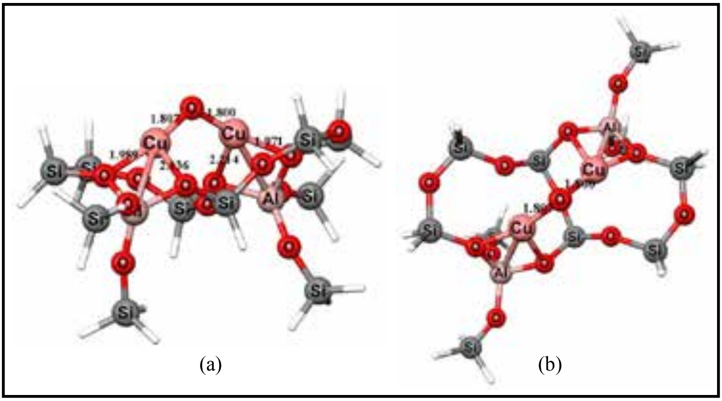

(a) (b)

Figure 1. The optimized structure and the selected geometry parameters of the $[Cu\text{-}O\text{-}Cu]^{2+}$/12T-ZSM-5 cluster (triplet spin state) viewed from (a) side view and (b) top view. Bond distances are in Å.

RESULTS

In this work, the electronic structure of the [Cu-O-Cu]/Z catalyst is the triplet spin state which is more stable than the singlet spin state by 15.22 kcal/mol. The conversion of methane to methanol consists of two elementary steps. The first step of the reaction is the methane activation. First, the methane adsorbs on the $[Cu\text{-}O\text{-}Cu]^{2+}$ active center of Cu-exchanged ZSM-5 with the adsorption energy of -5.51 kcal/mol. From these studies, the calculated barrier, when referring to the adsorption complex, is 20.65 kcal mol^{-1} for the first C−H bond activation of CH_4. Proton transfer from the activated C-H bond of the adsorbed methane to the bridging O atom of the extra framework copper cluster results in the formation of $[CH_3\text{-}Cu\text{-}HO\text{-}Cu]$ intermediate. Two-state reactivity (TSR) is involved in this step. The electronic state of the system is changed from the triplet spin state to the singlet spin state. Subsequently, a methanol molecule is formed via the recombination of two ligands bound on the copper active center. The activation energy for this step is predicted to be 16.71 kcal/mol. The formed methanol molecule is desorbed from the zeolite surface, resulting in a final complex $[2Cu]^{2+}/Z + CH_3OH$. The bridging O atom is regenerated by the decomposition of an oxidant.

REFERENCES

1. M. H. Groothaert, P. J. Smeets, B. F. Sels, P. A. Jacobs and R. A. Schoonheydt, *J. Am. Chem. Soc.*, 2005, **127**, 1394-1395.
2. P. Vanelderen, R. G. Hadt, P. J. Smeets, E. I. Solomon, R. A. Schoonheydt and B. F. Sels, *J. Catal.*, 2011, **284**, 157-164.
3. J. S. Woertink, P. J. Smeets, M. H. Groothaert, M. A. Vance, B. F. Sels, R. A. Schoonheydt and E. I. Solomon, *Proc. Natl. Acad. Sci.*, 2009, **106**, 18908-18913.
4. E. Kurnaz, M. F. Fellah and I. Onal, *MICROPOR MESOPOR MAT*, 2011, **138**, 68-74.

CHE -P- 17

The Effect of Small Gas Detection on Metal-Embedded Mos$_2$: DFT Study

Chanchai Sattayanon[1], Jittima Meeprasert[2], Chattarika Sukpattanacharoen[1],
Nawee Kungwan[1,C], and Supawadee Namuangruk[2,C]
[1]Department of Chemistry, Faculty of Science, Chiang Mai University,
Chiang Mai , 50200, Thailand
[2]National Nanotechnology Center (NANOTEC), National Science and Technology Development
Agency (NSTDA), Pathum Thani, 12120, Thailand

[C] ***E-mail****: naweekung@gmail.com, supawadee@nanotec.or.th;* ***Tel.*** *+66 8 4828 3641*

EXTENDED ABSTRACT

Keywords: DFT; Gas adsorption; MoS$_2$ monolayer; Metal-doped; Sensor.

INTRODUCTION

Effective gas sensing particularly for the detection of toxic gasses is of great importance for human health, biomedicine, agricultural production and environmental protection. For these reasons, gas sensors that are efficient in terms of energy consumption, cost, and reversibility are extremely needed. In general, the gas sensors that are made of semiconducting metal oxide nanowires are widely used on gas detection. However, the band gap is one of the most important factors for gas sensing materials. By comparison with the zero-band gap materials such as graphene, MoS$_2$ as a typically two-dimensional material has more potential value in the field of gas sensing application due to the suitable band gap of 1.3-1.8 eV and low price. Recently, two-dimensional metal embedded-MoS$_2$ have been reported as potential materials as gas sensing however the efficiency in term of gas adsorption of these metal embedded-MoS$_2$ is not systematically assessed. Therefore, in this study, the pristine molybdenum disulfide (MoS$_2$) and MoS$_2$ embedded (M-MoS$_2$; M=Co, Cu, Fe, Ni, Pd, and Pt) have been theoretically investigated to adsorb small gas molecules such as CO, NO, O$_2$, HCN and NH$_3$.

PROPOSED APPROACH

To investigate the small gas adsorption on pristine MoS$_2$ and metal-embedded MoS$_2$ (shown in Figure 1), the periodic density functional theory (DFT) has been performed to calculate the geometric, energetic, and electronic properties of gas adsorption on those materials using Vienna Ab initio Simulation Package (VASP). The adsorption energy, energy band gap and density of states will be analyzed to assess the possibility of metal-doped MoS$_2$ as gas sensors.

RESULTS

From the DFT calculations, we found that reactivity of MoS$_2$ is substantially improved by embedded metals. All small gas molecules prefer to adsorb on metal embedded-MoS$_2$ than pristine MoS$_2$ indicated by stronger adsorption energy. Especially, we found that NO (-2.94 eV) and CO (-1.71 eV) gases are strongly adsorbed on Co-embedded MoS$_2$ (CoMoS), while O$_2$ is weakly adsorbed (-1.61 eV). There is a correlation between adsorption energy and amount of charge transfer (between gas and surface). In case of distance, the shorter distance between gas and surface results in stronger adsorption energy. The density of state, charge transfer, conductivity changes and electronic property induced by the gas adsorption will be presented. Finally, this study should provide the suitable embedded metals for improving the performance of MoS_2-based gas detection.

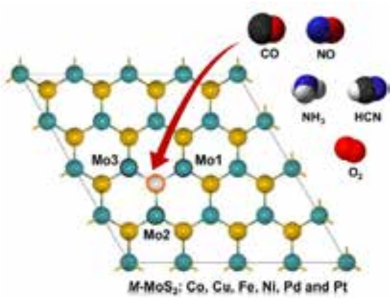

Figure 1. Graphical abstract of small gas detection on Metal-embedded MoS_2 in this study.

REFERENCES

1. F. Mehmood and R. Pachter. Journal of Applied Physics 2014, **16**, 115-123.
2. X. Ying Liu, J. Min Zhang. Applied Surface Science 2014, **293**, 216-219.
3. L. Maa, J. Min Zhanga, K. Wei Xuc, V. Ji. Applied Surface Science 2015, **343**, 121-127.
4. H. Luo, Y. Cao, J. Zhou, J. Feng, J. Cao, H. Guo. Chemical Physics 2016, **643**, 27-33.

CHE
-P-
18

The Influence of Silver Cluster Size and Carbon Nanotubes on CO Adsorption: A DFT Study

Chan Inntam[1,C]
[1]*Chemistry Department, Faculty of Science, Ubon Ratchathani University,*
Ubon Ratchathani, Thailand

[C] ***E-mail**: inntam@gmail.com; **Fax**: +66 45299379; **Tel.** +66 45288301*

EXTENDED ABSTRACT

Keywords: Ag cluster, CO adsorption, carbon nanotubes.

INTRODUCTION

Understanding the influence of metal nanoparticles and nanoaggregation is a great deal of current interest. Particularly, the catalytic activity of supported metal nanoparticles depends on the metal–support interaction and metal size. From previous works, it has been suggested that the silver nanoparticles on metal oxides support, e.g. TiO_2, SiO_2 and Al_2O_3, perform highly selective catalytic hydrogenation of crotonaldehyde to the desired unsaturated alcohol products as well as the various types of reactions [1-5]. However, single-walled carbon nanotubes (SWNTs) have also been widely used as a metal supporter in many recent fields due to the great unique properties. The goal of the present work is to identify the interactions of CO molecules on the various sizes of silver nanocluster supported on SWNTs, Ag atom to Ag_4 tetramer. This study is of particular interest as the hybrid metal-SWNTs materials are able to use as gases sensor at low concentration and as a highly efficient catalyst [4-7].

PROPOSED APPROACH

In this work, we used the armchair (5,5) SWNTs as a silver supporter (Ag-Ag_4) for investigating the adsorption of CO molecules. A quantum cluster model consisting of 99 carbon atoms of the SWNTs were applied to represent the bulk nanotube structure. All calculations were performed based on the density functional theory (DFT), employing Becke's three-parameter hybrid exchange functional combined with the Lee, Yang, and Parr correlation functional (B3LYP) [8] implemented in a Gaussian 03 program [9]. The basis sets used in the calculation were 6-31G(d) for C, N, O, S and H atoms. The relativistic effective core pseudopotential of Hay and Wadt functional was employed for Ag atom [10].

RESULTS

In this study, we focus on the energetic and structural properties of CO adsorption on the Ag_n-$C_{99}H_{20}$ cluster models which n = 1-4. Therefore, we have studied the adsorptions of CO molecules in the direction of on-top site of all Ag_n-$C_{99}H_{20}$ complexes. The optimized structures are shown in Figure 1. From our calculated adsorption energies, we found the interaction of CO molecule decreases sharply with increasing the Ag cluster size from 1 to 4 atoms. The corresponding adsorption energies of CO molecules are -18.9, -16.5, -4.8 and -5.8 kcal/mol for Ag-, Ag_2-, Ag_3- and Ag_4-$C_{99}H_{20}$ complexes, respectively. This result is in agreement with the structural property of the adsorption complexes. The Ag-CO distances of those complexes lengthen from 209 pm (Ag-$C_{99}H_{20}$) to 245 pm (Ag_4-$C_{99}H_{20}$) while the C-O bond length shorten slightly, 114.2 pm to 113.7 pm. This result can be explained by the transfer of electron between the adsorbated species and Ag_n-SWNTs, counteracted by the Pauli repulsion. As one can see from the results, the strong metal-metal interaction within the Ag_3 trimer and Ag_4 tetramer causes the weak adsorption of CO molecule. Consequently, the longer Ag-CO distances are observed for the Ag_3-$C_{99}H_{20}$ and Ag_4-$C_{99}H_{20}$ complexes. This interaction mainly contributes to the adsorption energy as well as the most stable geometry. Furthermore, the most stable adsorption complex relevant to other possible sites on the silver metal clusters is being investigated.

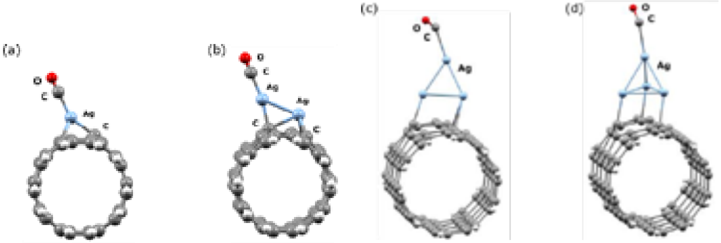

Figure 1. Sketches of the adsorption complexes concerning the CO molecules adsobed on the Ag_n-$C_{99}H_{20}$ cluster model: (a) CO···Ag-$C_{99}H_{20}$ complex, (b) CO···Ag_2-$C_{79}H_{20}$ complex, (c) CO···Ag_3-$C_{99}H_{20}$ complex, (d) CO···Ag_4-$C_{99}H_{20}$ complex.

REFERENCES

1. Peli, S., *et al. J. Phys. Chem. C.* **2016**. *120 (8),* 4673-4681.
2. Baksi, A.; Bootharaju, M.S.; Chen, X.; Hakkinen, H.; Pradeep, T. *J. Phys. Chem. C* **2014**, *118*, 21722−21729.
3. Hirunsit, P., *J. Phys. Chem. C*, **2014**, *118 (15)*, 7996–8006.
4. Perassi, E. M.; Coronado, E. A., *J. Phys. Chem. C* **2013**, *117*, 7744– 7750.
5. De, H. J.; Veldeman, N.; Claes, P.; Janssens, E.; Andersson, M.; Lievens, P. *J. Phys. Chem. A* **2011**, *115*, 2103−2109.
6. Yuan, X.; Luo, Z.; Zhang, Q.; Zhang, X.; Zheng, Y.; Lee, J. Y.; Xie, J. *ACS Nano* **2011**, *5*, 8800−8808.
7. Takei, T.; *et al. Adv. Catal.*, **2012**; *55*, 1–126.
8. Lee, C., Yang, W., Parr, R. G. *Phys. ReV.B* **1988**, *37*, 785−789.
9. Frisch, M. J. T., *et al. Gaussian 03,* revision *E.01*; Gaussian, Inc.: Wallingford, CT, 2004.
10. Hay, P. J., Wadt, W. R. *J. Chem. Phys.* **1985**, *82*, 299−310.

CHE -P- 19

Theoretical Mechanistic Investigation of Au_{20} and $Au_{16}Pd_4$ Catalyzed Aerobic Oxidation of Benzyl Alcohol to Benzaldehyde

Karan Bobuatong[1c]
[1]*Department of Chemistry, Faculty of Science and Technology,*
Rajamangala University of Technology , Pathumthani, Thailand

[C] ***E-mail**: karan_@rmutt.ac.th*

ABSTRACT

Density functional theory calculations have been performed to investigate the reaction mechanisms of the aerobic oxidation of benzyl alcohol to benzaldehyde catalyzed by Au_{20} and $Au_{16}Pd4_2$. Two consecutive reaction mechanisms have been carefully examined: (1) the oxidation of benzyl alcohol with non-dissociated O_2 towards the formation of benzaldehyde and H_2O_2 (2) the formation of benzaldehyde occurred through the reaction between dissociated O_2 and benzyl alcohol. Our calculations show that the aerobic oxidation of benzyl alcohol is energetically preferred to proceed via the latter mechanism which is in agreement with the experimental observations. It is demonstrated that the role of Au involves the activation of molecular oxygen to peroxide-like species which is capable of the H–abstraction of benzyl alcohol. The roles of Pd are directly related in the enhancement of the electron distribution to neighbor gold atoms that facilitates the activation of O_2 as well as significantly enhance the stability of adsorption complex and transition states by the interaction between positively charged Pd atoms of $Au_{16}Pd_4$ and π-bond of benzyl alcohol yielding as a consequence the lower activation barriers than those of Au_{20}.

Keywords: Gold, Palladium, oxidation, ethanol.

REFERENCES

1. Dhital, R. N.; Bobuatong, K.; Ehara, M.; Sakura, H. Chem. Asian. J. 2015, 10 (2015) 2669-2676
2. Bobuatong, K.; Karanjit, S.; Fukuda, R.; Ehara, M.; Sakurai, H. Phys. Chem. Chem. Phys. 2012, 14, 3103–3111.
3. Karanjit, S.; Bobuatong, K.; Fukuda, R.; Ehara, M.; Sakurai, H. Int. J. Quant Chem. 2012, 113, 428–436.
4. Dhital. R. N.; Kamonsatikul, C.; Somsook, E.; Bobuatong, K.; Ehara, M.; Karanjit, S.; Sakurai, H. J. Am. Chem. Soc. 2012, 134, 20250−20253.

CHE -P- 20

Theoretical Study on Carbon-Doped Boron Nitride Nanosheet as a Metal-Free Catalyst for NO Reduction Reaction

Tanabat Mudchimo[1], **Supawadee Namuangruk**[2,C], **and Siriporn Jungsuttiwong**[1,C]
[1]*Department of Chemistry, Faculty of Science, Ubon Ratchathani University,*
Ubon Ratchathani, 34190 Thailand
[2]*NANOTEC, National Science and Technology Development Agency (NSTDA),*
111 Phahon Yothin Rd, Klong Luang, Pathumthani, 12120 Thailand

[C] ***E-mail**: supawadee@nanotec.or.th (S.N.) and siriporn.j@ubu.ac.th (S.J.)*

EXTENDED ABSTRACT

Keywords: NO reduction, Metal-free catalyst, Carbon-doped boron nitride, DFT.

INTRODUCTION

Nowadays, the emission of poisonous gases from the combustion of fuel, vehicles, and industrial processes is considered to be the big environmental issues that must be resolved urgently. Among the poisonous gases, nitrogen oxide (NO) is one of the most prominent pollutants because it has many devastating effects on the atmosphere, ecosystems and human health.[1] Therefore, it is of great importance to reduce or remove NO molecules from the atmosphere. Presently, noble transition metal catalytic materials (such as Pt, Ag, Ru, Rh, Pd, and Au) are the one of most effective and commonly used for NO reduction with high efficiency. However, in term of the high cost, toxicity (from heavy metals) and limited supply about these metals are limited their application uses to some extent. Considering these problems, metal-free catalysts for NO reduction was emerged. Among the metal-free catalysts, hexagonal boron nitride nanosheets (h-BNs) is the one of most commonly used, which exhibits excellent mechanical properties and high thermal conductivity like graphene but with different chemical and physical properties due to the different electronegativity of B and N atoms. For these reasons lead to h-BN structure has more ionic properties, strongly interaction and charge transfer with deposited atoms than graphene.[2] Hence, in this work, we would carry out density functional theory (DFT) calculations to investigate the possible mechanism of NO reduction reaction on CBNs in term of kinetically and thermodynamically favorable via $(NO)_2$ dimer mechanism pathway following equation: $2NO \rightarrow N_2O + O^*$. To the best of our knowledge, all of these possible mechanisms will be study, which may be helpful to fabricate novel and metal-free NO reduction catalysts.

PROPOSED APPROACH

The DFT calculations were performed using the DMol^3 program with the exchange and correlation interactions of PBE functional and DNP basis set to explore the carbon-doped boron nitride nanosheets (CBNs) for NO reduction reaction. On the adsorption part, we have try all possible adsorption site and possible mechanism of NO reduction on C_BBNs and C_NBNs following equation: $2NO \rightarrow N_2O + O^*$. Form this study, we found 5 possible structures namely D1 to D5. In addition, we have studied the influence of charge transfer and adsorption energy of each structure. This current study might be helpful in the development of the new generation of metal-free catalyst for NO reduction with high efficiency, low cost and environmental friendly.

RESULTS

From the results show that all five pathways are exothermic and possible to reduction NO into N_2O gas via dimer mechanism by using a CBNs as a metal-free catalyst. From the comparisons of the five pathways on rate-determining step, we predicted that the mechanism of NO reduction on CBNs will occur via D5 pathway (see **Figure 1.**) with the smallest of rate-determining step of 0.59 eV and high exothermicity with total reaction energies (ΔE_r) of -1.16 eV. Moreover, our results show that the p-type semiconductor material as a C_NBNs show a more excellent efficiency toward catalytic behavior for NO reduction than n-type semiconductor material. Hence, we presented here suggest that C_NBNs can be a metal-free material in NO removal, which will reduce NO into green products with kinetically and thermodynamically.

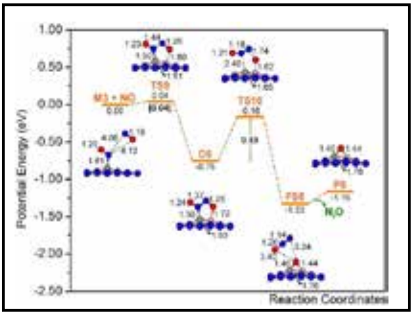

Figure 1. The potential energy profile of NO reduction mechanism on CBNs of D5 systems.

REFERENCES

1. A. Fritz and V. Pitchon, *Appl. Catal. B Environ.*, 1997, 13, 1-25.
2. M. Gao, M. Adachi, A. Lyalin and T. Taketsugu, *J. Phys. Chem. C.*, 2015, 120, 15993-16001.

CHE
-P-
21

Theoretical Study on Olefin Polymerization Catalyst: Half-Titanocenes Containing Aryloxo Ligands

Suppasith Assawabenjang[1], **Pornthep Sompornpisut** [1,C]
[1] *Computational Chemistry Unit Cell, Department of Chemistry, Faculty of Science, Chulalongkorn University, Bangkok, Thailand*

[C] ***E-mail:*** *Pornthep.S@chula.ac.th;* ***Fax:*** *+66 2 218 7598;* ***Tel.*** *+66 2 218 7603*

EXTENDED ABSTRACT

Keywords: Olefin Polymerization, Half-Metallocene Catalyst, Half-Titanocene

INTRODUCTION

In olefin polymerization process, the catalysts exhibiting remarkable activities with better comonomer incorporations are desired. Half-titanocenes are among the group of catalysts that provide this property. In resent computational work, it was showed that comonomer incorporations can be predicted using relative energy barrier of insertion between ethylene and alpha-olefin monomer using a high level method for energy evaluation [1]. However there is no straightforward prediction for the activity term. For nonbridged half-titanocenes, ligand modification is very important to achieve high activities. It was observed that substituents in the 2,6-position of aryloxo ligand are necessary for exhibiting the high activity as well as the Cp* ligand [2]. In this study, our goal is to rationalize the changes in activity for the systems with different ligand structures.

PROPOSED APPROACH

In order to study the effect of ligand, systems differ in ligand structures were set up to calculate the energy barrier of the insertion step, a key step in polymerization that might be RDS. And also the evaluation of conformers' energy after insertion was performed to see the effect of aryloxo ligand. M06-2X hybrid functional, reported to be appropriated for the energy barrier calculation with early transition meal complexes [3], was used in this DFT study. All the DFT calculations were performed with Gaussian 09 software package using M06-2X/6-311+G(2d,p)/LANL2TZ(f)//M06-2X/6-31G(d,p)/LANL2DZ level of theory.

RESULTS

The optimized geometries and energies of different conformation in ethylene binding state were obtained. The free energy barrier of insertion was calculated from the insertion transition state energy and the energy of the most stable ethylene binding conformation. The result showed that the complex with Cp* ligand gives 2.0 kcal/mol lower in energy barrier than one with Cp ligand (2.2 kcal/mol calculated from experiment [4]). While the unwanted beta-hydrogen transfer pathway has relatively much higher energy barrier in both cases. Moreover, the energetic study of models representing the structures after the insertion step gives irrelevant trend to the activity. The calculation result shows that the complexes with no substituent on 2,6-position, which exhibits low activity, give even more stable open conformation than ones having the substituents. This result implied that alkyl chain rotation has minor effect to activity comparing to the insertion barrier.

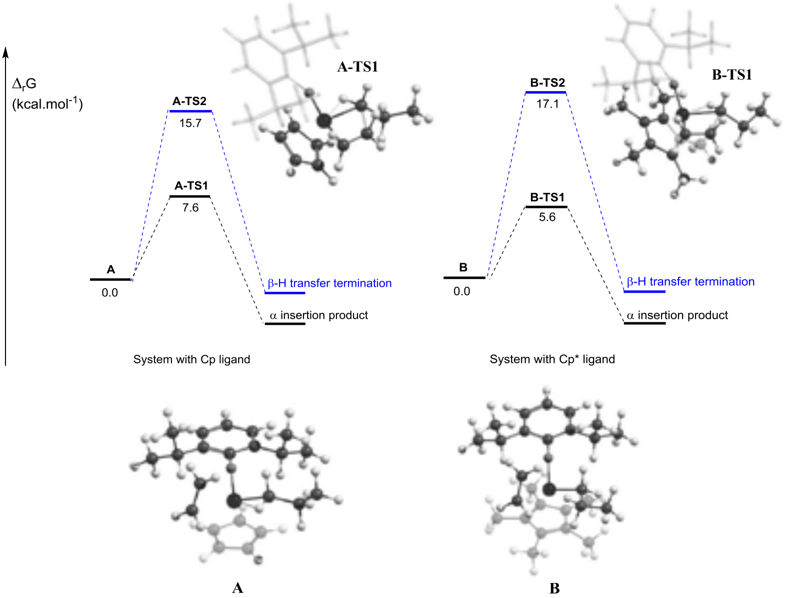
ΔrG
(kcal.mol-1)
A-TS2
15.7
A-TS1
7.6
A
0.0
β-H transfer termination
α insertion product
A-TS1
B-TS2
17.1
B-TS1
5.6
B
0.0
β-H transfer termination
α insertion product
B-TS1
System with Cp ligand
System with Cp* ligand
A
B

Figure 1. Free energy profiles for the ethylene polymerization using half-titanocenes.

REFERENCES

1. Zaccaria, F., et al., *ACS Catalysis*, 2017, **7(2)**, 1512-1519.
2. Nomura, K., J. Liu, *Organometallic Reactions and Polymerization*, Springer Berlin Heidelberg, 2014, 51-88.
3. Ehm, C., P.H.M. Budzelaar, and V. Busico, *Calculating accurate barriers for olefin insertion and related reactions.* Journal of Organometallic Chemistry, 2015. **775**: p. 39-49.
4. Nomura, K., et al., *Macromolecules*, 1998. **31**(22), 7588-7597.

CHE
-P-
22

Warped Nanographene $C_{80}H_{30}$ as a Promising Catalyst for Nitric Oxide Decomposition

Thantip Roongcharoen,[1] Nawee Kungwan,[1,*] Rathawat Daengngern,[2] Chanchai Sattayanon,[1] Supawadee Namuangruk[3,C]
[1] Department of Chemistry, Faculty of Science, Chiang Mai University, Chiang Mai 50200, Thailand
2 Department of Chemistry, Faculty of Science, King Mongkut's Institute of Technology Ladkrabang, Bangkok 10520, Thailand
3 National Nanotechnology Center (NANOTEC), 111 Thailand Science Park, Patumthani 12120, Thailand

[C] ***E-mail***: naweekung@gmail.com , supawadee@nanotec.or.th

EXTENDED ABSTRACT

Keywords: $C_{80}H_{30}$, nanographene, NO decomposition, DFT, reaction mechanism.

INTRODUCTION

The environmental concerns regarding hazardous gases (NO and NO_2) released mainly from various human sources such as vehicles, fossil fuel combustion, and industrial processes have drawn much attention from scientists around the globe. These harmful gases have caused many serious problems to both mankind and environment such as effects on forming tropospheric ozone (ozone in the ambient air that we breathe), powerful greenhouse gas leading to a global warming, environmental damage as acid rain and harmful to the respiratory system of human being. The prevention and sequestration as well as reduction of these gases from releasing into our atmosphere have attracted our concerns. Therefore, it is urgent to develop more effective catalysts for NO_x removal. Different kinds of catalytic materials for NO_x removal have been developed [1]. These include the selective catalytic reduction with ammonia (NH_3-SCR) which has been currently used in industry on NO_x emission control. However, the NH_3-SCR technology has a drawback which requires the additional ammonia from urea to the catalytic converting system from an external source, introducing a high cost into the system. One of the most efficient catalysts for NO decomposition is rare metal catalysts, for example, Pt, Ir, Pd, Ag, Au. Through these metals are very active for NO oxidation with low activation energy, the cost of these metals certainly limit their large-scale applications. Among new developed materials, In year 2013, *Nature Chemistry* [2] has reported an interesting work regarding the synthesis of a warped nanographene ($C_{80}H_{30}$), which has opened an exciting and new avenue for carbonaceous nanomaterial research. The structure of nanographene serves as a model for defects in graphene with distinct electronic and optical properties from carbon nanotubes and a planar graphene sheet [3]. Moreover, Dai et al. used DFT method to study the adsorption of small molecules such as O_2, H_2, CO, NO, NH_3, HCHO and SO_2 on $C_{80}H_{30}$ [4]. They found $C_{80}H_{30}$ can physically absorb NO but, O_2 strongly absorbed on $C_{80}H_{30}$ which is found in dissociative forms on the $C_{80}H_{30}$ resulting in the dramatically change the electronic properties of $C_{80}H_{30}$. The high reactivity of $C_{80}H_{30}$ to O_2 molecule and the electronic change of $C_{80}H_{30}$ after O_2 dissociative adsorption inspired us to investigate the catalytic properties of this warped $C_{80}H_{30}$ nanographene for NO oxidation after O_2 molecule dissociative adsorption on it.

PROPOSED APPROACH

All calculations were performed by Gaussian 09 program package. The density functional theory (DFT) method was applied using B3LYP functional at the 6-31G(d) basis set on all atoms for optimization of the structures of NO, O_2, $C_{80}H_{30}$ as well as the corresponding intermediates and transition states in the reactions. The adsorption energy (E_{ads}) of gas molecules on the ($C_{80}H_{30}$) surface were calculated based on the following expression:

$$E_{ads} = E_{C80H30-gas} - E_{C80H30} - E_{gas}$$

where $E_{C80H30-gas}E_{C80H30-gas}$, $E_{C80H30}E_{C80H30}$, and $E_{gas}E_{gas}$ are the total energy of the $C_{80}H_{30}$-gas adsorption complex, the total energy of $C_{80}H_{30}$ and the total energy of isolated gas molecule, respectively.

RESULTS

The oxygen molecules adsorbed on warped nanographene $C_{80}H_{30}$ is very reactive for NO oxidation in low temperatures suggested by low activation barrier at the rate-limiting step and highly exothermic reaction process. The reaction mechanism consists of three elementary steps; O_2 dissociation, first NO oxidation and second NO oxidation. The O_2 prefers to be dissociated at the central pentagon site of nanographene with the activation energy barrier 26.6 kcal/mol, which is considered as the rate-limiting step of the overall reaction pathway. The charge analysis reveals that charge transfers from nanographene to the dissociated O atoms make them very active to upcoming NO molecules by ER mechanism resulting in the low activation energies for the first NO (barrierless) and second NO (14-16 kcal/mol) oxidations. Desorption of NO_2 product which is the rate-limiting step of NO oxidation in some catalysts, is easily occurred in this nanographene (less than 2 kcal/mol) indicating the prevention of catalyst poisoning for NO removal. This opens a new avenue of using non-metal and non-poising catalyst in air purification technology.

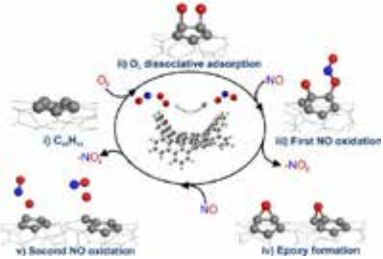

Figure 1. NO oxidation by O_2 dissociation on $C_{80}H_{30}$.

REFERENCES

1. S. Roy, A. Baiker, Chemical Reviews, 109 (2009) 4054-4091.
2. K. Kawasumi, Q. Zhang, Y. Segawa, L.T. Scott, K. Itami, Nat Chem, 5 (2013) 739-744.
3. Y. Dai, Z. Li, J. Yang, Journal of Physical Chemistry C, 118 (2014) 3313-3318.
4. Y. Dai, Z. Li, J. Yang, Carbon, 100 (2016) 428-434.

CHE-P-23

Coarse-Grained Molecular Dynamics Simulation of CorA Magnesium Channel in a Nanodisc

Warin Jetsadawisut[1], **Pornthep Sompornpisut**[1C]
[1] *Computational Chemistry Unit Cell, Department of Chemistry, Faculty of Science, Chulalongkorn University, Bangkok, Thailand*

[C] ***E-mail:*** *Pornthep.S@chula.ac.th;* ***Fax:*** *+66 2 218 7598;* ***Tel.*** *+66 2 218 7603*

EXTENDED ABSTRACT

Keywords: Magnesium channel, CorA, Nanodisc, Coarse-Grained Molecular Dynamics

INTRODUCTION

CorA is Mg^{2+}-dependent gating channels which are primarily found in prokaryotes. It is a homopentameric channel which selectively binds Mg^{2+} and allow its conduction across the membrane [1]. Studies of CorA showed that the channel undergoes conformational transition from the closed to open states upon removal of Mg^{2+} from the divalent-cation-sensor binding site located at the cytoplasmic domain of CorA. Recent, cryo-electron microscopy experiment of CorA reconstituted in lipoprotein nanodisc revealed the asymmetric open conformation, suggesting a break in the symmetry arrangement upon gating. The observation has been supported by chemical cross-linking experiments and electron paramagnetic spectroscopy of spin-labeled CorA [2].

PROPOSED APPROACH

In this study, our goal is to explore structural insight into the conformational rearrangement of CorA underlying gating using molecular dynamics (MD) simulation. For this work, we report a coarse-grained (CG) MD study of CorA magnesium channel to observe a large conformational changes. The structure of the CorA protein in the closed conformation was encapsulated by a lipoprotein nanodisc, a discoidal phospholipid bilayer surrounded by two molecules of membrane scaffold proteins (MSP) [3]. The CG-MD simulations of a nanoparticle assembly have been performed in solution using the NAMD program with the Martini force field.

RESULTS

The CG-MD simulations of Mg^{2+}-free CorA in a MSP nanodisc have been performed up to 3 µs. In the absence of Mg^{2+}, conformational changes of the closed conformation have been observed from the simulation. It appears that one of the five subunits move further away from the central axis of the symmetry while at least the other two subunits move closer to each other. The results suggest an asymmetry in the motion of the pentamer, supporting the gating mechanism model of CorA.

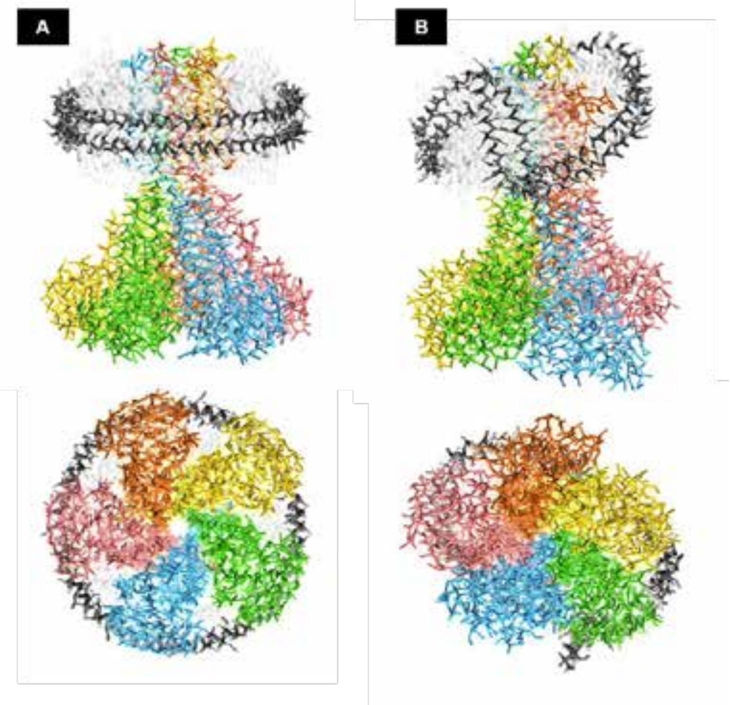

Figure. The MD snapshots of CorA magnesium channel lipoprotein nanodisc (A) at initial time and (B) at t = 2µs

REFERENCES

1. Maguire, M.E., *Magnesium transporters: properties, regulation and structure*. Front Biosci, 2006. **11**: p. 3149-63.
2. Matthies, D., et al., *Cryo-EM Structures of the Magnesium Channel CorA Reveal Symmetry Break upon Gating*. Cell, 2016. **164**(4): p. 747-56.
3. Bayburt, T.H. and S.G. Sligar, *Membrane protein assembly into Nanodiscs*. FEBS Lett, 2010. **584**(9): p. 1721-7.

CHE -P- 24

Computational Docking Study of 4-Oxo-*N*-(2-(Piperidin-1-Yl)Ethyl)-4*H* -Chromene-2-Carboxamide as Acetylcholinesterase and Butyrylcholinesterase Inhibitors

Paptawan Suwanhom[1], Vannajan Sanghiran Lee[2], Teerapat Nualnoi[3], Luelak Lomlim[1,C]

[1] *Department of Pharmaceutical Chemistry, Faculty of Pharmaceutical Sciences, Prince of Songkla University, Hat Yai, Songkhla, 90110, Thailand*

[2] *Department of Chemistry, Faculty of Science, University of Malaya,*
Kuala Lumpur, 50603, Malaysia

[3] *Department of Pharmaceutical Technology, Faculty of Pharmaceutical Sciences, Prince of Songkla University, Hat Yai, Songkhla, 90110, Thailand*

[C] ***E-mail:*** *luelak.l@psu.ac.th;* ***Fax****: +66 74 428 239;* ***Tel.*** *+66 74 288929*

EXTENDED ABSTRACT

Keywords : Acetylcholinesterase inhibitor; Butyrylcholinesterase inhibitor, Computational docking.

INTRODUCTION

Alzheimer's disease (AD) is a major problem in aging society. Lack of acetylcholine (ACh) in the brain is the main hypotheses for the pathogenesis of AD. Acetylcholinesterase inhibitors (AChEIs) have been used for elevating ACh level in the brain of AD patients and alleviate the symtomps but they cannot stop the progress of the disease. Therefore, new anti-AD drug candidates are still needed. Butyrylcholinesterase (BChE) is another cholinesterase found in the peripheral tissues. Inhibition of BChE might result in increased AChE level in the peripheral and subsequently side effects such as nausea and vomitting. Donepezil is a potent and selective AChEI widely used in the clinic. Therefore it is interesting to evaluate selectivity of new AChEIs and study interactions of these ligands with the enzymes in details. Compound 1 is a new, moderately potent AChEI developed in our group [1-3]. In contrast to donepezil, it exhibited less selectivity to AChE as compared to BChE. The IC_{50} values and selectivity index are summarized in Table 1**.** To obtain indept information about interactions between these ligands and the enzymes, which reflects the difference in potency and seletivity of the compounds, computational docking was employed in this study.

Table 1. Acetylcholinesterase and Butyrylcholinesterase inhibitory activities

Compound	IC_{50} ± SEM (*Ee*AChE)	IC_{50} ± SEM (*eq*BChE)	Selectivity* index
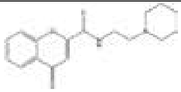 1	3.22 ± 0.12	20.59 ± 1.04	6.39
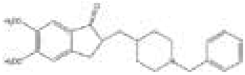 Donepezil	0.006 ± 0.001	1.06 ± 0.01	176.67

* Selectivity index = IC_{50} of *eq*BChE/IC_{50} of *Ee*AChE

PROPOSED APPROACH

Structures of *Tc*AChE and *Hu*BChE (PDB ID: 1EVE and 4BDS) were retrieved from protein data bank. The enzyme was prepared under the protein preparation protocol implemented in Discovery Studio 2.5. PROPKA was used to assign protonation states at pH 7 while the ligands were optimized using density functional theory at B3LYP/6-311G(d,p) level. Molecular docking with AutoDockVina [4] was performed towards the catalytic anionic site (CAS) and peripheral anionic site (PAS) of the enzymes. The residue interaction energy of the docked structure were then analyzed using the Discovery Studio 2.5 with CHARMM force field.

RESULTS

Computational docking revealed that both compounds acted as dual binding site inhibitors which had interactions with various amino acid residues both in the catalytic anionic site (CAS) and peripheral anionic site (PAS) of the enzymes. Compound 1 showed higher total interaction energy than donepezil which indicated that donepezil has a stronger interaction with both enzymes. These findings correlated well with the biological assay results. Total interaction energy values and key interactions between the ligands and the enzymes are summarized in Table 2. However from the structural analysis and interaction with the specific residues in CAS and PAS pockets, compound 1 could bind to both sites with comparable interaction energy towards AChE and BChE and it has less selectivity to AChE as compared to donepezil. This information is valuable for further development of new AChEIs with higher potency and selectivity.

Table 2. Total interaction energy and key enzyme-ligand interactions

Compound	***Torpedo califonica* Acetylcholinesterase (*Tc*AChE) PDB ID : 1EVE**		**Human Butyrycholinesterase (*Hu*BChE) PDB ID : 4BDS**	
	Type of interaction (amino acid residue)	**Total interaction energy (kcal/mol)**	**Type of interaction (amino acid residue)**	**Total interaction energy (kcal/mol)**
1	π-π (Trp278), cation-π (Phe329), Hydrophobic (Phe330)	-98.79	Hydrogen bond (Ser195, His433)	-72.40
Donepezil	π-π (Trp83), π-π (Trp278), Cation-π (Phe329), Hydrophobic (Phe330)	-119.63	π-π (Trp79), Hydrophobic (Tyr329)	-102.80

REFERENCES

1. Ellman, G., Courtney, K., Andres, V., and Featherstone R., *Biochem Pharm*, 1961, **7**(2), 88-95.
2. Gitay, K., Israel, S., Sussman, J.L., *Structure*, 1999, **7**(3), 297-307.
3. Liu, Q., Qiang, X., Li, Y., Sang, Z., Li, Y., et al., *Bioorg Med Chem*, 2015, **23**(5), 911-923.
4. Trott, O., and Olson, A.J., *J.Comput. Chem,* 2010, **31**(2), 455-461.

CHE -P- 25

Dimer Structure Stabilization of H_v1 C-terminal Domain by Salt Bridge Movements

Panisak Boonamnaj[1] **and Pornthep Sompornpisut** [1,C]
[1] *Department of Chemistry, Faculty of Science, Chulalongkorn University,*
Bangkok, Thailand

[C] ***E-mail**: Pornthep.S@chula.ac.th;* ***Fax**: +66 2 218 7598;* ***Tel.** +66 2 218 7604*

EXTENDED ABSTRACT

Keywords: Hv1, C-terminal domian, MD simulation.

INTRODUCTION

Voltage-gated proton-selective channel (H_v1) is a protein that allows protons (H^+) transport across cell membranes. H_v1 has known as a homodimer molecule buried in phospholipid bilayer[1]. C-terminal domain of H_v1, which is coiled-coil helix structure, is believed that may relate to structural stability and dimer assembly[2]. Here, we examined the contribution of the salt bridge pairs (E235 and K230) on C terminus affected dimer stabilization using MD simulations in a variation of pH and temperature.

PROPOSED APPROACH

MD simulations were performed with NAMD using the CHARMM27 force field. C-terminal domain of mH_v1cc crystal structure was used. Simulation systems were prepared with VMD. Ionization states of side chains were assigned based on pK_a using PROKA software. The protein was embedded in 100 mM NaCl solutions with TIP3P for water. Harmonic constraints were applied to I214 residues to maintain the dimer structure. Cut-off range of 12 Å was used for both of electrostatic interactions and van der Waals interactions. Langevin dynamics was employed for constant temperature.

RESULTS

At 298 K, salt bridge pairs of C-terminal domain (Figure 1.) showed the movements which may stabilize dimer structure and two subunits still held even at higher temperature (353 K). However, the structure is more energetically favorable at pH 4 than 7 form total solvation energy profiles. The helix-helix interactions of C-terminal domains are temperature- and pH-dependent manners.

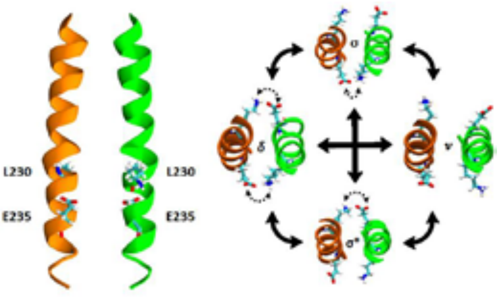

Figure 1. **Dimer structure of mHv1cc C-terminal domain and salt bridge movements. Conformation states of salt bridge pairs are labeled as follows: non-interacting pairs (ν), single-interacting pairs (σ,σ*) and double-interacting pairs (δ). Each can change to other as indicated with the solid arrows and the dash arrows denote the interacting pair of salt bridges.**

REFERENCES

1. DeCoursey, T.E., *Physiol. Rev.*, 2013, **93**(2), 599-652.
2. Fujiwara, Y., Kurokawa, T., Takeshita, K., Kobayashi, M., Okochi, Y., Nakagawa, A., Okamura, Y., *Nat. Commun.*, 2012, **3**, 816.

CHE
-P-
26

Enhanced Stability of Inclusion Complexes of Alpha-Mangostin with Hydrophilic Beta-Cyclodextrin; a Molecular Dynamics Simulation Study

Wiparat Hotarat[1], Saranya Phunpee[2], Chompoonut Rungnim[2], Peter Wolschann[3,4], Nawee Kungwan[5], Uracha Rukta Ruktanonchai[2], Thanyada Rungrotmongkol[6, 7], Supot Hannongbua[1, C]

[1]Computational Chemistry Unit Cell, Department of Chemistry, Faculty of Science, Chulalongkorn University, Bangkok 10330, Thailand
[2]National Nanotechnology Center (NANOTEC), Pathumthani, 12120 Thailand
[3]Department of Pharmaceutical Technology and Biopharmaceutics, University of Vienna, Vienna 1090, Austria
[4]Institute of Theoretical Chemistry, University of Vienna, Vienna 1090, Austria
[5]Department of Chemistry, Faculty of Science, Chiang Mai University, Chiang Mai 50200, Thailand
[6]Ph.D. Program in Bioinformatics and Computational Biology, Faculty of Science, Chulalongkorn University, Bangkok 10330, Thailand
[7]Department of Biochemistry, Faculty of Science, Chulalongkorn University, Bangkok 10330, Thailand

*[C] **E-mail**: supot.h@chula.ac.th; **Fax**: +66 2 218 7603; **Tel.** +66 8 1636 1975*

EXTENDED ABSTRACT

Keywords: Computational Science, Computational Conferences.

INTRODUCTION

Alpha-mangostin (αMGS), a traditional Thai medicine, is commonly used to treat skin inflections, diarrhea, and chronic wounds[1,2]. Its low solubility and stability lead to limitations in its pharmaceutical applications. Inclusion complexes with cyclodextrins (CDs) are well-known to enhance properties of hydrophobic compound[3,4]. In this study, both theoretical and experimental studies were applied to investigate the inclusion complexes between αMGS and beta-cyclodextrin (βCD) as well as its derivatives: 2,6-dimethyl-βCD (2,6-DMβCD), 2-hydroxypropyl-βCD (2-HPβCD), 6-hydroxypropyl-βCD (6-HPβCD), and 2,6-dihydroxypropyl-βCD (2,6-DHPβCD). The structural orientation, host-guest interaction and binding affinity of αMGS in the hydrophobic cavity of CDs as well as the solubility of inclusion complexes were focused upon in this work.

PROPOSED APPROACH

The starting conformations of αMGS were prepared by ab initio calculation using HF/6-31(d) in the Gaussian09 program. To predict the inclusion complex with CDs and its derivatives, each conformation of αMGS as a guest molecule was docked with 500 independent structures using the CDOCKER module in Accelys Discovery Studio Visualizer 3.0 program. Molecular dynamics (MDs) simulations were performed by the Amber 12 software package with the Glycam-06 bimolecular force field. The solubilities of the inclusion complexes were described by the Higuchi and Connors method.

RESULTS

From the MM-PBSA/GBSA calculations, it can be suggested that the van der Waals interaction is the main driving force of the inclusion complexes. The binding free energies of all inclusion complexes were ordered as 2,6-DHPβCD > 6-HPβCD > 2,6-DMβCD > 2-HPβCD > βCD, respectively. These results are in good agreement with the phase-solubility study that suggested that the complex formation between αMGS and DMβCD were more favorable than HPβCD and native βCD. From both theoretical and experimental results, the predicted binding free energy indicated that the βCD-derivatives (methyl and hydroxypropyl groups) can promote the stability of the inclusion complexes.

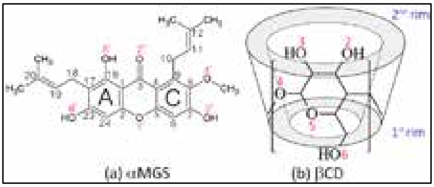

Figure 1. The chemical structure of (a) alpha-mangostin (αMGS) and (b) beta-cyclodextrin (βCD)

REFERENCES

1. Mahabusarakam, W., P. Wiriyachitra, and W.C. Taylor, *Chemical Constituents of Garcinia mangostana.* Journal of Natural Products, 1987. **50**(3): p. 474-478.
2. Nakatani, K., et al., *Inhibition of cyclooxygenase and prostaglandin E2 synthesis by gamma-mangostin, a xanthone derivative in mangosteen, in C6 rat glioma cells.* Biochem Pharmacol, 2002. **63**(1): p. 73-9.
3. Brewster, M.E. and T. Loftsson, *Cyclodextrins as pharmaceutical solubilizers.* Advanced Drug Delivery Reviews, 2007. **59**(7): p. 645-666.
4. Liu, L. and Q.-X. Guo, *The Driving Forces in the Inclusion Complexation of Cyclodextrins.* Journal of inclusion phenomena and macrocyclic chemistry, 2002. **42**(1): p. 1-14.

CHE
-P-
27

MD Simulation of M2 Proton Channel in Different Phospholipid Bilayer Models

Channarong Khrutto[1], **and Pornthep Sompornpisut** [1,C]
[1] *Department of Chemistry, Faculty of Science, Chulalongkorn University, Bangkok, Thailand*

[C] ***E-mail**: pornthep.s@chula.ac.th;* ***Fax**: +66 2 218 7598;* ***Tel.** +66 2 218 7604*

EXTENDED ABSTRACT

Keywords: M2 protein channel, Influenza A virus, molecular dynamics simulation

INTRODUCTION

The M2 channel from influenza A virus is pH-gated proton channels found in the viral lipid envelope. The M2 channel plays an essential role in the viral life cycle. The channel is a homotetramer with 97-amino-acid residues per subunit. Each chain consists of an extracellular N-terminal domain, a single transmembrane segment and an intracellular C-terminal domain. Studies of M2 showed the channel exhibits various conformations depending on the use of different membrane models, including detergent micelles and membrane bilayers. Here, we examined the conformation of the M2 protein channel using MD simulation with different phospholipid models.

PROPOSED APPROACH

Simulation systems were prepared by following a standard protocol for membrane protein tutorial with the VMD program. Initially, the formation of M2 tetramer was constructed using the NMR solution structure, solvated in a hydrated phospholipid bilayer and neutralized with 0.1M NaCl solution. In this study we used two phosphocholine lipids with different acyl chain length that are 1-palmitoyl-2-oleoyl-sn-glycero-3-phosphocholine (POPC) and 1,2-dilauroyl-sn-glycero-3-phosphocholine (DLPC). MD simulations were performed by NAMD using the CHARMM27 force field in 100 ns with Cut-off range 12 angstroms.

RESULTS

The MD simulation of M2 in POPC bilayer showed the stability of the channel. During the course of the simulation, the arrangement of the tetramer structure remained significantly unchanged with respect to the starting structure. On the other hand, a significant change in the orientation of transmembrane helices of M2 has been observed from the MD simulation of M2 in DLPC bilayer, a lipid with a shorter acyl chain. In this simulated system, the effect of hydrophobic mismatch is clearly seen by a large tilt of transmembrane helices. The results are consistent with a reduction of spin-spin coupling observed from an EPR study of spin-labeled M2.

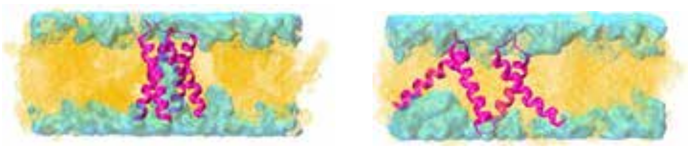

(a.) POPC (b.) DLPC

Figure 1. Conformation of M2 protein channel in POPC and DLPC

REFERENCES

1. Krisna C. Duong, Vikas Nanda, William F. Degrado, and Kathleen P. Howard, *Protein Scince*,2005,**14**,856-861.
2. Kei Saotome, Krisna C. Duong-Ly, Kathleen P. Howard ,*Peptide Scince*,2015,**104** 405-411.

CHE -P- 28	Millisecond Protein Dynamics Does Not Control Catalysis in Cyclophilin A – Evidence from Molecular Dynamics Simulations

Pattama Wapeesittipan[1,C], **Antonia Mey**[1], **and Julien Michel**[1]
[1] *EaStCHEM School of Chemistry, University of Edinburgh, EH9 3FJ, UK*

[C] ***E-mail**: s1467112@sms.ed.ac.uk email; **Tel.** +44 7 879720224*

EXTENDED ABSTRACT

Keywords: Cyclophilin A, Molecular dynamics, Protein dynamics, Catalysis.

INTRODUCTION

Cyclophilin A is member of the Cyclophilin family of peptidyl-prolyl isomerases which catalyzes the *cis-trans* isomerization of proline peptide bond. Previous biophysical studies have suggested that the CypA wild type (WT) active site interconverts between a 'major' catalytically active conformation and a 'minor' catalytically impaired conformation on millisecond timescales.[1] A serine to threonine (S99T) mutation distal (ca. 10 Å away) from the active site was devised to stabilize this minor conformation of CypA, leading to a dramatic 70 fold drop in catalytic turnover, similar in magnitude to activity changes upon mutation of key residues that make direct contacts with the substrate.[2] Although such example is frequently cited in support of the importance of millisecond dynamics for enzymatic function, the details of how the S99T mutation reduces catalytic activity are still unclear.

PROPOSED APPROACH

One way to obtain the free energy profile is to calculate the probability of state sampled during the MD simulation. However, classical MD simulation can only sample the configuration around local minimum and rarely sample at higher energy or other local minimum with high energy barrier. Therefore, the accelerated sampling methods have been applied to obtain free energy profile for all region of reaction coordinate. Umbrella sampling is the biased molecular dynamics for enhanced sampling of rare states to obtain free energy along a reaction coordinate.

In this research, molecular dynamic (MD) and biased MD simulations were carried out to investigate the link between conformational changes and catalysis in the WT and S99T mutant forms of CypA.

RESULTS

In the present study, we observe conformational changes between the proposed 'major' and 'minor' active site conformations on nanosecond timescales. Yet in agreement with previous experimental data, free energy profiles from our simulations showed that the S99T CypA-catalyzed amide isomerization reaction has a larger activation barrier than in WT CypA. Further analysis indicates that this is a result of weakened hydrogen bonding interactions between Asn102 and the transition state. Additional simulations established that weakened transition state stabilisation is caused by an overall increase in fast (nanosecond) dynamics of active site residues due to poorer side-chains packing in the S99T mutant.

In summary, our study disputes literature claims of a link between slow (millisecond) protein dynamics and catalysis,[1] and suggests instead that changes in fast (nanosecond) dynamics are sufficient to explain the reduced catalytic power of the S99T Cyclophilin A mutant.

REFERENCES

1. Eisenmesser, E. et al. *Nature*, 2005, **438**, 117-121.
2. Fraser, J. S. *et al. Nature*, 2009, **462**, 669-673.

CHE
-P-
29

Molecular Calculations on Host-Guest Inclusion Complexes of Natural Insecticides: Squamocin and Nicotine

Theerayut Khempach[1], **Phiraphol Nonsathaporn**[1], **Watcharapong Udomsinca**[1],
Luckhana Lawtrakul[1,C]
[1]*School of Bio-chemical Engineering and Technology,*
Sirindhorn International Institute of Technology, Thammasat University, Thailand

[C]***E-mail**: luckhana@siit.tu.ac.th*; ***Tel**: +66-2-986-9009*

EXTENDED ABSTRACT

Keyword: Molecular modeling, Host-guest chemistry, Natural insecticide

INTRODUCTION

Squamocin ($C_{37}H_{66}O_7$) and nicotine ($C_{10}H_{14}N_2$), two natural insecticides, which mainly extracted from the custard apple seeds and tobacco, respectively, are reported to be effective in controlling some tick parasites [1-2]. The main problem is these two compounds have very low environmental persistence. Therefore, we would like to use the encapsulation techniques to preserve the quality of them, enhance shelf lifetime as well as stability improvement without changing their chemical properties. In order to find the compatibility host molecule for Squamocin and Nicotine to form the host-guest inclusion complexes, quantum chemistry and molecular docking calculations are used to establish the molecular model between Squamocin and Nicotine (guests) and some common host molecules such as cyclotriveratrylene [3], calixarenes [4], and cyclodextrins [5]. Thermodynamics properties and molecular interactions are discussed in detail for further development the formulation of inclusion complexes of these two natural insecticides.

PROPOSED APPROCHED

The molecular docking is used to predict the compatibility of Squamocin and Nicotine with the hosts in order to make host-guest interaction or the inclusion complexes. Five common hosts have been used in this study: (i) Beta-cyclodextrin or BCD, (ii) Gamma-cyclodextrin or GCD, (iii) Cyclotriveratrylene or CTV, (iv) Calix[6]arene, and (v) Calix[8]arene. The ratio used between host and guest is 1:1 the method used for calculating the complexes' binding energy is semi-empirical PM3.

RESULTS

The binding energy of Squamocin and Nicotine inclusion complexes with five host molecules are calculated by the following equation:

$$\Delta E = E_{\text{inclusion}} - (E_{\text{host}} + E_{\text{guest}})$$

where ΔE is Binding energy,
$E_{inclusion}$ is Energy of inclusion complex,
E_{host} is Energy of host molecule,
E_{guest} is Energy of guest molecule.

As shown in Table 1, Squamocin and Nicotine have the most compatibility with BCD due to the lowest binding energy. The conformations and the host-guest molecular interactions in each of inclusion complex systems are further discussed in detail.

Table.1 The binding energy results from PM3 calculations.

Host-Guest Complex	**ΔE (kcal/mol)**
BCD/Squamocin	-21.55
GCD/Squamocin	7.44
CTV/Squamocin	-23.44
Calix[6]arene/Squamocin	-5.31
Calix[8]arene/Squamocin	-14.41
BCD/Nicotine	-13.48
GCD/Nicotine	24.32
CTV/Nicotine	-6.32
Calix[6]arene/Nicotine	3.72
Calix[8]arene/Nicotine	-3.31

REFERENCES

1. Smith, R.E., Tran, K., Shejwalkar, P., and Hara, K. *Austin Neurol & Neurosci.* 2016, **1**(1), id1005, (8 pages).
2. Isman M. B., and Seffrin, R., "Natural insecticides from the Annonaceae: a unique example for developing biopesticides," in *Advances in plant biopesticides*, ed: Springer, 2014, 21-33.
3. Hardie, M. J. "Cyclotriveratrylene and Cryptophanes," *Supramolecular Chemistry: From Molecules to Nanomaterials*., 2012., DOI: 10.1002/9780470661345.smc053
4. Y. Agrawal, J. Pancholi, and J. Vyas, "Design and synthesis of calixarene," *Journal of scientific and industrial research,* 2009, **68**, 745-768.
5. A. Magnusdottir, M. Másson, and T. Loftsson, "Self association and cyclodextrin solubilization of NSAIDs," *Journal of inclusion phenomena and macrocyclic chemistry,* 2002, **44**, 213-218.

ACKNOWLEDGEMENT

The authors gratefully acknowledge the financial support provided by Thammasat University Research Fund under the TU Research Scholar, Contract No. TP 2/21/2559.

**CHE
-P-
30**

Molecular Docking Study of WR99210 Analogues as Novel *M. tuberculosis* DHFR Inhibitors

Nattaya Mekjirawat[1], Patcharapon Praserth[1], Atcharapun Chockborvornpaisan[1], Suriyawut Kulatee[1], and Luckhana Lawtrakul[1,C]
*[1]School of Bio-Chemical Engineering and Technology,
Sirindhorn International Institute of Technology, Thammasat University
P.O. Box 22, Thammasat Rangsit Post Office, Pathum Thani 12121, Thailand*

[C] ***E-mail***: *luckhana@siit.tu.ac.th*

EXTENDED ABSTRACT

Keywords: Binding energy, Inhibition constant, Ligands-Protein Interaction.

INTRODUCTION

Tuberculosis (TB) is a disease which mostly caused by *M. tuberculosis*. Patients who are infected with TB need a prescribed medical treatment. However, estimated 9 million new TB cases had occurred globally, and more than 480,000 cases of multidrug-resistant (MDR) occur every year which 9% of them are affected by extensively drug-resistant (XDR) in 2015. Therefore, the development of new drug is urgently needed. Dihydrofolate reductase (DHFR) is an enzyme that reduces dihydofolate to tetrahydofate. The derivatives of tetrahydofate are essential for the cell proliferation and cell growth. According to the function of DHFR, it is reasonable to presume that DHFR of pathogenic organism could be a good target for drug. Hence, *M. tuberculosis* dihydrofolate reductase (mtbDHFR) is the selected drug target for this study. In this work, molecular modelling approach is used to investigate the interaction between mtbDHFR and WR99210 analogues. Molecular docking is applied to dock all analogues into the active site of mtbDHFR. The results are summarized to provide the characteristic of effective inhibitors for mtbDHFR, which leads to the development of new anti-tuberculosis drug.

PROPOSED APPROACH

The WR99210 analogues were used to inhibit mtbDHFR. The binding energy was used to determine the effectiveness of inhibitors. The initial structures of WR99210 analogues [1] against the *M. tuberculosis* were built using GaussView 5.0.8 and the geometry optimizations were performed using Gaussian 09 program at HF/6-31G (d,p) level of calculations. The crystal structure of mtbDHFR (PDB code 1DG7) [2] complexes with NADPH and 4-bromo WR99210 is provided in RCSB protein data bank. Discovery Studio Visualizer 4.0 was applied to remove ligands and water molecules from the crystal structure. Finally, the hydrogen atoms were added to the mtbDHFR enzyme.

Molecular docking of 1DG7 mtbDHFR with inhibitors was performed using Autodock 4.2.6 software package. The protein was fixed as a rigid molecule (protein) while the rotatable bonds within the inhibitors molecules (ligand) were allowed to be flexible during the docking simulation. One-hundred runs of docking were performed by using the Lamarckian Genetic Algorithm. The centre of grid box on the binding pocket located at the same binding site of 4-bromo WR99210 in crystal structure with a grid spacing of 0.375 Å. The number of points was set as 46 points in each of three dimensions. The conformation with lowest binding energy and highest frequency from molecular docking calculations were chosen for further analysis.

RESULTS

Table 1. Structures and relative potencies of the WR99210 series of compounds against the *M. tuberculosis dfrA* gene tested in yeast [1]. Binding energy (B.E.) and inhibition constant (K_i) from molecular docking calculations.

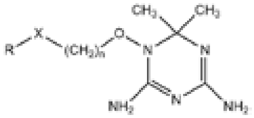

No.	R	X	n	Potency	B.E. (kcal/mol)	K_i (nM)
1	2,4,5-Trichlorophenyl (WR99210)	O	3	+ +	-9.20	180.16
2	2,4-Dichlorophenyl	O	3	+ +	-9.35	139.86
3	1-Naphthyl	O	3	+ +	-9.30	152.18
4	4-Bromophenyl	O	3	+ +	-9.44	120.15
5	3,4-Dichlorophenyl	O	3	+ +	-9.40	128.54
6	1-(4-Chloronapthyl)	O	3	+ +	-9.88	57.17
7	4-*t*-Butylphenyl	O	3	+ +	-9.66	82.88
8	2-(6-Bromonapthyl)	O	3	+	-10.07	41.48
9	4-Methoxyphenyl	O	3	+	-8.85	325.27
10	4-Chlorophenyl	O	3	+	-9.27	160.08
11	2-Naphthyl	O	3	+	-9.79	66.55
12	4-Nitrophenyl	O	3	-	-8.73	398.30
13	4-Chlorophenyl	CH_2	3	-	-9.43	122.19
14	4-Fluorophenyl	S	3	-	-8.71	411.97
15	2,4,5-Trichlorophenyl	O	2	-	-9.03	240.04
16	4-Chlorophenyl	SO_2	3	-	-8.35	756.45
17	4-Fluorophenyl	O	3	-	- 8.58	513.06
18	4-Chlorophenyl	O	4	-	- 9.02	244.13
19	3,4-Dichlorophenyl	CH_2	0	-	- 8.73	398.30

As shown in Table 1, the B.E. and the K_i values obtained from molecular docking are relatively consistent with the previous experimental results from the laboratory [1]. Our approach can classify the WR99210 series of compounds to be the effective compounds (No.1-8, 10-11, and 13) with K_i lower than 181 nM and non-effective compounds (No.9, 12, and 14-19) with K_i greater than 181 nM. However, there have a small differ due to the experiment potency data obtain from an engineered strain of the budding yeast but our docking calculation we used the crystal structure of mtbDHFR. The lower in B.E., the fewer of K_i values indicate the stronger binding affinity of compound on mtbDHFR. Our results indicate compound No.8 is the most effective inhibitor with K_i 41.48 nM. This molecule composes of 2-(6-Bromonapthyl) group at R position, three carbon atoms at the carbon linkage chain, and oxygen atom at X position. The detail of protein-ligand interactions have been also identified.

REFERENCES

1. A'Lissa, B. Gerum, et al. "Novel Saccharomyces cerevisiae screen identifies WR99210 analogues that inhibit Mycobacterium tuberculosis dihydrofolate reductase." *Antimicrobial agents and chemotherapy* 46.11 (2002); 3362-3369.
2. Li, Rongbao, et al. "Three-dimensional structure of M. tuberculosis dihydrofolate reductase reveals opportunities for the design of novel tuberculosis drugs." *Journal of molecular biology* 295.2 (2000): 307-323.

CHE -P- 31

Structure Based Drug Design of 4-Aminoquinilone Derivatives in DNA Gyrase B Subunit for Anti-Tuberculosis Agents Using Molecular Dynamic Simulations

Naruedon Phusi[1], Chayanin Hanwarinroj[1], Kampanart Chayajaras[1], Nitima Suttipanta[2], Pharit Kamsri[3], Auradee Punkvang[3], Khomson Suttisintong[4], Patchareenart Saparpakorn[5], Supa Hannongbua[5] and Pornpan Pungpo [1,C]

[1] *Department of Chemistry, Faculty of Science, Ubon Ratchathani University,85 Sthollmark Rd., Warinchamrap, Ubonratchathani, 34190, Thailand*
[2] *Faculty of Pharmaceutical Science, Ubon Ratchathani University,85 Sthollmark Rd., Warinchamrap, Ubonratchathani, 34190, Thailand*
[3] *Faculty of Science, Nakhon Phanom University, Nakhon Phanom, 48000, Thailand*
[4] *National Nanotechnology Center, 114 Thailand Science Park, Pathumthani, Thailand*
[5] *Department of Chemistry, Faculty of Science, Kasetsart University, Chatuchak, Bangkok, 10900, Thailand*

[C] *E-mail: pornpan_ubu@yahoo.com; Fax: + 66(45) 288 379; Tel. + 66(45) 353401-4 Ext.4124*

EXTENDED ABSTRACT

Keywords: 4-Aminoquinoline derivatives, GyrB, anti-TB agents, MD simulations.

INTRODUCTION

Tuberculosis (TB), caused by *Mycobacterium tuberculosis* (*M. tuberculosis*), remains a major global health problem. In 2016, an estimated 9.6 million people developed TB and 1.8 million died from the disease [1]. The clinical efficacy of fluoroquinolone drugs demonstrated over the past 20-30 years has validated DNA gyrase as a target in the area of broad-spectrum antibacterials [2]. Gyrase A subunit has been facing a major hurdle of their resistance developed by *M. tuberculosis* which makes gyrase B subunit a drug able target for discovery of potent anti-tuberculosis agents. DNA gyrase B subunit is involved in the process of ATP hydrolysis which in turn provides energy to gyrase A subunit for maintaining the DNA topological state [3]. So, GyrB has been genetically demonstrated to be a bactericidal drug target in *M. tuberculosis*, but there have not been any effective therapeutics developed against this target for TB [4]. Recently 4-aminoquinoline derivatives have been developed as anti-tuberculosis agents with moderate biological activities against *M. tuberculosis* and XDR *M. tuberculosis* [5]. Therefore, MD simulations approaches have been used to understand dynamic be heavier and the structural requirements of these derivatives. The obtained results showed aid to design new and more potent anti-tuberculosis agents.

PROPOSED APPROACH

The chemical structures and their experimental biological activities of 4-aminoquinoline derivatives were selected from the literature [5]. The biological activities of these compounds were expressed in terms of *Msm*GyrB assay (IC_{50} in μM) values. The chemical structures of these inhibitors were constructed using the standard tools available in GaussView 3.07 program and were then fully optimized using the HF/6-31G* method implemented in Gaussian 09 program. The initial coordinates for MD simulations of the complexes was obtained from molecular docking calculations using

Autodock 3.05 program. MD simulations were performed to predict the inhibitors in the GyrB binding pocket (PDB Code: 4B6C). TIP3P water model and Na^+ were chosen to represent water for salvation and ions for neutralize system. The root-mean square deviations (RMSDs) of the GyrB enzyme and the inhibitors, binding interactions were analyzed based on the equilibrium state obtained. The binding free energies were calculated to evaluate the binding affinities of inhibitors in GyrB binding pocket using the Molecular Mechanics Poisson-Boltzmann Surface Area (MM-PBSA) [6-9] and Normal-mode [10] methods.

RESULTS

In order to determine structural stability during MD simulation of the highest active compound in GyrB binding pocket, the RMSDs for all atoms of solute species relative to the initial structure over the 15 ns of simulation times were calculated and plotted in Figure 1 (a). The plateau characteristic of the RMSD plot over the simulation time is the criteria to indicate the equilibrium state of each solute species. Convergent RMSD plots indicate that the equilibrium state of the highest active compound was reached after 6 ns. The binding mode of the highest active compound is presented in Figure 1 (b). The hydrogen bond interaction between oxygen atom of methoxyl ($-OCH_3$) with Asn16 of DNA gyrase B subunit. Moreover, hydrophobic interactions with Arg46, Gly47, Val63 and Ile115 of DNA gyrase B. To gain quantitative insights into the affinity for binding of 4-aminoquinoline inhibitors in the GyrB binding site, the binding free energies of 4-aminoquinoline/GyrB complexed were calculated by the MM-PBSA method is -8.400 kcal/mol. It is notable that the calculated free binding energies of inhibitor are in the correct order as compared with the IC_{50} values. The obtained results could be successfully used to validate the MD procedure in this study.

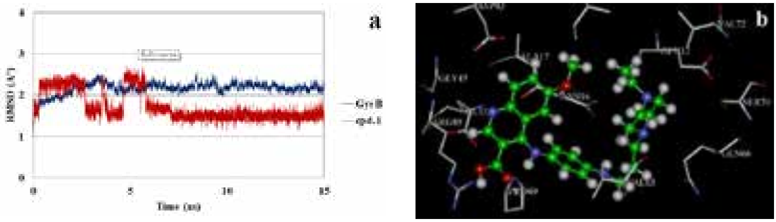

Figure 1. RMSD plots of compound with GyrB (a) and binding mode of compound in GyrB binding pocket derived from MD simulations (b).

REFERENCES

1. World Health Organization, Global tuberculosis report 2016, http://www.who.int /tb/publications/global_report/gtbr16_main_text.pdf
2. MaxwellA.1997. DNA gyrase as a drug target. Trends Microbiol.5:102-109. http://dx.doi.org/10.1016/S0966-842X(96)10085-8.
3. Lewis R.J., Singh O.M., Smith C.V., Skarzynski T., Maxwell A., Wonacott A.J., Wigley D.B., J.EMBO., 1996, **15**, 1412-1420.
4. Kaur P., Agarwal S., Datta S., PLoS One 2009, **4**, 5923.
5. Medapi B., Suryadevara P., Renuka J., Sridevi J. P., Yogeeswari P., Sriram D., J.Med.Chem., 2015, **103**,1-16.
6. Homeyer N., Gohlke H., Mol. Inf., 2012, **31**, 114–122.

7. Wang J., Hou T., Xu X., Curr Comput Aided Drug Des, 2006, **2**, 95-103.
8. Wang J., Morin P., Wang W., Kollman P.A., J. Am Chem Soc., 2001, **123**, 5221-5230.
9. Hou T., Wang J., Li Y., Wang W., J. Chem Inf Model, 2011, **51**, 69–82.
10. Kaledin M., Brown A., Kaledin A.L., Bowman J.M., J. Chem Phys, 2004, **121**, 5646-5653.

CHE-P-32

A Data Mining Approach to Determine the Hindered Internal Rotational Frequency for Chemical Species

Triet H. M. Le[1], **Tung T. Tran**[1], **and Lam K. Huynh**[2,C]
[1] *School of Computer Science and Engineering, International University –*
Vietnam National University, Ho Chi Minh City, Vietnam,
Quarter 6, Linh Trung Ward, Thu Duc District, HCMC, Viet Nam, 700000
[2] *School of Biotechnology, International University – Vietnam National University, Ho Chi Minh City,*
Vietnam, Quarter 6, Linh Trung Ward, Thu Duc District, HCMC, Viet Nam, 700000

[C] ***E-mail**: hklam@hcmiu.edu.vn, lamhuynh.us@gmail.com; **Fax**: (84-8) 3724.4271;*
***Tel.** (84-8) 2211.4046 (Ext. 3233)*

EXTENDED ABSTRACT

Keywords: Computational Chemistry, Data Mining, Machine Learning, Classification, Hindered Internal Rotation

INTRODUCTION

In order to obtain reliable thermodynamic properties for chemical species, special treatments beyond the harmonic vibrational approximation for the possible internal rotors are needed. A rigorous treatment for the internal rotors was proposed by Mai and co-workers [1]. Such an approach requires detailed information about the rotor namely rotational axis, group, frequency, symmetry and hindrance potential. However, it is complicated and troublesome for chemists, even experts, to obtain those parameters correctly. Recently, there has been an effort to help the chemists with this tedious process [2]. In this work, one of the most significant contributions is the algorithm to assign the correct rotational frequency to the rotors. Apparently, it has been demonstrated to work well for simple cases. However, due to its dependence on some predefined rules, the algorithm had difficulty handling more complex species. Furthermore, the most optimal frequencies are to select from a list of all possible vibrational modes of a molecule, which can be categorized as a binary classification problem. Therefore, in this study, we propose a more flexible approach to work with a wider range of cases thanks to the support of data mining. Such idea is possible thanks to adaptive learning pattern unveiled from regularly updated data. We conducted some experiments with the pre-processed dataset using several machine learning algorithms. The results were found to be promising for different types of chemical systems. This study also sheds light on the usefulness of data mining in other fields of computational science.

PROPOSED APPROACH

The essence of our approach is the use of data mining which allows evolutionary capability (cf. Figure 1). Firstly, our proposed solution preprocesses the electronic structure calculation data of the chemical species produced by an electronic structure program (e.g., GAUSSIAN). More specifically, based on both domain knowledge and expert's experience, the system extracts requisite raw data features for the detection of the rotational frequency. We then clean, integrate and transform the raw data to prepare the dataset for the subsequent classification process. After that, we select the most optimal classification algorithms based on the pre-defined training dataset and 10-fold cross-validation technique. Such model is used to automatically predict the best choices of rotational frequency for each rotor. Finally, the result is provided to the chemists/users in MSMC-GUI (i.e., Graphical User Interface of Multi-Species Multi-Channel [3]) to support the thermodynamic calculations. More significantly, the chemists/scientists can collaborate with each other to add sufficiently verified data of new species to the existing dataset. By this way, the algorithm can evolve and adapt to more general cases over time.

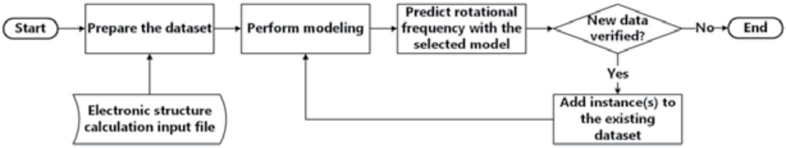
Start
Prepare the dataset
Perform modeling
Predict rotational frequency with the selected model
New data verified?
No
End
Yes
Electronic structure calculation input file
Add instance(s) to the existing dataset

Figure 1. Overall workflow of the data mining approach to detect the rotational frequency of hindered internal rotation.

RESULTS

The electronic structure calculation data used for the experiment were mostly adapted from [2]. The selected features were then extracted to build the dataset. Subsequently, three well-known machine learning algorithms of the scikit-learn library in Python [4] (i.e., logistic regression, support vector machines) were trained and then validated using 10-fold cross-validation on the dataset. For each round, *Accuracy*, *Precision*, *Recall* and *F-Score* following the equations in [5] of each algorithm were calculated as follows

$$Accuracy = \frac{TP+TN}{TP+FP+TN+FN}$$

$$Precision = \frac{TP}{TP+FP}, \quad Recall = \frac{TP}{TP+FN}$$

$$F-Score = \frac{2 \times Precision \times Recall}{Precision + Recall}$$

		Prediction result	
		Positive	**Negative**
Actual value	**True**	True positives (TP)	False negatives (FN)
	False	False positives (FP)	True negatives (TN)

Finally, the average values along with standard deviations of the aforementioned metrics of each algorithm were recorded in Table 1 to demonstrate their performance. It was found that the proposed method worked well for various types of species, ranging from simple hydrocarbons to more complex compounds with multiple bonds, ring, and even complicated transition states. Compared to rule-based methods, our approach can adapt to the emergence of new species thanks to its ability to recognize new general patterns from the updated data. In the next step, we will try to reduce the number of features to decrease drastically the complexity of our models. In the meantime, we can evaluate the impact of each feature on the output. The optimal model will be integrated into MSMC-GUI (https://sites.google.com/site/msmccode/manual/gui-1) to enhance the robustness of the determination of hindered internal rotation parameters.

Table 1. Performance comparison among several machine learning algorithms using Accuracy, Precision, Recall, F-score and their corresponding Standard Deviations (Std.) ***Notes:*** **Support Vector Machine (SVM), Radial Basis Function (RBF)**

Algorithm	*Accuracy*	*Accuracy Std.*	*Precision*	*Precision Std.*	*Recall*	*Recall Std.*	*F-Score*	*F-Score Std.*
RBF SVM	0.968	0.029	0.940	0.074	0.882	0.150	0.900	0.101
Linear SVM	0.972	0.025	0.916	0.101	0.936	0.068	0.922	0.064
Logistic Regression	0.971	0.025	0.920	0.097	0.927	0.089	0.918	0.066

REFERENCES

1. Mai TVT, Duong Mv, Le XT, Huynh LK, Ratkiewicz A, *Struct Chem*, *2014*, **25**(5), 1495-503.
2. Le THM, Do ST, Huynh LK, *Comp Theor Chem*, *2017*, **1100**, 61-9.
3. Duong MV, Nguyen HT, Truong N, Le TNM, Huynh LK, *Int J Chem Kinet*, *2015*, **47**(9), 564-75.
4. Pedregosa F, Varoquaux G, Gramfort A, Michel V, Thirion B, Grisel O, et al., *Journal oachine Learning Research*, *2011*, **12**(Oct), 2825-30.
5. Witten IH, Frank E, Hall MA, *Data Mining: Practical Machine Learning Tools and Techniques*, Morgan Kaufmann Publishers Inc., 2011.

BIO -P- 1

Amylose Wrapping on Single-wall Carbon Nanotube by Computational Study

Wanwisa Panman[1], Thanyada Rungrotmongkol[2,3,] , Oraphan saengsawang[4],
and Supot Hannongbua[5,C]
[1]*Multidisciplinary Program of Petrochemistry and Polymer Science, Faculty of Science, Chulalongkorn University, Bangkok 10330, Thailand*
[2]*Structural and Computational Biology Research Group, Department of Biochemistry, Faculty of Science, Chulalongkorn University, Bangkok 10330, Thailand*
[3]*Ph.D. Program in Bioinformatics and Computational Biology, Faculty of Science, Chulalongkorn University, Bangkok 10330, Thailand*
[4]*Office of Corporate R&D, IRPC Public Company Limited, Rayong, 21000, Thailand*
[5]*Department of Chemistry, Faculty of Science, Chulalongkorn University, Bangkok 10330, Thailand*

[C]***E-mail**: supot.h@chula.ac.th; **Fax**: +66 2 218 7603; **Tel.** +66 2 218 7602*

EXTENDED ABSTRACT

Keywords: Carbon nanotube, Molecular Dynamics Simulation, Amylose

INTRODUCTION

Carbon nanotube (CNT) is a tube-shape material with diameter in nanometer scale and length up to several centimeters, high curvature, and extra-large surface area. CNTs are composed of carbon atoms linked in hexagonal shapes, with each carbon atom covalent bonded to three other carbon atoms. CNTs have attracted great research interests due to their unique properties such as high electrical and thermal conductivity, excellent stiffness against bending, high tensile strength, highly flexible, low mass density, very elastic, and good electron field emitters. Their various applications are thermal conductivity, field emission, energy storage, conductive adhesive and biomedical applications. However, the serious problems is aggregation of CNT. To solve such problem, the surface modification by the covalent functionalization or non-covalent functionalized with some polymers or biopolymers has been applied. In this work, the amylose wrapped around CNT was studied by molecular dynamics simulation.

PROPOSED APPROACH

The initial structure of single-walled carbon nanotube ((10, 0) zigzag SWNT) and amylose was shown in Figure 1. The Glycam and AMBER ff14SB force fields were applied for amylose and SWNT, respectively. The system was simulated in the vacuum model for 100 ns by AMBER 16 software package at room temperature.

RESULTS

Molecular dynamics simulation indicated how amylose wrapped around SWNT in aqueous solution. Amylose can well bind with CNT on the outer surface by non-covalent interaction. This simulated structure of amylose wrapped around SWNT will be further used for modelling the amylose and polypropylene wrapped on SWNT in order to prevent agglomeration of CNT.

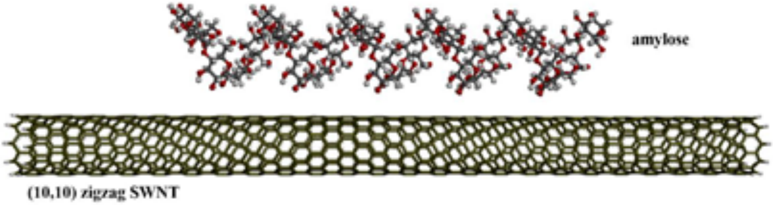

Figure 1. The initial structure of amylose wrapped around SWNT.

REFERENCES

1. Y.H. Xie, A.K. Soh, Investigation of non-covalent association of single-walled carbon nanotube with amylose by molecular dynamics simulation, *Materials Letters*, 59 (2005) 971-975.
2. Syamal S. Tallury and Melissa A. Pasquinelli, Molecular Dynamics Simulations of Flexible Polymer Chains Wrapping Single-Walled Carbon Nanotubes, *J. Phys. Chem. B*, 114 (2010) 4122-4129.

BIO
-P-
2

Computer-Based Drug Screening of Mansonone G Analogs Against Human DNA Topoisomerase II ATPase Domain

Panupong Mahalapbutr[1], **Yi Qin Gao**[2], **and Thanyada Rungrotmongkol**[1,3,C]
[1] *Structural and Computational Biology Research Group, Department of Biochemistry, Faculty of Science, Chulalongkorn University, Bangkok 10330, Thailand*
[2]*College of Chemistry and Molecular Engineering, Peking University, Beijing 100871, China*
[3]*Ph.D. Program in Bioinformatics and Computational Biology, Faculty of Science, Chulalongkorn University, Bangkok 10330, Thailand*

[C]***E-mail**: thanyada.r@chula.ac.th* ***Fax**: +66 2 218 5418;* ***Tel.** +66 2 5416-7*

EXTENDED ABSTRACT

Keywords: DNA topoisomerase II, quinone, *In silico* drug screening

INTRODUCTION

Cancer is one of the leading causes of death worldwide ranked only behind the heart disease[1]. Chemotherapeutic drugs are designed to target not only rapidly dividing cells but also normal cells. Cancer targeted therapies use the drugs or other substances to interact with specific molecules involved in tumorigenesis. DNA topoisomerase IIα (TopoIIα) is an important enzyme that regulates the DNA topology for promoting replication, transcription, and cell division[2]. TopoIIα is up-regulated in the rapidly proliferating cells and radically peaks at G2/M phase of cell cycle, making it as an important target for cancer targeted therapy[3]. Quinone-containing compounds showing the great cytotoxicity against various cancer cell lines and TopoIIα was the primary target for quinones[4]. Mansonone G (MG), an *ortho*-naphthoquinone-containing compound, exhibits the various biological activities including antitumor potential. In the present study, MG and its 18 synthesized derivatives were screened to find the potent compounds against TopoIIα using molecular docking, classical molecular dynamics (MD) simulations, and MM/PB(GB)SA binding free energy calculations.

PROPOSED APPROACH

The initial structures of Human DNA topoisomerase II were obtained from Protein Data Bank (PDB), whereas the starting structures of ligands were built and fully optimized using HF/6-31(d) basis set. The CDOCKER module in the Accelrys Discovery Studio 3.0$^{\text{Accelrys Inc}}$ was used to prepare the ligand-protein complexes with 100-independent docking runs (rigid condition). The potent docked complexes were then studied by molecular dynamics (MD) simulations using AMBER 14 packages for 80-ns and binding free energy calculations based on MM/PB(GB)SA approaches.

RESULTS

Based on docking results, the entire series of MGs specifically target to the ATPase domain rather than the etoposide pocket and the central domain. The eight compounds (MG4, MG5, MG6, MG12, MG13, MG14, MG15, and MG17) that showed the lower interaction energy than that of the ATP-competitive inhibitor, salvicine, were selected for MD study. The decomposition free energy data revealed that the key binding amino acids involved in ligand binding were residues 87-88, 91, 94-95, 98, 125, 141-142, 148-149, 160-161, 164-168, 215, and 217 located in the ATP-binding pocket of ATPase domain. The vdW interactions played a crucial role for stabilizing protein-ligand complexes rather than electrostatic and H-bond interactions. Based on MM/PB(GB)SA binding free energy calculations, the best three MGs will be further explored.

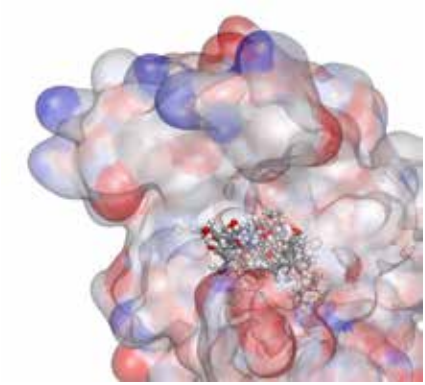

Figure 1. Docked complex of salvicine and MGs with TopoII*α* ATPase domain.

REFERENCES

1. Baudino TA, *Curr Drug Discov Technol*, 2015**, 12**(1), 3-20.
2. Jiménez-Alonso, S., et al., *J. Med. Chem*, 2008, **51**(21), 6761-6772.
3. Pommier, Y., et al., *Chem Biol*, 2010, **17**(5), 421-33.
4. Gurbani, D., et al., *Toxicol Sci*, 2012. **126**(2), 372-90.

BIO -P- 3

Dynamics Behaviors of Active and Inactive EGFR TK Domains with Erlotinib Bound

Phakawat Chusuth[1], Supot Hannongbua[2], Shinji Saito[3], Thanyada Rungrotmongkol [1,4, C]
[1]*Department of Biochemistry, Faculty of Science,*
Chulalongkorn University, Bangkok 10330, Thailand
[2]*Computational Chemistry Unit Cell, Department of Chemistry, Faculty of Science,*
Chulalongkorn University, Bangkok 10330, Thailand
[3]*Institute for Molecular Science, Myodaiji, Okazaki, Aichi 444-8585, Japan*
[4]*Ph.D. Program in Bioinformatics and Computational Biology, Faculty of Science,*
Chulalongkorn University, Bangkok 10330, Thailand

[C] ***E-mail**: t.rungrotmongkol@gmail.com; **Fax**: +66 2 218 5418; **Tel.** +66 8 1255 3575*

EXTENDED ABSTRACT

Keywords: EGFR, erlotinib, secondary mutation.

INTRODUCTION

Epidermal growth factor receptor (EGFR) is a transmembrane tyrosine kinase receptor that can stimulate mitosis, cell proliferation and inhibition of apoptosis. EGFR consists of three domains: (1) extracellular domain (2) transmembrane domain and (3) tyrosine kinase (TK) domain. Mutations in EGFR TK domain can lead to an abnormal growth of cells which ultimately can be the cause of cancers. L858R is one of the major mutations that normally found in Asian cancer patients, especially non-small cell lung cancer (NSCLC). In targeted cancer therapy, erolotinib is the tyrosine kinase inhibitor (TKI) that binds to EGFR TK domain leading to a decrease in cancer cell growth. The secondary mutation, T790M, causes the erlotinib-resistance.

PROPOSED APPROACH

Ligand structure was obtained from crystallographic coordinates. Consequently, ligand was optimized the geometry, computed the single point energies and charges with HF/6-31G* theory. Quantum mechanical computations were performed by Gaussian09 and antechamber module in AMBER 14. The generalized amber force field (GAFF) was used for erlotinib. The AMBER ff14SB force field was used for protein. The simulation was performed without restraint until 100 ns by the PMEMD module in AMBER.

RESULTS

Based on the MM/PBSA and MM/GBSA methods, the binding affinity of erlotinib to these two forms were not significantly different, while van der Waals force was the main contribution in binding with the targeted protein likely through the side chains of surrounding residues. In addition, the residues M793 and C797 formed hydrogen bonds with drug in both forms. Although, the mutated residue M790 in both active and inactive forms contributed to the erlotinib binding, the active form significantly exhibited higher amplitude of motion than the other form in particular at the activation loop close to the drug binding site.

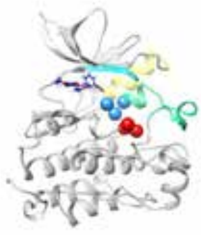

Figure 1. EGFR TK domain complexed with erlotinib.

.

REFERENCES

1. Park H. J., Liu Y., Lemmon A. M., Radhakrishnan R., *Biochem. J.*, 2012, **448**, 417-423.
2. Sharma V. S., Bell W. D., Settleman J., Haber A. D., *Nat Rev Cancer*, 2007, **7**, 169-181.

**BIO
-P-
4**

How a T-cell Antigen Receptor Recognizes Self-peptide Leading Autoimmune

Sirilak Kongkaew[1, 2], Thanyada Rungrotmongkol[3, 4, C], Supot Hannongbua[2, C]
[1] *Program in Biotechnology, Faculty of Science, Chulalongkorn University, Bangkok, Thailand*
[2] *Computational Chemistry Unit Cell, Department of Chemistry, Faculty of Science, Chulalongkorn University, Bangkok, Thailand*
[3] *Department of Biochemistry, Faculty of Science, Chulalongkorn University, Bangkok, Thailand*
[4] *Ph.D. Program in Bioinformatics and Computational Biology, Faculty of Science, Chulalongkorn University, Bangkok, Thailand*

[C] ***E-mail**: t.rungrotmongkol@gmail.com; supot.h@chula.ac.th*

EXTENDED ABSTRACT

Keywords: T-cell receptor, human leucocyte antigen, autoimmune, molecular dynamic simulation

INTRODUCTION

T-cell receptor (TCR) molecule recognizing antigenic peptide laid on human leukocyte antigen presenter (pHLA) is the first step in the T cell-mediated immune responses [1]. A T-cell can recognize over a million different antigenic peptides [2]. Normally, the immune system detects "foreign" –antigens such as viral or bacterial peptides, whilst "self" –antigens are misrecognized by immunity causing autoimmune diseases [3]. Autoimmune is the system of immune responses an organism against its own healthy cells and/or tissues. Many theories suggested autoimmune triggers involving environmental and chemical irritants, drugs and biological invader [4]. Limitations of immune response to take against an antigenic peptide if *i)* this peptide is not detected by HLAs or *ii)* pHLA does not recognized by TCR [1]. In this work, we modeled T cell-mediated autoimmune responsibility from factors risk to be autoimmunity, which represented in Behçet's disease (BD). Based on the previous reports, genetic markers with BD-association are revealed HLA-B*51:01 protein and MICA peptide (especially, a sequence of AAAAAIFVI) cohesion [5, 6]. HLA-B*51:01 is wildly known a strong BD association as well as a resistant HIV infection [7]. The self-autoantigen recognition by TCR, physical properties and binding interaction with viral infected system were studied by molecular dynamics simulation. Followed by our hypothesis, the autoimmune system might show the binding orientation and energy quite similar into the infection system.

PROPOSED APPROACH

The immune recognition on diversity cases were investigated in protein complex of TCRpHLA with different peptides (p).*a)* Autoimmune system: MICA peptide (9 amino acids length of AAAAAIFVI) *b)* Infected system: HIV peptide (8 amino acids length of TAFTIPSI) The TCR/HIV peptide/HLA-B*51:01 was obtained from the crystal structure in Protein Data Bank under PDB code 4MJI. For the autoimmune system, the original HIV-peptide was changed to the MICA sequence through mutagenesis technique using the Discovery studio 3.0 (Accelrys, Inc.) program. The LEaP module in Assisted Model Building with Energy Refinement (AMBER) version 14 was used to add all missing atoms in the starting structures with the ff03.r1 force field. Protein complexes were soaked in TIP3P water model. Counter ions were added to neutralize protein charge. Then, the SANDER module of AMBER 14 was applied to minimize all water molecules and protein complexes, consecutively. Atoms of protein were fixed with a weak force of 60.0 kcal·mol^{-1}·Å^{2} for 100-ps simulation, and the system was heated up to 298 K at atmospheric pressure. The fully MD simulations were performed until 150 ns. The trajectories extracted from 40-150 ns were accumulated to resolve into elements.

RESULTS

To investigate TCRpHLA binding, the MM/PBSA method was applied over the 200 frames on the steady state. TCR mainly interacted pHLA by van der Waals force. Relative MM/PBSA binding energy was separately calculated in part of HLA/p and TCR/p. HLA had similar binding energy value with MICA (-33.48 kcal/mol) and HIV (-34.68 kcal/mol) peptides. On the other side, MICA and HIV peptides were attracted by TCR at -19.85 and -10.97 kcal/mol, respectively. Two peptides prefer to bind into HLA groove than TCR, because HLA had larger surface to interact. From the relative binding, MICA peptide, self-antigen, was recognized at the least values of HIV peptide on either HLA or TCR side. Not only binding affinity was demonstrated but also binding orientation. Because of immune responded by signal transduction, binding location on ternary complex was studied by inter-pairwise residue contact. Amino acids were closely located can connect within 7 Å cutoff of chemical interactions. The distance between the C_α atoms of pairwise residue was measured and recorded. Basic interfaces in MICA system was appeared like HIV contact lists, additionally increasing of HLA—TCR interface. It was preliminarily implied as immune can response MICA peptide similar to infection lead to autoimmune production. Our findings may be more understanding autoimmunity on fundamental immune and be treated autoimmune disease in the next step.

REFERENCES

1. van der Merwe, P. A.; Dushek, O. Mechanisms for T cell receptor triggering. *Nat Rev Immunol* 2011, **11** (1), 47-55.
2. Wooldridge, L.; Ekeruche-Makinde, J.; Hugo, A.; van den Berg, H. A.; Skowera, A.; John, J.; Miles, J. J.; Tan, M. P.; Dolton, G.; Clement, M.; Llewellyn-Lacey, S.; Price, D. A.; Peakman, M.; Sewell, A. K. A Single autoimmune T cell receptor recognizes more than a million different peptides. *Journal of biological chemistry* 2012, **287** (2), 1168 –1177.
3. Simmonds, M. J.; Gough, S. C. L. Genetic insights into disease mechanisms of autoimmunity. *British Medical Bulletin* 2005, **71**, 93–113.
4. Poletaev, A. B.; Churilov, L. P.; Stroev, Y. I.; Agapov, M. M. Immunophysiology versus immunopathology: Natural autoimmunity in human health and disease. *Pathophysiology* 2012, **19** (3), 221-31.

5. Kongkaew, S.; Yotmanee, P.; Rungrotmongkol, T.; Kaiyawet, N.Meeprasert, A.; Kaburaki, T.; Noguchi, H.; Takeuchi, F.; Kungwan, N.; Hannongbua, S. Molecular Dynamics Simulation Reveals the Selective Binding of Human Leukocyte Antigen Alleles Associated with Behcet's Disease. *PLoS One* 2015, **10** (9), e0135575.
6. Yasuoka, H.; Okazaki, Y.; Kawakami, Y.; Hirakata, M.; Inoko, H.; Ikeda, Y.; Kuwana, M. Autoreactive CD8+ cytotoxic T lymphocytes to major histocompatibility complex class I chain-related gene A in patients with Behcet's disease. *Arthritis Rheum* 2004, **50** (11), 3658-62.
7. Motozono, C.; Kuse, N.; Sun, X.; Rizkallah, P. J.; Fuller, A.; Oka, S.; Cole, D. K.; Sewell, A. K.; Takiguchi, M. Molecular basis of a dominant T cell response to an HIV reverse transcriptase 8-mer epitope presented by the protective allele HLA-B*51:01. *J Immunol* 2014, **192** (7), 3428-34.

BIO
-P-
5

In Silico Screening of Chalcones Against Epstein-Barr Nuclear Antigen 1 Protein

Nitchakan Darai[1], **Chompoonut Rungnim**[2], **Thanyada Rungrotmongkol**[3,4,C]
[1]*Program in Biotechnology, Faculty of Science, Chulalongkorn University, Bangkok 10330, Thailand*
[2]*National Nanotechnology Center (NANOTEC), National Science and Technology Development Agency (NSTDA), 111 Thailand Science Park, Pathumthani 12120, Thailand*
[3]*Structural and Computational Biology Research Group, Department of Biochemistry, Faculty of Science, Chulalongkorn University, Bangkok 10330, Thailand*
[4]*Ph.D. Program in Bioinformatics and Computational Biology, Faculty of Science, Chulalongkorn University, Bangkok 10330, Thailand*

[C]***E-mail**: t.rungrotmongkol@gmail.com; **Fax**: +66 2 218 5418; **Tel.** +66 4 375 4246*

EXTENDED ABSTRACT

Keywords: Epstein-Barr Nuclear Antigen 1 protein, Chalcones, Molecular docking

INTRODUCTION

Epstein–Barr Virus (EBV) is the herpesvirus 4 discovered by using electron microscopy of cells cultured from Burkitt's lymphoma tissue by Epstein, Achong, and Barr. EBV has infected more than 90% of people worldwide and persisted for the lifetime of the person. EBV has induced changes to the cell and best known as the cause of infectious mononucleosis and long-term EBV infections are associated with higher risk of lymphoma, ovarian cancer, stomach cancer and other types of cancer. After infection, this virus establishes a lifelong latency in infected cells. During latent infection, EBV does express a limited set of viral gene products that promote host-cell survival and proliferation. The maintenance of the latent viral genome depends on the functions of the Epstein-Barr Nuclear Antigen 1 protein (EBNA1), which is the only viral protein that is consistently expressed in all forms of latency, essential for viral genome maintenance and for infected-cell survival. However, there are not widespread vaccine or therapeutic drugs for controlling EBV infection. Due to its important role, Epstein-Barr Nuclear Antigen 1 protein (EBNA1) is an attractive target protein for drug design of anti-EBV agents. In this study, we aimed to screen chalcones, which can exhibit several biological activities including anticancer activity, in order to disrupt EBNA1-DNA binding.

PROPOSED APPROACH

The EBNA1 structure was prepared from X-ray crystal structure in protein data bank (PDB), entry code 1VHI. Ligand-protein interactions was investigated using CHARMM based docking software (CDOCKER) of the Discovery Studio 3 (Accelrys Inc., San Diego, CA, USA) suite of program, and CDOCKER protocol was used to prepare the protein and ligand as inputs. The algorithm offers flexible ligand docking and protein was held rigid during the entire process.

RESULTS

Based on the CDOCKER interaction energy values obtained from the profiles of 47 chalcones (Figure 1) with the target protein EBNA1, the compound 33d, 33f and 44l (Figure 2) have the lowest interaction energy. Their orientations in the ligand binding pocket of EBNA1 were likely similar as shown in Figure 1. In addition, H-bonding interaction between SER513, LYS586, LYS477 of EBNA1 and chalcones was observed by mean of molecular docking approach.

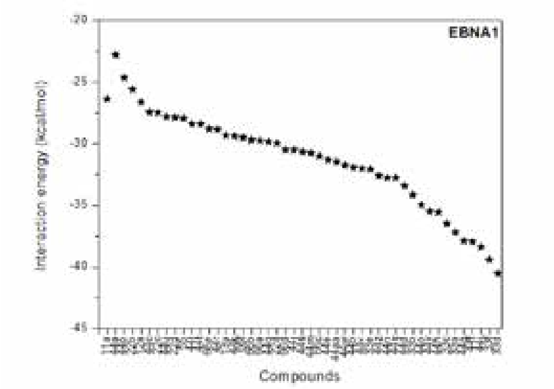

Figure 1. Interaction energy between 47 chalcones and EBNA1 protein.

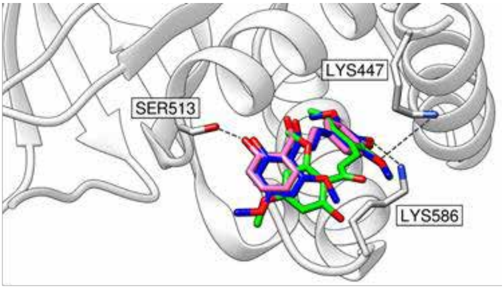

Figure 2. The complex structures of EBNA1 (gray) with compound 33d (blue), compound 33f (green) and compound 44l (pink) bound from docking procedure

REFERENCES

1. E. Gianti, T. Messick, P. Lieberman, R. Zauhar, Computational analysis of EBNA1 drug ability suggests novel insights for Epstein-Barr virus inhibitor design, *J Compute Aided Mol Des*, (2016).
2. N. Li, S. Thompson, D. Schultz, W. Zhu, et al. , Discovery of Selective Inhibitors Against EBNA1 via High Throughput In Silico Virtual Screening, *PLoS ONE*, (2010).

BIO
-P-
6

In silico Screening of Targeted Proteins for Developing Anticancer Agents

Kamonpan Sanachai[1] **and Thanyada Rungrotmongkol**[1,C]
[1]*Structural and Computational Biology Research Group, Department of Biochemistry, Faculty of Science, Chulalongkorn University, Bangkok 10330, Thailand*

[C]***E-mail****: t.rungrotmongkol@gmail.com;* ***Fax****: +66 2 218 5418;* ***Tel.*** *+66 4 375 4246*

EXTENDED ABSTRACT

Keywords: HPV E6, HPV E7, EBNA1, HCV protease, Mansonones, Molecular docking

INTRODUCTION

Cancer is related to a condition where cells in a specific part of the body grow and reproduce uncontrollably. The cancerous cells can invade and destroy surrounding healthy tissue, including organs. Infection with specific subtypes of *Human papillomavirus* (HPV) has been strongly implicated in cervical carcinogenesis. Hepatitis B is a potentially life-threatening liver infection caused by hepatitis B virus (HBV). It can cause chronic infection and puts people at high risk of death from cirrhosis and liver cancer. Hepatitis C is a liver disease caused by the hepatitis C virus (HCV). This virus can cause both acute and chronic hepatitis, ranging in severity from a mild illness lasting a few weeks to a serious, lifelong illness. The last one, Epstein–Barr nuclear antigen 1 (EBNA1) is the only nuclear Epstein-Barr virus (EBV) protein expressed in both latent and lytic modes of infection. Infection with EBV is associated with lymphoproliferative disorders, especially in immunocompromised hosts, and with various tumors, including nasopharyngeal carcinoma and Burkitt lymphoma. In this research, the mansonone G (MG) compounds were used to search for the cancer protein targets in order to further anticancer drug development.

PROPOSED APPROACH

The 3D structures of HPV E6 (4XR8.pdb), HPV E7 (2B9D.pdb), and EBV EBNA1 (1VHI.pdb) proteins were obtained from Protein Data Bank (PDB), whereas the SWISSMODEL server was used to prepare the HBV polymerase and HCV protease from 1IUD.pdb and 3P8N.pdb, respectively. The 20 MG derivatives were docked into the drug/inhibitor binding site of each protein for 100 independent docking runs (rigid condition) using CDOCKER module in the Discovery Studio 3 (Accelrys Inc., San Diego, CA, USA). The ligand-protein interaction energies of all MGs were ranked and compared with the known drugs and/or inhibitors.

RESULTS

The interaction energies of all 20 MGs toward the selective proteins including HPV E6, HPV E7, HBV polymerase, HCV protease, and EBNA1 resulted from molecular docking were compared with the commercially available drugs or inhibitors. The overall MGs with the lowest interaction energy for each protein were summarized in

Table 1. From docking results, MG5 showed the better binding affinity against the HPV E6 and EBNA1 than that of the known active compounds. The hydrogen bond (H-bond) formations between 3,5,7-trihydroxy -2-(2,4,5-trihydroxyphenyl)- 4H-chromen-4-one and MG5 within HPV E6's pocket were occurred at Glu381 and Glu382. Additionally, MG5 and chalcone could form H-bond interactions with Lys514 residue of EBNA1. The interaction of MG12 (-34.89 kcal/mol) with HPV E7 protein was slightly stronger than that of podophyllotoxin (-33.22 kcal/mol), by which His67 and Arg71 were the key residues for H-bond formations. In case of HBV polymerase, MG13 (-57.90 kcal/mol) showed the greater binding efficiency than that of lamivudine (-46.01 kcal/mol) but significantly lower than tenofovir (-167.81 kcal/mol). The H-bond interactions were found at (*i*) Arg22 and Asn219, (*ii*) Asp64, and (*iii*) Ala67, Ala68, and Gln243 for MG13, lamivudine, and tenofovir, respectively. Altogether, the potent MGs against cancer protein targets shared the same binding site for each protein. Unfortunately, there are no MG analogs targeted toward the HCV protease.

Table 1. The screened MG compound with the lowest interaction energy with the protein target relative to the known drugs, inhibitors, and potent compounds

Proteins	Compounds	Interaction energy (kcal/mol)
HPV E6	3,5,7-Trihydroxy-2-(2,4,5-trihydroxyphenyl)-4H-chromen-4-one	-38.76
	MG5	-55.09
HPV E7	Podophyllotoxin	-32.22
	MG12	-34.89
HBV polymerase	Lamivudine	-46.01
	Tenofovir	-167.81
	MG13	-57.90
HCV protease	Boceprevir	-59.97
	Telaprevir	-57.53
	MG5	-43.71
EBNA1	Chalcone	-46.49
	MG5	-52.28

REFERENCES

1. Sivachandran N, Wang X, Frappier L, Functions of the Epstein-Barr virus EBNA1 protein in viral reactivation and lytic infection, *Journal of Virology*, (2012), 86, 6146-6158.
2. Zhang S, Gao S, Zhao M, Liu Y, Bu Y, Jiang Q, Zhao Q, Ye L, Zhang X, Anti-HBV drugs suppress the growth of HBV-related hepatoma cells via down-regulation of hepatitis B virus X protein, *Cancer Letters*, (2017), 392, 94-104.

BIO -P- 7 | MD Simulations of Three Designed TSX Structures with 50% Galactose-Removal in Explicit Water Solvent

Napat Kongtaworn[1], **Namon Hirun**[1,2], **Thanyada Rungrotmongkol**[3,4], **Supaporn Dokmaisrijan**[1,C]
[1]*Theoretical and Computational Modeling (TCM) Research Group, School of Science, Walailak University, Nakhon Si Thammarat 80161, Thailand*
[2]*School of Pharmacy, Walailak University, Nakhon Si Thammarat 80161, Thailand*
[3]*Structural and Computational Biology Research Group, Department of Biochemistry, Faculty of Science, Chulalongkorn University, Bangkok 10330, Thailand*
[4]*Ph.D. Program in Bioinformatics and Computational Biology, Faculty of Science, Chulalongkorn University, Bangkok 10330, Thailand*

[C]***E-mail**: sdokmaisrijan@yahoo.com; **Tel.** +66 75672045*

EXTENDED ABSTRACT

Keywords: Molecular Dynamics Simulations, Tamarind Seed Xyloglucan, modified TSX

INTRODUCTION

Tamarind seed xyloglucan (TSX) can dissolve in water at high temperatures (ca. 60 °C) and has been widely used in drug delivery because of its non-toxicity and biocompatibility. The TSX has three types of repeating units including heptasaccharide (H, XXXG), octasaccharide (O1, XXLG or O2, XLXG), and nonasaccharide (N, XLLG) (where G, X, and L are glucose (Glu), xylose (Xyl) substituted glucose, and galactose (Gal) substituted xylose, respectively). Moreover, nonasaccharide unit has been reported to be the most abundant form of the TSX.

Gelation of the modified TSX polymer has been of great interests for biomedical applications. A TSX solution cannot form a gel by itself, but it can become gel when the galactose molecules are partially removed by the β-galactosidase. It was believed that the lack of galactose residues might be able to promote the association of the β-glucan main chains through the hydrophobic interactions and result in the gelation. Moreover, the sol-gel transition temperature decreases as the galactose removal ratio increases. For TSX with 50% of galactose removal ratio, its gelling temperature is around 10 °C. In this study, the possible structures of modified TSX have been designed and studied in the explicit water model using molecular dynamics (MD) simulation technique. Those designed TSX structures can provide the roles of galactose residue and the β-glucan main chain arrangements in association and aggregation of TSX as well as their intermolecular interactions between modified TSX chains.

PROPOSED APPROACH

Three modified TSX models were designed as two chains of O1 (model1), two chains of O2 (model2), and chains of O1 and O2 (model3). The O1 and O2 structures and example of double-chain TSX are shown in Figure. 1a and 1b, respectively.

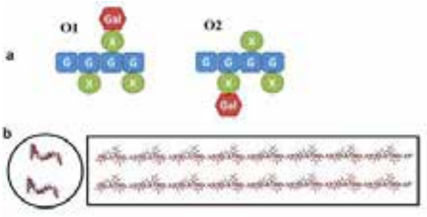

Figure. 1 Two types (O1 and O2) of octasaccharide (a) and modified TSX double chain (b).

All modified TSX models and a model of cellulose were built and solvated by the TIP5P water molecules in a triangular box. The GLYCAM_06j-1 parameters were applied to describe the molecular characteristics of TSX. Each model was performed in the same way using the NVT-MD simulation technique embedded in the AMBER16 program. The non-bonded cutoff radius of 10 Å was applied. After steps of minimization, heating the system to 283 K for 50 ps and 1-ns dynamics, all modified TSX models were further simulated for 50 ns of dynamics for a trajectory collection.

RESULTS

The MD results of all modified TSX and cellulose models revealed that the main chains of all models were bent and twisted. For the cellulose model, the G main chain is in close contact and there is no gap formed between the two chains. Contrarily, each modified TSX model showed different structural feature. The model1 displayed that two main chains prefer to form in the parallel-like structure, even there is a small gap formed between these chains. The model2 and model3 have some association points formed from intermolecular hydrogen bonds (H-bonds) between the -OH groups of main chain and xylose and galactose side chains.

REFERENCES

1. H. Urakawa, M. Mimura, K. Kajiwara, Diversity and Versatility of Plant Seed Xyloglucan. Trends in Glycoscience and Glycotechnology, *J Trends in Glycoscience and Glycotechnology*, (2002) 14:355–376
2. N. Hirun, S. Rugmai, T. Sangfai, V. Tantishaiyakul, SAXS and ATR-FTIR studies on EBT–TSX mixtures in their sol–gel phases, *International Journal of Biological Macromolecules*, (2012) 4:423-430
3. N. Hirun, V. Tantishaiyakul and W. Pichayakorn, Effect of Eriochrome Black T on the gelatinization of Xyloglucan investigated using rheological measurement and release behavior of Eriochrome Black T from xyloglucan gel matrices, *International Journal of Pharmaceutics*, (2010) 1-2:196-201
4. S. Yamanaka, Y. Yuguchi, H. Urakawa, K. Kajiwara, M. Shirakawa, K. Yamatoya, Gelation of Enzymatically Degraded Xyloglucan Extracted from Tamarind Seed, *Sen'i Gakkaishi*, (1999) 11:528-532

BIO
-P-
8

Molecular Dynamics Study on MCR-1 in Mono-Zinc and Di-Zinc Forms

Chonnikan Hanpaibool[1], Eric Lang[2], Philip Hinchliffe[3], Thanyada Rungrotmongkol[1,4,C], Jame spencer[3], Adrian Mulholland[2]

[1] Structural and Computational Biology Research Group, Department of Biochemistry, Faculty of Science, Chulalongkorn University, Bangkok 10330, Thailand
[2] School of Chemistry, Faculty of Science, University of Bristol, Bristol BS8 1TS, UK
[3] School of Cellular and Molecular Medicine, Faculty of Science, University of Bristol, Bristol BS8 1TS, UK
[4]Ph.D. Program in Bioinformatics and Computational Biology, Faculty of Science, Chulalongkorn University, Bangkok 10330, Thailand

*[C]**E-mail:** t.rungrotmongkol@gmail.com ; **Fax:** +66 2 218 5418; **Tel.** +66 218 5426*

EXTENDED ABSTRACT

Keywords: Antimicrobial resistance, MCR-1, molecular dynamics

INTRODUCTION

Colistin is one of the last resort antibiotics used in clinical treatment. It competitively replaces Mg^{2+} and Ca^{2+} ions from negative charged phosphate on the lipid A of bacterial membrane with a consequence of outer membrane disruption. MCR-1 catalyzes the phosphoethanolamine transfer reaction to lipid A on outer membrane of gram-negative bacteria in order to neutralize the negative charge with a reduction on colistin binding which cause the bacteria resistance to the colistin.

PROPOSED APPROACH

The starting geometry of the MCR-1 containing mono-zinc and di-zinc ions was taken from Protein data bank with entry codes: 5lrn and 5lrm. Protonation state of MCR-1 protein was predicted by propka server. Both systems were simulated in octahedral water box and were heated to 310K within 200-ps using with 2-fs time step. 100-ns MD simulation was performed at the same temperature. The Zinc coordination in these two systems was analyzed and compared by the distance measurement between Zn and surrounding residues as well as waters.

RESULTS

Based on the 100-ns MD results of the MCR-1 containing mono-zinc and di-zinc ions, the catalytic Zn1 was likely more stable than the Zn2. In both systems, the coordinated ligands of Zn1 were D465, E246, H466, T285, and a water molecule (Figure 1). Interestingly, the Zn2 left out the catalytic site after 95-ns of simulation. The obtained information from this study suggested that the active conformation of MCR-1 may require only a single zinc ion.

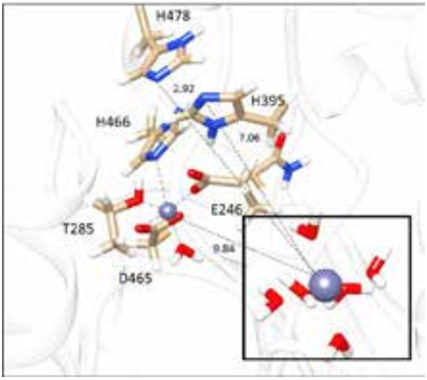

Figure 1. Average distance between Zn ion and its coordinated ligands resulted from the simulation of MCR-1 containing di-zinc ions

REFERENCES

1. Hinchliffe, P., Yang, Q. E., Portal, E., Young, T., Li, H., Tooke, C. L., Carvalho, M. J., Paterson, N. G., Brem, J., Niumsup, P. R., Tansawai, U., Lei, L., Li, M., Shen, Z., Wang, Y., Schofield, C. J., Mulholland, A. J., Shen, J., Fey, N., Walsh, T. R., & Spencer,J. (2017). Insights into the Mechanistic Basis of Plasmid-Mediated Colistin Resistance from Crystal Structures of the Catalytic Domain of MCR-1.Scientific Reports, 7, 39392.

BIO
-P-
9

Structural Dynamics and Binding Free Energy of Neral Cyclodextrins Inclusion Complexes: Molecular Dynamics Simulation

Peerapong Wongpituk[1], **Bodee Nutho**[2], **Wanwisa Panman**[3], **Nawee Kungwan**[4], **Thanyada Rungrotmongkol**[5,6,7*], **Nadtanet Nunthaboot**[1*]
[1]Department of Chemistry and Center of Excellence for Innovation in Chemistry, Faculty of Science, Mahasarakham University, Mahasarakham 44150, Thailand
[2]Program in Biotechnology, Faculty of Science, Chulalongkorn University, Bangkok 10330,Thailand
Tel: +66 22 186426, +66 43 754246; Fax: +66 22 186418, +66 43 754246

***E-mail**: thanyada.r@chula.ac.th, nadtanet@gmail.com*

EXTENDED ABSTRACT

Keywords: Cyclodextrin, neral, citral, inclusion, molecular dynamics simulation.

INTRODUCTION

Lemon grass (*Cymbopogon citratus* Stapf) is a widely used herb in Thailand and is extensively applied as an ingredient in Thai cuisine. The broad biological activities of lemon grass oil have been reported, including anti-bacterial, anti-fungal, and insecticidal activities. Citral has been reported to exhibit high antibacterial activity against gram-negative and gram-positive organisms. Due to their limitations on poorly water solubility, and sensitivity towards high temperature, oxygen and light consequently leading to a loss of therapeutic properties on oxidation, a stabilization process has become an imperative necessity. Among various encapsulation techniques, one of the interesting methods is the entrapment of such volatile compounds in a proper cavity of cyclodextrins (CDs) to increase their physicochemical properties.

PROPOSED APPROACH

The inclusion complexation of neral, a *cis*-isomer of citral found in lemon grass (*Cymbopogon citratus* Stapf), and four different types of cyclodextrin, β-cyclodextrin (βCD), 2,6-dimethyl-βCD (2,6DMβCD), 2,6-dihydroxypropyl-βCD (2,6DHPβCD), and 2-hydroxypropyl-βCD (2HPβCD), were investigated using molecular docking and molecular dynamics simulation approaches. The simulations show that the neral/CD inclusion complex could be formed in aqueous solution with 1:1 ratio. Three possible binding orientations were assessed for the encapsulation of neral (^{1}neral, ^{7}neral, and ^{u}neral) inside the hydrophobic interior of the host molecule. The ^{u}neral in which both aldehyde and alkyl terminals point outward the secondary rim of CD was observed as the most preferential conformation in all neral/CD complexes. The theoretical calculation of binding ability of host-guest inclusion complexes were agree well with the experimental data supporting that neral could bind inside the hydrophobic cavity of all CDs with nearly the same potency.

RESULTS

To determine the system stability of all neral/CD complexes, the 1D-RMSD and 2DRMSD for all atoms of inclusion complexes with two different modes of ligand binding (^{1}neral and ^{7}neral) along 70-ns simulation were plotted in Figure. 1. The 1DRMSD result suggested that all simulated systems had reached equilibrium at 50 ns and thus the snapshots taken from the last 20-ns simulation were selected for further analysis.

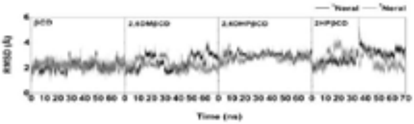

Figure 1. 1D-RMSD plots of all atoms for ¹neral/CDs (black) and ⁷neral/CDs (gray) whereCDs are βCD, 2,6DMβCD, 2,6DHPβCD and 2HPβCD.

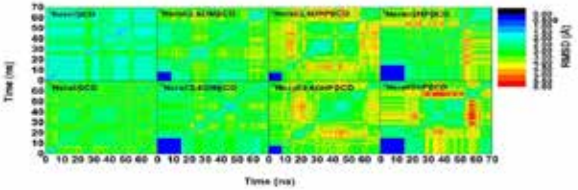

Figure 2. 2D-RMSD plots of all atoms for ¹neral and ⁷neral/CDs complexes where CDs are βCD, 2,6-DMβCD, 2,6-DHPβCD and 2-HPβCD

REFERENCES

1. Leimann FV, Gonçalves OH, Machado RAF, Bolzan A. Antimicrobial activity of microencapsulated lemongrass essential oil and the effect of experimental parameters on microcapsules size and morphology. *Mat Sci Eng C.* **2009;** *29:*430-436.
2. Nguefack J, Dongmo JBL, Dakole CD, Leth V, Vismer HF, Torp J, Guemdjom EFN, Mbeffo M, Tamgue O, Fotio D, Zollo PHA, Nkengfack AE. Food preservative potential of essential oils and fractions from Cymbopogon citratus, Ocimum gratissimum and Thymus vulgaris against mycotoxigenic fungi. *Int J Food Microbiol.* **2009;** *131:* 151-156.
3. Oyedele AO, Gbolade, AA, Sosan MB, Adewoyin FB, Soyelu OL, Orafidiya OO, Formulation of an effective mosquito-repellent topical product from Lemongrass oil. *Phytomedicine.* **2002;** *9*: 259-262.
4. Onawunmi GO, Yisak WA, Ogunlana EO. Antibacterial constituents in the essential oil of Cymbopogon citratus (DC.) Stapf. *J Ethnopharmacol.* **1984;** *12*: 279-286.
5. Kimura K, Nishimura H, Iwata I, Mizutani J, Deterioration mechanism of lemon flavor. 2. Formation mechanism of off-odor substances arising from citral. *J Agr Food Chem.* **1983;***31:* 801-804.

BIO -P- 10

Susceptibility of Potent Inhibitors Against NS2B/NS3 Serine Protease of Zika Virus: a Molecular Dynamics Study

Bodee Nutho[1] **and Thanyada Rungrotmongkol**[2,3,C]
[1]*Program in Biotechnology, Faculty of Science, Chulalongkorn University, Bangkok 10330, Thailand*
[2]*Structural and Computational Biology Research Group, Department of Biochemistry, Faculty of Science, Chulalongkorn University, Bangkok 10330, Thailand*
[3]*Ph.D. Program in Bioinformatics and Computational Biology, Faculty of Science, Chulalongkorn University, Bangkok 10330, Thailand*

[C]***E-mail**: thanyada.r@chula.ac.th; **Fax**: +66 2 218 5426; **Tel.** +66 4 375 4246*

EXTENDED ABSTRACT

Keywords: Zika virus, NS2B/NS3 serine protease, Molecular Dynamics Simulation

INTRODUCTION

Zika virus (ZIKV), a mosquito-borne flavivirus, was first isolated from sentinel rhesus monkey in the Zika Forest of Uganda in 1947. Originally, it was not considered as a relevant human pathogen because the majority of its infections is asymptomatic until the large outbreak starting in Brazil in 2015. The virus is transmitted to humans by *Aedes* species mosquitoes. Nonetheless, there are now growing evidences showing that ZIKV infections might be related to fetal and newborn microcephaly with serious neurological complications particularly for Guillain–Barré syndrome. In addition, ZIKV can cross the placenta and results in microcephaly. The incidences of Guillain–Barré syndrome and microcephaly associated with ZIKV infection have led the World Health Organization (WHO) to declare ZIKV infection as a global public health emergency in February of 2016. Unfortunately, there are no currently available vaccine or therapeutic drugs for preventing or controlling ZIKV infection; thus, drug design and development of anti-ZIKV agents with effective and safe properties have become an imperative necessity. One of the attractive drug targets for ZIKV treatment is the NS2B/NS3 serine protease, which plays a crucial role during viral replication process. Herein, classical molecular dynamics (MD) simulations and free energy calculation methods were employed to investigate the dynamics behaviors and binding affinities of the enzyme-inhibitor complex at the molecular level.

PROPOSED APPROACH

To obtain the initial structures, the NS2B/NS3 protease of ZIKV in complex with peptide-boronic acid inhibitor was prepared from crystal structure in protein data bank (PDB), entry code 5LC0. The partial atomic charges and empirical force field parameters for each ligand were developed in accordance with the standard procedure. Briefly, the atomic charges of each inhibitor were calculated using HF/6-31G(d) method with the Gaussian09 software. The electrostatic potential (ESP) charges were consequently computed with the same method. Afterward, the ESP charges of each inhibitor were fit into restrained ESP (RESP) charges using the ANTECHAMBER module in AMBER16. The atom types and the other molecular parameters of protein and ligand were assigned by the AMBER ff14SB force field and the generalized AMBER force field (GAFF), respectively. It should be noted that all classical MD simulations of 50 ns were performed using AMBER16 software package. All structural analyses were computed by the cpptraj module, while the binding free energy was calculated using the MMPBSA.py module.

RESULTS

Theoretically, it was observed that there was conformational fluctuation of the RMSDs of all atoms relative to those of the initial structure *versus* the simulation time around 0.25 Å from 10 ns till the end of simulation in both systems. Therefore, the snapshots from the last 20 ns of the trajectory were extracted for further analysis. The MM/PBSA method was applied in this study to estimate and compare the inhibitory efficiency of the two studied inhibitors against the ZIKV NS2B/NS3 protease in terms of the binding free energy (ΔG_{bind}). Our results indicated that the favourable ΔG_{bind} from the MM/PBSA approach of peptidyl boronic acid Bz-[4-(CH_2NH_2)]Phe-Arg-B$(OH)_2$ (Figure 1A) was better than Bz-(4-NH_2)Phe-Arg-B$(OH)_2$ (Figure 1B), which was consistent with the experimental data. By including the solvation free energy, the vdW term ($\Delta G_{\mathrm{nonpolar,sol}} + \Delta E_{\mathrm{vdW}}$) is a favourable contribution to the total binding free energies of both NS2B/NS3 inhibitor complexes, which were opposed by the unfavourable electrostatic term ($\Delta G_{\mathrm{ele,sol}} + \Delta E_{\mathrm{ele}}$). This is due to relatively high positive values of polar solvation resulting from PB model. It indicated that the vdW interaction played a key role in the ZIKV NS2B/NS3 protease with inhibitors. Therefore, the ability of the classical MD simulations presented here could be informative and useful for further for further drug design and development.

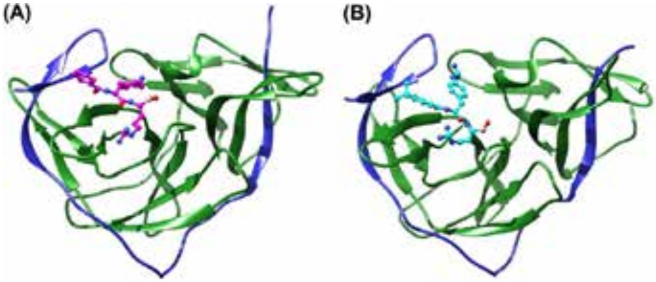

Figure 1. 3D structure of NS3 protease (green) and NS2B cofactor (blue) in complex with (A) Bz-[4-(CH_2NH_2)]Phe-Arg-B$(OH)_2$ (magenta) and (B) Bz-(4-NH_2)Phe-Arg-B$(OH)_2$ (cyan).

REFERENCES

1. H. Lee, J. Ren, S. Nocadello, A. J. Rice, I. Ojeda, S. Light, G. Minasov, J. Vargas, D. Nagarathnam, W. F. Anderson, M. E. Johnson, Identification of novel small molecule inhibitors against NS2B/NS3 serine protease from Zika virus, *Antiviral Research*, 139 (2017), 49-58.
2. W. W. Phoo, Y. Li, Z. Zhang, M. Y. Lee, Y. R. Loh, Y. B. Tan, E. Y. Ng, J. Lescar, C. Kang, D. Luo, Structure of the NS2B-NS3 protease from Zika virus after self-cleavage, *Nature Communications*, 7 (2016), 1-8.

BIO
-P-
11

Virtual Screening for Tripeptide Inhibitors in Nnrti Binding Pocket of HIV-1 Reverse Transcriptase

Nattawat Tantijaratchai[1], Duangnapa kiriwan[1], Bundit Boonyarit[1], Supa HannongBua[2], and Kiattawee Choowongkomon[1,C]
[1] *Laboratory of Protein Engineering and Bioinformatics, Department of Biochemistry, Faculty of Science, Kasetsart University, 50 Ngamwongwan, Chatuchak, Bangkok 10900, Thailand*
[2] *Department of Chemistry, Faculty of Science, Kasetsart University, 50 Ngamwongwan, Chatuchak, Bangkok 10900, Thailand*

[C] ***E-mail:*** *kiattawee.c@ku.th;* ***Fax****: +6625614627;* ***Tel.*** *+6685551480*

ABSTRACT

The HIV-1 (Human Immunodeficiency Virus type-1) and AIDS (Acquired Immunodeficiency Syndrome) epidemic have long been recognized as one of the world's most serious health and development challenges. The Reverse transcriptase (RT) is potential drug target for anti-HIV therapy and a critical enzyme of the HIV life. The HIV type-1 RT is an asymmetric heterodimer composed of p66 and p51 subunits. The p66/p51 heterodimer contains a single DNA polymerization active site and one RNase H active site. Commonly, the NNRTIs (Non-nucleoside reverse transcriptase inhibitors) have interfered with RT as non-competitive inhibitors which bind to a single site in the p66 subunit of the HIV-1 RT. The NNRTI binding pocket is 10Å from the polymerase active site[1]. The NNRTIs inhibit HIV-1 RT in a way that is distinct from the NRTIs[2]. Moreover, the important problem is the resistance of HIV-1 to the drugs by mutation of HIV-1 RT[3, 4, 5, 6]. About 8000 tripeptides[7, 8] were screened against HIV-1 RT by Gold docking program[9, 10] . The screening criterion is based on Gold fitness scores. Interestingly, several peptides show Gold fitness scores higher than Rilpivirine[11, 12 ,13], a third generation of HIV-1 drug. The top five tripeptides were selected for further analysis using molecular dynamics simulation.

Keywords: Tripeptides, HIV-1, Reverse Transcriptase, NNRTI, Gold docking, molecular dynamics simulation, inhibitor

REFERENCES

1. Kohlstaedt, L.A., Wang, J., Friedman, J.M., Rice, P.A. and Steitz, T.A., Crystal structure at 3.5 A resolution of HIV-1 reverse transcriptase complexed with an inhibitor, *Science*, 1992a., **256**(5065), 1783-1790.
2. Schauer, G.D., Huber, K.D., Leuba, S.H., and Sluis-Cremer, N., Mechanism of allosteric inhibition of HIV-1 reverse transcriptase revealed by single-molecule and ensemble fluorescence, *Nucleic Acids Research*, 2014, **42**(18), 11687–11696.
3. Balzarini, J., Auwerx, J., Rodriguez-Barrios, F., Chedad, A., Farkas, V., Ceccherini-Silberstein, F., Garcia-Aparicio, C., Velazquez, S., Clercq, E. D., Perno, C.F., Camarasa, M.J. and Gago, F., The amino acid Asn136 in HIV-1 reverse transcriptase (RT) maintains efficient association of both RT subunits and enables the rational design of novel RT inhibitors, *Mol. Pharmacol.*, 2005, **68**(1), 49-60.

4. Zheng, X., Mueller, G.A., Cuneo, M.J., Derose, E.F., and London, R.E., Homodimerization of the p51 subunit of HIV-1 reverse transcriptase, *Biochemistry*, 2010, **49**(13), 2821-2833.
5. Braz, V.A., Barkley, M.D., Jockusch, R.A., and Wintrode, P.L., Efavirenz binding site in HIV-1 reverse transcriptase monomers, *Biochemistry*, 2010, **49**(49), 10565-10573.
6. Anta, L., Llibre, J.M., Poveda, E., Blanco, J. L., Álvarez, M. , Pérez-Elías, M.J., Aguilera, A., Caballero, E., Soriano, V., de Mendoza, C., Rilpivirine resistance mutations in HIV patients failing non-nucleoside reverse transcriptase inhibitor-based therapies, *AIDS*, 2013, **27**(1), 81–85.
7. D. Seeliger and Bert L. de Groot, Protein thermostability calculations using Alchemical free energy simulations, *Biophys. J,* 2010, **98**(10), 2309-2316.
8. V. Gapsys, S. Michielssens, D. Seeliger, and B. L. de Groot., pmx: Automated protein structure and topology generation for alchemical perturbations, *J. Comput. Chem,* 2015, **36**, 348–354.
9. Almeida, H., Leroux V.,, Motta, F. N., Grellier, P., Maigret, B., Santana, J.M., Bastos, I.M.D., Identification of novel Trypanosoma cruzi prolyl oligopeptidase inhibitors by structure-based virtual screening, *J .Comput. Aided Mol. Des.*, 2016, **30**, 1165–1174
10. Timothy D. H. B, Maria T. R., Agnes M., Shirin J., Inhibition of phospho-MurNAc-pentapeptide translocase (MraY) by nucleoside natural product antibiotics, bacteriophage /X174 lysis protein E, and cationic antibacterial peptides, *Bioorg. Med. Chem.*, 2016, **24**,6340–6347
11. Shi, S., Nguyen, P.K., Cabral, H.J., Diez-Barroso, R., Derry, P.J., Kanahara, S.M., and Kumar, V.A., Development of peptide inhibitors of HIV transmission, *Bioactive Materials*, 2016, **1**(2), 109–121.
12. Kaushik-Basu, N., Basu, A., and Harris, D., Peptide inhibition of HIV-1: current status and future potential, *Biodrugs*, 2008, **22**(3), 161-175
13. Wan-Gang Gu, Xuan Zhang, and Jun-Fa Yuan, Anti-HIV drug development through computational methods, *AAPS Journal*, 2014, **16**(4), 674- 680.

CSE
-P-
1

A Numerical Model for Optimizing a Magnetic Regenerator

Pairat Tulyaprawat[1], **Yuranan Hanlumyuang** [2,C],
[1] *Department of Materials Engineering, Faculty of Engineering, Kasetsart University, Bangkok, Thailand*

[C] ***E-mail:*** *fengynh@ku.ac.th;* ***Fax:*** *+66 2 955 1811;* ***Tel.*** *+66 2 7970999 ext. 2119*

EXTENDED ABSTRACT

Keywords: Numerical Model, Magnetrocaloric Effect. Layered- bed

INTRODUCTION

The rising energy consumption has become one of the most important problems in modern world. It is known that more than 50% the energy is spent in cooling systems, both in industry and household. Therefore, there is a need, now more than ever, to develop a better energy-saving refrigerant alternative. Recently, cooling-system engineers and scientists have spurred into investigating magnetic refrigerators because of their efficiency; 20-30% improvement over those of current vapor-compression refrigerators. However, there is still a gap of knowledge on the interplay among magnetic work, thermal work, and fluid flow inside a magnetic refrigerator. Our work is aimed to develop a model of the heat exchanging among all those three main components. The developed numerical model allows experimentalists and engineers to optimize the cooling-system design, and predict the operating temperature span. Finite difference method is used in solving relevant heat equations. In order to determine temperature span for the highest cooling performance applicable for household usage, initial conditions are studied and various variables are identified

PROPOSED APPROACH

The simulations are performed using a Matlab program, designed to predict the coefficient of performance of a magnetic refrigerant system. Several physical parameters in the cooling system are identified and tuned to achieve the optimal efficiency.

RESULTS

The resultant coefficients of performance of the layered- bed design are shown against that of the layered-bed design at different temperature levels.

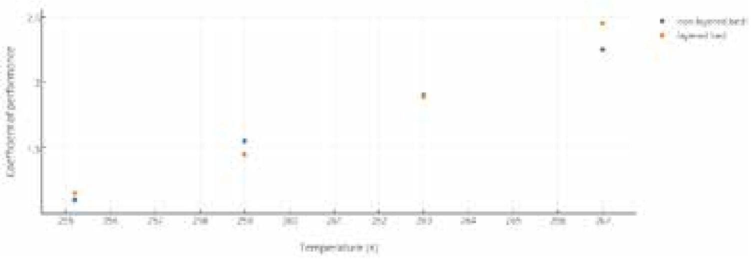

Figure 1. Coefficients of performance of the layered- bed design non-layered-bed design

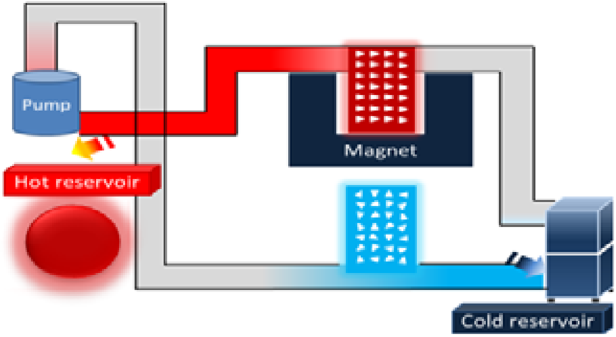

Figure 2. Magnetic refrigerator system

REFERENCES

1. Engelbrecht, K. L. , Nellis, G. F. , Klein, S. A. , 2005. A numerical model of an activemagnetic regenerator refrigeration system. Cryocoolers 13, 44-128
2. Franco, V., et al. (2012). "The Magnetocaloric Effect and Magnetic Refrigeration Near Room Temperature Materials and Models." Annu. Rev. Mater. Res.: 42.
3. Bouchekara, H., et al. (2008). "Prediction and optimisation of geometrical properties of the refrigerant bed in an AMRR cycle." international journal of refrigeration: 1224-1230.
4. Nikkola, P., et al. (2014). "1D model of an active magnetic regenerator." international journal of refrigeration: 43-50.
5. Tusek, J., et al. (2013). "Geometrical optimization of packed-bed and parallel-plate active magnetic regenerators." international journal of refrigeration: 1456-1464.
6. Lei, T., et al. (2015). Study of geometries of active magnetic regenerators for room temperature magnetocaloric refrigeration. Applied Thermal Engineering: 19.
7. Tusek, J., et al. (2011). "Dynamic operation of an active magnetic regenerator (AMR): Numerical optimization of a packed-bed AMR." international journal of refrigeration: 1507-1517.

CSE
-P-
2

Automatic Control for Water Droplet on Metal Surface

Prasarnphun Saisin[1], **Santi Wannippanto**[2], **Yongyut Pattanapong**[3,]
[1,2,3]*Graduate of Electrical Engineering, Faculty of Science and Technology*
Pathumwan Institute of Technology, Bangkok 10330, Thailand

E-mail *: e1saisin_p@hotmail.com, e2santi@pit.ac.th, e3yongyut.pattanapong@gmail.com ;*
Fax : +66 4 241 2458; **Tel.** +66840286923

EXTENDED ABSTRACT

Keywords: Automatic control, Droplet, Dew point, Smart room.

INTRODUCTION

Factories in Thailand mainly import machinery used in manufacturing to the use of force and to produce large quantities. Machinery used mainly made of metal, which is the component of steel and shaped characteristics vary according to use. And require regular maintenance. The problems encountered in the maintenance of the rust caused a lot of water vapor in the air condenses on the surface of the metal and the condensation reaction between iron and oxygen in the air. Rust stains are red or reddish brown on a surface of the metal. And the Condensation on the surface of the metal, machinery and equipment industry is another reason that causes rust. As a result, cause a short circuit of the electronics and cause damage. The dew point refers to the point at which condensation of water vapor occurs due to the amount of water vapor in the air is fully saturated and the air temperature drop causes the condensation water naturally. If we can control the condensation on the surface, especially in the machining of large industrial plants to prevent damage different. The aim of researchers are interested to learn how to control condensation on metal surfaces and cause condensation to occur by increasing the temperature to a metal surface. This method seems to control condensation and may be another way to reduce the damage of a mechanical device.

THEORY AND RELATED WORKS

The relative humidity (f) and the dewpoint temperature (T_D) are two widely used indicators of the amount of moisture in air. The exact conversion from f to T_D, as well as highly accurate approximations, are too complex to be done easily without the help of a calculator or computer. However, there is a very simple rule of thumb that found to be quite useful for approximating the conversion for moist air.Relative humidity is commonly defined in one of two ways, either as the ratio of the actual water vapor pressure *e* to the equilibrium vapor pressure over a plane of water *es* (often called the "saturation" vapor pressure).Dew Point Equations Formulas CalculatorMeteorology Weather Water Vapor

- Solving for dew point temperature

$$T_D = \left(\frac{f}{100}\right)^{1/8}(112 + 0.9T) + 0.1T - 112$$

EXPERIMENTAL

1. Preparation Materials. The materials for this study consist of as follows:
    1.1 Aluminium plate with size width 7.62 cm, length 11.43 cm, thick 0.5 cm
    1.2 Thermoelectric plate has the size 92 watts 12 volts.
    1.3 Fin heat sink and the cooling fan with size 12 volts.
    1.4 Thermocouple
    1.5 Heater or resistance wire
    1.6 The DHT-22 (also named as AM2302)
2. Preparation of Laboratory

    For preparation of laboratory, all materials are composed and designed circuit are made for studying the behavior of the water droplets on the specimen and controlling the occurrence of water droplets on Aluminium surface.
3. Method of Experiment

    12 volts DC power was fed through the semiconductor type: n-type and p-type, which is inside the thermoelectric plate. One of the thermoelectric plate sides would be cool and another side of the plate would be hot. Cool thermoelectric plate side would attach to Aluminium surface. This made the Aluminium surface cool and a cause of condensation to be the water droplets on the surface. However, the controller could get rid of the water droplets on the surface.

RESULTS

This paper is found that in-house tests that control air conditions can remove droplets on the work surface and meet the intended purpose as shown in figure 1.

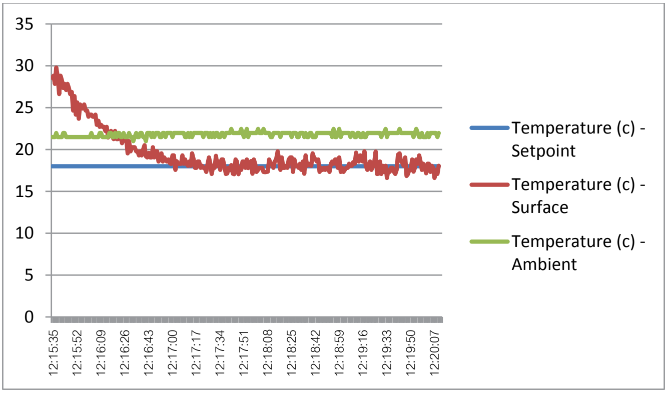

Figure 1. **Set point (18 degree)**

REFERENCES

1. Luca FERRARIS, Paolo FERRARIS, "Improvement of a static system for water condensation supplied with Photo Voltaic energy", IEEE TRANSACTIONS ON PLASMA SCIENCE, 2016, pp. 1-5,
2. Tzung Han Yang1, Chin Pan1, and Hon Ming Hsieh, "Molecular Dynamics Simulation of Interactions between a Nano Water Droplet and an Isothermal Platinum Surface", Proceedings of the 3rd IEEE Int. Conf. on Nano/Micro Engineered and Molecular Systems, January 6-9, 2008, Sanya, China, pp. 1129-1133

3. Richard W. Bonner III, “Dropwise Condensation in Vapor Chambers”, 26th IEEE SEMI-THERM Symposium, 2010, pp. 224-227.
4. Dr.D.Senthil Kumar, R.Yuvaraj, “Simulation of Dropwise Condensation on a Superhydrophobic Inclined Substrate”, 2013, pp. 217-222.
5. Xiao Tan, Yunhao Qiu, Yong Yang, Dawei Liu, Member,IEEE, XinPei Lu, Senior Member, IEEE, and Yuan Pan, “Enhanced Growth of Single Droplet by Control of Equivalent Charge on Droplet”, 2016, pp. 1-5.
6. Martin Wanielista, Robert Kersten and Ron Eaglin. 1997. Hydrology Water Quantity and Quality Control. John Wiley & Sons. 2nd ed.

ANSCSE21
SPONSORED BY

Let's start your journey with us IBM

Reduce your simulation Cost &Time from Days to Hours
Handle extreme amount of data with incredible speed
Improve platform Efficiency & Scalability
New Technology Supported AI/Machine Learning /Deep Learning
WHAT IF IBM CAN?
Power Systems

Hewlett Packard
Enterprise

enterprise.nxt

Digital disruption impacts every industry. Here's how to win in an era of constant change.

WRITTEN BY MIKE SHAW

Hewlett Packard
Enterprise

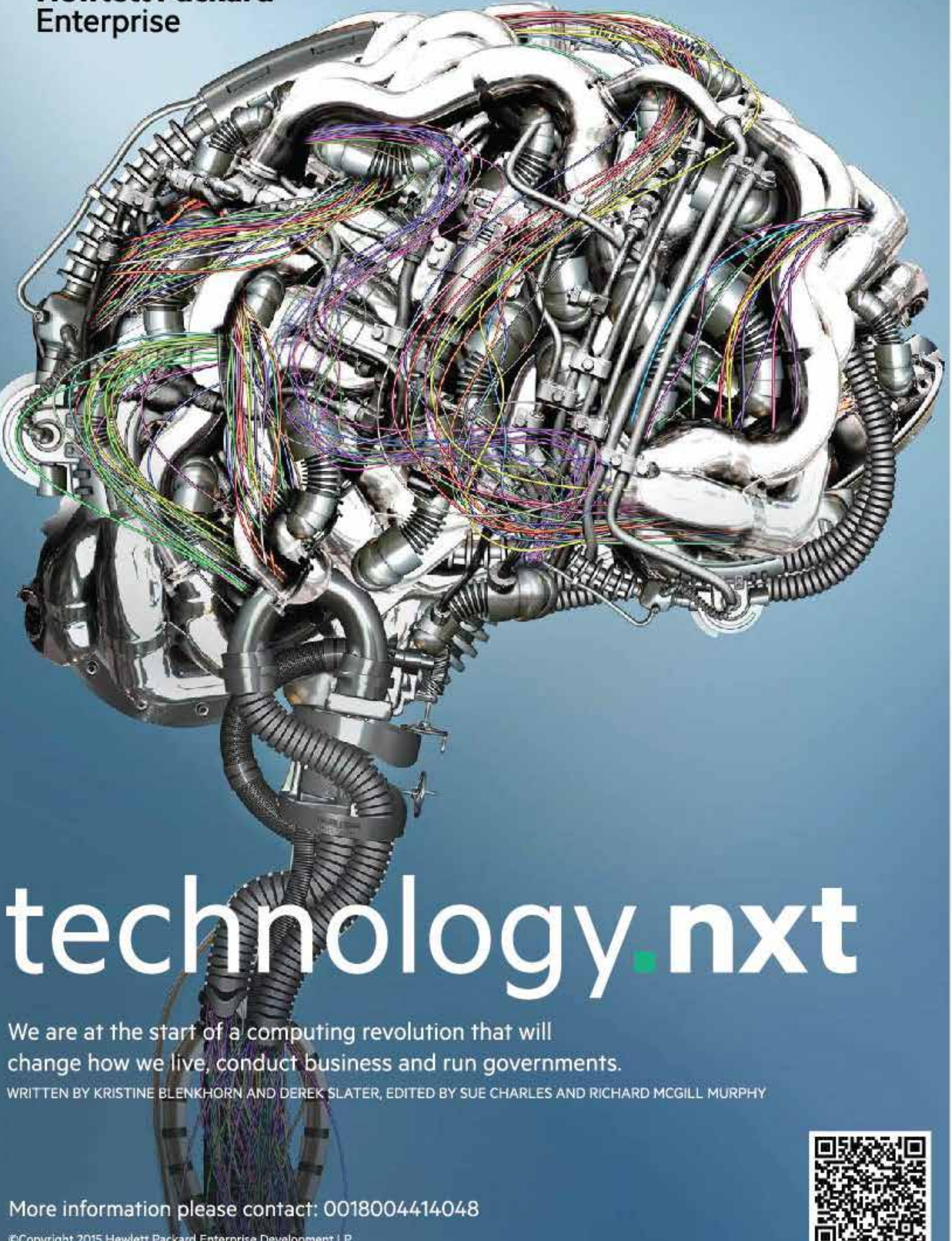

technology.nxt

We are at the start of a computing revolution that will change how we live, conduct business and run governments.

WRITTEN BY KRISTINE BLENKHORN AND DEREK SLATER, EDITED BY SUE CHARLES AND RICHARD MCGILL MURPHY

More information please contact: 0018004414048

©Copyright 2015 Hewlett Packard Enterprise Development LP.

มหาวิทยาลัยอุบลราชธานี

อตฺตานํ ทมยนฺติ ปณฺฑิตา
มหาวิทยาลัยเชียงใหม่ พ.ศ.๒๕๐๗